PHYSICO-CHEMICAL STUDIES ON SOFT MATTER: BEHAVIOUR OF SURFACTANT AGGREGATE AND BIODEGRADABLE POLYMER SYSTEMS

Thesis Submitted for the Degree of Doctor of Philosophy (Science)
Of the University of North Bengal

By

Mrinmay Jha, M.Sc.

GUIDE

Prof. Swapan K. Saha

DEPARTMENT OF CHEMISTRY
University of North Bengal
Darjeeling, West Bengal
India

2015

DECLARATION

I declare that the thesis entitled "**PHYSICO-CHEMICAL STUDIES ON SOFT MATTER: BEHAVIOUR OF SURFACTANT AGGREGATE AND BIODEGRADABLE POLYMER SYSTEM**" has been prepared by me under the guidance of Dr.S.K.Saha, Professor of Chemistry, University of North Bengal. No part of this thesis has formed the basis for the award of any degree or fellowship previously.

Mrinmay Jha 13.3.15

Mrinmay Jha

Department of Chemistry,
University of North Bengal
Darjeeling-734013
West Bengal
India

DATE

University Of North Bengal

Professor S. K. Saha
DEPARTMENT OF CHEMISTRY
Email: ssahanbu@hotmail.com

Ref.

Ph: (0353) 2776 381
Fax: (0353) 2699 001
P.O. North Bengal University
Raja Rammohunpur
Dt. Darjeeling.
PIN – 734 013
Dated: **March 13, 2015**

CERTIFICATE

I certify that Mrinmoy Jha, M.Sc. has prepared the thesis entitled " PHYSICO-CHEMICAL STUDIES ON SOFT MATTER: BEHAVIOUR OF SURFACTANT AGGREGATES AND BIODEGRADABLE POLYMER SYSTEMS" for the award of Ph.D. degree of the University of North Bengal, under my guidance. He has carried out the work at the Department of Chemistry, University of North Bengal.

Dr. Swapan K. Saha
Professor of Chemistry
University of North Bengal
Siliguri, Dist. Darjeeling
PIN 734 013

Acknowledgements

I take this opportunity to express my heartfelt gratitude to my supervisor, prof.S.K. Saha, Department of Chemistry, North Bengal university for his wise guidance and incessant encouragement throughout the entire period of work.

I would like to extend my thanks to Council of scientific and Industrial Research (CSIR), New Delhi, for fellowship support and appreciate the authorities of North Bengal University for extending laboratory facilities.

The cooperation and help from the teachers, officers and other staff members of the Department of Chemistry, North Bengal University are thankfully acknowledged.

I extend my sincere thanks to Mr.S.Bardhan, Miss.G. Chakraborty,.Dr.M.Ali,Dr.G.Bit,Dr.B.Debnath,Dr.A.Chakraborty,Mr.S.Ch akraborty, and Dr.S.K.Das of this laboratory for their good gesture and generous help. I must appreciate them for their kind cooperation and sharing many happy moments during the years.

I am particularly indebted to my mother Late Labanaya Jha, for her encouragement and enthusiasm which supported me for a long period of my research work. Without her it was not possible for me to join the craft and art of this scientific research.

I express my best regards to my father and other elders of my family for their ceaseless blessings and inspiration throughout the period of my work.

I would like to extend my thanks to my wife, Soma and our little son Devraaj for their constant support under all circumstances.

Last but not least I want to thank all fellow research scholars of the Department who made possible my life highly enjoyable during research period.

Date: 13.03.2015

University of North Bengal

Mrinmay Jha

(Mrinmay Jha)

ABSTRACT

Many everyday materials – food, medicines, cleaning agents, paints, plastics – are highly complex at the microscopic levels and consist of several kinds of molecules or tiny particles, which are held together by weak electrostatic forces in a highly organized way. At room temperature, these forces are usually not strong enough to prevent the materials from deforming under stress – which is why they are 'soft'. Generally the materials which are consist of very large molecules and easily deformable are usually referred to as "soft matter". The concept of "soft matter" covers a large class of molecular materials, including e.g. polymers, thermotropic liquid crystals, micellar solutions, microemulsions and colloidal suspensions, and also includes biological materials, e.g. membranes and vesicles. Two major focuses of the present study have been fixed. In Section A of the thesis, a detail study has been undertaken on the surfactant aggregation in aqueous solutions in presence of additives. Special emphasis has been given to the spherical to rod/worm like micelle transition at low surfactant concentrations, particularly in presence of neutral additives. Rheological and spectroscopic behaviour of the systems are also examined. The section B of the thesis constitutes studies on the physicochemical characteristic of some biopolymer viz, Sodium alginate and Poly (vinyl alcohol) in solution phase.

The unfavorable contact between water and the apolar part of surfactant molecules lead to their congregation into well organized entities, viz., micelles, vesicles, fibers, discs and tubes. Although micelles are usually spherical in shape, under certain conditions, e.g., concentration, salinity or in the presence of hydrophobic counter ions, etc., they may undergo uniaxial growth. This subsequently results in the formation of significantly long yet highly flexible aggregates referred to as "worm-like micelles (WLM)" . The research of WLM has drawn considerable interest because its rheology is very challenging due to the presence of multiple pertinent length scales and stress relaxation mechanisms. This relatively new material has many applications including that of fractured fluids in oil fields, efficient drag reducing agent in hydrodynamic engineering and home care, personal care and cosmetic products . Among the different additives, the hydrotrope, sodium salicylate, is very effective in triggering WLM formation in cationic surfactants even at very low concentrations. However, the use of salicylate as the promoter of WLM formation suffers from some

limitations, especially in the oil fields due to its complex forming tendency with metal ions impurities. In spite of a large number of publications in the field, WLM formation by metal-inert promoters which may work under salt free condition is rather rare and intensive research in this area is warranted. In view of the importance of an efficient WLM promoter, which might be effective for various applications at low surfactant concentrations under salt-free condition, organic π-conjugated molecules with H-bonding functionality, viz., naphthols are highly promising. Moreover, since the dissociation of hydroxyl groups of naphthols is tunable by controlling the pH of the system, a facile route to design pH-responsive morphology transition of WLM can be achieved via customized charge screening as a function of pH. This would find application in drug delivery processes. Stimuli-responsive viscoelastic gels of long wormlike micelles are formed at low surfactant concentrations in the presence of neutral naphthols, where H-bonding plays a key role in micellar shape transition in the absence of any charge screening. Micelle-embedded naphthols also act as novel self-fluorescence probes for monitoring viscoelasticity of the system as a function of applied shear. While UV absorption and Fourier transform infrared studies confirm the presence of intermolecular H-bonds in micelle embedded naphthols, transmission electron micrographs of vacuum-dried samples at room temperature demonstrate the transition in shape from sphere to rodlike micelles.

The viscoelastic gels formed in presence of naphthols are thermoreversible in nature, and the viscosity-temperature profile of each system passes through a maximum. ^{1}H NMR confirms that solubilization sites of naphthols in the micelle are located near the surface. The above study also shows that, on the NMR time scale, the motion of the naphthol molecules is highly restricted in viscoelastic phase, but water molecules rotate freely. While fluorescence quenching via H-bond strengthening is not observed in the micellar phase, UV absorption spectra demonstrate the presence of inter- molecular H bond in micelle-embedded naphthols in their ground electronic states as mentioned above, which was confirmed by FTIR. The ESPT of 2-naphthol is facilitated in presence of CTAB in the submicellar concentration range due to the catalytic effect of surfactant charge where as, ESPT is hindered in postmicellar concentrations due to lack of water accessibility. The micropolarity of OH sites of micelle-embedded naphthols is measured by observing pK_a-shift at the micellar surface relative to bulk water. Based on hydroxyaromatic

dopants, a simple and effective route to design pH-responsive viscoelastic worm-like micelles and the vesicles of single tail cationic surfactant (CTAB) is reported. Results are confirmed by observing cryogenic – transmission electron microscopy (cryo-TEM) images. The success of naphthols in effecting microstructural transition of micelles lies in their unique ability to form H-bonding with interfacial water molecules, which have shown unusual H-bond donating property compared to bulk water. The OH groups of micelle-embedded naphthols are protruded toward the Stern layer through ~1 A and the dielectric constant of OH sites has been measured as 45±2 by observing pK_a-shift of acid-base equilibrium of naphthols at the interface relative to that in bulk water. The result of unusual H-bonding may be relevant, not only when considering the H-bonding of the interfacial water molecules in the specific micelle and dopant studied here, but also for the H-bonding interaction of other micelle-dopant systems as well. This offers an interesting route for fluorescence monitoring of unperturbed viscosity as a function of applied shear. In a viscous medium, a fluophore cannot transfer energy efficiently via nonradiative means because of delayed collisions with the surrounding molecules resulting in the increased emission quantum yield.

The results of the investigation on the unperturbed dimension, interaction parameter and related aspects of poly(vinyl alcohol) and sodium alginate in binary solvent mixtures viz. water-acetone, water-ethoxy ethanol for sodium alginate and water-acetone, water-tetrahydrofuran for poly(vinyl alcohol) have been described in Section B of the present thesis. The intrinsic viscosity [η] of three different samples of the polymers (Sodium Alginate; Type-A, Type-B and Type-C) and poly(vinyl alcohol) having different molecular weights were measured in various fractions of solvent composition (Φ_{ace} and Φ_{ee}). Acetone and ethoxy ethanol are the poor solvent for sodium alginate but water-acetone and water- ethoxy ethanol mixtures act as a co-solvent in certain proportions. On the other hand, acetone and tetrahydrofuran are poor solvents for poly(vinyl alcohol) but water-acetone and water- tetrahydrofuran mixtures act as a co-solvent in certain proportions for the poly(vinyl alcohol). From the relation between [η] and [Molecular mass(M)], the unperturbed dimension and molecular expansion factor have been measured. The Huggins constant value in each case was also determined in order to have ideas on the influence of co-solvent system on the aggregation of the polymers. The

evaluation of the above interaction parameters and molecular dimensions of sodium alginate, a linear polysaccharide and that of poly(vinyl alcohol) using fundamental laws governing polymer chemistry and physics give new insight regarding the character of such macromolecular chains in binary solvent mixtures. A better understanding of their behavior in solution would help in opening new direction of research with immense application.

Contents

Chapter -3 41-107

Studies on microstructural transition of micellar aggregates in presence of hydroxyaromatic compounds: rheology and spectroscopy

Chapter – 4 108-129

Interaction of cationic micelles with 1 and 2 naphthols: self fluorescence monitoring of stimuli-responsive viscoelasticity and location of surface activity

Chapter 1

General Introduction

1. Introduction

1.1 Soft Matter Research:

The pace of worldwide research in the areas like macromolecular and association colloids, emulsions and microemulsions, gels, membranes, liquid crystals, nano particles etc. in recent years is amazing. This has led to the emergence of "soft matter" science and technology as a distinct interdisciplinary area of Chemistry, Physics, Life Sciences, Chemical Engineering, Pharmacy and Material Science. The study of soft matter aims at identification of molecules that form specific structures in a particular environment and probing into the causes that induce the structures formation, understanding of the specific functional aspects of the structures formed, designing specific structure with desired properties of the structures formed. Biological systems provide ample examples of structure and compartment formation. A clear understanding may help drug design, encapsulation, targeting and delivery. Natural process may be conveniently mimicked to advantage for applications in pharmacy, medicine, agriculture and industry.

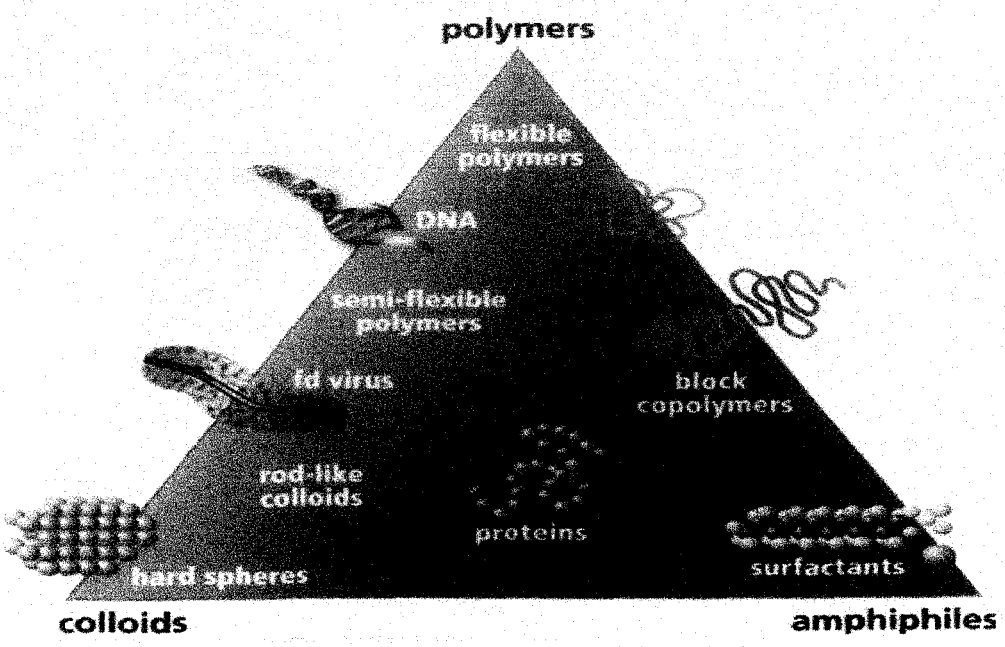

Figure1.1: The "soft -matter triangle": it encompasses a broad, continuous range of materials, from colloidal suspensions of particles to flexible long-chain polymer molecules and amphiphilic or soap-like, systems. Many biological systems such as proteins, DNA and virus have the characteristics of all these soft-matter types.

1.2 Self-Assembly of Amphiphilic Molecules

Amphiphilic molecules have been the realm of interest in chemistry for over a hundred years with attention not only in pure science but also in their wide applications to industry. Self-assembly is a spontaneous organization of molecules driven by noncovalent interactions into stable aggregates. Self-assembly is also well recognized in biological systems, e.g., lipid bilayers, the DNA duplex, and tertiary and quaternary structure of proteins. The process of spontaneous aggregation of single molecules in solution into larger structures with a certain order is also an important phenomenon in every-day-life as well as in science. The best known example of aggregation in every-day-life is the formation of micelles by detergent molecules. The most important type of aggregation, which is essential to life, is the formation of the lipid bilayer membrane by phospholipids. It has inspired chemists and physicists to study and mimic this and other types of aggregates [1]. Aggregation of molecules often occurs at the borderline of solubility. An important molecular property in this respect is polarity, for which solubility follows the rule 'like dissolves like'. Polar (hydrophilic) compounds are well soluble in polar solvents, e.g. salt in water, and the same goes for apolar (hydrophobic) compounds and solvents, e.g. vitamin E in oil. Furthermore, polar compounds are insoluble in apolar solvents and vice versa. Things become more interesting when a compound has amphiphilic properties, i.e. when it contains a polar as well as an apolar part. The polar part is called "head" and the apolar part usually a long chain hydrocarbon is called "tail" (see Figure 1.2). These compounds are most comfortable in a situation when each part is located in an appropriate environment, which is only possible at the interface between two media. Therefore, amphiphilic compounds are also called surface-active agents, or in short, surfactants [2]. The head group may be anionic, cationic or nonionic and accordingly the surfactants are classified as anionic, cationic or nonionic.

Figure 1.2: Schematic representation of an amphiphile.

There are some surface active amphiphilic molecules that contain both anionic and cationic centers at the head group. These are called zwitterionic surfactants. Surfactants can also have two hydrocarbon chains attached to a polar head and are called double chain surfactants. On the other hand, surfactants containing two hydrophobic and two hydrophilic groups are called "gemini" surfactants. Amphiphilic molecules can also have two head groups (both anionic, both cationic or one anionic and the other cationic) joined by hydrophobic spacer [3]. These types of molecules are termed "bola-amphiphiles" commonly known as "bolaforms". Surface activity of these molecules depends on both the hydrocarbon chain length and the nature of head group(s). Amphiphiles with longer hydrocarbon chains are found to be more surface-active compared to those having shorter hydrocarbon tail [4]. It is observed that amphiphiles with fluorocarbon chain are more surface-active than those with hydrocarbon chain. This is because the fluorocarbon chain is more hydrophobic than hydrocarbon chain [5].

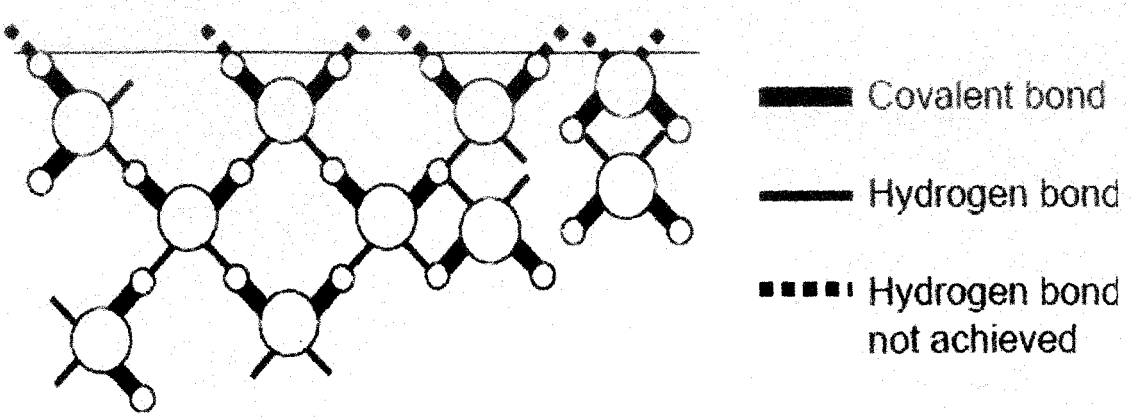

Figure 1.3: Water molecules at the liquid-air interface

Water is a very cohesive liquid due to the formation of a 3-dimensional hydrogen bond network (Figure 1.3) in addition to attractive van der Waals interactions.

This induces that the amount of work required to expand the interface air-water, characterized by the surface tension, is relatively high (72.6 mNm^{-1}, for pure water at 20°C). When surfactants are added to water, they adsorb at the water-air interface, which actually arises from their dualistic character. In aqueous solution the hydrophobic chain interacts weakly with the water molecules, whereas the hydrophilic head interacts strongly via dipole or ion-dipole interactions. It is this strong interaction that renders the surfactant soluble in water. However, the cooperative action of dispersion and hydrogen bonding between the water molecules tends to squeeze the surfactant chain out of the water (hence, these chains are referred to as hydrophobic). Therefore, surfactants tend to accumulate at the surface, which allows lowering the free energy of the phase boundary, i.e. the surface tension.

1.3 Structure and Shape of Aggregates: The Packing Parameter

The concept of molecular packing parameter has been widely cited in chemistry, physics, and biology literature because it allows a simple and intuitive insight into the self-assembly phenomenon [6]. The packing parameter approach permits indeed to relate the shape of the surfactant monomer to the aggregate morphology [7-9].

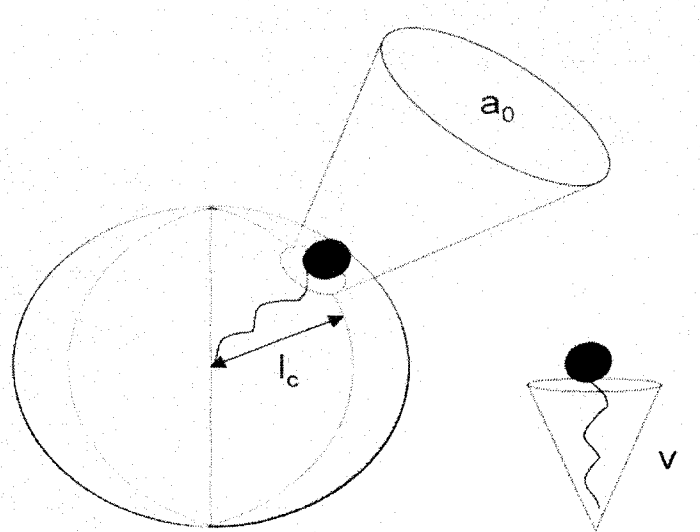

Figure 1.4: The critical packing parameter P (or surfactant number) relates the head group area, the extended length and the volume of the hydrophobic part of a surfactant molecule into a dimensionless number $P=V/a_0l_c$

The molecular packing parameter P is defined as the ratio $v/a_o l_c$, where v and l_c are the volume and the extended length of the surfactant tail, respectively and a_o is the *equilibrium* area per molecule at the aggregate interface (or mean cross-sectional {effective} head-group surface area), as illustrated in Figure 1.4. If we consider a spherical micelle with a core radius R, made up of N_{agg} molecules, then the volume of the core is $V = N_{agg} \times v = 4\pi R^3/3$, the surface area of the core $A = N_{agg} \times a_o = 4\pi R^2$. Hence, it can be deduced that $R = 3v / a_o$, from

Table1.1 Schematic representation of surfactant structures and shapes derived from various packing parameters

Possible surfactant type	P(=V/$a_o l_c$)	Shape	Structures formed
Single-tail surfactants with large head groups	p< 1/3	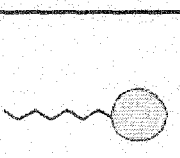	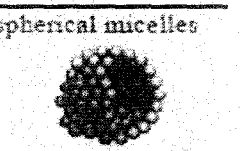
Single chain surfactants with small head groups	1/3<P<1/2	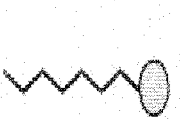	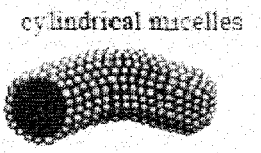
Double chain surfactants with large headgroups and flexible chains	1/2<P<1	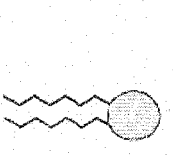	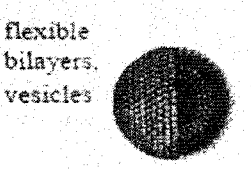
Double-chain surfactants with small head groups or rigid, immobile chains	P~1		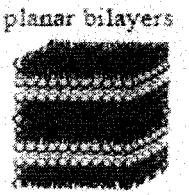
double-chain surfactants with small head groups, and bulky chain	P>1	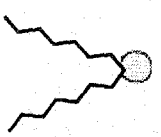	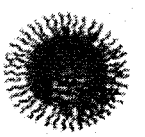

simple geometrical relations. If the micelle core is packed with surfactant tails without any empty space, then the radius R cannot exceed the extended length l_c of the tail. Introducing this constraint in the expression for R, one obtains $0 \leq v / a_o l_c \leq 1/3$, for spherical micelles. These geometrical relations, together with the constraint that at least one dimension of the aggregate (the radius of the sphere or the cylinder, or the half-bilayer thickness, all denoted by R) cannot exceed l_c, lead to the following well-known connection between the molecular packing parameter and the aggregate shape [7]. $0 \leq v / a_o l_c \leq 1/3$ for sphere, $1/3 \leq v / a_o l_c \leq 1/2$ for cylinder, and $1/2 \leq v / a_o l_c \leq 1$ for bilayer. Inverted structures are formed when $P>1$. Therefore, if the molecular packing parameter is known, the shape and size of the equilibrium aggregate can be readily identified as shown above. Noteworthy, a_o is often referred to as the "headgroup area" in the literature. This has led to the erroneous identification of a_o as a simple geometrical area based on the chemical structure of the headgroup in many papers, although a_o is actually an equilibrium parameter derived from thermodynamic considerations [6]. Needless to say, that for the same surfactant molecule, the area a_o can assume widely different values depending on the solution conditions such as temperature, salt concentration, additives present, etc.; hence, it is meaningless to associate one specific area with a given head group. For example, sodium dodecylbenzene sulfonate forms micelles in aqueous solution whereas bilayer structures are formed when alkali metal chlorides are added [10]. Moreover, the role of the surfactant tail has been virtually neglected. This is in part because the ratio v /l_c appearing in the molecular packing parameter is independent of the chain length for common surfactants (0.21 nm^2 for single tail surfactants) and the area a_o depends only on the head group interaction parameter. Nagarajan showed that the tail length influences the head group area (consideration of tail packing constraints) and thereby the micellar shape [6].

1.4 Self-Assembled Structures of Amphiphilic Molecules in Water

1.4.1 Micelles

The most intensely studied and debated type of molecular self-assembly and perhaps the simplest in terms of the structure of the aggregate is the micelle. Micelles formed by ionic amphiphilic molecules in aqueous solution are dynamic associations of surfactant molecules that achieve segregation of their hydrophobic portions from the solvent via self-assembly. They are loose, mostly spherical aggregates above their critical micellisation concentration

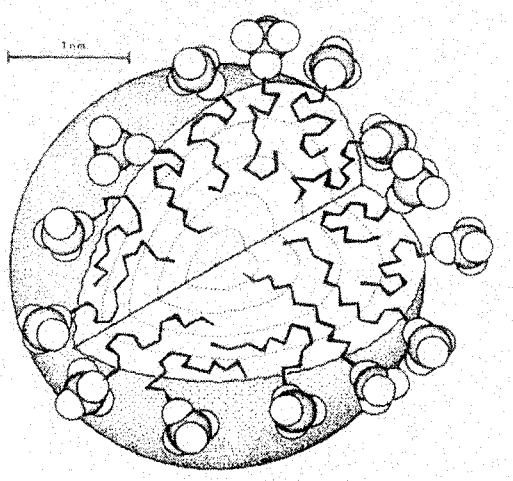

Figure 1.5: Schematic representation of a spherical micelle in aqueous solution.

(cmc) in water or organic solvents [1]. Also, micellar aggregates are short-lived dynamic species, which rapidly disassemble and reassemble [11]. Hence, only average shape and aggregation numbers of micelles can be determined. Micellization of surfactants is an example of the hydrophobic effect. In micellization there are two opposing forces at work. The first is the hydrophobicity of the hydrocarbon tail, favouring the formation of micelles and the second is the repulsion between the surfactant head groups. The mere fact that micelles are

formed from ionic surfactants is an indication of the fact that the hydrophobic driving force is large enough to overcome the electrostatic repulsion arising from the surfactant head groups. Figure 1.5 represents a spherical micelle formed in aqueous solution, where the hydrophobic chains are directed towards the interior of the aggregate and the polar head groups point towards water, hence allowing the solubility / stability of the aggregate (no phase separation). Micelles are also known to be disorganized assemblies whose interiors consist of mobile, non-stretched hydrophobic chains [12]. Note in addition that water molecules can penetrate partially into the micelle core to interact with surfactant hydrophobic tails [13]. There are a huge number of publications related to the micelles, micelle structures, and the thermodynamics of micelle formation. A huge amount of experimental and theoretical work devoted to the understanding of the aggregation of surface-active molecules has been carried out [14-16].

Micelles are generally formed by cationic, anionic, zwitterionic as well as nonionic surfactants having short alkyl chains. The environment of a micelle varies in a regular manner as a function of distance from the center of the micelle, going from a relatively dense aliphatic medium near the center to a relatively diffuse region known as either Stern layer in ionic micelles, or as Palisade layer in neutral micelles [17-19] where the head groups, bound counterions, and solvent molecules coexist. The remaining counterions are contained in the Gouy-Chapman portion of the double layer that extends further into the aqueous phase. Fluorescence probe studies have indicated that micellar core is nonpolar, but less fluid than hydrocarbon solvents of equivalent chain length [20]. On the other hand, the Stern layer has polarity equal to that of alcohols [21].

When a nonpolar group is introduced into an aqueous solution, the hydrogen bonding network formed by the existing water molecules is disrupted and the water molecules order themselves around the nonpolar entity to satisfy hydrogen bonds (Figure 1.6 A). This results in an unfavourable decrease in entropy in the bulk water phase. As additional nonpolar groups are added to the solution, they self-associate thus reducing the total water-accessible surface of the complex relative to the monodisperse state. (Figure 1.6 B) Now, fewer water molecules

are required to rearrange around the collection of nonpolar groups. Therefore, the entropy associated with the complex is less unfavorable than for the monodisperse detergents. In short, hydrophobic association and the formation of micelles is driven by the favorable thermodynamic effect on the bulk water phase.

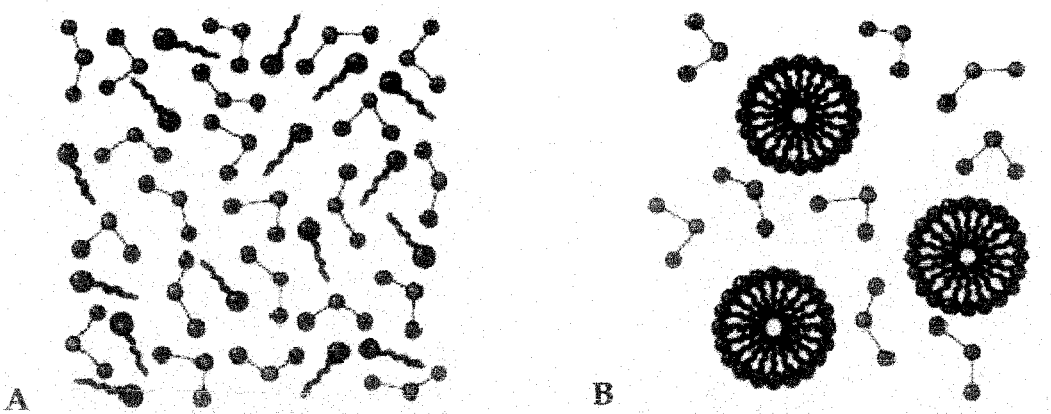

Figure 1.6: Water molecules ordered around surfactant monomers (**A**). Loss of total water-accessible surface as a result of micellisation (**B**).

A great deal of work has been done on elucidating the various factors that determine the cmc at which micelle formation becomes significant, especially in aqueous media. An extensive compilation of the cmcs of surfactants in aqueous media has been published [22]. Among the factors that are known to affect the cmc in aqueous solution are (i) the structure of the surfactant, (ii) the presence of added electrolyte (in the case of ionic surfactants) in the solution, (iii) the presence of various organic compounds in solution, and (iv) temperature of the solution.

Surfactant structure. In general, the ionic surfactants have higher cmc values compared to nonionic surfactants. The cmc in aqueous media decreases as the hydrophobic character of the surfactant increases. It has been observed that the cmc is halved by the addition of one methylene group to a straight-chain hydrocarbon tail. For nonionics and zwitterionics, the cmc value is decreased to one fifth of its previous value. The branching of the hydrocarbon chain appears to have about one-half the effect of carbon atoms of a straight chain. When C-C double bond is present in the hydrocarbon chain the cmc value is higher than that

of the corresponding saturated compound. An introduction of a polar group such as –O or –OH into the hydrophobic chain generally causes a significant increase in the cmc value in aqueous medium at room temperature. However, replacement of hydrocarbon chain by a fluorocarbon chain of same length causes a decrease in cmc value. For n-alkyl ionic surfactants, the cmc decreases in the order aminium salts > carboxylates > sulfonates > sulfates. It has been found that in quaternary cationics, pyridinium compounds have smaller cmcs than the corresponding trimethylammonium compounds.

Counterion. The degree of counterion binding, β (=1-α), has also an effect on the cmc value of ionic surfactants. The larger the hydrated radius of the counterion ($NH_4^+ > K^+ > Na^+ > Li^+$ and $I^- > Br^- > Cl^-$), the weaker the degree of binding, and hence larger the cmc. Thus in aqueous medium, for anionic lauryl sulfates, the cmc increases in the order $Ca^{2+} < N(C_2H_5)_4^+ < N(CH_3)_4^+ < NH_4^+ < Cs^+ < K^+ < Na^+ < Li^+$. On the other hand, for cationic dodecyltrimethylammonium and dodecylpyridinium salts, the order of decreasing in aqueous medium is $I^- < Br^- < Cl^- < F^-$.

Electrolyte. In aqueous solution, the presence of electrolyte causes a decrease in the cmc, the effect being more pronounced for anionic and cationic than for zwitterionic surfactants and more pronounced for zwitterionic than for nonionics. This is a consequence of decreased electrostatic repulsion between ionic headgroups in the micelle. The change in cmc of nonionics and zwitterionics upon addition of electrolyte is mainly due to the "salting out" or "salting in" of the hydrophobic group in aqueous solvent.

Organic additives. Water-soluble polar organic compounds such as alcohols and amides reduce the cmc at much lower concentrations. Shorter-chain alcohols are mainly adsorbed in the water-micelle interfacial region. The longer-chain compounds are adsorbed in the outer portion of the micelle core, between the surfactant molecules. Additives that have more than one group capable of

forming hydrogen bonds with water appear to produce greater depression of cmc. On the other hand, additives like urea, formamide, N-methylacetamide, guanidinium salts, short-chain alcohols, ethylene glycol, and other polyhydric alcohols, such as fructose and xylose increase cmc at relatively higher concentrations by modifying the interaction of water with surfactant molecules.

Temperature. The effect of temperature on the CMC of surfactants in aqueous medium is complex, the value appearing first to decrease with temperature to some minimum and then to increase with further increase in temperature. Increase of temperature causes decrease of hydration of the hydrophilic group, which favors micellization and also causes disruption of the structured water surrounding the hydrophobic group, which disfavors micellization. The relative magnitude of these two opposing effects, therefore, determines increase or decrease of CMC.

1.4.2 Worm-like micelles

Worm-like micelles are long, flexible, cylindrical chains with contour lengths of the order of a few micrometers. The entanglement of these wormlike chains into a transient network imparts viscoelatic properties to the solution [23-24]. Single chain ionic surfactants, e.g., cetyltrimethylammonium bromide (CTAB), favor convex-up surface geometry of the micelles due to strong headgroup repulsion and form spherical or near spherical micelles at the critical micelle concentration (cmc), while either at much higher surfactant concentrations (~1.0 M) or in the presence of high inorganic salt concentrations (>0.1 M), morphological changes occur to rod-like micelles and vesicles [27-30]. Hydrotropic salts like sodium salicylate (NaSal) also promote sphere to worm-like micellar transition at considerably lower concentration (e.g., ~1.0 mM in CTAB) by increasing the packing parameter above the critical value of 1/3 via efficient charge screening of the surfactant head groups [31]. These worm-like micellar solutions at low concentrations show complex and unusual rheological phenomena.

The dynamics of these systems differs from those of conventional polymers in that the wormlike micelles are continuously breaking apart and recombining. The rheological behavior of these surfactant solutions is known to follow "reaction-reptation model" which is an extension of the reptation model of polymer relaxation to cylindrical micelles of surfactant molecules undergoing reversible scission and recombination processes [25]. The linear and nonlinear viscoelastic properties of surfactant solutions have been extensively studied over past few years, both theoretically [26,27] and experimentally [28-38]. In general, it is observed that there is a critical shear rate above which the viscosity dramatically increases for dilute concentration of surfactant solution. The cause of this shear thickening phenomenon is believed to be the flow-induced structure of surfactant solution under shear flow [28,34].

Figure 1.7: Microstructure of a typical wormlike micelle.

With increasing flow intensity, the micelles undergo coalescence or tend to be stretched toward the flow direction, and as shear flow is going with time, the shear-induced structure of wormlike micelles continuously breaks down and re-forms at high shear rate [39]. This shear-induced structure (SIS) behaves like a gel and shows strong flow birefringence in solution state [31]. The classic example of such an 'abnormal' system is a solution containing cationic surfactant cetyl pyridinium chloride (CPC) with sodium salicylate (NaSal) as the additive. For

semidilute surfactant solutions, zero shear viscosity initially increased with concentration, reached a maximum, and then decreased [24,32,40]. Also, the shear viscosity of semi-dilute CPC/NaSal solutions showed almost a constant value until the critical shear rate and then shear thinning began, followed by shear thickening at higher shear rate.

The average micellar length is a thermodynamic quantity, and it responds to changes in solution composition and temperature. Normally when a wormlike micellar solution is heated, the micellar length decays exponentially with temperature [23,41]. The reduction in micellar length leads to an exponential decrease in viscosity of the solution. The reduction in micellar length, in turn, leads to an exponential decrease in rheological properties such as the zero-shear viscosity η_0 and the relaxation time t_R. Accordingly, an Arrhenius plot of ln η_0 versus 1/T (where T is the absolute temperature) falls on a straight line, the slope of which yields the flow activation energy E_a. Values of E_a ranging from 70 to 300 kJ/mol have been reported for various micellar solutions [41-43].

Inorganic and organic salts have been widely used as additives to facilitate the structural transition of micelles in ionic surfactant solutions [44-47]. Inorganic counterions promote gradual micellar growth by reducing the head group repulsions in the ionic micelles. On the other hand, organic salts in aqueous micellar systems, dissociate to produce ionic species with a hydrophobic moiety, which affects the packing of the surfactant tails and leads to changes in the effective packing parameter. The growth of cationic surfactant such as CTAB micelles has been extensively studied in the presence of salts such as KBr [48], sodium salicylate [49,50] chlorobenzoates [51], and benzyl sulfonates [52]. The increased salt concentrations cause the microstructure to change from globular to wormlike micelles. Addition of anionic surfactant, for instance, sodium dodecyl benzenesulfonate (SDBS) to solutions of cationic surfactants has also been found to generate wormlike micelles [53]. Kaler and coworkers have reported a million-fold increase in viscosity for mixtures of alkyltrimethylammonium bromide surfactants and sodium oleate (SO) relative to the single component solution [54]. The effect of nonionic additives on micellar shape has also been investigated by

many research groups. Hedin and co-workers have reported the elongation of CTAB micelles upon the solubilization of benzene [55]. Zhang and coworkers investigated the effect of benzyl alcohol on CTAB/KBr micellar systems through a combination of rheology and NMR and have suggested elongation of micelles upon alcohol solubilization [56]. The addition of alcohols has also been shown to promote growth of worm-like micelles in such transitions [57-59].

Although, studies related to the microstructural transitions of micelles to worm-like micelles and vesicles have been going on for quite some time, a common element in most of the works summarised above is the presence of an anion salt like NaSal. A number of studies on micellar shape transition in cationic, anionic, and catanionic surfactant systems induced by polar and nonpolar organic species have been reported the literature [55, 60-62]. However, these systems trigger the shape transition only at very high concentrations and make themselves unsuitable for certain applications. Recent studies show that the above mentioned transitions takes place even in presence of neutral aromatichydroxy dopants like 1- and 2-naphthols. Studies on the microstructural modifications by neutral aromatichydroxy compounds are rather recent and will be discussed later in more detail.

1.4.3 Vesicles

Vesicles are closed bilayered structures similar to those of the lamellar phase characterized by two distinct water compartments, one forming the core and other the external medium [63,64]. Like micelles, the formation of vesicles is a result of energetically favorable hydrophobic association of the hydrocarbon tail(s) of an amphiphilic molecule. However, unlike micelles vesicles have two distinct domains: the lipophilic membrane and the interior aqueous cavity.

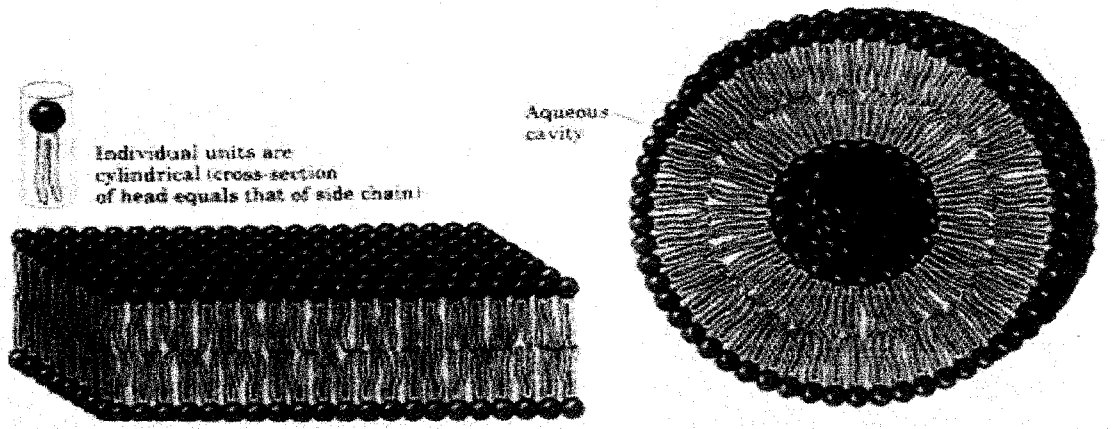

Figure 1.8: Figure showing bilayer and the individual unit of the surfactant forming the bilayer. The folding of the bilayer due to hydrophobic interaction forms the vesicle.

Specifically, the surface of micelles is a lipid monolayer, while the surface of liposomes is a lipid bilayer and the inner core of micelles is composed of hydrocarbon chains, while the inner core of vesicles is an aqueous phase. Vesicles have been found useful as agent in many practical applications and also a basis for several theoretical investigations. Micelles can solubilize amphiphiles and organic compounds, while vesicles can solubilize (or encapsulate) organic compounds and amphiphiles found in the lipid bilayer, and inorganic compounds and amphiphiles found in the aqueous core.

Vesicles can be prepared as small unilammellar vesicles (SUV), large unilamellar vesicles (LUV) or large multilamellar vesicles (liposomes). Multilamellar vesicles can be large having diameter of several μms and they are also termed as onions [65,66]. Vesicles are classified in terms of number of lamellae and size. Figure 1.7 presents a schematic view of the major liposome types. Multimembrane vesicles are divided into three groups: multilamellar vesicles (MLVs) also called as onion-shaped vesicles, oligolamellar vesicles (OLVs), and multivesicular vesicles (MVVs). OLVs are composed of several lamellae.

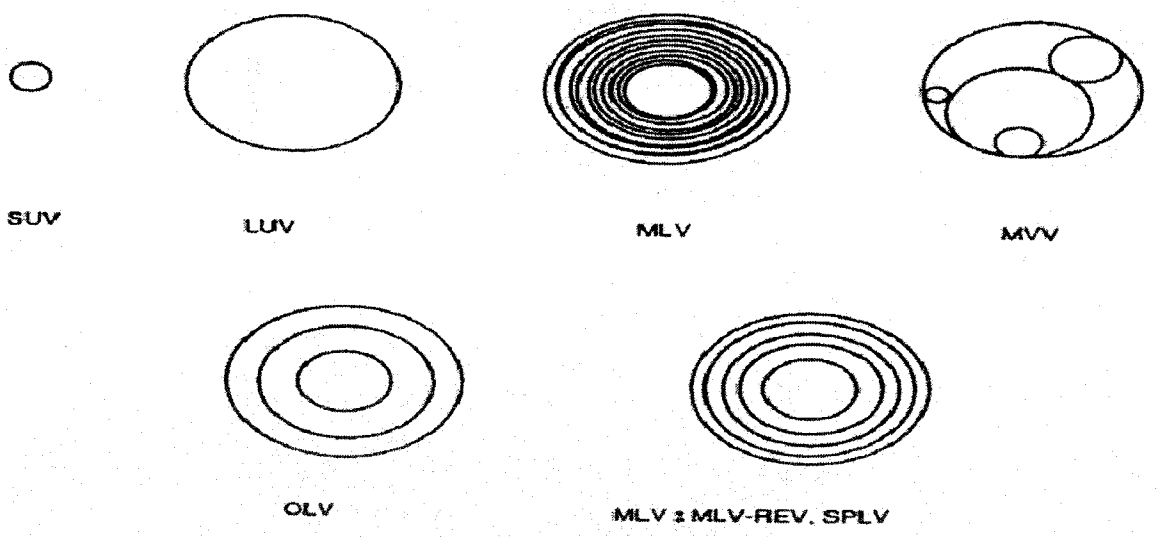

Figure 1.9: Morphology of different vesicle structures

Unilamellar vesicles consist of a lipid bilayer separating an aqueous solution from the bulk phase, forming roughly spherical structures with an inner aqueous core [67,68]. These vesicles (ULVs) are usually divided into three groups in terms of size: small unilamellar vesicles (SUVs), large unilamellar vesicles (LUVs), and giant unilamellar vesicles (GUVs). Vesicles under 100 nm are normally considered as SUVs, whereas those greater than 100 nm are LUVs. GUVs are those, which have sizes greater than 10 μm. The disadvantage of MLVs is their heterogeneous size distribution. The advantage of SUVs is the homogeneous size distribution and their disadvantage is low encapsulation efficiency. For LUVs, encapsulation efficiency is relatively high and macromolecules can be encapsulated. Vesicles have been found to form from synthetic surfactants containing one, two, or three alkyl hydrocarbon chains and quaternary ammonium, carboxylate, sulfate, sulfonate, hydroxide, or phosphate, zwitterionic or functionalized head groups. Vesicles are also generated by polymeric surfactants and block copolymers.

Role of Hydrogen Bonding Interaction in Self-Assembly Formation

Hydrogen bonds play very important role in biological systems. Hydrogen bonds have directional property and are moderately strong (4-25 kJ mol^{-1}) [69,70]. One of the important features of hydrogen bonding is that the bond formation can be reversibly switched under mild conditions by physical stimuli such as heat. In fact, hydrogen bonds have become a tool in liquid crystal (LC) [71,72] and polymer [73,74] chemistry. The role of hydrogen bonding on the gelation of organic solvents and water is well documented in the literature [74,75]. Recent studies have shown that short range attractive interactions, such as hydrogen bonding could be a driving force in the formation of bilayer self-assemblies of single-chain surfactants [76,77, 78-80]. In fact, hydrogen bonding between the amide groups is responsible for the favorable aggregation of some cationic surfactants that carry amidegroup spacer between the hydrophobic tail and the quaternary ammonium ion [81-84]. It has also been shown that intermolecular hydrogen bonding (IHB) between secondary amide groups in the hydrophobic tail of sodium 11-acrylamidoundecanoate induces a stable linear state [48].

It is well known that the spontaneous curvature of a surfactant aggregate is related to the relative sizes of the hydrophilic head and hydrophobic tail of the surfactant molecule. Increase of attractive forces between the headgroups can cause a decrease in effective head-group area, and hence a decrease in the curvature of the aggregate. In other words, this is a driving force for aggregate growth. LBM studies at the air-water interface have suggested that OH-substitution near (2 or 3-position) the headgroup results in a loss of ordering which is caused by the headgroup enlargement by the neighboring –OH group and a misfit of the alkyl chains in hydroxypalmitic acid [85]. On the other hand, well-shaped condensed phase domains were found after the phase transition in 9-hydroxypalmitic acid in which the -OH group is near the center of the hydrocarbon chain. The stability of the LC phase formed by the fatty acid derivatives bearing the -OH group is influenced by the ability of the substituent to form IHB and cause little disorder in the packing of the alkyl chain. The hydrogen-

bonding role of -OH group in molecular cohesion in condensed monolayer, helical ribbon, and gel formation by 12-hydroxyoctadecanoic acid has been reported by Tachibana and coworkers [86,87].

1.5 Biodegradable Polymers:Poly(vinylalcohol) and Sodium alginate.

Increasing concern exists today about the preservation of our ecological systems. Most of today's synthetic polymers are produced from petrochemicals and are not biodegradable. Persistent polymers generate significant sources of environmental pollution, harming wildlife when they are dispersed in nature. For example, the disposal of non-degradable plastic bags adversely affects sea-life. It is widely accepted that the use of long-lasting polymers in products with a short life-span, such as engineering applications, packaging, catering, surgery, and hygiene, is not adequate. Moreover, incineration of plastic waste presents environmental issues as well since it yields toxic emissions (e.g., dioxin). Synthetic plastics are resistant to degradation, and consequently their disposal is fuelling an international drive for the development of biodegradable polymers. Biodegradable polymers have been a subject of interest for many years because of their potential to protect the environment by reducing non-biodegradable synthetic plastic waste [88–92]. Biodegradation involves enzymatic and chemical degradation by living microorganisms [93–95].In essence, the enzymatic degradation of polymers takes place by hydrolysis and oxidation.The Biodegradable polymers, i.e.biopolymers are polymers formed in nature during the growth cycles of all organisms; hence, they are also referred to as natural polymers. Their synthesis generally involves enzyme-catalyzed, chain growth polymerization reactions of activated monomers, which are typically formed within cells by complex metabolic processes.

The applications of biodegradable polymers have been focused on three major areas:medical, agricultural, and consumer goods packaging. Some of these have

resulted in commercial products. Because of their specialized nature and greater unit value, medical device applications have developed faster than the other two.

1.5.1 Poly (vinyl alcohol) :

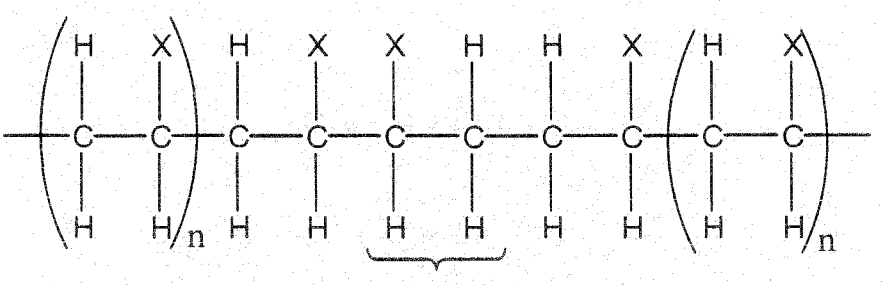

where X is- OH

Figure 1.10: A general structure of poly vinyl alcohol

(Poly vinyl alcohol)(PVA) is the most readily biodegradable of vinyl polymers. It is readily degraded in waste-water-activated sludges. The microbial degradation of PVA has been studied, including its enzymatic degradation by secondary alcohol peroxidases isolated from soil bacteria of the Pseudomonas strain [96–99]. It was concluded that the initial biodegradation step involves the enzymatic oxidation of the secondary alcohol groups in PVA to ketone groups. Hydrolysis of the ketone groups results in chain cleavage. Other bacterial strains, such as Flavobacterium [99] and Acinetiobacter [100] were also effective in degrading PVA. The controlled chemical oxidation of PVA was carried out to yield poly(enol-ketone) (PEK), which has a similar structure to the intermediate formed as PVA is biodegraded [101].Poly (vinyl alcohol) (PVA) has attracted much attention in recent years due to its excellent flexibility, transparency,toughness, and relatively low cost, especially in the era of highprice petroleum. PVA has been widely used in different fields such as textile sizing and has been utilized as a finishing agent, an emulsifier, a photosensitive coating, and as an adhesive for paper, wood,

textiles, and leather [102,103]. In addition, it is a biologically friendly polymer because of its biodegradability and biocompatibility[104].

Poly (vinyl alcohol) is an industrially important polymer, and this is shown by the fact that its production increases every year [105-109]. It exhibits a high degree of compatibility with inorganic salt solutions[110] natural and synthetic resins, and other chemicals [111,112]. Small amounts effectively stabilize emulsions [113] dispersions, and suspensions[114] It also forms chemical complexes of practical importance [115]. The intrinsic viscosity [η], a measure of the size of the isolated molecules,and Huggin's constant K_H [116],a measure of their interactions with solvent, are both influenced by changes of solvent power [117] and temperature [118] .Besides theoretical interest,such measurements are also important for technical reasons including polymer addition in motor oil recovery. Advances in the preparation of stereoregular polymers have stimulated the need to characterize their microtacticity and fine structure [119]. A number of studies and experimental techniques were used to characterize the nature of polymers in different solvents, but there seems to be few systematic studies of the dilute solution properties in different solvents and that too restricted to one or two temperatures[120,121]. As far as the polymers are concerned, the viscosity method can be successfully employed for the determination of the nature of the compound and their behavior in different solvents. Viscosity is affected by a number of parameters such as molecular mass, shape, and size of molecules, concentration, temperature, and intermolecular attractions, viz., ion-ion and ion-solvent interactions [110,122] .Ahmed et al.Takada et al., and Wang et al.[123-125] studied the thermodynamics of supermolecular order of the polymer PVA in aqueous solutions by the viscometric behavior and light scattering studies [124,125]

1.5.2 Sodium Alginate

Sodium alginate is a family of linear, binary co-polymers of (1→4) linked β-D-mannuronate (M) and α-L- guluronate residues arranged in a non-regular,

blockwise fashion along the chain [126,127]. The chain is composed of homopolymeric blocks of mannuronate (MM) and guluronate (GG),and blocks with an alternating sequence (Fig-1.11) The chain conformations of M- block and G- block were suggested to be "flat-ribbon" and "buckled-ribbon" forms,respectively [128].From light scattering and viscometric data, Smidsrod showed that the relative extension in the unperturbed state of the three types of blocks increase in the order of MG block ‹ MM block ‹ GG block [129]. Thus alginate polymer with high content of guluronate and long G-blocks generally showed a more extended, less flexible chain conformation than long M-block alginates. In general, the relative dimensions for the neutral unperturbed alginate chain at theta condition, a measure of chain stiffness, was higher than that of carboxyl methyl cellulose, dextran and amylase, but lower than double stranded DNA [130]

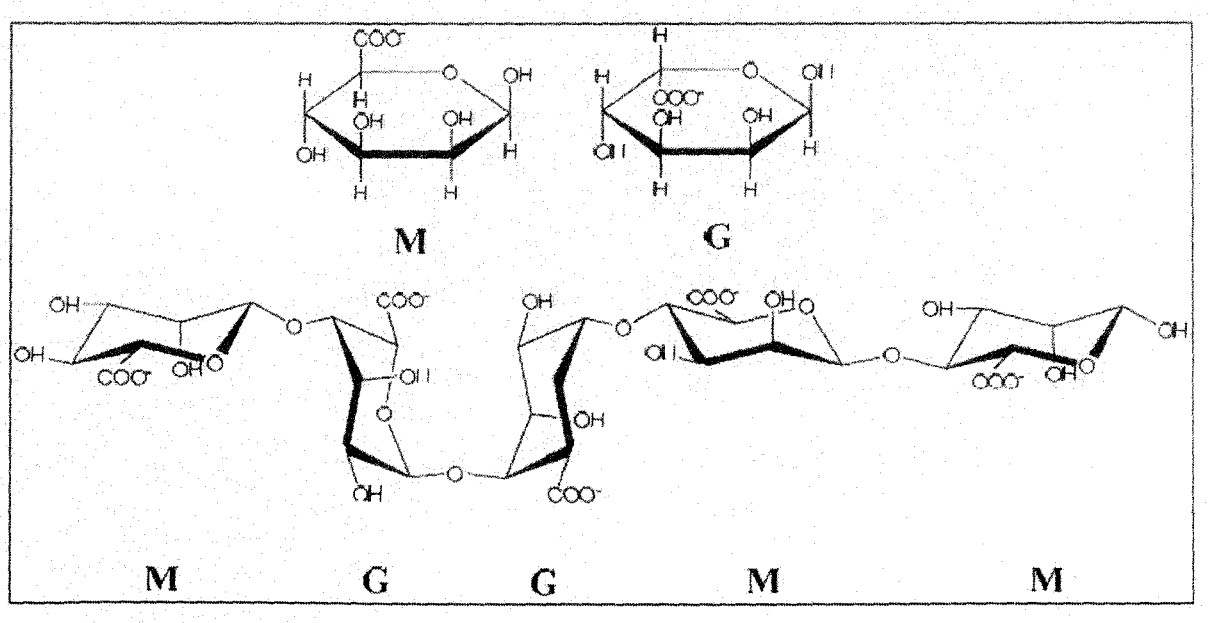

Figure 1.11: The chemical structure of alginate; the top figure illustrates the two monomers: mannuronic acid (M) and gluronic acid (G) residues in their Haworth conformation where as the bottom figure shows a sample block structure of alginate.

The biological properties of polysaccharides, especially of the algínates, have been explored since many decades in countless medical and surgical

applications. Those properties, and the solubility in water, are due to the presence of inorganic ions in the alginate structure[131]. Alginic acid form water-soluble salts with monovalent cations but is precipitated upon acidification. Alginates of many bivalent cations, particularly of $Ca^{2+,}$ Sr^{2+} and $Ba^{2+,}$ are insoluble in water and can be prepared when sodium ions of NaAlg are sodium alginate has been employed in the preparation of gels for the delivery of biomolecules such as drugs, peptides and proteins [136].Toxicological data replaced by di- and trivalent cations This property is used in the isolation of alginic acid from algae [132,133]. Due to their physical and chemical properties alginic acid (HAlg)and sodium alginate (NaAlg), have widely been used in food processing, medical and pharmaceutical industries [134] such as drug carrier [135], moreover, showed that alginates are safe when used in food. HAlg and its derivatives acts as stabilizers and thickeners facilitating the dissolution and improving viscosity of the ingredients preventing the formation of crystals that will prejudice the appearance and homogeneity, mainly in frozen products [137].

Alginates are fainly characterized of the marinepolysaccharides [138].Most commercial alginates are extracted from brown seaweed. However alginates can also be synthesized by some bacterial species such as Azotobacter and Pseudomonas[138]. Bacterialalginates are additionally O-acetylated on the 2 and/or 3 positions of the D-mannuronic acid residues, and exhibit a greater water binding ability [139,140]. Among the brown algal species, the most widely used are Laminaria hyperborea, Macrocystis pyrifera, and Ascophyllum nodosum due to their abundance [141] for extracting alginates.

1.6 Reference

1. J.H. Fuhrop and J. Köning, In *Membranes and Molecular Assemblies: the `Synkinetic `Approach*, The Royal Society of Chemistry - Cambridge, (1994).
2. J.H.Clint, *Surfactant Aggregation*, Blackie - Glasgow/London, (1992).
3. J.H.Fhurhop and J.Mathieu, *J. Chem Soc., Chem. Commun* , 144 (1983).
4. M.J.Rosen,*Surfactants and Interfacial Phenomena*, Wiley-Interscience,p.60. (2004).
5. E.Kissa, In *Fluorinated Surfactants and Repellents*, 2nd ed.; Marcel Dekker:`New York; p103 (2001).
6. R. Nagarajan *Langmuir*, **18**, 31 (2002)
7. J.N.Israelachvili ; D.J. Mitchel, and B.W. Ninham, *J. Chem. Soc., FaradayTrans.* **72(2)**, 1525 (1976).
8. J.N. Israelachvili In *Intermolecular and Surface Forces*; Academic Press: London, (1994).
9. R.Nagarajan; Ruckenstein, E. In *Equations of State for Fluids and Fluid Mixtures*; `J.V.Sengers, R.F.Kayser, C.J. Peters, Jr.White and H.J. Eds.; *Elsevier*: Amsterdam, `Chapter 15 (2000).
10. A. Sein and J. B. F. N. Engberts, *Langmuir,* **11**, 455 (1995).
11. A.Patist, S.G.Oh, R.Leung and D.O.Shah, *Coll. Surf. A*, **176**, 3 (2001)
12. F.M. Menger, R Zana and B.Lindman, *J. Chem. Ed.* **75**, 115 (1998).
13. K.Tsujii, In *Surface Activity: Principles, Phenomena, and Applications*; Academic Press Ed.: San Diego, London, New York, Tokyo, (1997).
14. R.G.Laughlin, *The aqueous phase behavior of surfactants*; Academic Press: `London,(1994).
15. J. H. Fendler *Membrane Mimetic Chemistry*, Wiley: New York, (1982).
16. J.H. Fuhrhop and W. Helfrich, *Chem. Rev.*, **93**, 1565 (1993).
17. S.S.Berr, E.Caponetti, J. S.Johnson, R.R.M. Jones and L. Majid, *J. Phys. `Chem*, **90,** 5766 (1986).

18. S. S. Berr , M.J. Coleman, R. R.M. Jones and J. S. Johnson, *J. Phys. Chem.*, **90**, 6492 (1986).

19. S. S. Berr ,*J. Phys. Chem.*, **91**, 4760 (1987).

20. N. J.Turro, M.Gvätzel and A. M. Brann, *Angew. Chem. Int. Ed.*, **19**, 675 (1980).

21. R. Zana, In *Surfactant Solutions. New Methods of Investigation*, R. Zana, and`M.Dekker New York, Chapter 5 (1987).

22. P.Mukherjee and K. J. Mysels, *Critical Micelle Concentrations of Aqueous Surfactan Systems*, NSRDS-NBS 36, U. S. Dept. of Commerce, Washington, DC, (1971).

23. M. E. Cates and S. J. Candau, *J. Phys.: Condens. Matter*, **2**, 6869 (1990).

24. H. Hoffmann In *Structure and Flow in Surfactant Solutions*; C. A. Herb and R.K.Prudhomme, Eds.; American Chemical Society: Washington, DC, ***2,3*** pp 2-31(1994).

25. M.E.Cates, *Macromolecules* **20**, 2289 (1987).

26. M.E.,Cates, In Theoretical modeling of viscoelastic phases, C.A. Herb, and R.K. Prudhomme (eds), *ACS Symposium Series* **578**, 32 (1994).

27. M.E.Cates, and S.J.Candau,Statics and dynamics of worm-like surfactant micelles, *J. Phys.* **2**, 6869 (1990).

28. H. Hu, R.G. Larson and J.J. Magda, *J. Rheol.* ***46***, 1001 (2002).

29. T.Shikata, M. Shiokawa, S. Itatani and S. Imai, *Korea Australia Rheol. J.* `***14***,129 (2002).

30. Z. Lin, A. Mateo, E. Kesselman, E. Pancallo, D.J. Hart, Y. Talmon, T.H.Davis, L.E. Scriven and J. Zakin, *Rheol. Acta* **41**, 483 (2002).

31. Z.Lin, B. Lu, J. Zakin, Y. Talmon, Y. Zheng, T.H. Davis and L.E. Scriven, *J. Colloid Interface Sci.* ***239***, 543 (2001).

32. H. Rehage and H. Hoffmann *Mol. Phys.*,**74**, 933 (1991).

33. H.Hoffmann, H. Löbl, H. Rehage and I.Wunderlich *Tenside Detergents,* **22**,290 (1985)

34. H. Rehage and H. Hoffmann *Phys. Chem.*,**92**, 4712 (1988).

35. T.Shikata, K.Hirata and T.Kotaka *Langmuir.*,**3**, 1081 (1987)

36. T.Shikata., K. Hirata and T. Kotaka, *Langmuir,* **4**, 354 (1988)

37. T.Shikata., K. Hirata and T. Kotaka, *Langmuir*, **5,** 398 (1989)

38. T.Shikata., K. Hirata and T. Kotaka, *J. Phys. Chem,* **94**, 3702 (1990)

39. W.J. Kim and S.M. Yang, *Langmuir* **16**, 4761 (2002).

40. R.Zana, *Adv. Colloid Interface Sci.* **97**, 205 (2002).

41. S. R., Raghavan and E. W. Kaler, *Langmuir*, **17**, 300 (2001)

42. R. Makhloufi and R.Cressely, *Colloid Polym. Sci.* **270**, 1035 (1992).

43. A., Ponton, C., Schott and D. Quemada, *Colloids Surf. A.*, **37**,145 (1998).

44. O. R.Pal, V. G. Gaikar, J. V. Joshi, P. S.Goyal and V. K. Aswal, *Langmuir*, **18**, 6764(2002).

45. G. Porte and J.Appell, *J. Phys. Chem,* ***85***, 2511 (1981).

46. E. W. Kalu, K. L. Herrington, D. J. Iampietro, B. Coldren, H. T. Jung, A. J. Zasadzinski, In *Mixed Surfactant Systems* 2nd Ed.; M. Abe, J.Scamehorn, Eds.; Marceel Dekker: New York (2005).

47. D.Angeleseu, A. Khan and H. Caldaram, *Langmuir*, **19**, 9155 (2003).

48. V. K.Aswal and P. S. Goyal, *Chem. Phy. Lett.*, **357**, 491 (2002).

49. H. Hoffmann, H. Rehage, G.Platz, W. Schorr, H.Thurn and W. Ulbricht, *Colloid Polym. Sci*, **260**, 1042 (1982).

50. P. A.Hassan and J. V. Yakhmi, *Langmuir*, **16**, 7187 (2000).

51. U.R.K. Rao, C. Manohar, B. S. Valaulikar, R. M. Iyer, *J. Phys. Chem.*, **91,** 3286 (1987).

52. O. R. Pal, V.G. Gaikar, J. V. Joshi, P. S. Goyal and V. K. Aswal, *Langmuir*, **18**,6764 (2002).

53. E.W.Kalu,K.L.Herrington D.J.lampietro,B.Coldren,H.T.Jung, A.J. Zasadzinskiln *Mixed Surfactant Systems* 2nd Ed.; M. Abe, J.Scamehorn, Eds.; Marceel Dekker: NewYork (2005).

54. D. Angeleseu, A. Khan and H. Caldaram, *Langmuir*, **19**, 9155 (2003).

55. N.Hedin, R.Sitnikov, I.Furo, U.Henriksson and O.Regev, *J.Phys.Chem.B* ,**103**, 9631 (1999).

56. W.C.Zhang, G.Z. Li, Q. Shen and J.H. Mu, *Colloids Surf., A, **170**,* 59 (2000).

57. S.Chiruvolu, H. E. Warriner, E.Naranjo, S.H.J.Idziak, J.O.Rädler, R.J.Plano, J.A .Zasadzinski and C. R. Safinya, *Science*, **266**, 1222 (1994).

58. (a) H. Hoffmann, C.Thunig and M. Valiente, *Colloids Surf* ,**67**, 223 (1992). (b) H.Hoffmann, U. Munkert, C.Thunig and M. Valiente *J. Colloid Interface `Sci.*, **163**, 217(1994). (c)M.Gradzielski, M. Bergmeier, M. Müller, H. Hoffmann, *J. `Phys.Chem B*, **101**, 1719 (1997).

59. R. Oda, L. Bourdieu, M. Schmutz, *J. Phys. Chem. B*, **101**, 5913 (1997)

60. C.Manohar, In *Micelles, Microemulsions, and Monolayers*; *Science and Technology*;D. O. Shah, Ed.; Marcel Dekker, Inc.: New York, p 145 `(1998).

61. P. M. Lindemuth and G. L. Bertrand, *J. Phys. Chem,* **97**, 7769 (1993).

62. H.Yin, S.Lei, S.Zhu, J.Huang and J.Ye, *Chem.-Eur. J*, **12**, 2825 (2006).

63. D.B. Fenske, N. Maurer and P. R. Cullis, In *Liposomes: a practical approach*, 2nd ed.; V.Weissig, Ed.; Oxford University Press: Oxford, p 167-191 (2003).

64. K. M. G. Taylor and S. J. Farr In *Liposomes in drug delivery*; H. M. Patel, Ed.; Harwood Academic Publishers: Chur, Switzerland, **2**, 95 (1993).

65. H. Hoffmann, and W. Ulbricht, *Recent Res. Devel. in Physical Chem.*, 2 (1998).

66. Susanne Nilsson, Krister Thuresson, Per Hansson and Björn Lindman, *J Phys.*

Chem. B, 102,7099 (1998).

68. D.D. Lasic, *Liposomes. From Physics to Applications*, Elsevier, Amsterdam,(1993).

69. I.I. Yaacob and A. Bose, *J. Colloid Interface Sci*, ***178,*** 638 (1996).

70. R.D. Koehler, S. R. Raghavan and E. W. Kaler, *J. Phys. Chem.`B*,**104**,11035(2000).

71. L. L. Brasher, K. L. Herrington, E. W. Kaler ,*Langmuir*, **11**, 4267(1995).

72. M. T. Yatcilla, K. L. Herrington, L. L. Brasher, E. W. Kale , S.Chiruvolu and J. A. Zasadzinski . *J. Phys. Chem*, **100**, 5874 (1996).

73. A. J. O'Connor, T. A. Hatton and A. Bose, *Langmuir*, **13,** 6931(1997).

75. N.Filipović-Vinceković, M. Bujan, , I. Šmit Lj.Tušek-Božić, and I. Štefanić, *J. Colloid Interface Sci.*, **201**, 59 (1998).

77. Y. Talmon, D. F.Evans and B. W. Ninham, *Science*, **221**, 1047 (1983).

78. K. K. Karukstis, S. W. Suljak, P. J. Waller, J. A.Whiles and E. H. Z. Thompson, *J. Phys.Chem*, **100**, 11125(1996).

80. E.F. Marques, A.Khan, M. da Graca Miquel and B. Lindman *J. Phys. Chem.*, **97**, 4729 (1993).

81. E.F. Marques, A.Khan and B. Lindman, *Thermochim Acta*, **394**, 31(2002).

82. G. Bai, Y. Wang, J. Wang, B. Han and H. Yan, *Langmuir*, **17**, 3522 (2001).

83. A.Das Burman, T. Dey, B.Mukherjee and A. R. Das, *Langmuir*, **16**, 10020 `(2000).

84. A. Bumajdad, J. Eastoe, P. Griffiths, D. C. Steytler, R. K. Heenan and J. R Lu, *et al. Langmuir*, **15**, 5271 (1999).

85. Y.Kondo, H. Uchiyama, N. Yoshino, K.Nishiyama and M. Abe, *Langmuir*, **11,**`2380 (1995).

86. E. F.Marques, O.Regev, A. Khan, M. da Graca Miquel, and B. Lindman, *J. Phys. Chem. B*, **103**, 8353 (1999).

87. D.J Iampietro,.L.L.Brasher, E.W. Kaler,A. Stradner and O. Glatter, *J.Phys. Chem B*, ***102***, 3105 (1998).

88. Y.Doi and K .Fukuda, editors. In *Biodegradable plastics and polymers* : *Elsevier* Amsterdam, (1994).

89. W.M. Doane, C.L.Swanson and Fanta GF. *Emerging technologyes for materials and chemicals from biomass*. ACS Symposium Series;**476**:,197 (1992).

90. D .Raghavan. *Polym-Plast Technol Eng*; **34**,41 (1995)

91. J.M. Krokhta, D. Mulder and C.L.C Johnston. In: *Biodegradable polymers `from agricultural products*. ACS Symposium Series ,**647**,120 (1996).

92. A.M. Thayer, *Plastics recycling efforts spurred by concerns about soli waste*. In:J.E, Glass, and G Swift, editors. *Agricultural and synthetic `polymers `Biodegradability and utilization*. ACS Symposium Series;**433**,38 (1990).

93. P.A. Wagner, B.J. Little, K.R Hart and R.I Ray *Int Biodeterior Biodegrad*,**38**,125 (1996).

94. L. Tilstra, D. J .Johnsonbourgh, *Environ Polym Degrad* **1**,247 (1993).

95. M. Vert, L.Feijen, A. Albertsson and G. Scott, editors. *Biodegradable polymers and plastics*.Wiltshire, UK: Redwood Poss Ltd, The Royal Society of Chemistry (1992).

96. T. Suzuki, *J. Appl. Polym. Sci. Appl. Polym. Symp.*, **35,** 431(1979).

97. Y.Watanabe, M.Morita, N. Hamade, and Y. Tsujisake, *Agric. Biol. Chem.*, **39,** 2447(1975).

98. M. Morita, and Y.Watanabe, *Agric. Biol. Chem.*, **41,** 1535 (1977) .

99. Y.Watanabe, N. Hamada,., M. Morita, and J.Tsuisake, *Arch. Biochem. `Biophys.*, **174,**575 (1976)

100. F.Fukanage, S.Sumina,K.Neda, T.Takemasa, and K.Tachibana, *Jpn. kokai*,**794**,471(1977).

101. F.Fukunaga, K. Nesta, K.Tuchibana, T. T Akemara, and S. Sumina, *Jpn. kokai*,**25**,786 (1976).

102. C. A. Finch, *Poly Vinyl Alcohol*; Wiley: New York, pp 1-3 and12-18 (1992).

103. N.Nakano, S.Yamane and K.Toyosima, *PoVal(polyVinyl-alcohol)*; Japan Polymer Society: Kyoto, p 3 (1989).

104. E.Chiellini, A.Corti, S. D Antone and R. Solaro, Biodegradation of poly (vinyl `alcohol) based materials. *Prog. Polym. Sci.*, **28**, 963 (2003).

105. N.Gungor and S. Dilmac, The effects of some salts and (NaPO3)*n* `polymer on viscosity of Na-Montmoillanite slurry. *J. Chem. Soc.Pak.*, **19**,14 (1997).

106. F.Uddin, V.Saeed and R. Talib, Temperature Dependence of the Intermolecular Activation Energy for Flow in Strontium Nitrate And Barium Nitrate Solution in Aqueous 2-Propanol Mixtures. *J. Saudi Chem. Soc.*, **2**, 101(1998).

107. R.H Stokes and R.Mills, *Viscosity Electrolyte and Related `Properties*;Pergamon Press: New York, 1965.

108. N. Ahmed, SAkber, I.Khan, and A. Saeed, Viscosity Parameters and `Energy of Activation of Dilute Aqueous Polyvinyl Alcohol (PVOH) `Solutions. *J. Chem. Soc Pa* **10**, 43(1998).

109. M. S.Khan and F. Kanwal, Degradation of PVC in Air. *J. Chem. Soc. Pak.*, **19**, 8 (1997).

110. H.Yang, P. Zhu, C. Peng, S. Ma, Q. Zhu and C. Fan, Viscometric Study of Polyviny Alcohol in NaCl/Water Solutions ranged from Dilute to Extremely Dilute Concentration.*Eur. Polym. J.* **9**, 1939 (2001)

111. N.M. Claramma, and N. M. Mathew, Rheological Behavior of Prevuleanized

Natural Rubber Latex; Huething Gm B H: Heidelberg, Germany, (1998).

112. T. Okaya, H. Kohna, K.Terada, T.Sato, H.Maruyams and J. Yamauchi,. Specific Interaction of Starch and Polyvinyl Alcohols having Long Alkyl Groups. *J. Appl.Polym. Sci.* **45**, 1127(1992).

113. M. Nakamae, K. Yuki, T.Sato and H. Maruyama, *Colloids and Surfaces, A, Physicochemical and Engineering Aspects*; Elsevier Science Publishers B. V Amsterdam, The Netherlands, (1997).

114 W. S. Lyoo, S. M. Lee, K. Koo, J. S. Lee, H. D. Ghim, J. P. Kim and J. Lee,Effect of Emulsion Polymerization Conditions of Vinyl Acetate on Viscosity Fluctuation and Gelatinous Behavior of Aqueous Poly (Vinyl`Alcohol) Solution. *J. Appl. Polym. Sci.* **82**, 1897(2001)

115. M.Shibayama, F. Ikkai, R. Moriwaki, and S. Nomura, Complexation of Poly (Vinyl Alcohol) - Congo Red Aqueous Solutions. 1*Viscosity Behav. Gelatin Mech. Macromol* , ***27***, 1738 (1994).

116. K.Lewandowska,D.UStaszewska,andM.Bohdanecky,Huggins Viscosity Coefficient of Aqueous Solutions of Poly (Vinyl Alcohol). *Eur. `Polym. J.*, **37**, 25(2001).

117. G. O Yahya,.; A. Ali, M. Al-Naafa and A. E. Z. Hammad, *J. Appl. Polym. Sci.*`**57**,343(1995).

118. K.Koga, A.Takada and N. Nemoto, Dynamic Light Scattering and Dynamic Viscoelasticity of Poly (Vinyl Alcohol) in Aqueous Borax Solutions. 5. Temperatures Effects. *Macromolecules*, ***32***, 8872(1999).

119. N.Ahmed,.and B. Ahmed, Intrinsic Viscosity, Huggins Constant and Unperturbed Chain Dimension of Poly Vinyl Pyrolidone. *J. Chem. Soc. Pak.*, **12**, 246(1990).

120. S.Shaikh, S. K. A Ali ;A. E. Z. Hamad, M.Al-Nafaa, A. Al- Jarallah and B. Abu-Sharukh, Synthesis,Characterization and Solution Properties of Hydrophobically Modified Poly (Vinyl Alcohol). *J. Appl. Polym. Sci.*, **70**, 2499 (1998).

121. M.Liu,R.Cheng,C.Wu and R.Qian, Viscometric Investigation of `Intramolecular Hydrogen Bonding Cohesional Entanglement in Extremely Dilute Aqueous Solutions of Polly Vinyl Alcohol. *J. Polym. Sci., Part B: Polym. Phys.*, **35**, 2421(1997).

122. G.Jones, and M. Dole, The Viscosity of Aqueous Solutions of Strong Electrolytes with Special Reference of Barium Chloride. *J. Am. Chem. Soc. (*1929).

123. N. Ahmed, A. Rasheed, M. S. Khan and A. K. A. Bhettani, Thermodynamic Study of Supermolecular Order in AqueousSolution of Poly (Vinyl Alcohol) *J. Chem. Soc.`Pak.* **12**, 221(1990).

124. A.Takada M.Nishimura, A. Koike and N. Nemoto, Dynamic Light Scattering and Dynamic Viscoelasticity of Poly (Vinyl Alcohol) in Aqueous Borax Solutions. 4. Further Investigation on Polymer Condition and Weight `Dependencies. *Macromolecules*, **31**,436 (1998).

125. B.Wang, S. Mukataka, M. Kodama and E. Kokufuta, Viscometric and Light Scattering Studies on Microgel Formation byç-raylrradiation to Aqueous Oxygen-Free Solutions of Poly (Vinyl Alcohol).*Langmuir*,**13**,6108(1997).

126. A.Hauge,B.Larsen and O.Smidsrod *Acta Chem.Scand*,**20**,183(1966).

127. Z.Wang,Q.Zhang,M.Kono and S. Saito, *Biopolymers,***34,**737 (1994).

128. E.D.T Atkins ,W.Mackie,K.D. parker and E.ESmolko,*J.polymer Sci.*part, lym. Lett,**9**, 311(1971).

129. O.Smidsrod,A.Haug and S.G.Whittington ,*Acta Chem.Scand,***26**,2563 (1972).

130. Flory, P. J.John Rehner, J., Statistical Mechanics of Cross-Linked Polymer Networks II.Swelling. *The Journal of Chemical Physics,* **11**, 521(1943).

132. K. Nakamura, E. Kinoshita, T. Hatakeyama and H. Hatakeyama, *Thermochim. Acta* **171**, 352 (2000).

133. A. I. Usov, *Russ. Chem. Rev.*, **68,** 957 (1999).

134. A. Ikeda, A. Takemura, and H. Ono, *Carbohydr. Polym.* ,**42** , 421 (2000).

135. G.O. Aspinall, The polysaccharides, Academic Press, New York, vol. 2 (1983)

136. T. W. Wong, L. W. Chan, S. B. Kho and P. W. S. Heng, *J. Controlled Release* ,**84**, 99 (2002).

137. D. F. Othmer and R. E. Kirk, Encyclopedia of Chemical Technology, John Wiley, New York 3rd., (1980).

138. C. K. Yeom and K. H. Lee, Characterization of sodium alginate membrane crosslinked with glutaraldehyde in pervaporation separation. *Journal of Applied Polymer Science* **67 (2),** 209 (1998).

139. M.Iza, S. Woerly, C.Danumah, S. Kaliaguine and M. Bousmina, Determination of pore size distribution for mesoporous materials and polymeric gels by means of DSC measurements: thermoporometry. *Polymer* **41(15)**,5885(2000).

140. P. J.Flory,. *Statistical mechanics of chain molecules*. Repr. ed. with corrections ed.;Oxford University Press: New York, (1989).

141. B. Amsden and N.Turner, Diffusion characteristics of calcium alginate gels. *Biotechnology and Bioengineering,* **65** (**5**), 605 (1999).

Chapter 2

Scope and Object

Scope and Object

Many everyday materials – food, medicines, cleaning agents, paints, plastics – are highly complex at the microscopic levels and consist of several kinds of molecules or tiny particles, which are held together by weak electrostatic forces in a highly organized way. At room temperature, these forces are usually not strong enough to prevent the materials from deforming under stress – which is why they are 'soft'. Generally the materials which are consist of very large molecules and easily deformable are usually referred to as "soft matter". The concept of "soft matter" covers a large class of molecular materials, including e.g. polymers, thermotropic liquid crystals, micellar solutions, microemulsions and colloidal suspensions, and also includes biological materials, e.g. membranes and vesicles.

Various types of soft matter with their sizes

Polymers	10 nm-1μm
Colloids	10 nm-1μm
Surfactant micelles	5 nm-100μm
Liquid Cristals	5 nm-100μm
Bio Molecules	2 nm-5μm

These substances have a wide range of applications including structural and packaging materials, foams and adhesives, detergents and cosmetics, paints, food additives, lubricants and fuel additives, rubber in tyres etc., and our daily life would be unimaginable without them. In spite of the various forms of these materials, many of their very different properties have common physicochemical origins such as a large number of internal degrees of freedom, weak interactions between the structural elements and a delicate balance between entropic and enthalpic contributions to the free energy. These properties lead to large thermal fluctuations, a wide variety of forms,

sensitivity of the equilibrium structures to external boundary conditions, macroscopic softness and various metastable states.

Vesicles and micelles represent two of the important classes of self-assembled structures that can be formed by amphiphiles in dilute or semidilute solution. Vesicles are hollow spheres enclosed by a bilayer of the amphiphiles and are commonly used to encapsulate labile hydrophilic molecules within their interiors. Micelles tend to occur in a range of morphologies, including spherical, ellipsoidal, and wormlike micelles. Among the most fascinating of these are the 'wormlike micelles', which are flexible cylindrical chains with radii of a few nanometers and contour lengths up to several micrometers. Considerable interests have been generated recently in studying physico-chemical properties of self assembled surfactant aggregates, especially micelles, and unilamellar vesicles . Although many reasons can be cited for the wide spread interest in elucidating the physico-chemical properties of these self organized systems, primarily there are three reasons. Firstly, one can consistently and easily prepare aqueous micellar and vesicular solutions which contain aggregates of colloidal dimensions with characteristic size, shape and surface properties. Hence micellar and vesicular system have been employed as a model system in investigations concerned with understanding colloidal physico-chemical phenomena. Secondly, the similarities between self-assembled surfactant aggregates, such as micelles and vesicles, and biological lipid membranes prompted researchers to employ micelles and vesicles as model biological systems. Quite often they provide microenvironments very similar to the biological environments – thus allowing trial experiments prior to in-vivo study . Thirdly, it has been found that micelles and vesicles can act as unique reaction media. Therefore, investigation on physico-chemical characteristics of micelles and vesicles forms a considerable volume of literature .

The self aggregation of amphiphilic molecules, either in the simplest form of monolayers or in the form of micelles, vesicles, liposomes and microemulsions, all provide unique opportunities to bring other molecules closer together, to orient them in specific way and

to alter their reactivities. Thus, much of the impetus for the study of reactions in micelles, vesicles or microemulsions is that they model, to some extent, reactions in biological assemblies. Normal micelles that form within aqueous surfactant solutions above a surfactant concentration (or a concentration range), usually called critical micelle concentration (cmc), are a topic of major interest due to their unusual physicochemical properties as a result of surfactant aggregation. A complete understanding of the micellization phenomena, its fundamental aspects, use of related studies for technological developments, and understanding molecular behavior require a comprehensive knowledge of the forces and factors controlling the process. One approach that is widely being practiced for the said knowledge has been the study of effect of additives, especially electrolytes, on the micellization characteristics of ionic surfactants. The alteration or modifications of important physicochemical properties of aqueous surfactant solutions is highly desirable as far as potential applications of such systems are concerned.

Hence, it may be recalled that at low concentrations, the aggregates , especially there of changed surfactant are generally round , globular micelles. In some charged surfactant systems, long worm like micelles are formed at higher concentrations upon addition of salt and acid. However, with anions that associate strongly with surfactant cations, such as salicylate , wormlike micelles grow rapidly at low surfactant and salt concentrations. The rheological behaviour exhibited by these systems is viscoelastic analogous to that observed in solutions of flexible polymers. However, wormlike micelles have a more dynamic structures than that of a polymer since the former break and reform reversibly. The rheological behaviour is, therefore, more complex and fascinating. When sheared below a critical shear rate which depends on temperature and on surfactant and salt concentrations, dilute worm like micellar solution shear thin. In contrast, above a critical shear rate, micellar solutions exhibit time dependent behavior, initially the solutions shear thin, and after an induction period shear thickens.

The shape of the micelles depend strongly upon the actual packing parameters in micellar assembly. The counter ion binding suppresses the micellar charge and decrease the surface area per surfactant head group by reducing the electrostatic repulsion between the head groups, thus promoting the spherical to worm like micelle transition. The addition of different types of molecules leads to large deviation of packing parameters. Many counter ions and cosurfactants are strongly adsorbed at the micellar interface, depending on the amount of separation, this may change the mean distance between polar head groups or increase the volume of the micellar core. However, the theory of spherical to worm like micelle transition and the theory of rheological behaviour of the worm like micellar solutions presently lack strongly predictive powers and therefore, it is important to establish a good descriptive data base of systems undergoing the spherical - to -worm like micelle transition.

Keeping the above in view two major focuses of the present study have been fixed. In section A of the thesis, a detail study will be undertaken on the surfactant aggregation in aqueous solutions in presence of additives. Special emphasis will be given to the spherical to rod/worm like micelle transition at low surfactant concentrations, particularly in presence of neutral additives. Rheological and spectroscopic behaviour of the system will also be examined.

The section B of The thesis constitutes physicochemical characteristic of some biopolymer viz, Sodium alginate and Poly (vinyl alcohol) in solution phase. According to hydrodynamics, the specific viscosity of a Newtonian liquid containing a small amount of dissolved material should depend in the first approximation only upon the volume concentration and the shapes of the suspended particles. The unperturbed dimension (UD) of a given polymer in a solvent does not depend on the nature of the solvent, as long as the solvent has no influence on the rotation of the chain segments. This is true in many cases, especially for nonpolar polymer-solvent pairs, but in the cases of polar polymer - polar solvents systems, the unperturbed dimension vary considerably with the nature of the solvent. Most of the polymeric materials are soluble only in a limited

number of primary solvents, but they could be made soluble in all proportions in mixtures consisting of two or more solvents, which may be individually poor solvent for the polymers. Several mixtures of nonsolvents are also known which produce good solvent systems or at least increase the solvency power of primary solvents. Many present and possible industrial applications of high molecular weight polymer arise from unusual properties they induce to their solutions. The study of their solution property is a prerequisite for the development of this modern domain. The characterization of high molecular weight polymers raises a number of problems. Therefore, systematic studies arising from the coupling of different experimental techniques are required for the elucidation of diverse theoretical and experimental aspects. The most important parameters characterizing macromolecular chains in dilute solution are the molecular weight, the mean square radius of gyration and the intrinsic viscosity. Their determination for very high molecular weight polymers opens a large area for discussing, on the basis of different theoretical approximations. The area of discussion includes such subjects as influence of molecular weight and solvent power on concentration domain, theta condition and unperturbed dimensions, chain flexibility in perturbed and unperturbed state, the type of interaction (short range and long range), the conformational characteristics including the transition phenomena influenced by temperature and solvent.

Section-A

π -conjugated systems have been extensively used in advanced applications such as sensors and in electronics . For these applications, π -functional materials are required that are able to form organised supramolecular assemblies of which the properties can be controlled as a function of the self assembly process and the chemical structure. Such a control is important for the improved performance of existing materials and to create new materials with tunable optical and electronic properties. The rational strategy often is to exploit the self assembly of small functional molecules into supramolecular polymers in solution or in the solid state.

Hydrogen bonds (H bonds) are ideal noncovalent interactions to construct supramolecular architectures since they are highly selective and directional. H bonds are formed when a donor (D) with an available acidic hydrogen atom is interacting with an acceptor (A) carrying available non bonding electron lone pair. The strength depends mainly on the solvent and number and sequence of the H bond donors and acceptors. In order to construct a significant amount of desired H bonded assemblies, high association constants are required. In many cases, however, relatively weak H-bond interactions are used so that additional supramolecular interactions are required to obtain nanosized assemblies.

As has been already mentioned, the unfavourable contact between water and the apolar part of surfactant molecules lead to their congregation into well organized entities, viz., micelles, vesicles, fibres, discs and tubes .Although micelles are usually spherical in shape, under certain conditions e.g., concentration, salinity or in the presence of hydrophobic counter ions, etc., they may undergo uniaxial growth. This subsequently results in the formation of significantly long yet highly flexible aggregates referred to as "wormlike micelles (WLM)". The research of WLM has drawn considerable interest because its rheology is very challenging due to the presence of multiple pertinent length scales and stress relaxation mechanisms. This relatively new material has many applications including that of fractured fluids in oil fields, efficient drag reducing agent in hydrodynamic engineering and home care, personal care and

cosmetic products.Viscoelastic WLMs are formed in various surfactant systems , which include mixtures of cationic and anionic surfactants , non-ionic surfactants[24-26], zwitterionic surfactants and ionic surfactants in the presence of different additives. Among the different additives, the hydrotrope, sodium salicylate, is very effective in triggering WLM formation in cationic surfactants even at very low concentrations. Formation of WLM occurs via efficient charge screening of the surfactant head groups and the systems display very fascinating rheological behaviour as well. However, the use of salicylate as the promoter of WLM formation suffers from some limitations, especially in the oil fields due to its complex forming tendency with metal ions impurities. In spite of a large number of publications in the field, WLM formation by metal-inert promoters which may work under salt free condition is rather rare and intensive research in this area is warranted.

In view of the importance of an efficient WLM promoter , which might be effective for various applications at low surfactant concentrations and in the presence of metal ion impurities, organic π-conjugated molecules with H bonding functionality, viz., naphthols are highly promising. Moreover, since the dissociation of hydroxyl groups of naphthols is tunable by controlling the pH of the system, a facile route to design pH- responsive morphology-transition of WLM can be achieved via customized charge screening as a function of pH. This would find application in drug delivery processes. Intensive research for a fundamental understanding of the interaction of a range of hydroxyl aromatic compounds in general, and 1- and 2-napthols in particular, with that of cationic surfactants of different head groups are therefore considered to be important from the practical as well as from the fundamental understanding points of view. Role of these π-conjugated aromatic molecules in the dynamics of the formation of WLMs and their networks is worth investigating.

Viscoelastic wormlike micelles are relatively new materials which have found applications as fractured fluids, drag reducing agents and as model systems to study the basic features of different flow induced phase transitions. In view of the importance

of an efficient WLM promoter, which might be effective at low surfactant concentrations and in the presence of metal ion impurities, organic π –conjugated molecules with H bonding functionality viz hydroxyl aromatic compounds, are highly promising . A detailed study on the physicochemical characteristics of the interaction of these organic systems with micellar aggregates of cationic surfactants under Newtonian flow regime, will be undertaken. The rheological characteristics and microstructures of WLM under non-Newtonian flow regime, and its morphological transition as functions of different parameters including shear, pH and temperature will be examined.

Chapter 3

Studies on microstructural transition of micellar aggregates in presence of hydroxyaromatic compounds: rheology and spectroscopy

3.1. Introduction and Review of Previous Works

The self-assembly of amphiphilic molecules often develops a variety of interesting structures of different shapes and sizes. Among the most fascinating of these are the 'wormlike micelles', which are flexible cylindrical chains with radii of a few nanometers and contour lengths up to several micrometers. The formation of wormlike micelles is linked to the emergence of viscoelasticity in the solution [1,2]. Micellar aggregates that can grow anisotropically under appropriate conditions, changing their shapes from spheres to rods or highly flexible wormlike aggregates, provide some analogies between giant flexible cylindrical micelles and conventional polymeric solutions [3]. However, unlike ordinary polymers, micellar chains posess the unique ability to reversibly break and then recombine. They reform by addition and loss of individual amphiphiles or by the scission and recombination of entire micelles [1]. The polymerlike micelles which are formed by certain ionic surfactants in solution exhibit very interesting rheological properties. At high concentrations, these solutions show typical viscoelastic behaviour while at very low concentrations more complex and unusual rheological phenomena is observed. Wormlike micelles are formed spontaneously at ambient temperature from cationic surfactants with e.g. 16 carbon atoms in the aliphatic chain. This is the case for cetyltrimethylammonium bromide (CTAB) [4-6] and cetylpyridinium bromide (CPB) [7]. Because of electrostatics the transition between spherical to cylindrical aggregates occurs at relatively high surfactant concentrations. However, the growth of the aggregates can be promoted even at lower concentrations of the surfactant if cosurfactants or other low molecular weight additives are incorporated to the solutions. These additives are short alcohol chains, strongly binding counterions, oppositely charged surfactants etc. Some of the different classes of surfactants and cosurfactants/additives which form such structures are given bellow.

A – Surfactant and simple salt. The addition of simple salts such as sodium chloride (NaCl) or potassium bromide (KBr) to ionic surfactant solutions results in

the screening of the electrostatic interactions between the charges, and thus in the growth of the aggregates. Example of this class is CTAB with KBr [8-10]. Halide counterions bind moderately strongly to cationic surfactant aggregates, and therefore, micellar growth is gradual. Other well-known examples are sodium dodecyl sulfate (SDS) with monovalent [11, 12] or multivalent counterions [13,14]. Micellar geometry of the different microstructures formed by amphiphiles in solution can be understood on the basis of a term called the critical packing parameter or CPP, which is defined as as the ratio $v/a_o l_c$ (as has been discussed in chapter 1). The larger the headgroup area (a_o) compared to the tail area (l_c), the more curved the aggregate. Thus, a CPP of ⅓, corresponding to a cone shape, leads to spherical micelles while a CPP of ½ (truncated cone) corresponds to cylindrical micelles. Finally, molecules shaped like cylinders, i.e., having $a_o \approx l_c$ and CPP = 1, tend to assemble into bilayer structures (vesicles). When added to water, CTAB tends to form spherical micelles because the ionic headgroups have a large, effective area due to their electrostatic repulsions. However, when salt is added to CTAB, the added ions screen the repulsions between the cationic headgroups, reducing the headgroup area, and increasing the CPP from ⅓ to ½. As a result, CTAB forms cylindrical micelles that grow uniaxially into long chains.

B – Surfactant and cosurfactant. where the cosurfactant is a short alcohol chain. Classical examples are the ternary systems of sodium alkylsulfate-decanol- water (Sodiumdecylsulfate -Decanol [15,16], Sodiumdodecylsulfate-Decanol [17,18] and Cetylpyridinium Chloride-hexanol-brine (CPC-Hex) [19,20]. In these systems, the ratio between the alcohol and surfactant concentrations controls the polymorphism of the self-assembly. The theoretical arguments developed for neutral chains should apply to this class, namely those for which the cylindrical aggregates are intermediate structures between spheres and bilayers.

C – Surfactant and strongly binding counterion. Strongly binding counterions are small molecules of opposite charge with respect to that of the surfactant. They are also called hydrotopes. Well-known examples of hydrotopes are salicylate, tosilate and chlorobenzoate counterions, which all contain an aromatic phenyl group. CTAB and CPC with sodium salicylate (NaSal) have been probably the most studied micellar systems during the last two decades. Contrary to simple salts (class A), a large proportion of these counterions (~ 80 %) is assumed to be incorporated into the micelles. It was found that in CPC-NaSal, long wormlike micelles are immediately formed at the cmc (0.04 wt. %), without passing through an intermediate spherical morphology [21, 22].

D – Cationic and anionic mixtures. Oppositely charged surfactants have shown synergistic enhancements of rheological properties, and notably through the formation of mixed wormlike micelles. The growth of the micelles is assumed to arise from the charge neutralization of the surface potential (as in C) and from the related increase of the ionic strength (as in A). Recent examples are the mixtures of sodium dodecylsulfate (SDS) and dodecyltrimethylammonium bromide (DTAB) [23,24], or the mixtures made from cetyltrimethylammonium tosilate and sodium dodecyl benzenesulfonate [25,26].

That surfactant solutions can be strongly viscoelastic was noticed by several authors in as early as 1950's. Nash for instance identified the role of additives such as naphtalene derivatives in the onset of viscoelasticity in CTAB solutions [27]. One intriguing result was that the viscoelasticity of the solution was showing up well below the cmc of the surfactant. Some years later, Gravsholt and coworkers recognized that other types of additives, such as salicylate or chlorobenzoate counterions are actually solubilized by the micelles, lowering the c.m.c. of the surfactant [28,29]. It was suggested by the authors that the viscoelasticity had the same physical origin as that of polymer solutions [30].

A step further in the description of the micellar dynamics was made by the first quantitative measurements of the linear mechanical response, also known as

Maxwellian Behaviour, of these solutions. The pioneering works in this field were those of Rehage and Hoffmann [31-33], Shikata [34-37] and Candau [38,39] and their coworkers. Rehage and Hoffmann had used rheology to demonstrate that the micellar growth resulted in an increase of the fluid viscosity. They observed that the effect of addition of NaSal to CPC increased the viscosity of the system sharply until the concentration reached slightly above a 1:1 molar ratio of CPC/ NaSal and then the viscosity dropped off drastically. This feature was observed for several concentrations of CPC and there does not seem to have any satisfactory explanation of this phenomenon until this date. The most fascinating result that Rehage, Hoffmann, Shikata and Candau and their coworkers have observed by quantitative measurements was that the viscoelasticity of these surfactant solutions was characterized by a single exponential response function. This rule is indeed so general that it is now commonly admitted that a Maxwellian behavior is a strong indication of the wormlike character of self-assembled structures. In a detailed study of the tetradecyltrimethylammonium salicylate system, they also reported that an increase in flow birefringence accompanies the stress growth. Actually, both the stress and flow birefringence curves show an induction period before rapid growth commences. In addition to the general features as described, the induction time is shown to be inversely proportional to the applied shear rate and is independent of the flow direction. On the basis of this information, a kinetic coagulation mechanism, first introduced by Rehage, Wunderlich and Hoffmann [31] was proposed to account for the rheopectic phenomenon. According to this model, the initial small micelles collide with each other more frequently in shear flow than in quiescene, resulting in the formation of large micelles. The same results are also obtained when the influence of sodium salicylate and sodium bromide concentration on the shear thickening behaviour of aqueous micellar solutions of CTAB and NaSal is studied experimentally.

The effect of Sodium 3 hydroxy 2 naphtoate (3,2 SHCN) on the micellar shape transition of CTAB was investigated by Manohar and co workers [40-47]. The 3,2 SHNC which is structurally comparable to NaSal is strongly adsorbed on

the micellar surface with the carboxylic and hydroxyl group protruding out of the micelle. The presence of naphthalene ring in HNC^- was expected to confer more hydrophobicity on the molecule as compared to NaSal. It was also proved from surface tension measurements that SHCN is mildly surface active and considering the concentrations for such surface activity, it could be regarded as a hydrotope. The molecular orientation is consistent with the surface active nature of SHNC (compared to NaSal). However, the CTAB-SHNC system differs in a major way from CTAB-NaSal system through the presence of a sequence of phases viz., small micelle aggregates, an isotropic gel phase (non-birefringent rodlike micelle, L_1-Phase), anisotroic liquid crystal (birefringent Lamellar, L_α-Phase) -precipitate-liquid crystal etc. Recently Raghavan and co-workers have shown that when a mixture of a cationic surfactant with an erucyl (C_{22}, mono-unsaturated) tail and an organic salt, sodium hydroxynaphthalene carboxylate (SHNC) is heated their zero-shear viscosity, instead of dropping exponentially, increases over a range of temperatures [48-50]. Using small angle neutron scattering (SANS) technique, these authors, have shown that the increase in viscosity is caused by an increase in the contour length of cylindrical micelles.

In this chapter the effects of neutral 1- and 2-naphthols and also the dihydroxy derivatives, 2,3- dihydroxynaphthalene (2,3-DHN) and 2,7-dihydroxynaphthalene (2,7-DHN), on the shape transition of CTAB micelles have been studied. The intermolecular H bonding between OH groups of micelle embedded naphthol molecules and the interfacial water molecules plays a key role in micellar shape transition in absence of any charge screening of head groups and thus imparts strong viscoelasticity to the dilute aqueous surfactant solution.

Since the effect of hydrogen bonding on the electronic spectra of organic molecules has been unambiguously detected and explained, the ultraviolet and visible spectroscopies are applied by a number of authors to study the hydrogen bond in solution. Investigation of the effect of hydrogen bonding on photodissociation of 1-naphthol was reported first by Takemura et. al. [51,52].

The ground state (UV-Vis absorption) and the excited state (fluorescence) solvatochromism of several naphthalene derivatives was analysed by Mataga and Kaifu [53] in terms of nonspecific solute-solvent interactions and specific hydrogen-bonding interactions. The influence of hydrogen bonding on the UV-Vis and emission spectra of naphthols has been studied by Baba and Suzuki [54] and Tramer and Zaborowska [55]. Switching of the lowest excited states of 1-naphthol, from ^1L_b state to ^1L_a state, as a result of better stabilisation due to hydrogen-bond interactions was suggested. While such studies on phenols and naphthols have been carried out in the presence of a variety of polar proton acceptor or donor solvent components in an inert solvent (or mixed solvents), similar investigations in organised media (micelles and vesicles) are scarce. Compared to a single solvent or a homogeneous mixture of solvents, organised assembly of nano dimensions possess many unique properties. The most significant property of an organised assembly is its ability to stabilise and bind solute molecules that are typically insoluble or sparingly soluble in bulk pure solvent [56]. Therefore, a detail investigation on the electronic spectra of indicator (probe) molecules in organised assemblies of CTAB, in particular and other alkyltrimethylammonium bromides in general, have been carried out to understand the mechanism of the phenomena of microstructural transitions in further detail.

The possibilities of the H bonding and π-π interaction in naphthols have been checked by observing the effect of CTAB micelles on the absorption spectrum of the hydroxyaromatic compounds. UV absorption spectra are modified due to the presence of an intermolecular H-bond of micelle-embedded naphthols with the interfacial water in their ground electronic states. The excited state proton transfer (ESPT) of 2-naphthol is facilitated in the presence of CTAB in the submicellar concentration range due to the catalytic effect of surfactant charge, whereas ESPT is hindered in post-micellar concentrations due to lack of water accessibility [57]. However, the exact nature of H-bonding in the micellar phase is not understood completely. Moreover, together with hydrogen bonding, the π-π and cation-π interactions between favorably arranged micelle-embedded

dopant molecules may also be involved in modifying the absorption spectra [58]. Therefore, in order to further examine the exact nature of the noncovalent interaction that is involved in the above modification of the spectra, it is tempting to check what would happen if the hydroxyl group of the promoter naphthol molecules is replaced by methoxy groups. Methoxynaphthalenes (MN) possess a similar structure and hydrophobicity to that of the hydroxyl naphthalene (HN) molecules but cannot act as hydrogen bond donors. It would be interesting to compare the efficiency of methoxynaphthalene with that of naphthols in effecting microstructural transitions of micelles and to discuss the result in the light of spectroscopic observations. Further, it may be anticipated that a simple and effective route to design a pH responsive microstructure could well be based on the neutral naphthol dopants, which form salts only at high pH ($pKa > 9.2$). As a function of pH, ionization of the OH group of naphthol molecules may switch the onset of charge screening, paving the way to effect further morphological transitions (viz., vesicle formation). An objective of the present work is, therefore, to design a simple effective route of pH-responsive morphological transition for the aqueous molecular aggregates of single chain cationic surfactant, viz., CTAB from micelles to long wormlike micelle to unilamelar vesicles. Finally, it is important to note that although the last two decades have witnessed a strong excitement among the researchers on the microstructural transitions of micelles at low concentrations, induced by hydrotropes like sodium salicylate and other similar dopants, leading to stimuli-responsive viscoelasticity, the exact role and the location of the protruded polar groups (e.g., OH groups) of the hydrotropes toward the Stern layer have not been firmly ascertained. This is particularly an interesting basic element to investigate for the present system where intermolecular H-bonding through OH groups of the micelle-embedded naphthols seems to play the pivotal role in the transition of the micellar morphology.

The formation of wormlike micelles have been studied for various type of surfactants in recent years, and new applications have been found in different areas from oil fields, drag reducing agents in district heating systems, home and personal care products to templates for asymmetric and aligned nanostructures.

Viscoelastic wormlike cationic surfactants have been successfully used as fracturing fluids in oil fields. Conventional polymer base fluid has comparable sand pack pore size residue left in reservoirs after fracturing. This reduces the fracturing permeability or conductivity. Surfactants, however, being small molecules, recovers back completely. Wormlike micelles are used commercially in district heating and cooling fluid as drag-reducing agents. The environmental friendly drag-reducing properties of N-alkyl, N, N-dimethylglycinate combined with sodium alkylbenzene sulfonate at a 4:1 molar ratio was found useful for such applications [59,60]. Viscoelastic property is needed in many home care products and microfluidity of wormlike micelle has such properties. A typical example of such application is hard surface cleaners and drain-opener liquid plumber, where the excellent thickening and cleaning capacity combined with easy flow and drag reduction properties have distinct advantages over other microscopic fluids such as lamellar or polymeric fluids. New applications should appear as our understanding increases and more and more application scientists understand the wormlike micelle system.

3.2 Materials and Methods

1- and 2-Naphthols (puriss, Aldrich) were purified by vacuum sublimation followed by crystallization from 1:1water methanol mixture. 1- and 2-Methoxynaphthalenes (Acros-Organics, Belgium) were recrystallized from 1:1 aqueous methanol before use. 2,3-dihydroxynaphthalene and 2,7-dihydroxynaphthalene were recrystalised twice from ethanol-water mixture and finally from ethanol alone. The structure of dopant molecules (probe) are shown in figure 3.1. All the probe molecules were stored in the dark. The surfactants viz.,

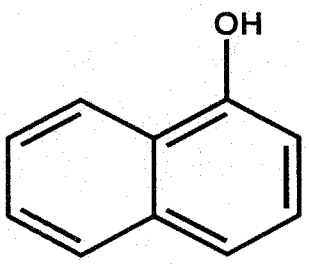

1-Naphthol

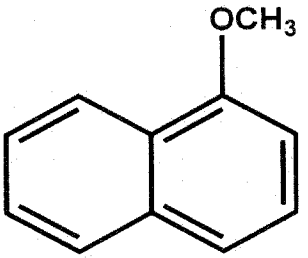

1-Methoxynaphthalene

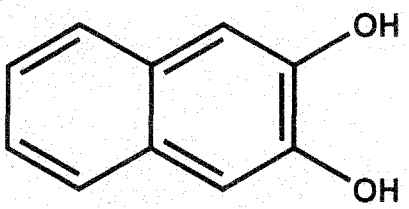

2,3-Dihydroxynaphthalene

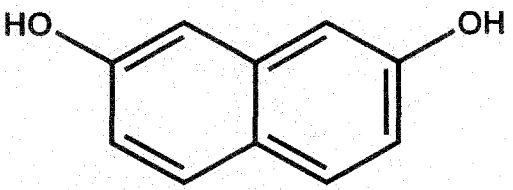

2,7-Dihydroxynaphthalene

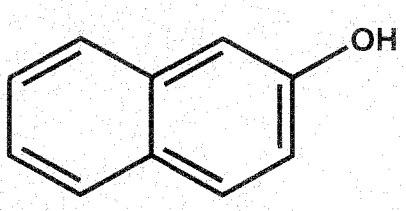

2-Naphthol

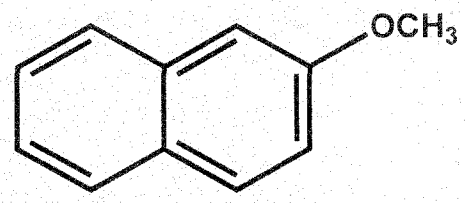

2-Methoxynaphthalene

Figure 3.1: Structures of the aromatichydroxy and methoxyaromatic dopants used in the present investigation.

Dodecyltrimethylammonium bromide (DTAB), Tetradecyltrimethylammonium bromide (TTAB), Cetyltrimethyl-ammonium bromide (CTAB) and Sodiumdodecyl sulphate (SDS) were of puriss grade procured from Aldrich and were used as received. Shear-induced viscosity was measured on a rotational viscometer (Anton-Paar, DV-3P; accuracy (1% and repeatability (0.2%)) equipped with a temperature controller and with the facility of varying shear rates. Here, the viscosity measurement is based on measuring the torque of spindle rotating at a given speed in the sample solution kept in a concentric cylinder, which is maintained at a constant temperature. The temperature of the viscometer was

regulated with a water circulating thermostat. The diameter and length of the inner cylinder are 2.5 cm and 9 cm respectively, whereas diameter and length of the outer cylinder are 2.8 cm and 14 cm respectively. The shear rate is calculated as rpm x 1.2236 s^{-1} (assuming the characteristics of the spindle). UV absorption spectra were recorded on a Jasco (V-530) Spectrophotometer using a matched pair of glass cuvettes. The instrument was attached with a water circulating thermostat. ^1H NMR spectra were recorded on a Bruker spectrometer (Germany) operating at 300 MHz. The water used for preparation of solutions was doubly distilled. The dopants (probes) were sparingly soluble in water at low pH but highly soluble in surfactants. Therefore, appropriate amount of the dopants were added directly to CTAB solutions. In some experiments dilute alcoholic solution of the dopants were used and alcohols were dried off before the addition of surfactant in the experimental set. Utmost care was taken to prepare naphthol-CTAB and other hydroxyaromatic dopant-CTAB solutions with minimum shaking. For the shear induced viscosity studies, the samples were equilibrated at desired temperatures in a thermostat (attached to the rotational viscometer) for 2 days before study.

3.3 Results and discussions

3.3.1 Shear Induced Viscosity Studies

Aqueous CTAB (2-10 mM) and 1- or 2-naphthol (2-10 mM in 2-5% methanol, naphthols being sparingly soluble in water) solutions show viscosities similar to those of water. But as soon as these solutions are mixed together at room temperature, a thick gel-type fluid with high viscoelasticity is developed. Since viscoelasticity tends to disappear in high methanol concentrations, experimental solutions are prepared routinely by transferring the required amount of naphthol solutions (in pure methanol) in the experiment vial first, and then the alcohol was evaporated off completely before the addition of aqueous surfactant solution. From the initial visual observation it was found that the viscosity of the gel was very much dependent on the concentration of CTAB and the additives. Therefore,

we first determined the CTAB/dopant mole ratio at which the gel shows maximum viscosity. Much like the CTAB-NaSal system,

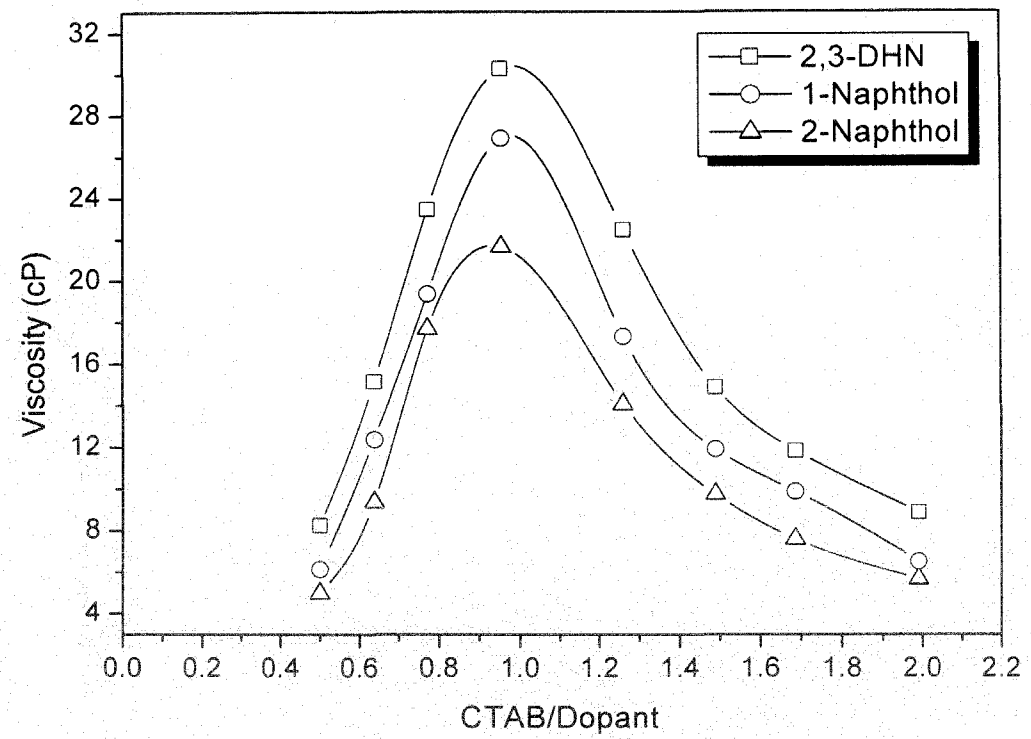

Figure 3. 2: Variation of viscosity as a function of mole ratio of CTAB and the dopants that form viscoelastic gels.

naphthols also display maximum viscoelasticity at a 1:1 molar ratio of surfactant and the promoter (figure 3.2). On the other hand, the effect of the dihydroxynaphthalenes (2,3-DHN and 2,7-DHN) on micelles of CTAB are interesting. Equimolar mixtures of only CTAB and 2,3-DHN gives a highly viscous gel in aqueous solutions but 2,7-DHN/CTAB does not. Therefore further attempts were not made to study the viscosity of 2,7-DHN/CTAB system. The argument that an excess or deficiency of charge on the micelles due to adsorption of hydrotrope anions (e.g., NaSal) would shorten the micellar life time and size is not apparently true for the present system because under the present experimental condition of solution pH (~6.5), the naphthols and the dihydroxynaphthalenes are mostly protonated, i.e., uncharged (p*Ka*'s > 9.0). Therefore, it seems apparent that the symmetrical distribution of surfactant and the promoter molecules, leading to highly compact spherical micelles, facilitates to attain an

optimum surface curvature in presence of H bonding (discussed later), and this results in the sphere to rod transition easily. For further experiments, dopant to surfactant ratio was chosen to produce strongest viscoelasticity, i.e., 1:1 mole ratio. At low concentrations (<1 mM), CTAB-naphthol solutions show shear thinning properties, typically observed in the case of a non-Newtonian fluid. Typical plots of viscosity against shear rate for 1- and 2-naphthols in CTAB solutions are shown in figures 3.3 and 3.4 respectively. Increasing the concentration range from 1 mM to 2 mM, the system shows a shear thinning property up to a shear rate of 25 s^{-1} and then the shear thickening phenomenon starts to occur, but above a shear rate of 60 s^{-1}, the fluid shows a Newtonian type behavior (figure 3.5 and 3.6). However, an overall non-Newtonian nature is apparent as the concentration of the CTAB and naphthol (1:1) system is raised above 1.0 mM. At still higher concentrations (>5.0 mM), the nature of the rheological response changes dramatically and the system starts displaying an unusual rheology as a function of shear rate. The variation of viscosity of CTAB/1-naphthol system as a function of shear rate at two different concentrations, 5.0 mM and 7.5 mM (1:1) is shown in figure 3.7. Up to a shear rate of 60 s^{-1}, the fluid shear thins. An onset of viscosity rise is observed at the shear rate of 60 s^{-1}, and the system again shear thins, passing through a maximum at 109 s^{-1}. At further higher concentrations (7.5 mM), the viscosity-shear rate profile again changes feature; the initial shear thinning characteristics disappear. The overall behaviour is consistent with building up of long worm-like micellar bundles at relatively high concentrations. Therefore, it appears that the shear thinning viscosity in low shear rates is indicative of the flow-induced alignment toward the flow directions. Equal concentrations of 2-naphthol/CTAB systems show similar features in the viscosity-shear rate profile (figure 3.8); the maximum viscoelasticity being displayed at 100 s^{-1}. Meanwhile, when the CTAB concentration is above 10.0 mM in the equimolar CTAB/naphthol solutions, the micelles are much longer and entangled with each other in

the solution. In this case, the shear viscosity increases much higher and the micellar solution behaves like entangled polymer solutions exhibiting typical nonlinear viscoelastic behavior such as a stress plateau. The contour length of the worm-like micelles is highly dependent on the concentrations of the surfactant and the promoter. The viscosity shear rate profile for the 2,3-DHN/CTAB systems are shown in figures3.9 to 3.11. The rheological characteristics shown by this system is almost similar to those of the CTAB-naphthol systems. Systems which display shear induced nonlinear rheological changes (as the present systems) bring about formidable problem in measuring the unperturbed solution viscosity because, the measuring techniques

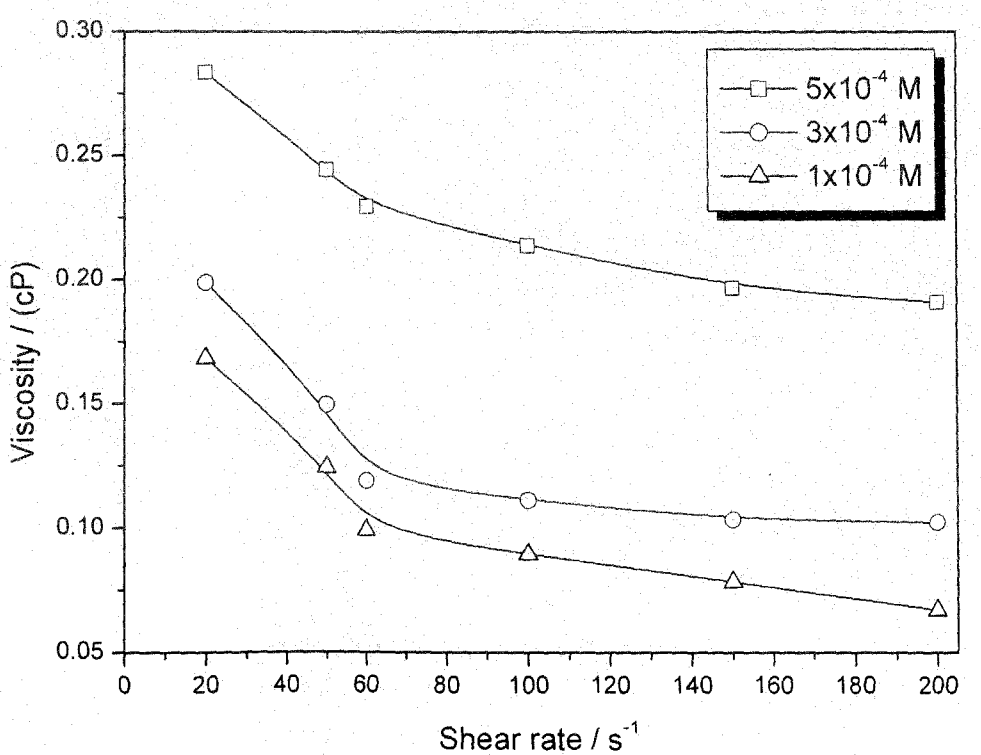

Figure3.3: Variation of viscosity of 1-naphthol/CTAB system as a function of shear rate at different molar ratios.

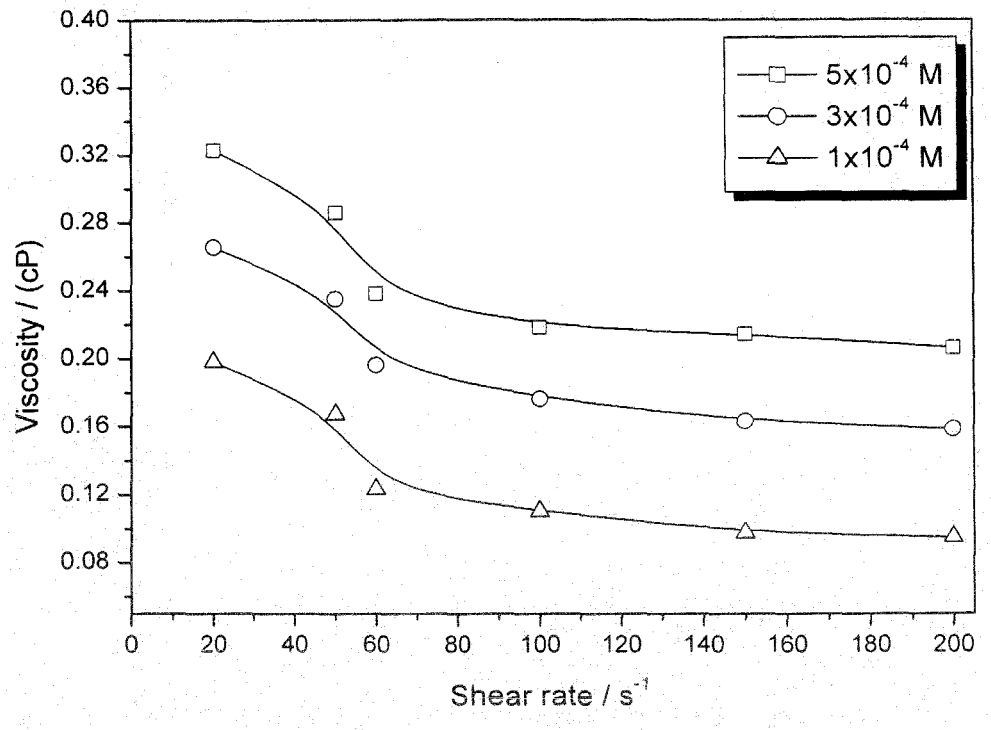

Figure 3.4: Variation of viscosity of 2-naphthol/CTAB system as a function of shear rate at different molar ratios.

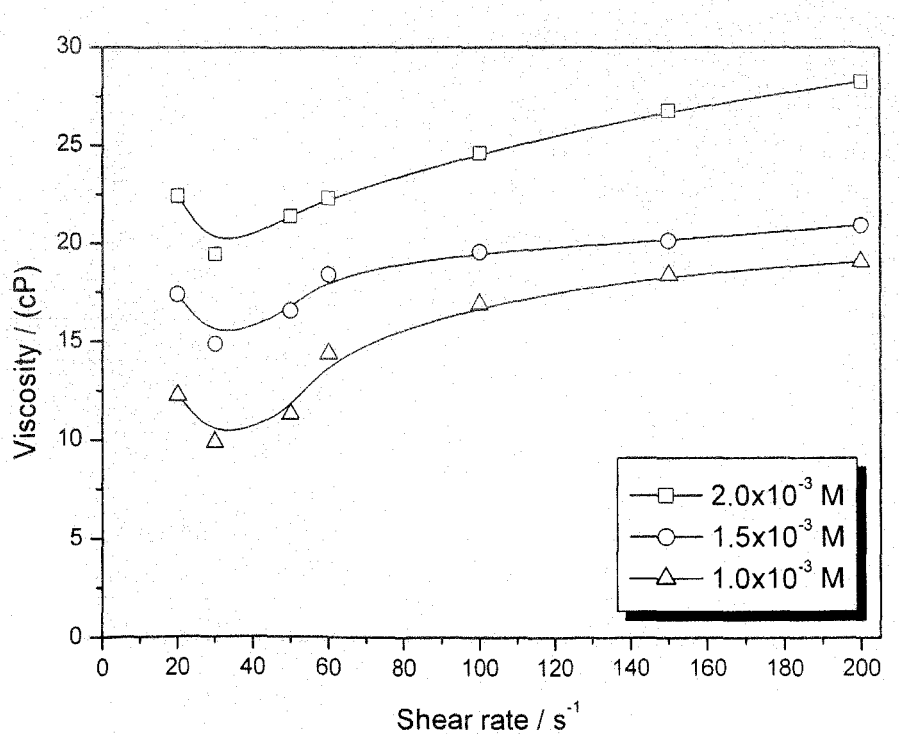

Figure 3.5: Variation of viscosity of 1-naphthol/CTAB system as a function of shear rate at different molar ratios.

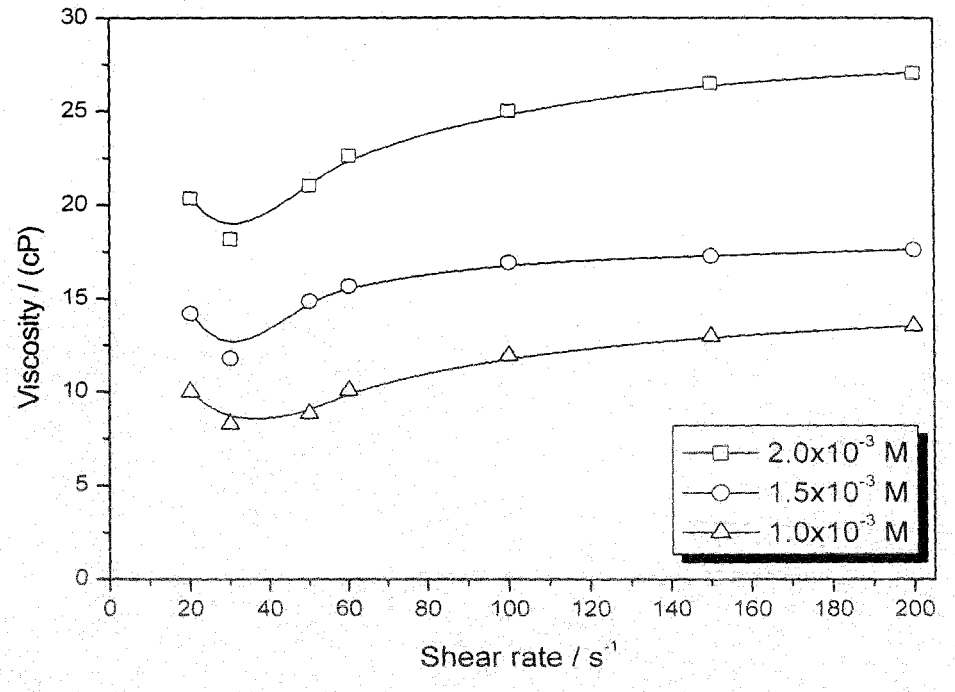

Figure 3.6: Variation of viscosity of 2-naphthol/CTAB system as a function of shear rate at different molar ratios.

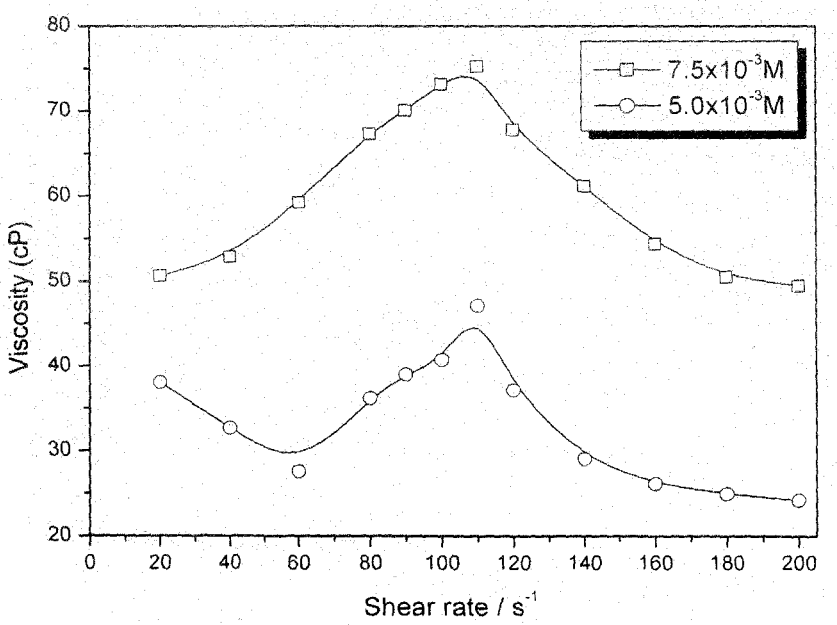

Fig ure 3. 7: Variation of viscosity of 1-naphthol/CTAB system as a function of shear rate at different molar ratios.

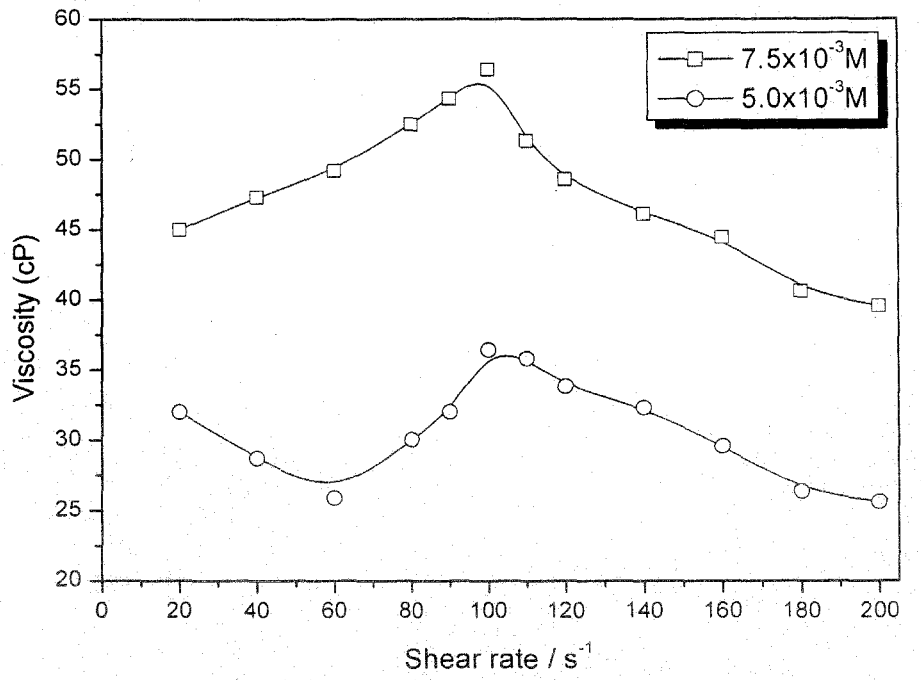

Figure 3.8: Variation of viscosity of 2-naphthol/CTAB system as a function of shear rate at different molar ratios.

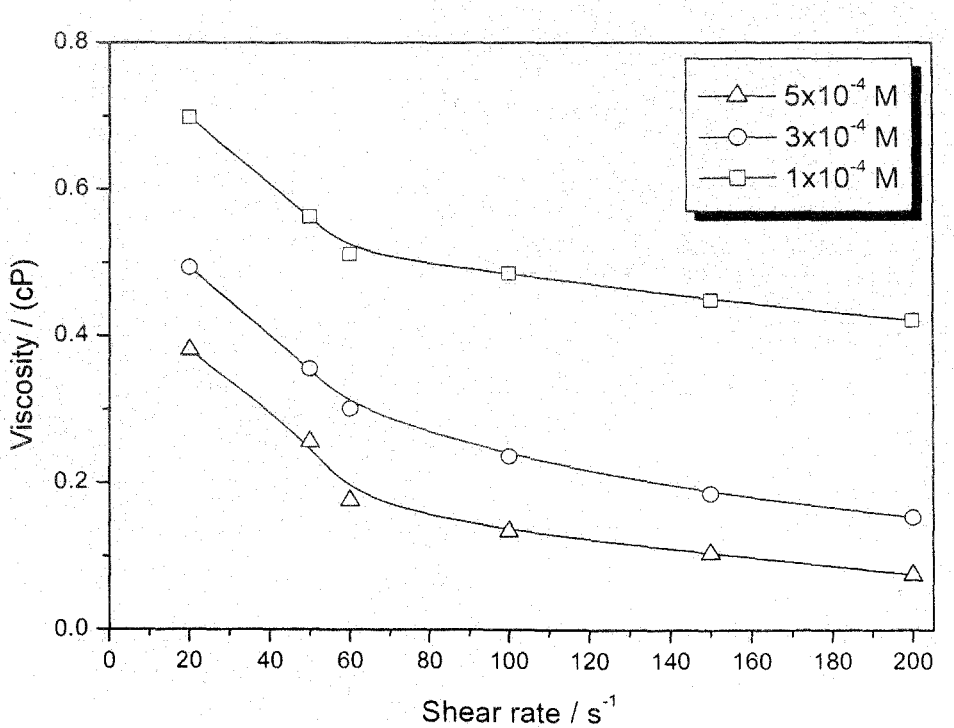

Figure 3.9: Variation of viscosity of 2,3-dihydroxynaphthalene/CTAB system as a function of shear rate at different molar ratios.

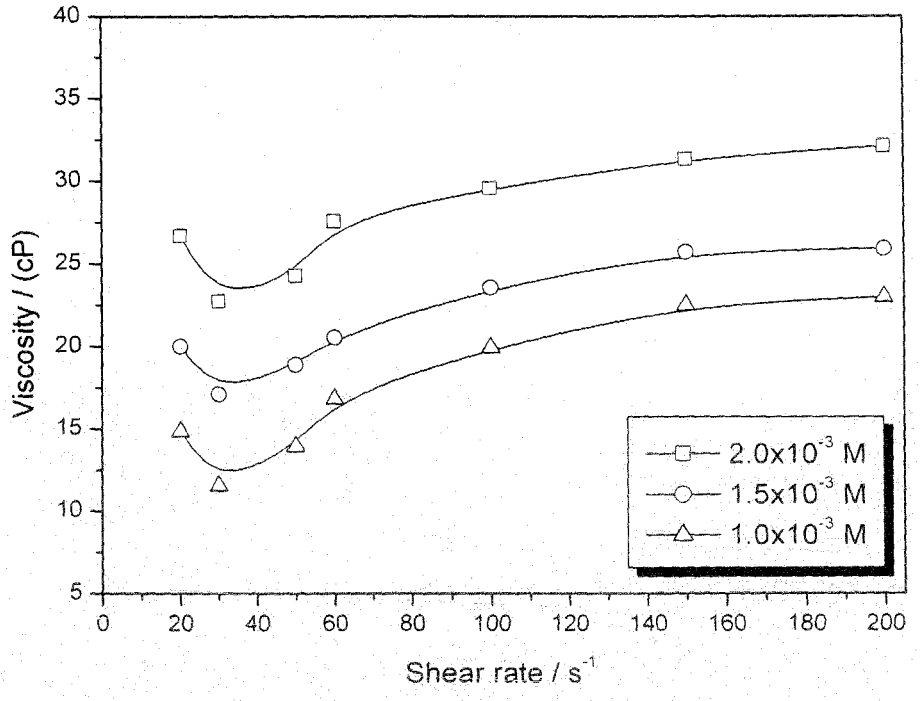

Figure 3.10: Variation of viscosity of 2,3-dihydroxynaphthalene/CTAB system as a function of shear rate at different molar ratios.

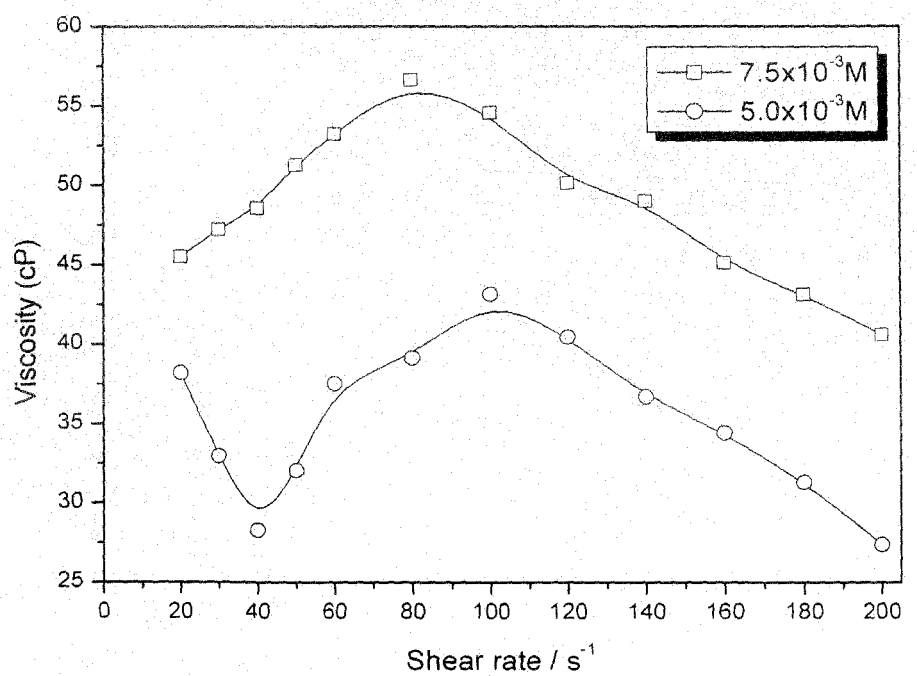

Figure 3.11: Variation of viscosity of 2,3-dihydroxynaphthalene/CTAB system as a function of shear rate at different molar ratios.

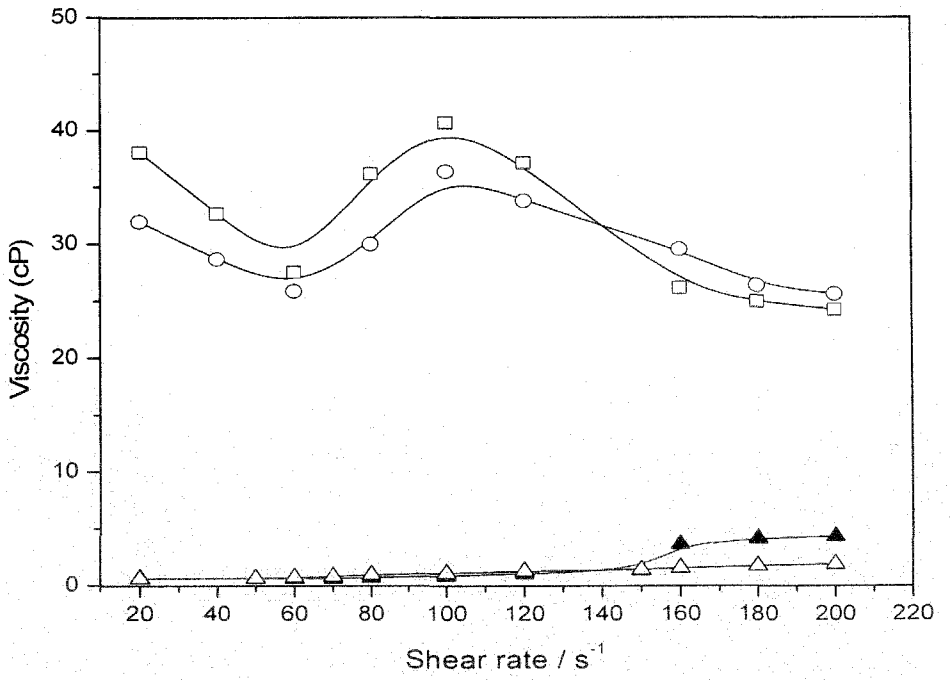

Figure 3.12: Comparision of viscosity modification of aqueous CTAB by 1-methoxy-naphthalene (Δ), 2- methoxynaphthalene (▲), 1-naphthol (□) and 2-naphthol (O) at 25°C. The concentration of the dopant and the surfactant was fixed at 5 mM (1:1).

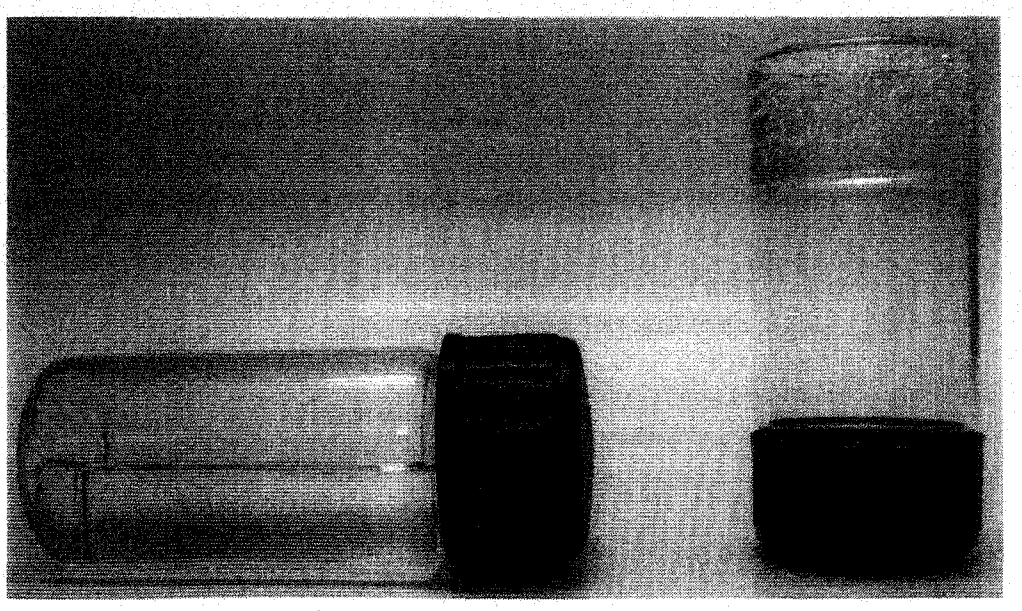

Figure 3.13: Photographs of the viscoelastic-gel (right) of aqueous 1-naphthol/CTAB (0.1 M, 1:1) and free flowing 'water like' solution (left) of 1-methoxy-naphthalene/CTAB system (0.1 M, 1:1).

(e.g., torsional shear rheometry) often apply considerable stress on the system during measurement, and thus the zero-shear viscosity becomes obscure.

The methoxynaphthalene-CTAB systems (1-methoxynaphthalene/CTAB and 2-methoxynaphthalene/CTAB), on the other hand, neither display the ability to develop viscoelasticity in the system nor exhibit any viscosity modification with applied shear, and behave completely like a Newtonian liquid. This result is quite surprising in view of the fact that much like 1- and 2-naphthols, both 1- and 2-methoxynaphthalenes are expected to embed into the micelles of CTAB. The plot of viscosity against shear rate for both the methoxynaphthalenes are shown in figure 3.12. For comparision the values of the naphthols at similar concentrations and conditions are also included in the figure. The images of the naphthol/CTAB and methoxynaphthalene/CTAB systems at 25°C are shown in figure 3.13. Though methoxynaphthalenes (MN) possess similar structure and hydrophobicity to that of the hydroxynaphthalene (HN) molecules but because the methoxynaphthalenes cannot act as hydrogen bond donors, they fail to assist the micellar shape transition and can not impart viscoelasticity to the CTAB solution. The exact role of hydrogen bonding in micellar shape transition has been discussed later in the light of spectroscopic observations.

3.3.2 Effect of Temperature

Typically, when a wormlike micellar solution is heated, the micellar contour length decays exponentially with temperature. At higher temperatures, surfactant unimers can move more rapidly between the cylindrical body and hemispherical end cap of the worm (the end cap is energetically unfavorable over the body by a factor equal to the end-cap energy). Thus, because end-cap constraint is less severe at higher temperatures, the worms grow to a lesser extent. However, an opposite trend in the rheological behavior is observed in CTAB-naphthol systems. Plots of viscosity against temperature, at shear rates of 35, 70, 120 and 200 s^{-1} for 1-naphthol, 2-naphthol and 2,3-dihydroxynaphthalene in presence of CTAB solutions are shown in figures 3.14-3.16. Instead of a decrease in viscosity, it is increased with temperature steadily up to a critical temperature value (26°C for

CTAB-naphthols) and then decreases. This transition as a function of temperature is reversible, i.e., if the temperature is lowered down from a high value, viscosity of the system follows the same viscosity-temperature profile. This observation is unusual, and the only example of this kind is found in a recent reference where wormlike micelle formation was promoted by sodium salt of hydroxynaphthalene carboxylate (SHNC) [48]. The micellar growth in the above systems is attributed to a desorption of weakly bound HNC counterions from the micelle at elevated temperatures. Such a desorption is believed to reduce the charge density at the micellar interface and thereby promote the growth of cylindrical structures. However, any explanation emphasizing charge screening of surfactant head groups by the added salt anions as has been put forward in above experiments is not applicable to the present system. On the other hand, hydrophobic interaction between micellar core and the aromatic ring of the dopant molecules seems to be an important factor, which imparts the thermoreversible viscoelastic property to the present system. As temperature is increased, naphthol molecules (uncharged) are more soluble and perhaps are partitioned more strongly in the micellar phase.

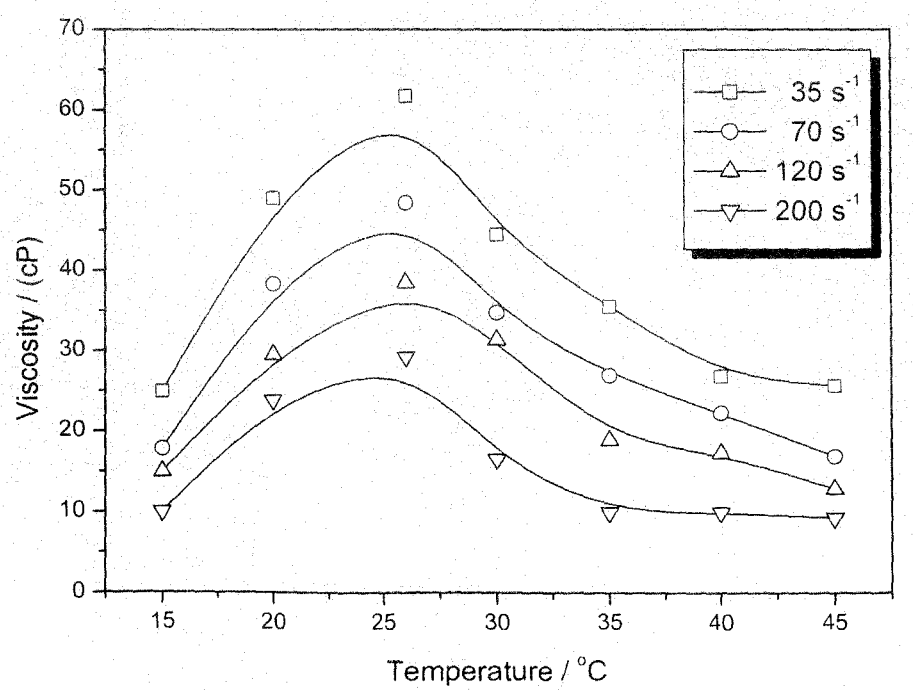

Figure 3.14: Variation of viscosity of 1-naphthol/CTAB system (10 mM; 1:1) with temperature at different shear rates.

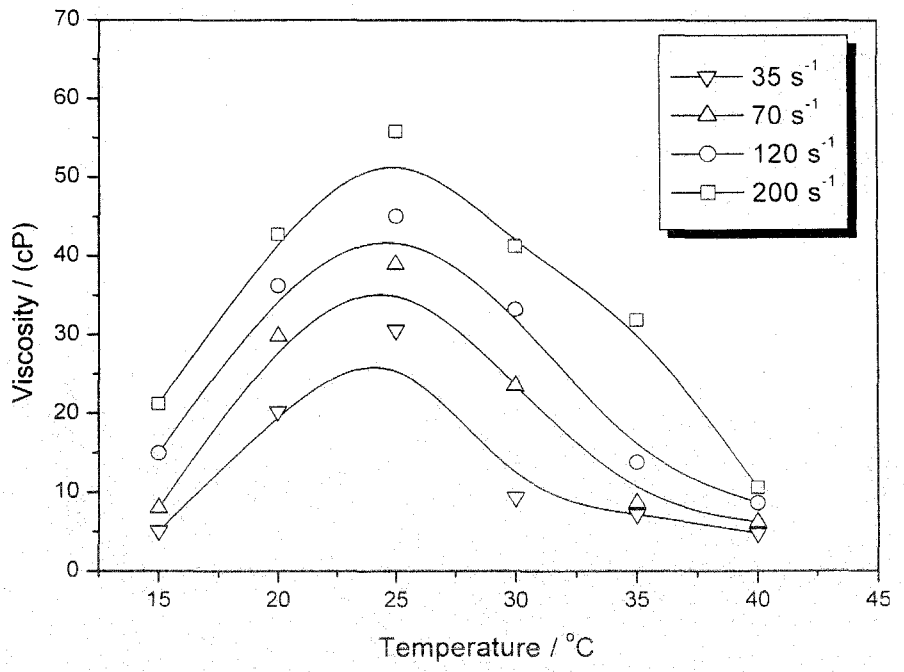

Figure 3.15: Variation of viscosity of 2-naphthol/CTAB system (10 mM; 1:1) with temperature at different shear rates.

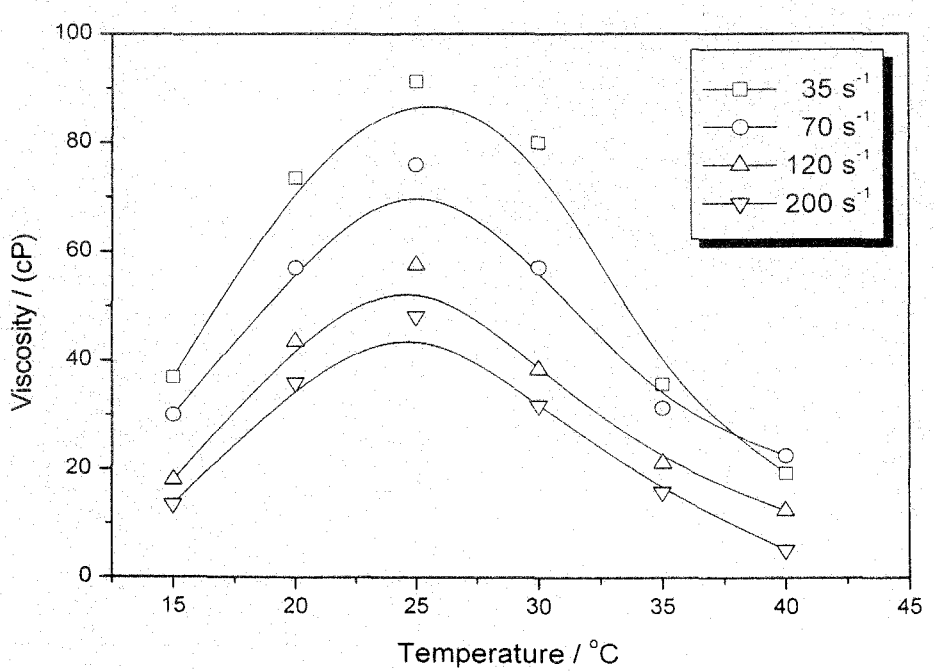

Figure 3.16: Variation of viscosity of 2,3-dihydroxynaphthalene/CTAB system (10 mM; 1:1) with temperature at different shear rates.

This favors the formation of longer wormlike micelles up to the critical temperature, above which the increased kinetic energy allowing surfactant unimers to hop more frequently between the body and the end cap results in the breaking up of the wormlike micelles [48].

3.3.3 Shear-Induced Viscosity and pH

The role of neutral hydroxyaromatic dopants, viz., 1- and 2-naphthols, which are found to be efficient in bringing about microstructural transition in CTAB micelles, stimulates the idea of designing a route for pH-responsive vesicle formation [57]. This idea stems from the fact that the dopants, which under neutral conditions activate the formation of worm-like micelles at pH ~5.0, may on partial ionization of the OH group increase the packing parameter further via charge screening [61]. This idea tempted the investigator to study the pH dependent viscosity changes of the present viscoelastic gel system. Figures 3.17 and 3.18 shows the viscosity-pH profiles of the 1-naphthol-CTAB and 2-naphthol-CTAB systems at constant shear of 122 and 184 s^{-1}, respectively. The general nature of the variation of viscosity as a

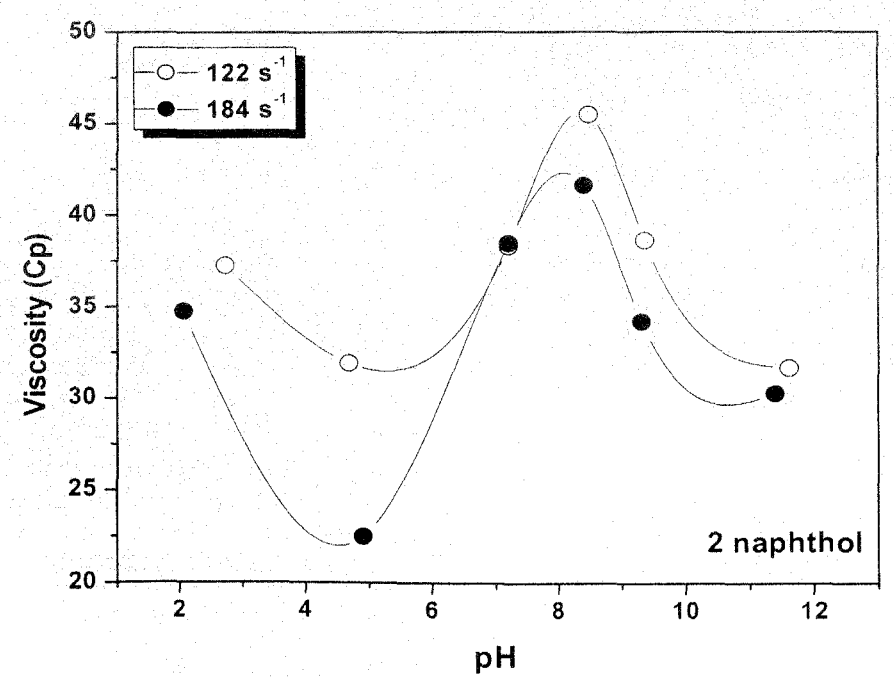

Figure 3.17: Viscosity vs pH profile for 2-naphthol/CTAB systems at fixed shear rates of 122 and 184 s^{-1}.

function of pH for both 1- and 2-naphthol-CTAB systems is similar in high shear regime (viz., 122 and 184 s^{-1}, respectively). However, morphological responses are not identical for both of the systems. While the viscosity of both, 2- as well as 1-naphthol-CTAB systems, is quite high (35-45 cP) due to formation of long worm-like micelles at low pH, the viscosity of the former system falls initially, indicating formation of shorter micelles until pH ~5.0 is reached. Charge screening by the anions from the added acid may be responsible for this observation. On the other hand, for 1-naphthol-CTAB, the onset of viscosity rise as a function of pH is found to occur from very low pH (pH ~2.0). For 2-naphthol-CTAB, the onset of viscosity rise is observed at higher pH (>5.0) and the viscosity-pH profile passes through a maximum at pH ~8.5. The onset of viscosity rise is observed due to the partial titration of OH group, leading to charge screening of surfactant head groups by the naphtholate anion and at pH ~8.5 the worm-like micelles grow maximum. Additional increase in pH results in the ionization of OH group further, and the packing parameter probably exceeds the critical value of 1/2 via enhanced charge screening, leading to vesicle formation (for naphthols, p*K*a > 9, which means 50% ionization of the OH group at pH ~9.0).

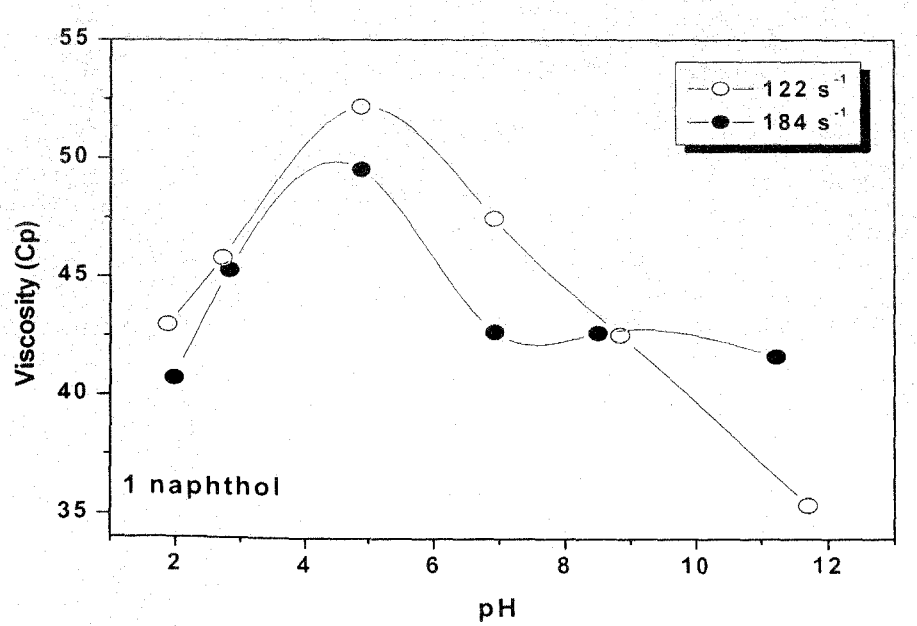

Figure 3.18: Viscosity vs pH profile for 1-naphthol/CTAB systems at fixed shear rates of 122 and 184 s^{-1}.

This results in the fall of viscosity of the system. Since 1-naphthol could modulate the micellar surface curvature of CTAB more efficiently, a little dissociation of the OH group (at low pH range) leads to an appreciable decrease of surface curvature via charge screening and promotes long worm-like micelle formation. In fact, for the 1-naphthol-CTAB system, vesicles start to form even at slightly higher than pH ~5.0 (Figure 3.18). A simple and effective route to design pH responsive viscoelastic worm-like micelles and less viscous globular vesicles based on naphthol dopants may be tuned by controlling the degree of charge screening of CTAB micelles via controlled ionization of naphtholic OH groups. The result of pH-responsive morphology modification is further investigated by means of cryo-TEM (discussed later).

3.3.4.1 ^{1}H NMR study

To ascertain the location and orientation of the additive naphthol molecules in the micelles and to understand the nature of interaction in micellar shape transitions, ^{1}H NMR experiments may be helpful along with the absorption spectroscopies. NMR spectrum of 2-naphthol in D_2O (in absence of CTAB) shows clusters of signals centered at δ values of 7.850 and 7.382, respectively, due to the resonance of the aromatic ring protons (figure 3.19 a). These two sets of signals are shifted upfield, broadened, and merged to give two broad signals at δ values of 7.337 and 6.991, respectively, when D_2O solution of CTAB and naphthols are mixed in 1:1 molar ratio (1.0 mM; Figure 3.19 b). This large shift of aromatic proton resonance to low δ values clearly indicates the location of naphthol rings in the less polar environment than that of water. Previous studies with CTAB-NaSal system also showed similar upfield shift of proton resonance of the aromatic moiety of NaSal molecule, and it was argued that this was due to insertion of Na Sal molecules into the micelles [50]. On the other hand, CH_3 protons of CTAB head group and the adjacent CH_2 protons, which resonate at 3.132 and 3.289, respectively, in D_2O (Figure 3.19 c), are shifted upfield and resonate at 2.746 and 2.397, respectively, in the presence of 2-naphthol (Figure

3.19 d). However, CH_2 protons adjacent to CTAB head group, are affected most in the presence of naphthols, and unlike pure CTAB, the signal from CH_2 protons emerges on the other side of CH_3 protons of CTAB head groups in the presence of naphthols. This identification is important because it indicates the presence of aromatic ring of naphthol near the surfactant head groups and close to adjacent CH_2 group. Signals from protons of other parts of hydrocarbon chain, however, remain unaffected in presence of naphthols (Figure 3.19 e). The NMR spectra of 10 mM CTAB-2-naphthol (1:1) have further subtle features (Figure 3.20). While the signals from water protons remain well resolved (not shown), the signals from the aromatic protons of the naphthol molecules are broadened dramatically (Figure 3.20 a). This means that on the NMR time scale, the motion of the naphthol molecules is highly restricted in viscoelastic phase, but water molecules rotate freely [62]. The signals from CTAB protons are, however, broadened to a lesser extent but appear structureless preventing further analysis (parts b and c of Figure 3.20). It seems that the naphthol molecules are held tightly in the micelles by means of strong hydrophobic interaction and H bonding (discussed later). Above observation conclusively proves that the solubilized naphthol molecules are penetrated not deep inside the micellar core but present near the surface probably with a well-defined orientation in which the OH groups are protruded from the micellar surface toward the polar aqueous phase.

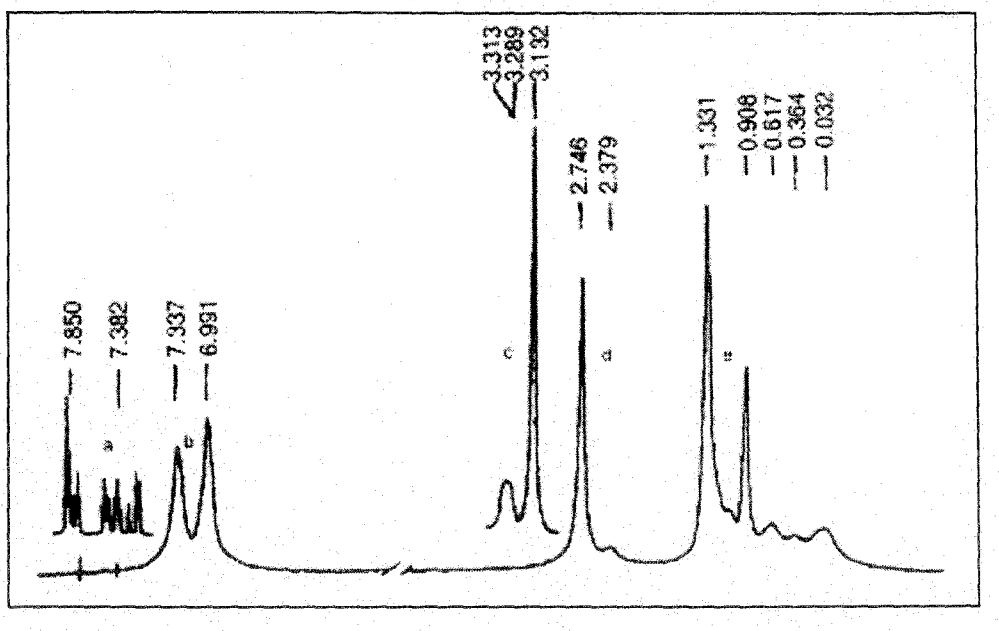

Figure 3.19: ^{1}H NMR spectra of CTAB-2-naphthol system. (a) ^{1}H signal from 2-naphthol, (c) ^{1}H signal from CTAB, (b, d, e) NMR spectrum of CTAB-2-naphthol (1 mM, 1:1).

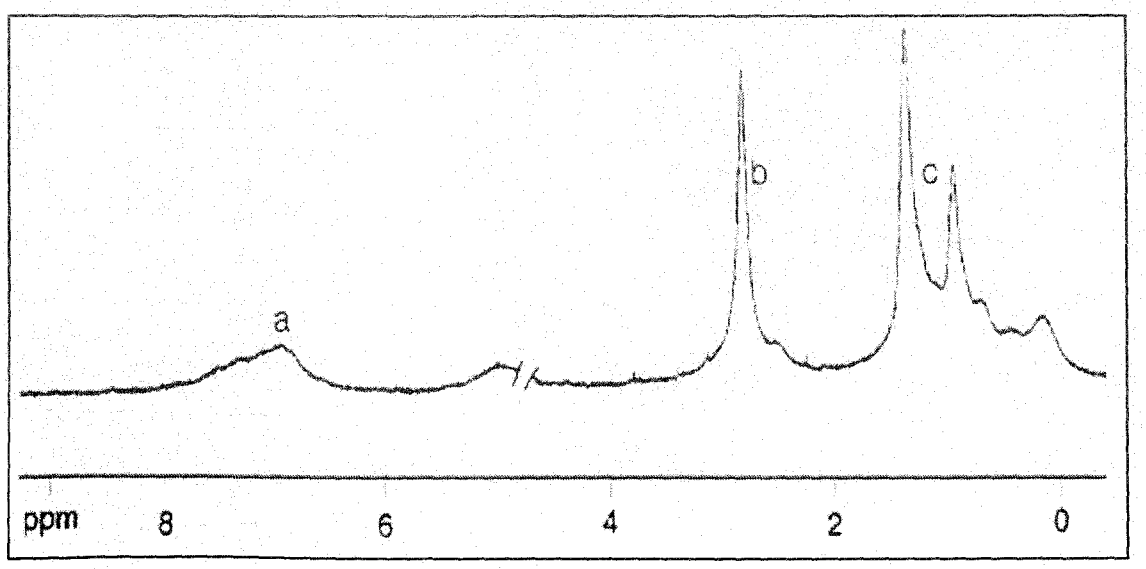

Figure 3.20: ^{1}H NMR spectra of CTAB–2--Naphthol system; abc: NMR spectrum of CTAB–2–Naphthol (10.0 mM, 1:1).

A previous study on the measurement of "apparent" shift of p*K*a of 1-naphthol at the micellar surface of CTAB yielded an effective dielectric constant value of ~45, indicating that the location of OH groups of naphthol at the micellar surface is fairly polar in nature [63, 64].

The orientation of 2,3-DHN and 2,7-DHN molecules within the micelle is greatly determined by the position of the substituents (–OH) on the aromatic ring. Though H-bonding between the water molecules and the micelle embedded dihydroxynaphthalenes is possible for both 2,3-DHN and 2,7-DHN, it is to be noted that equimolar mixtures of only CTAB and 2,3-DHN gives a transparent and highly viscous gel in aqueous solutions but 2,7-DHN/CTAB does not. Therefore, to ascertain the location and orientation of 2,3-DHN and 2,7-DHN molecules in the micelles and to understand the nature of interaction in micellar shape transitions, ^{1}H NMR studies of both the probes in CTAB micelles were also carried out in D_2O. NMR spectrum of 2,3-DHN in D_2O (in absence of CTAB) shows three sets of signals centered at δ values of 7.236, 7.283 and 7.652 respectively, due to the resonance of the aromatic ring protons (Figure3.21). All the three sets of signals are shifted upfield, broadened, and merged to give broad signals at δ values of 6.732, 6.895 and 7.143, respectively, when D_2O solution of CTAB and 2,3-DHN are mixed in 1:1 molar ratio (3.0 mM;). The large shift of aromatic proton resonance to low δ values indicates the location of naphthalene rings in the less polar environment than that of water. The broadening of aromatic proton signals is typical for a wormlike micellar solutions. The NMR spectrum of 2,7-DHN, on the other hand, in D_2O (in the absence of CTAB) shows three sets of signals at δ values of 6.932, 7.051 and 7.712, respectively, due to the resonance of the aromatic ring protons (Figure 4.22). These three sets of signals are shifted slightly upfield and resonate at δ values of 6.753, 6.782 and 7.401, respectively, when D_2O solution of CTAB and 2,7-DHN are mixed in 1:1 molar ratio (1.0 mM). Unlike the 2,3-DHN/CTAB system, the signals are not broadened and remain well resolved. The upfield shift of proton resonance for the 2,7-DHN in CTAB micelles is small compared to that of 2,3-DHN. This shows that in micellar solutions of CTAB, the 2,7-DHN molecules are portioned in somewhat

less polar environment than that of water, but resides in a far more polar surroundings than that of 2,3-DHN molecule

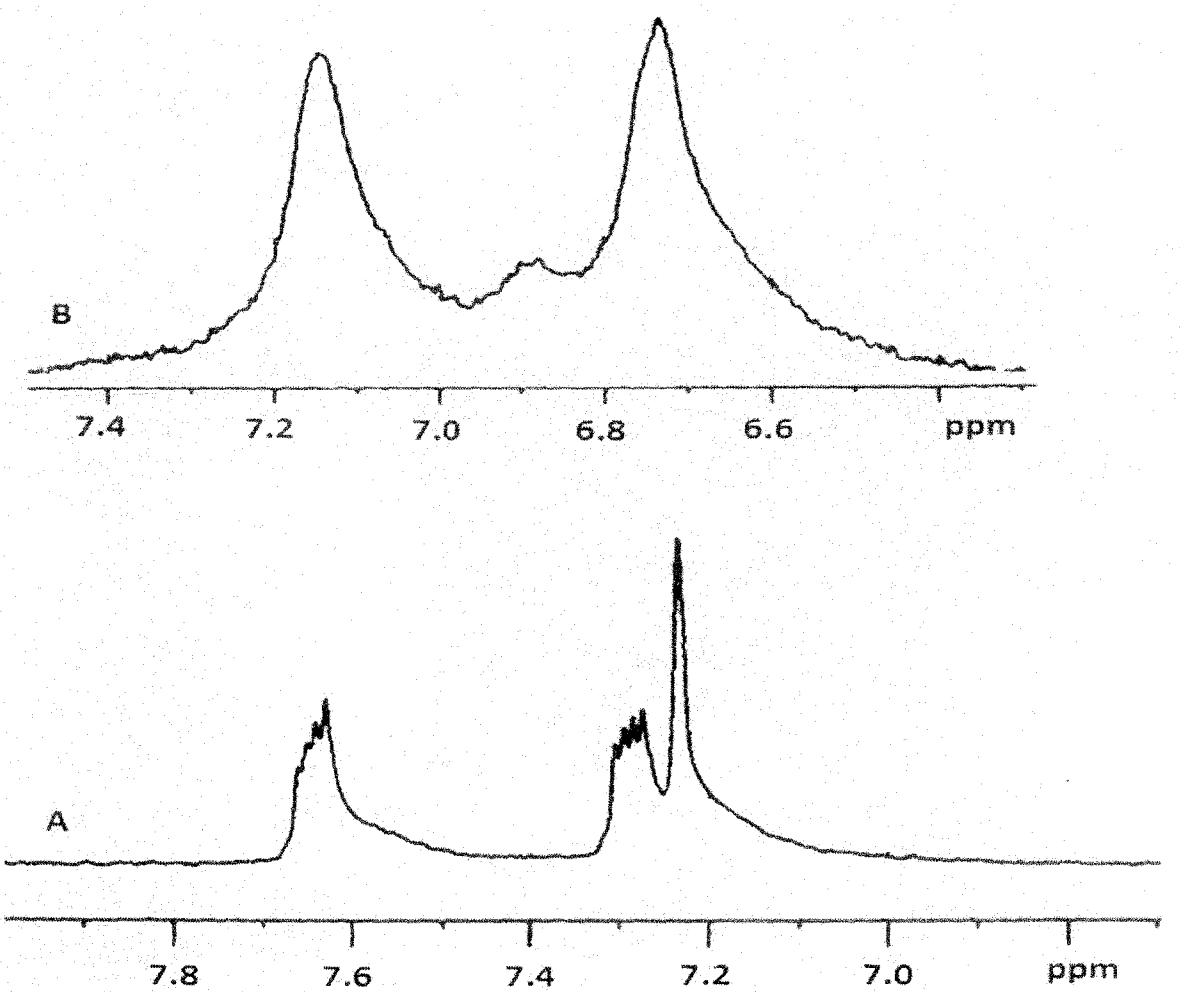

Figure 3.21 : ^{1}H NMR spectra of 2,3-dihydroxynaphthalene in the absence (A) and presence (B) of CTAB (7.5 mM, 1:1).

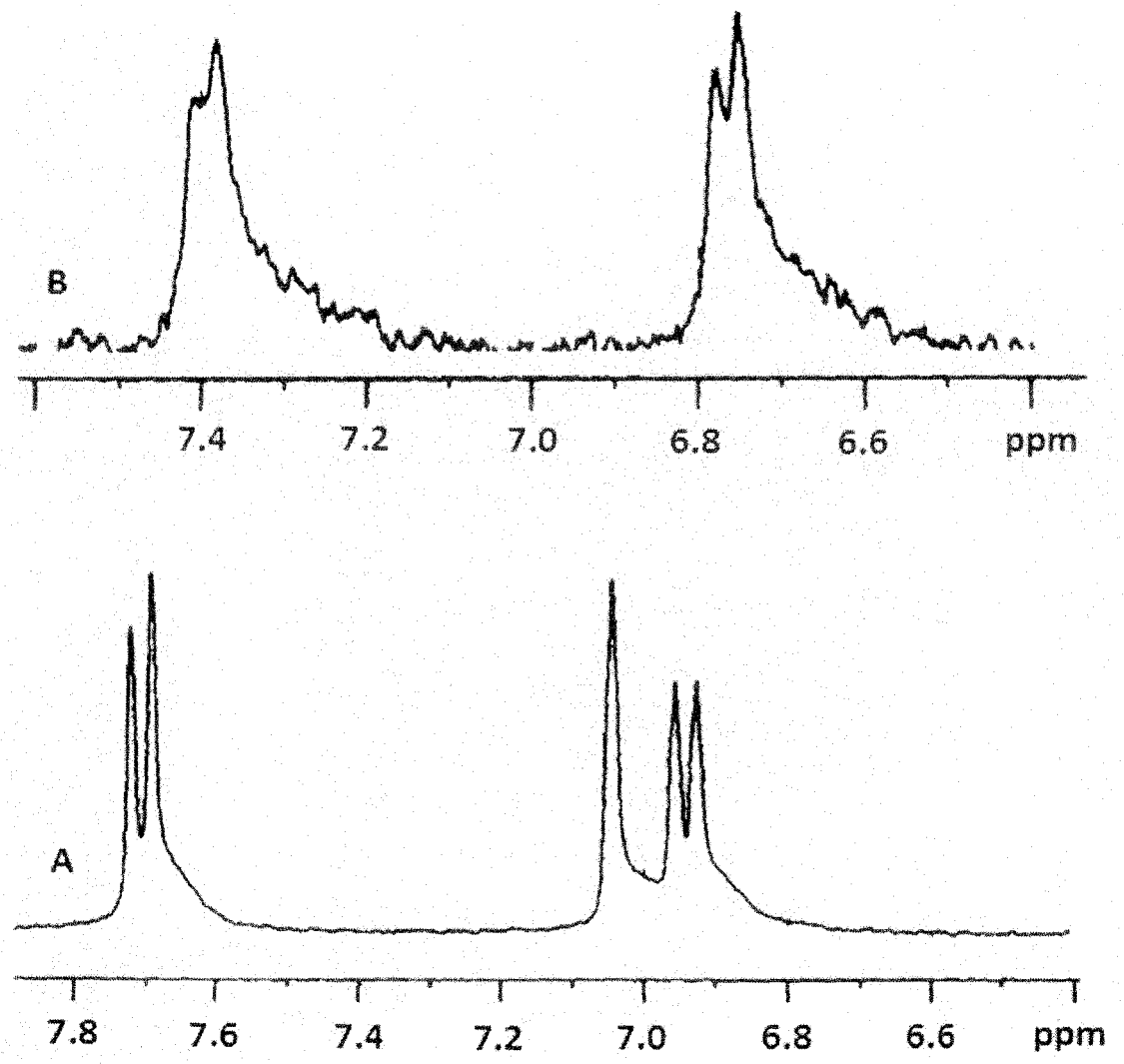

Figure 3.22 : ^{1}H NMR spectra of 2,7-dihydroxynaphthalene in the absence (A) and presence (B) of CTAB (7.5 mM, 1:1).

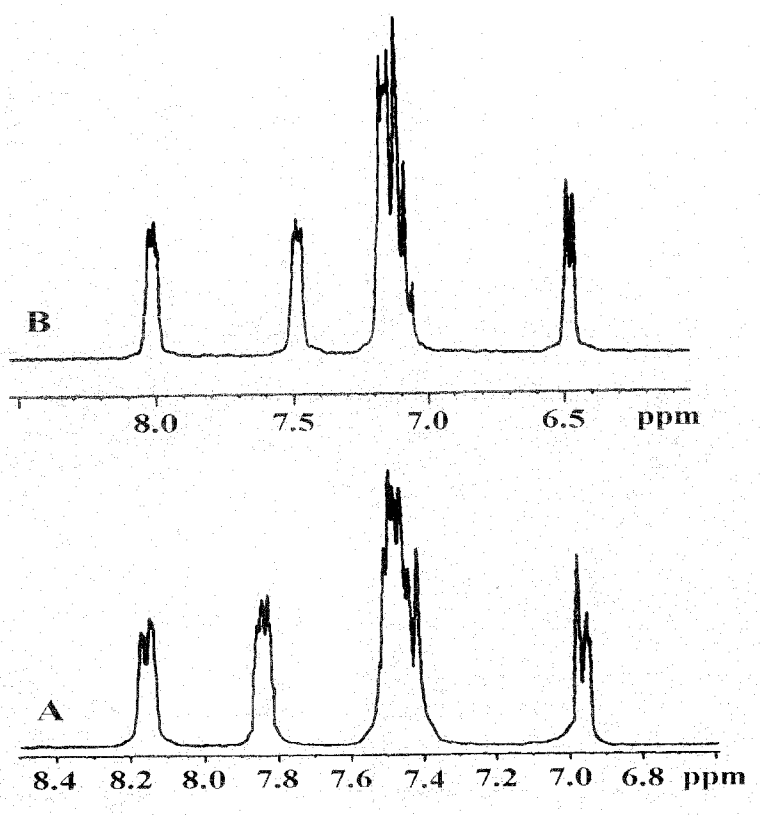

Figure 3.23: ^{1}H NMR spectra of 1-methoxynaphthalene in the absence (A) and presence (B) of CTAB (7.5 mM, 1:1).

Also, the absence of line broadening and presence of well resolved structures of the NMR signals clearly indicates fast rotation of naphthalene rings in the CTAB-2,7-DHN systems. To understand the nature of interaction of the additive methoxynaphthalene (1 MN and 2 MN) molecules with the CTAB micelles, ^{1}HNMR experiments were also performed (figure 3.23). NMR spectrum of 1MN in D_2O (in absence of CTAB) show signals centered at δ values of 8.151, 7.853, 7.482, and 6.947 respectively, due to the resonance of the aromatic ring protons

(figure 3.23 A). All the four sets of signal are shifted upfield, remain well resolved and appear at δ values of 8.013, 7.492, 7.147 and 6.487 respectively, when D_2O solution of CTAB and 1 MN are mixed in 1:1 molar ratio (7.5 mM; Figure 3.23 B). Similarly, the methoxy protons which resonate at a δ value of 3.953 in water (not shown) are also shifted up-field and resonate at a δ value of 3.561 in CTAB. This large shift of aromatic proton resonance as well as the methoxy proton signals to low δ values again indicates the location of naphthalene rings and methoxy protons in the less polar environment than that of water. Unlike naphthol-CTAB systems, absence of line broadening and the well resolved structures of the NMR signals clearly indicates fast rotation of naphthalene rings in the CTAB-MN systems (on NMR time scale). However, the degree of upfeild shift of the signals is less in 1 MN than that in naphthols; this indicates a stronger partitioning of naphthol molecules in the micelles than those of methoxynaphthalene (figure 3.23).

3.3.4.2 UV-Visible spectroscopy

Spectral Modification of Micelle-Embedded Dopants: Contribution of H-Bonding, π-π or Cation-π Interactions?

In view of the differences in the viscoelastic responses and the morphological transitions of CTAB micelles (Figure 3.12) induced by neutral naphthols and the methoxynaphthalenes, UV absorption spectra of these dopants may be interesting to study in micellar media. To understand the kind of interactions which are operative in the micelle-dopant systems, the key element of the present study is to compare the spectral characteristics of naphthols (which contain OH) with those of methoxynaphthalene (which do not contain OH) under various conditions in order to visualize a consistent molecular picture eliminating the untenable suggestions. Aromatic compounds, e.g., naphthalene, in general, have two strongly overlapped bands in the near UV region, viz., the longitudinally polarized $^1L_a \leftarrow {}^1A$ band and the transversely polarized $^1L_b \leftarrow {}^1A$ band. While the vibrational structure of these bands appears differently in different substituted compounds, effects of extending conjugation in 1 and 2 positions by OH or CH_3O

groups in naphthol and methoxynaphthalene molecules, respectively, are interesting. Both in 1-naphthol and 1-methoxynaphthalene conjugation is extended in the transverse direction and, therefore, it affects the transverse polarized ^1L_a band. In 2-naphthol and 2-methoxynaphthalene, on the other hand, conjugation is primarily extended in the longitudinal direction, affecting both the intensity and the frequency of the longitudinally polarized ^1L_b band compared to the unsubstituted naphthalene.

It is well known that the near UV spectra of aromatic compounds are affected by specific interactions like hydrogen bonding. Noncovalent interactions like π-π and cation-π also cause shifts in the electron distributions of the molecule. The OH group of naphthols can act as both a proton donor as well as a proton acceptor in forming intermolecular hydrogen bonding. A hydrogen bond in which the hydroxyl groups of naphthols is a proton donor releases electron density from the O-H bond toward the oxygen and hence, by an inductive effect, toward the aromatic ring. This causes a red-shift of the π-π^* transition. Conversely, if a hydrogen bond is formed in which the hydroxyl oxygen is a proton acceptor, electrons are withdrawn from the naphthalene ring, and an opposite shift is anticipated. If both bonds could form at the same time and with equal ease, since their effects on the partial charges of the oxygen are opposite, the net change on the oxygen and hence on the aromatic ring may be small. Therefore, in such a situation, the spectral shift relative to the position of the band in a nonhydrogen-bonding situation ought to be small [65].

The near UV absorption of 1-naphthol which arises from two strongly overlapped π-π^* transitions remain unaffected in the presence of submicellar aqueous CTAB solution, indicating the absence of any appreciable interaction (Figure 3.24). However, interestingly, significant red-shift starts to occur (6.4 nm at λ_{max} ~293 nm) in the presence of CTAB just above its cmc (0.96 mM) with a well-defined isobestic point at 296 nm. Such shifting of λ_{max} continues until most of the naphthol molecules are partitioned in the micellar phase at high surfactant/ naphthol ratio. The absorption spectra of 2-naphthol as a function of CTAB concentration shows similar features but consist of more than one isobestic

points (figure 3.25). The result suggests that the protruded OH groups of micelle-embedded naphthols form a H bond with interfacially located (D_{eff} ~45) water molecules and act as a H-donor. It may also be argued that at a mole ratio of 1:1 of naphthol and the CTAB, at which maximum viscoelastic response is observed under shear, due to the presence of entangled worm like micelles, not all of the naphthol molecules are embedded in the micelles, but some are located in the stern layer. These naphthols may, however, be involved in H-bond network formation with embedded molecules via interfacial water. The spectral feature and the nature and degree of shift undoubtedly resemble the spectra of 1-naphthol in isooctane at various dioxane concentrations (Figure 4.26) (red-shift of 6.3 nm at λ_{max} ~293 nm, as compared to a red-shift of 6.4 nm at λ_{max} ~293 nm, Figure 3.24) where naphthol acts as the hydrogen bond donor and dioxane as acceptor [54].

Previously, it has been shown that, in the ground state, 1-naphthol interacts with water via oxygen, whereas with alcohols (ethanol and isopropanol) and acetonitrile it interacts via hydrogen of the hydroxyl group [66]. The nature of spectral modification encountered by micelle free naphthol molecules in the presence of water is shown in figure 3.27. This figure shows that on every addition of water (up to 10% v/v) substantial gain in intensity is displayed by 1-naphthol spectra (in acetonitrile) with little change of wavelength. The nature of spectral modification of 1-naphthol due to H-bond formation is quite different from that of micelle-embedded naphthol. It may be argued that, like alcohols and acetonitrile media, naphthols at the interface (D_{eff} ~45) act as H-donating agents and water as a H-acceptor at the oxygen site. This is indeed interesting. The low D_{eff} value found for the interfacial microenvironment of CTAB micelles may be attributed to a low interfacial water activity. Nevertheless, it has also been argued that the low interfacial D_{eff} value may be a result of the H-bond donor properties of the water in the interfacial region being different from that of bulk water, and/or the presence of electrostatic image interactions caused by the proximity of the low dielectric hydrocarbon core. Present experiments indeed justify the former conjecture precisely [67]. It is known that the water molecules at the micellar

interface have some strange properties [68,69]. The solvation dynamics are slowed down by several orders of magnitude relative to bulk water. The reorientational motion is also restricted. The dynamics of water molecules near an aqueous micellar interface has been a subject of intense current interest because such a system serves as a prototype of complex biological system. Furthermore, oxygen absorption and emission spectra of water molecules in the micellar interface also show that the local electronic structure of water molecules is dramatically different from that of bulk water [70]. The relatively less polar and less mobile water molecules compared to bulk water form a strong H-bond with the OH group of embedded naphthols, which act as H-donors and result in an optimum orientation of aromatic π-electron systems in the micelles to shield the surfactant headgroup charges efficiently; maybe via cation-π interaction; i.e., cation charge of surfactant

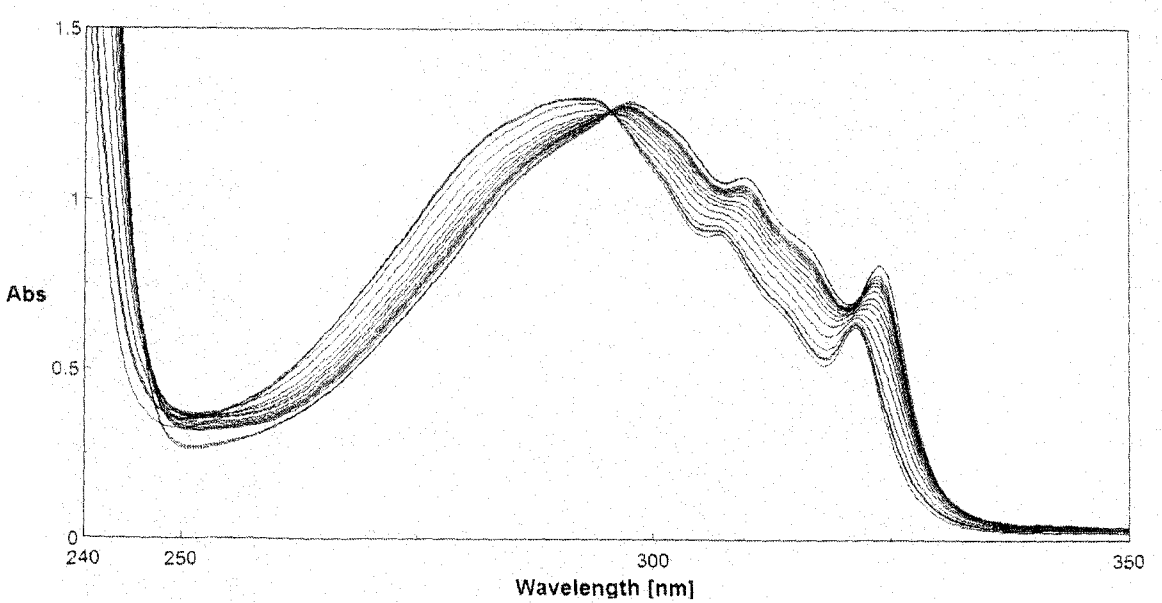

Figure 3.24: Absorption spectra of 1-Naphthol (0.25 mM) in water at varying concentrations of CTAB at 25 °C. [CTAB]: (1) 0.0, (2) 0.44, (3) 0.55, (4) 0.75, (5) 1.00, (6) 1.25, (7) 1.50, (8) 1.75, (9) 2.00, (10) 2.50, (11) 3.00, (12) 3.50, (13) 4.00, (14) 5.00, (15) 15.00, (16) 20.00 mM.

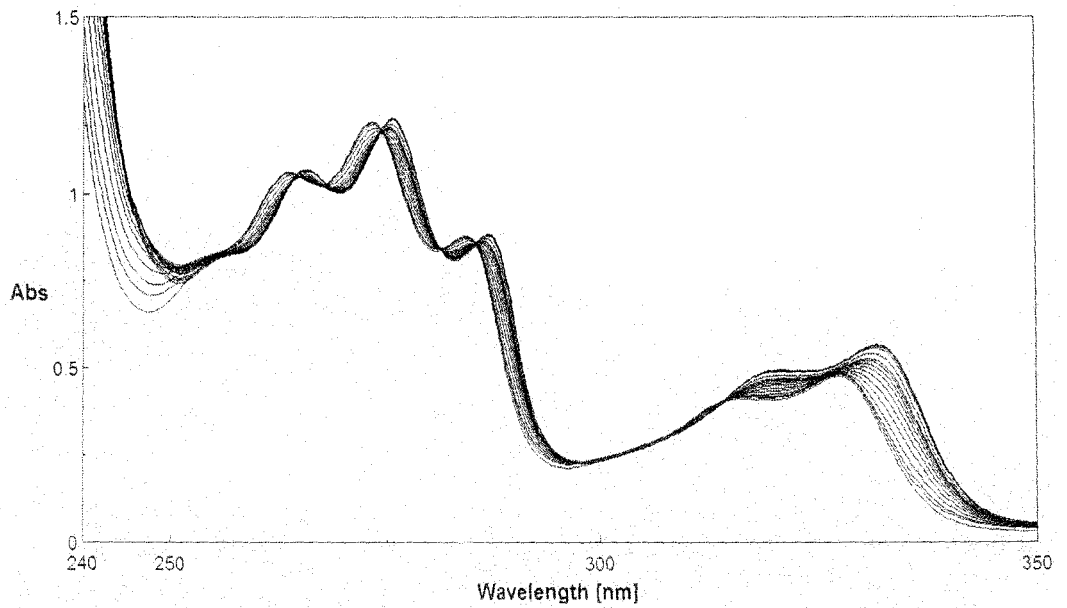

Figure 3.25: Absorption spectra of 2-Naphthol (0.25 mM) in water at varying concentrations of CTAB at 25 °C. [CTAB]: (1) 0.0, (2) 0.65, (3) 0.79, (4) 0.94, (5) 1.13, (6) 1.36, (7) 1.63, (8) 1.96, (9) 2.35, (10) 2.82, (11) 3.39, (12) 5.08, (13) 7.63, (14) 11.44, (15) 17.16, (16) 20.60 mM.

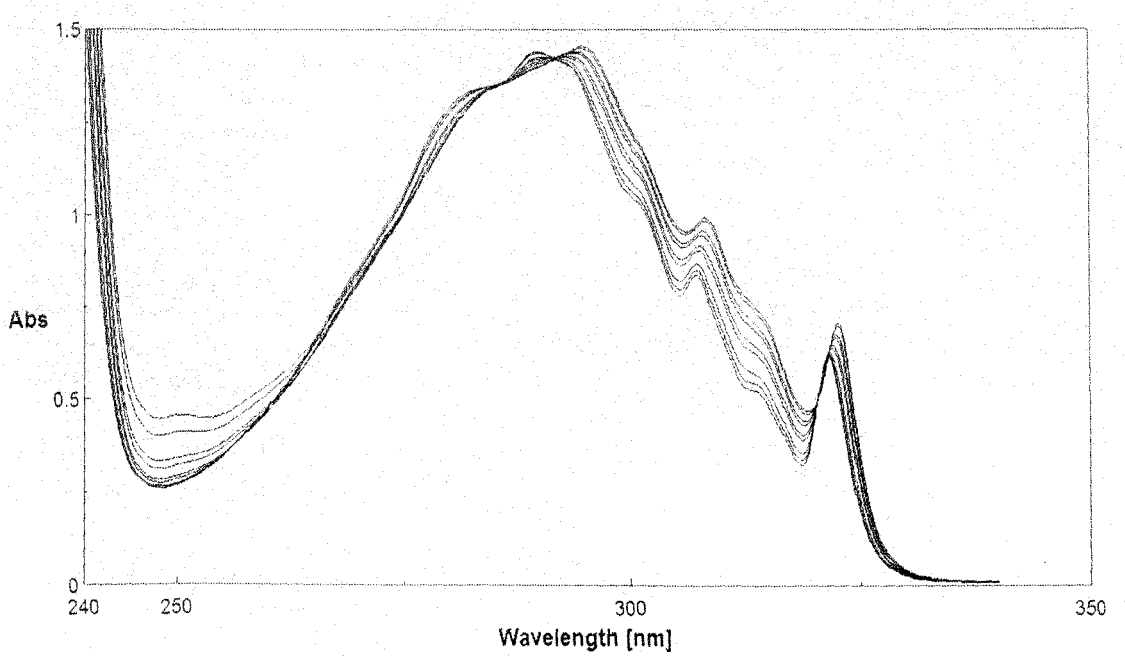

Figure 3.26: Absorption spectra of 1-Naphthol (0.25 mM) in isooctane at varying concentrations of 1,4-dioxane at 25 °C. [Dioxane]: (1) 0.0, (2) 13, (3) 20, (4) 40, (5) 50, (6) 80, (7) 100, (8) 160, (9) 200 mM.

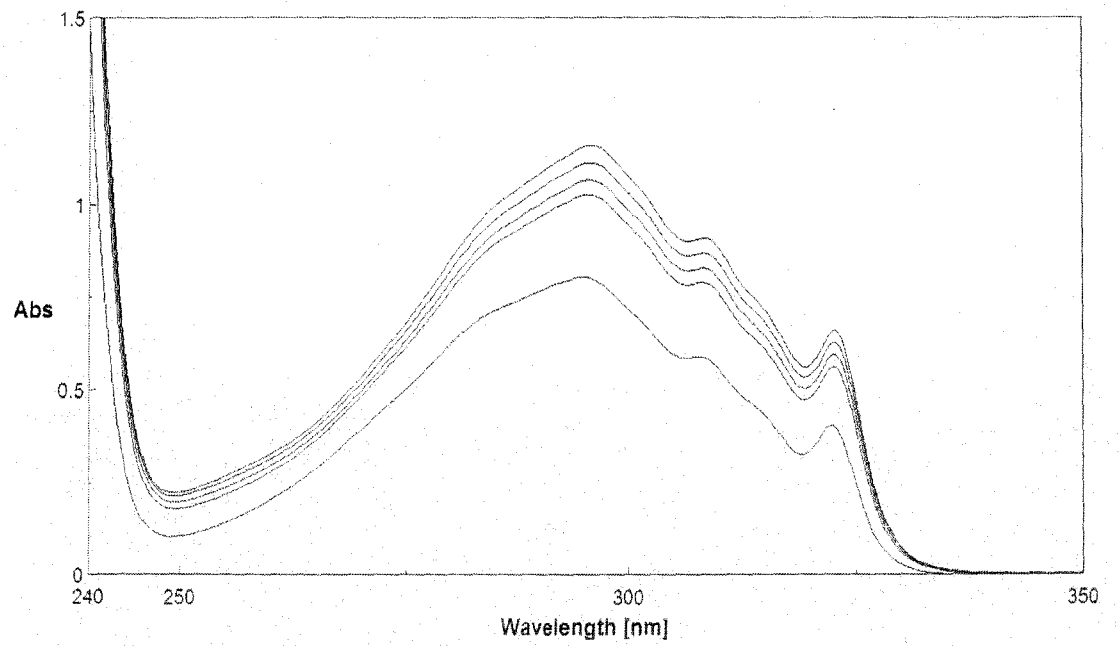

Figure 3.27: Absorption spectra of 1-Naphthol (0.25 mM) in acetonitrile at different percentages of water at 25 °C. % of water: (1) 0.00 %, (2) 4.00 %, (3) 6.00 %, (4) 8.00 %, (5) 10.00 %.

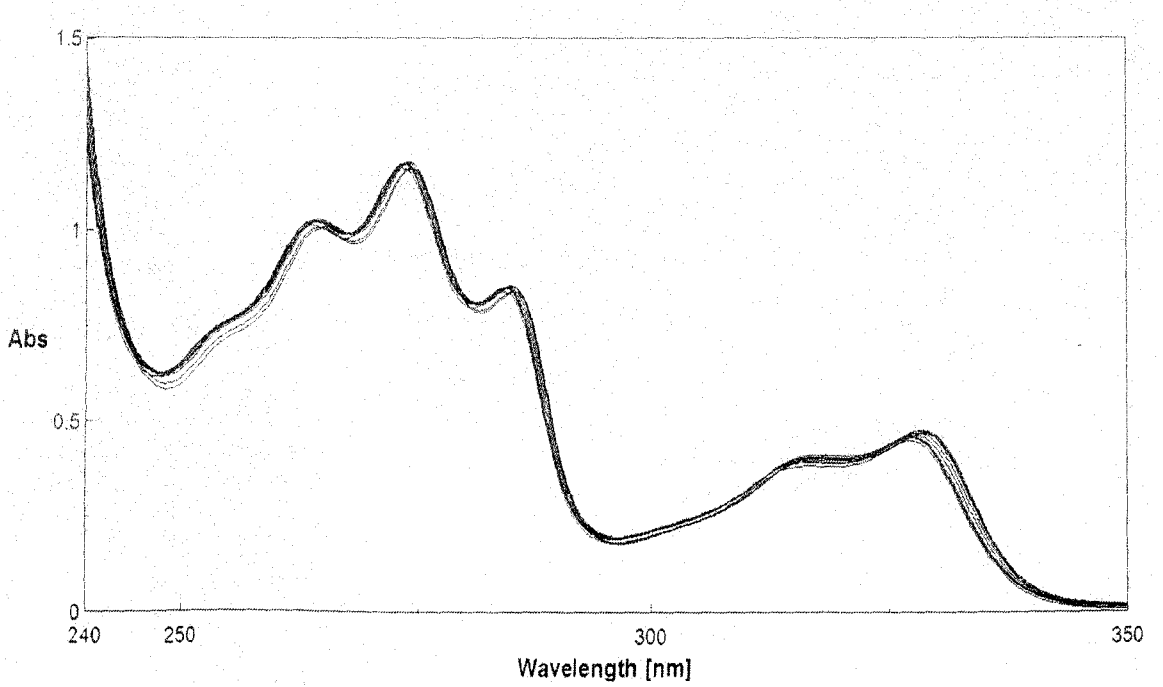

Figure 3.28: Absorption spectra of 2-Naphthol (0.25 mM) at varying concentrations of SDS in water at 25 °C. [SDS]: (1) 0.0, (2) 5.6, (3) 6.91, (4) 8.30, (5) 9.96, (6) 11.95, (7) 14.34, (8) 17.21, (9) 30.97 mM.

head groups interacts with the quadrupole moment of the aromatic π-system of naphthols. Cation-π interaction energies are of the same order of magnitude as hydrogen bonds and play an important role in molecular recognition [58]. To further strengthen the above view (involvement of cation-π interaction), the absorption spectra of the naphthols were recorded in aqueous SDS of varying concentrations. The possibility of a cation-π interaction in SDS can directly be ruled out due to the anionic head group of the surfactant. Figure 3.28 shows the absorption spectra of 2-naphthol in aqueous SDS. As expected, no appreciable shift at any of the vibrational bands of the probe molecule was observed. Moreover, very small enhancement in the absorbance of the peaks was seen.

On the other hand, as the H atom of OH is replaced by a CH_3 group (viz., the methoxynaphthalene molecules), the ability of intermolecular H-bond formation disappears. Instead, the H-accepting tendency from a potential donor is enhanced. The absorption spectra of 1- and 2- methoxynaphthalene in aqueous CTAB are shown in figures 3.29 and figure 3.30 respectively. The nature of changes

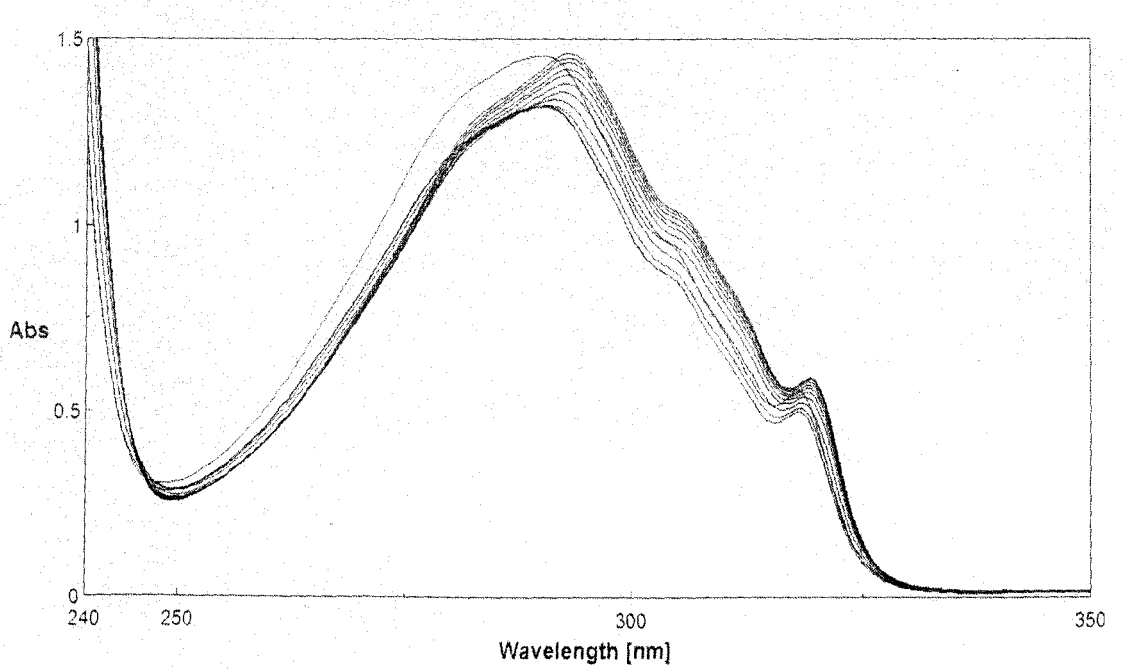

Figure 3.29: Absorption spectra of 1-Methoxynaphthalene (0.25 mM) in water at varying concen-trations of CTAB at 25 °C. [CTAB]: (1) 0.0, (2) 0.33, (3) 0.55, (4) 0.75, (5) 1.00, (6) 1.50, (7) 2.00, (8) 2.50, (9) 3.00, (10) 3.50, (11) 4.00, (12) 5.00 mM.

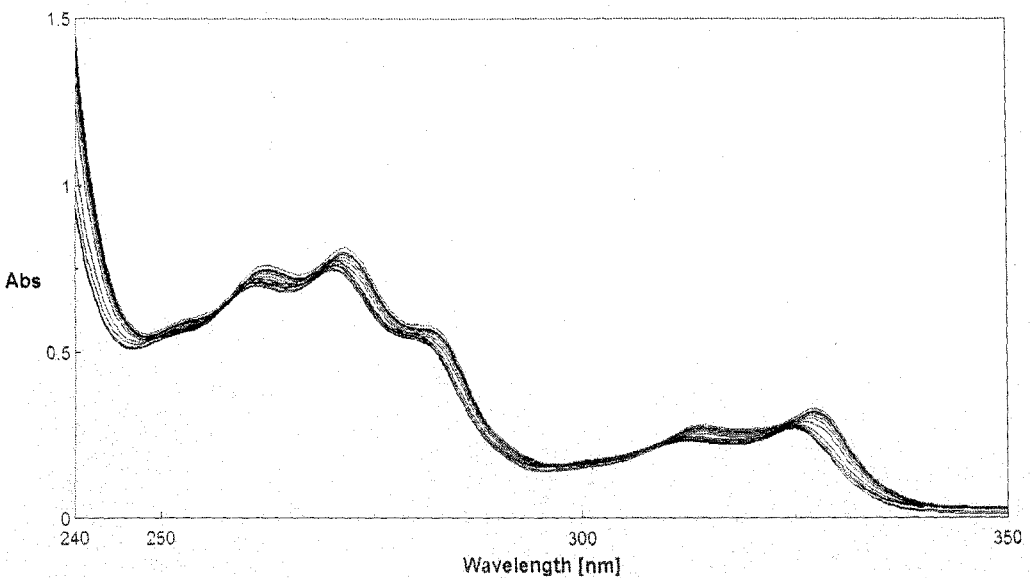

Figure 3.30: Absorption spectra of 2-Methoxynaphthalene (0.25 mM) in water at varying concent-rations of CTAB at 25 °C. [CTAB]: (1) 0.0, (2) 0.33, (3) 0.50, (4) 0.75, (5) 1.00, (6) 1.50, (7) 2.00, (8) 2.50, (9) 3.00, (10) 3.50, (11) 4.00, (12) 5.22 mM.

encountered in the UV spectra of 1- and 2- methoxynaphthalene on the addition of CTAB above its cmc indicates the permeation of the probe molecules in the micelles. The small red-shift, with the absence of any isobestic point(s), compared to that in naphthols indicates that a weaker noncovalent interaction takes place. The large drop in intensity on first addition of 0.33 mM CTAB is the signature of breaking of H-bonds with bulk water molecules. To examine the stabilities of the hydrogen bonding and the cation-π interactions in the 1-naphthol/CTAB and 1-methoxynaphthalene/CTAB systems respectively, the absorption spectra were recorded at higher temperatures. Interestingly, the spectra of 1-naphthol/CTAB system at 70°C (figure 3.31) shows dentical features as that at 25°C. Moreover, the shift in the λ_{max} is also the same (as that at 25°C). Therefore, it may be argued that the H-bonds which are formed at the interface are strong and remain stable even at 70°C. On the other hand, the 1-methoxy-naphthalene/CTAB system, with only cation-π interactions, behave differently even at 50°C (compared to that at 25°C). The spectra of probes show only gain in intensity on addition of surfactants (with negligible shift at the maximum wavelength) due to the increasing presence of non polar environment in the micellar phase (figure 3.32).

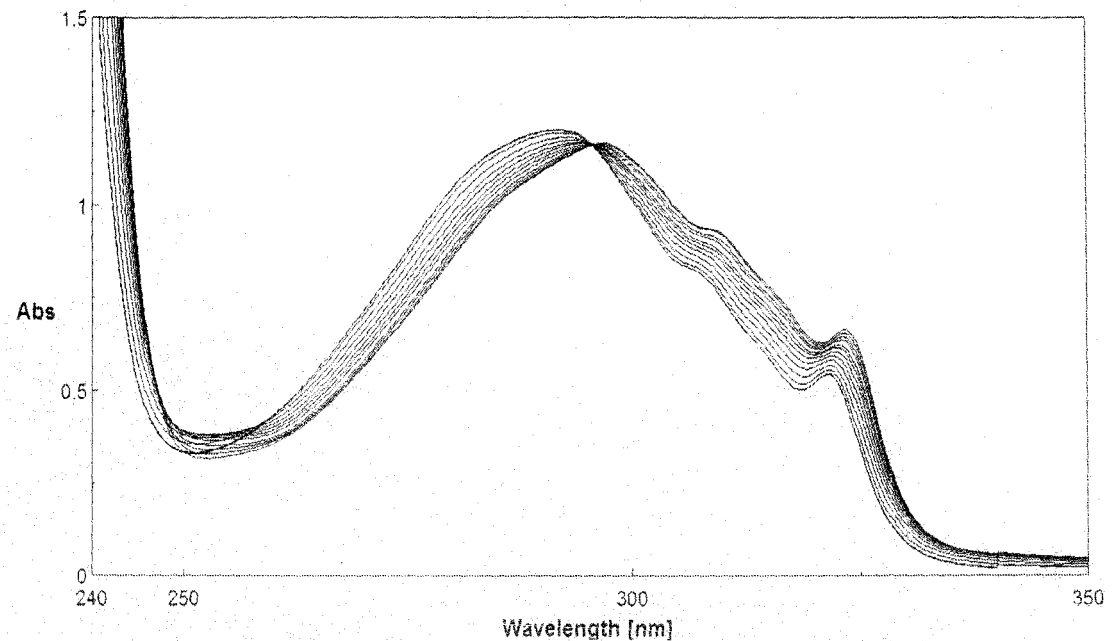

Figure 3.31: Absorption spectra of 1-Naphthol (0.25 mM) in water at varying concentrations of CTAB at 70 °C. [CTAB]: (1) 0.0, (2) 0.73, (3) 0.98, (4) 1.31, (5) 1.63, (6) 2.04, (7) 2.56, (8) 3.2, (9) 4.00, (10) 5.00, (11) 7.50, (12) 10.00, (13) 15.00, (14) 20.30 mM.

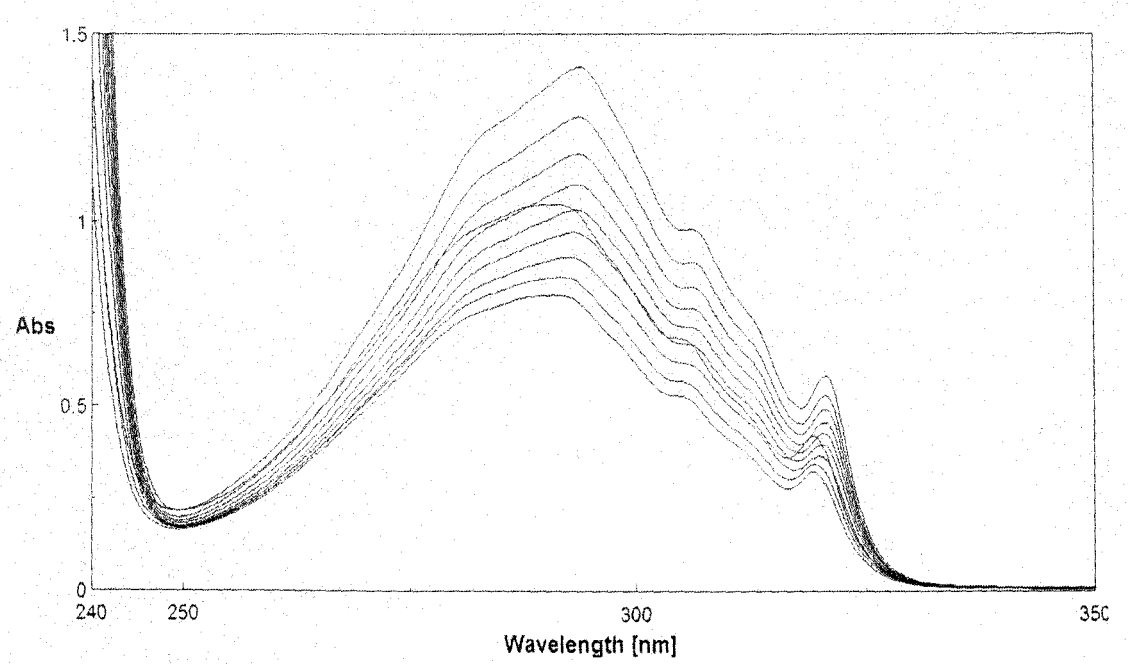

Figure 3.32: Absorption spectra of 1-Methoxynaphthalene (0.25 mM) in water at varying concen-trations of CTAB at 50°C. [CTAB]: (1) 0.52, (2) 0.78, (3). 1.75, (4) 2.63, (5) 3.95, (6) 5.92, (7) 8.88, (8) 13.33, (9) 20.00 mM.

Due to their directionality and spatial arrangement, complementary multiple H-bonding interactions at the micellar interface lead to engineering well defined supramolecular structure via micellar headgroup charge shielding by π-electron systems of naphthols (Figure 3.33). This result of unusual H-bonding may be relevant, not only when considering the H-bonding of the interfacial water molecules in the specific micelle and dopant studied here but also for the H-bonding interaction of other micelle-dopant systems as well. Therefore, unlike methoxynaphthalenes, naphthols interact with micelles strongly and the UV spectra of naphthols are modified showing significant red shifting and display sharp isobestic point due to strong H-bonding interaction with interfacial water molecules.

The spectral modifications of the probe molecules in CTAB micelles (with C_{16} hydrocarbon chain), promted to extend the spectroscopic investigation with other members of the alkyltrimethylammonium bromide series, viz; DTAB (C_{12}) and TTAB (C_{14}). It is well known that the compactness of the head group of the alkyltrimethylammonium surfactants increase with an increase in the surfactant

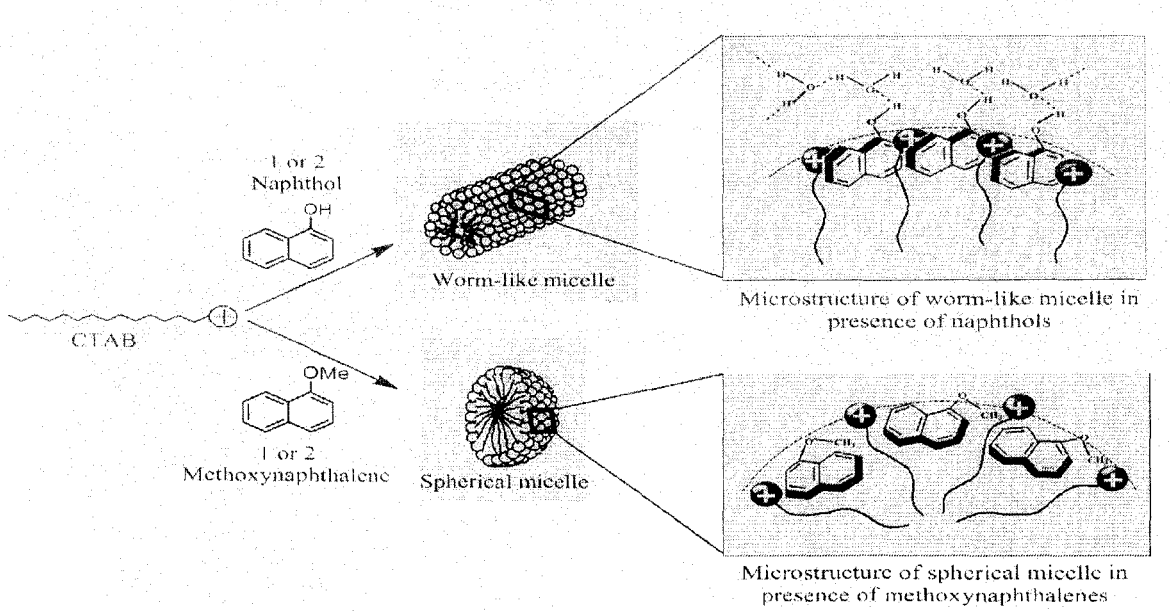

Figure 3.33: Schematic representation of the microstructures found in worm-like micelles formed by naphthols and spherical micelles formed by methoxynaphthalenes with CTAB.

chain length. Neutron scattering experiments on micelles having different surfactant chain lengths reveal that the head group structures of the micelles differ significantly [71,72]. For example, in DTAB water penetrates into the head group region to a depth of ~4 carbons, whereas in TTAB water penetrates to a depth of ~2.5 carbons [73]. Therefore, to check the effect of surfactant chain length and the validity of the water penetration (micellar hydration) model on the absorption characterstics of the hydroxynaphthalenes, studies with DTAB and TTAB were also carried out in aqueous media (figures 3.34 to 3.37). Interestingly, shifts in the maximum wavelengths of the probe molecules are the same irrespective of the hydrocarbon chain length of the surfactants. For example, the longest wavelength band of 1-naphthol in water which arises at 321.2 nm shifts to a maximum of 323.8 nm in presence of 10 mM CTAB. At this concentration all the naphthols are supposed to be fully bound to the CTAB micelles. The same shift is also observed for the probe molecule in micelles of TTAB and DTAB when fully bound. Moreover, the position of the isobestic point too remains unmoved with changes in the hydrophobicity of the surfactant. Arguing in line with the water penetration

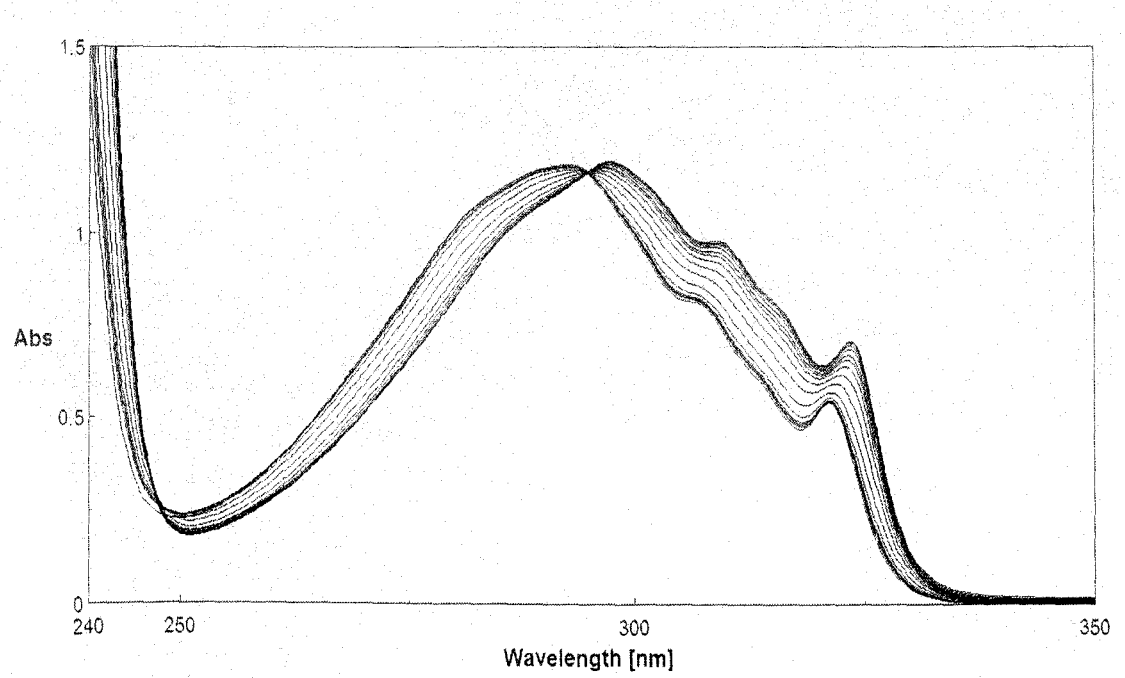

Figure 3.34: Absorption spectra of 1-Naphthol (0.25 mM) in water at varying concentrations of DTAB at 25 °C. [DTAB]: (1) 0.0, (2) 8.40, (3) 10.08, (4) 11.00, (5) 12.00, (6) 13.09, (7) 14.28, (8) 15.58, (9) 17.00, (10) 18.55, (11) 20.24, (12) 24.29, (13) 29.15, (14) 34.98, (15) 41.98, (16) 50.37, (17) 60.45 mM

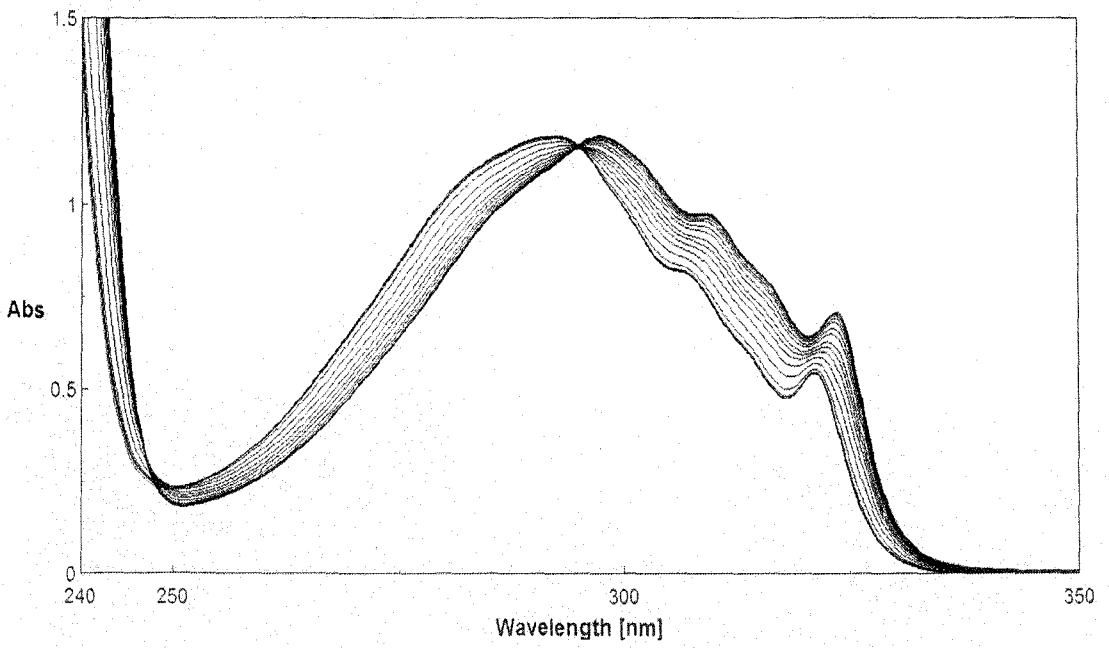

Figure 3.35: Absorption spectra of 1-Naphthol (0.25 mM) in water at varying concentrations of TTAB at 25°C. [TTAB]: (1) 0.0, (2) 1.96, (3) 2.62, (4) 3.15, (5) 3.43, (6) 3.75, (7) 4.09, (8) 4.47, (9) 4.87, (10) 5.32, (11) 6.39, (12) 7.67, (13) 10.23, (14) 13.64, (15) 18.19, (16) 24.26, (17) 29.11, (18) 39.94 mM

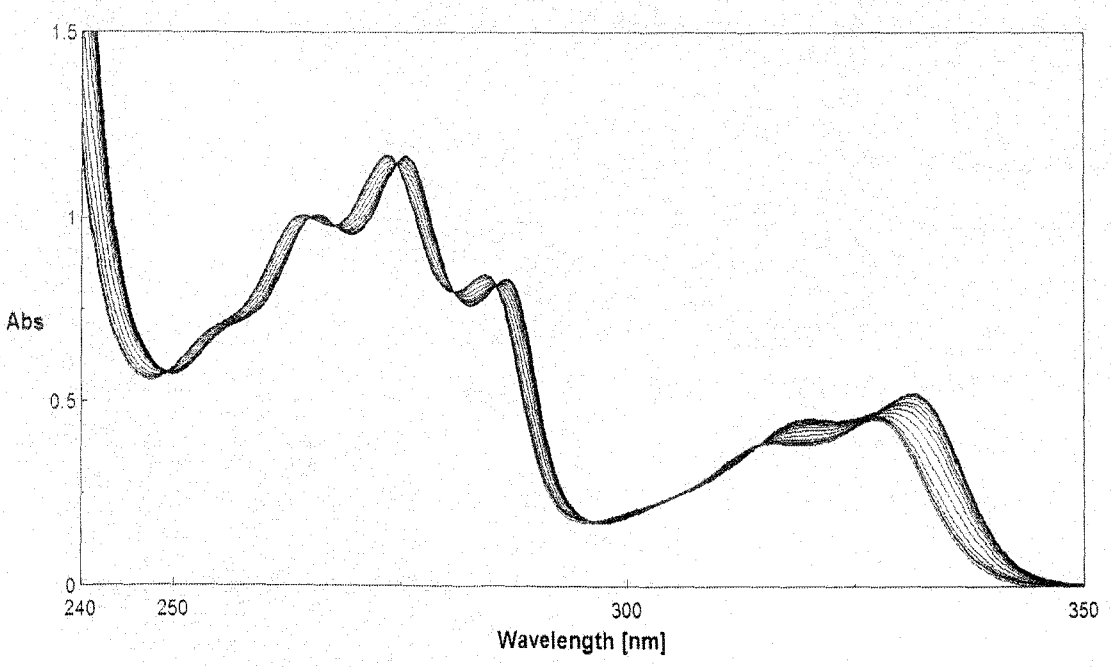

Figure 3.36: Absorption spectra of 2-Naphthol (0.25 mM) in water at varying concentrations of DTAB at 25 °C. [DTAB]: (1) 0.0, (2) 8.31, (3) 9.97, (4) 11.96, (5) 13.05, (6) 14.24, (7) 15.53, (8) 16.94, (9) 18.49, (10) 20.17, (11) 24.22, (12) 29.05, (13) 34.86, (14) 41.84, (15) 50.21, (16) 60.26 mM.

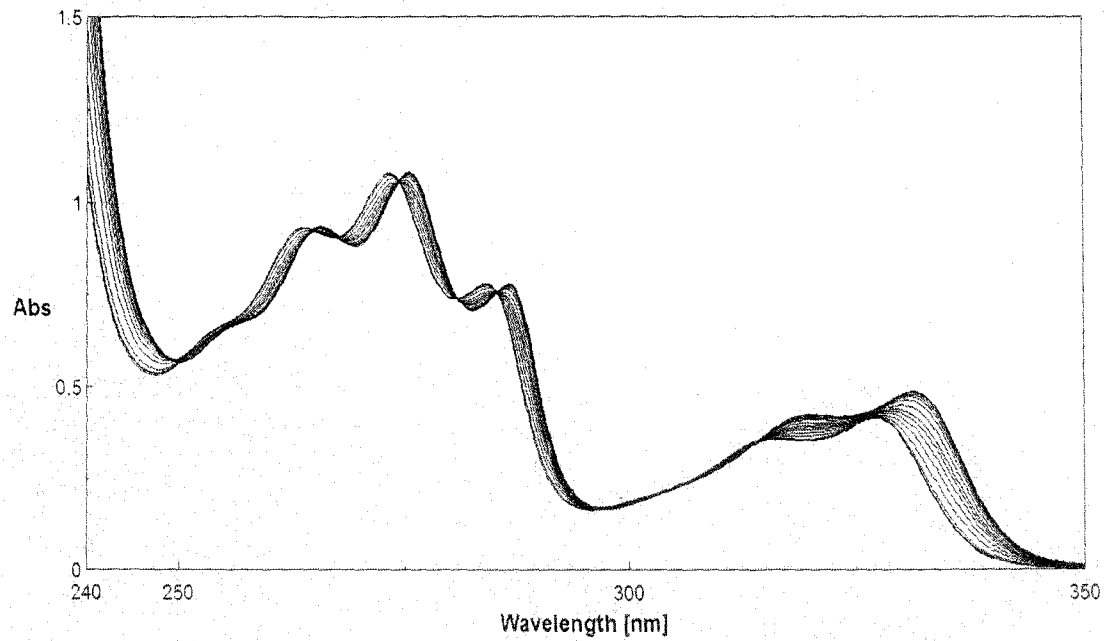

Figure 3.37: Absorption spectra of 2-Naphthol (0.25 mM) in water at varying concentrations of TTAB at 25°C. [TTAB]: (1) 0.0, (2) 2.33, (3) 2.80, (4) 3.36, (5) 3.67, (6) 4.01, (7) 4.37, (8) 4.77, (9) 5.21, (10) 6.25, (11) 8.33, (12) 11.11, (13) 14.81, (14) 19.75, (15) 26.33, (16) 31.60 mM.

penetration model, the increased micellar hydration in DTAB (as compared to TTAB and CTAB) would have caused lesser spectral shifts because the microenvironment faced by the probe in DTAB micelles would be more polar. This was however, not observed. From the foregoing observations we conclude that the spectral modification of the hydroxynaphthalenes (both 1- and 2-naphthols) in cationic micelles of alkyltrimethylammonium bromides is solely a consequence of hydrogen bonding with the interfacial water molecules in combination with cation-π interactions and that other factors like micellar hydration and temperatures seems insignificant.

3.3.4.3 Spectral modifications of Dihydroxyaromatic compounds in micellar media

While both the monohydroxynaphthalenes (1- and 2-naphthols) imparts strong viscoelasticity in the solution of CTAB micelles, the behaviour of the dihydroxynaphthalenes (DHN), viz., 2,3-dihydroxynaphthalene and 2,7-

dihydroxynaphthalene towards micellar solutions of CTAB is quite different. 2,3-dihydroxynaphthalene when mixed with aqueous CTAB, formed a viscoelastic gel, the maximum viscosity occurring at a mole ratio of 1:1 (figure 3.2). On the other hand 2,7-dihydroxynaphthalene could not form viscoelastic solutions with CTAB. Therefore, spectroscopic investigation of the dihydroxy dopants in aqueous CTAB have been carried out. The effect of other alkyltrimethylammonium bromides (DTAB and TTAB) on the absorption properties of 2,3 and 2,7 -dihydroxynaphthalenes have also been investigated.

The near UV absorption spectrum of 2,3 and 2,7-DHN exhibits several sharp vibrational components among which the longest wavelength band, the π-π^* band arises mainly due to the $^1L_b \leftarrow {}^1A$ transition. The interaction of alkyltrimethylammonium bromide surfactants with 2,3 and 2,7-DHN were studied at several concentrations range so as to cover both the submicellar and post micellar regions. Unlike 1 and 2-naphthols, where the absorbance remained constant upto the cmc of the added surfactant, the absorbance at the longest wavelength band of 2,3 and 2,7-DHN (324 nm for 2,3-DHN and 325.6 nm for 2,7-DHN) experienced an initial sharp decrease with increasing CTAB concentration. The decrease in absorbance at 324 nm continued upto the cmc of the surfactant and then a sharp rise in the absorbance with a red-shift of ~3.0 nm is observed. The absorption spectra of 2,3-DHN in aqueous CTAB is shown in figure 3.38. Well defined isobestic points at 282, 307.1, 311.2, 321 and 324 nm shows that equilibrium between the micelle bound and the free probe molecules exists. The longest wavelength band at 324 nm undergoes a gradual blurring of vibrational fine structure with a significant red shift (~3 nm). Although blurring or broadening occurs in the vibrational structure, there exists a similarity between the spectra of the free and the micelle embedded molecules. The blurring of vibrational structure and the shift to longer wavelength continues only upto a concentration of 5 mM CTAB and beyond 5 mM, the loss of vibrational structure is regained and no further shift in the λ_{max} is observed indicating that the probes are being increasingly incorporated within the micelles. Therefore, at a concentration of 5 mM all the 2,3-DHN molecules are fully embedded in the micelles and are

hydrogen bonded with the interfacial water molecules surrounding the micelles. Previously, a similar red-shift of absorption spectra band of 2-naphthol in AOT reverse micelle was observed, where AOT acts as hydrogen-bond donor and the perturbation on π electrons caused by the negative charge carried on oxygen atom of the partner molecule due to H-bonding occurs [74]. The same reasoning applies to the present case also and the nature of spectral change indicates in favour of H bonding between dihydroxy naphthalene molecules which are embedded increasingly in the micelle as the CTAB concentration (>1.0 mM) is increased. The spectra of 2,7-DHN/CTAB system showed similar red shifts with isobestic points at 293.4, 323.6 and 326.9 nm only (figure3.39). The absorption spectra of 2,3-DHN and 2,7-DHN in aqueous solutions of DTAB and TTAB are shown in figures 3.40 to 3.43. Though 2,3-DHN and 2,7-DHN produces completely different effects on CTAB micelles, for instance, 2,3-DHN induces microstructural transition from spherical to worm-like micelles and imparts strong viscosity to CTAB solutions but 2,7-DHN does not, not much difference in the absorption pattern is observed. The only difference in the spectral features of the two dihydroxy naphthalenes lies in the number of isobestic points (5 for 2,3-DHN and 3 for 2,7-DHN). Nevertheless

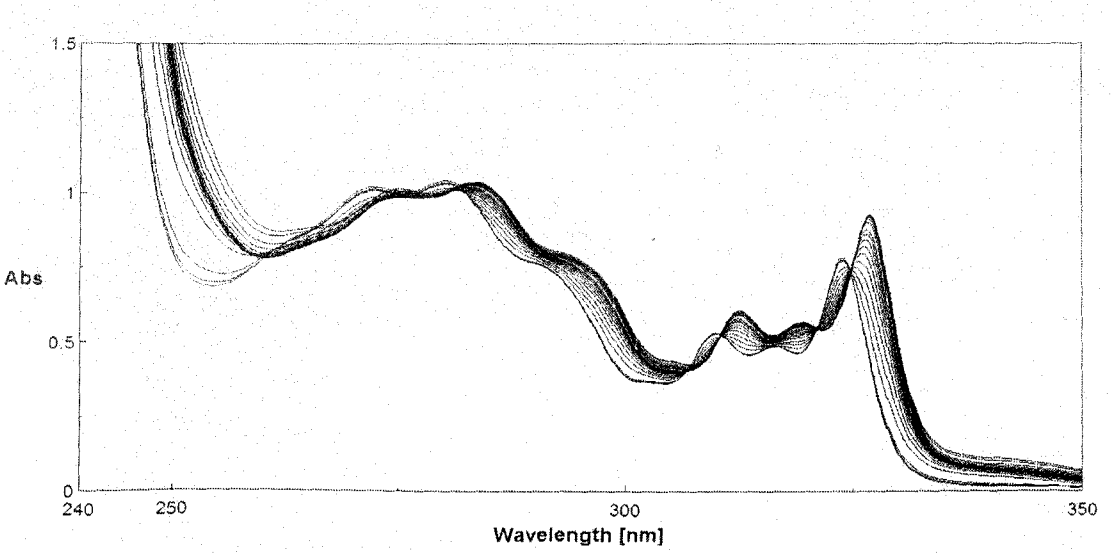

Figure 3.38: Absorption spectra of 2,3-dihydroxynaphthalene (0.25 mM) in water at varying concen-trations of CTAB at 25°C. [CTAB]: (1) 0.00, (2) 0.41, 0.61, (3) 0.61, (4) 0.92, (5) 1.10, (6) 1.32, (7) 1.59, (8) 1.91, (9) 2.29, (10) 2.75, (11) 3.30, (12) 3.96, (13) 5.94, (14) 7.92, (15) 10.56, (16) 14.08, (17) 18.78, (18) 25.04, (19) 30.05 mM

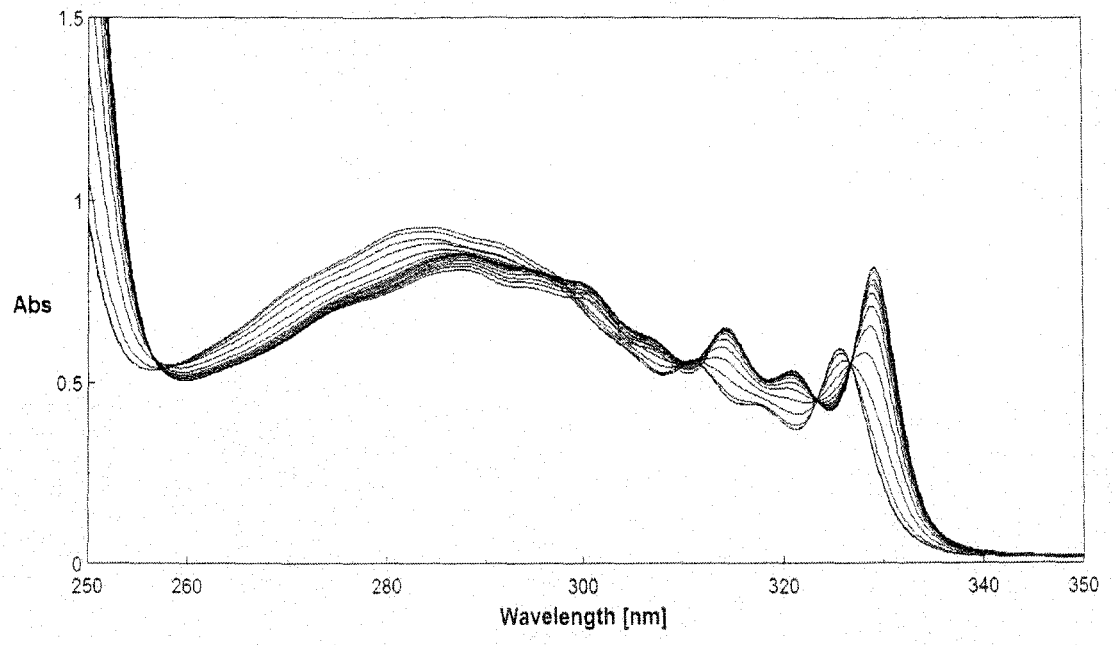

Figure 3.39: Absorption spectra of 2,7-dihydroxynaphthalene (0.25 mM) in water at varying concen-trations of CTAB at 25°C. [CTAB]: (1) 0.00, (2) 0.37, (3) 0.56, (4)0.84, (5) 1.27, (6) 1.69, (7) 2.25, (8) 3.00, (9) 4.00, (10) 5.34, (11) 7.12, (12) 9.49, (13) 12.65, (14) 16.87, (15) 22.50, (16) 30.10 mM

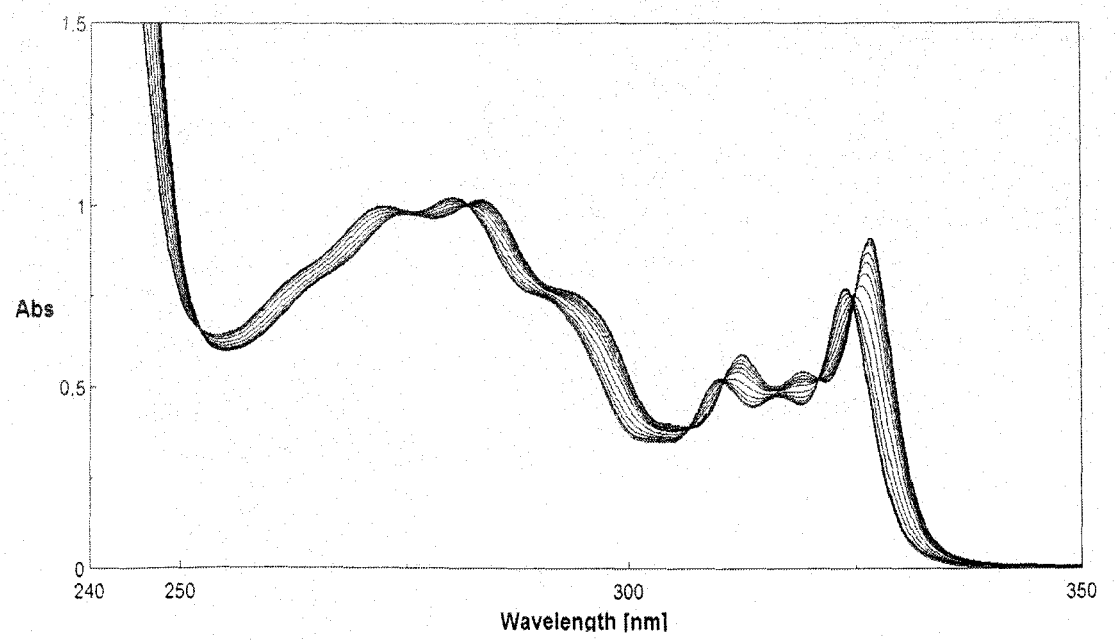

Figure 3.40: Absorption spectra of 2,3-dihydroxynaphthalene (0.25 mM) in water at varying concen-trations of DTAB at 25°C. [DTAB]: (1) 0.00 , (2) 6.92, (3) 8.31, (4) 9.97, (5) 11.96, (6) 13.05, (7) 14.24, (8) 15.53, (9) 16.95, (10) 18.49, (11) 20.17, (12) 24.20, (13) 29.05, (14) 34.86, (15) 41.84, (16) 50.20, (17) 60.25 mM

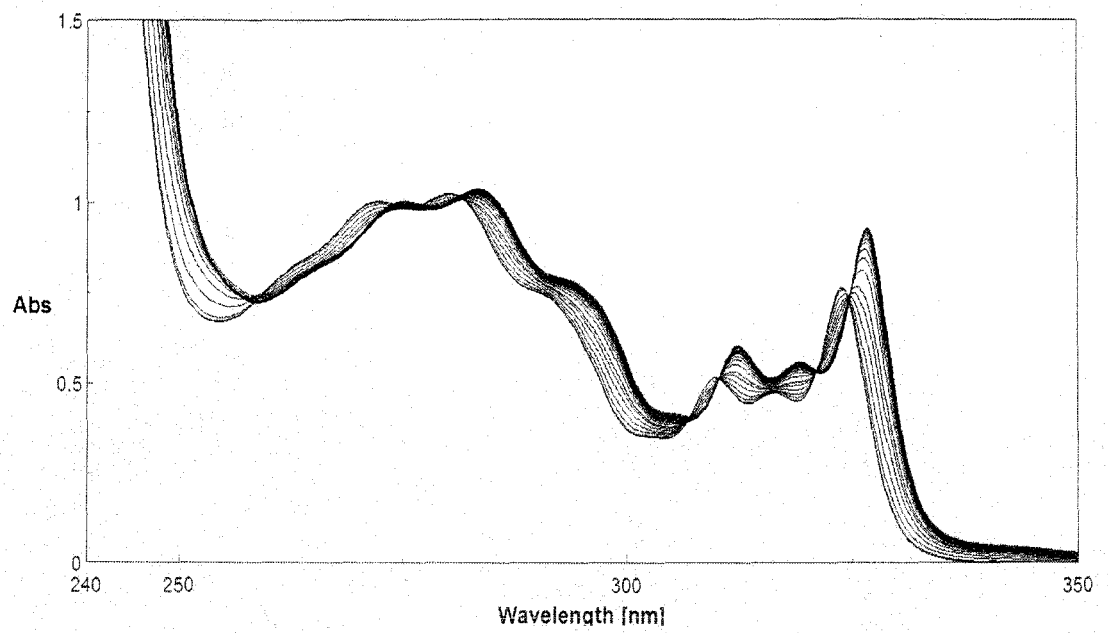

Figure 3.41: Absorption spectra of 2,3-dihydroxynaphthalene (0.25 mM) in water at varying concen-trations of TTAB at 25°C. [TTAB]: (1) 0.00 , (2) 1.78 , (3) 2.67, (4) 3.21, (5) 3.50, (6) 3.82, (7) 4.16, (8) 4.54, (9) 5.45, (10) 6.54, (11) 7.85, (12) 9.42, (13) 11.31, (14) 13.57, (15) 16.29, (16) 19.54, (17) 23.45, (18) 28.15, (19) 33.78, (20) 40.53 mM

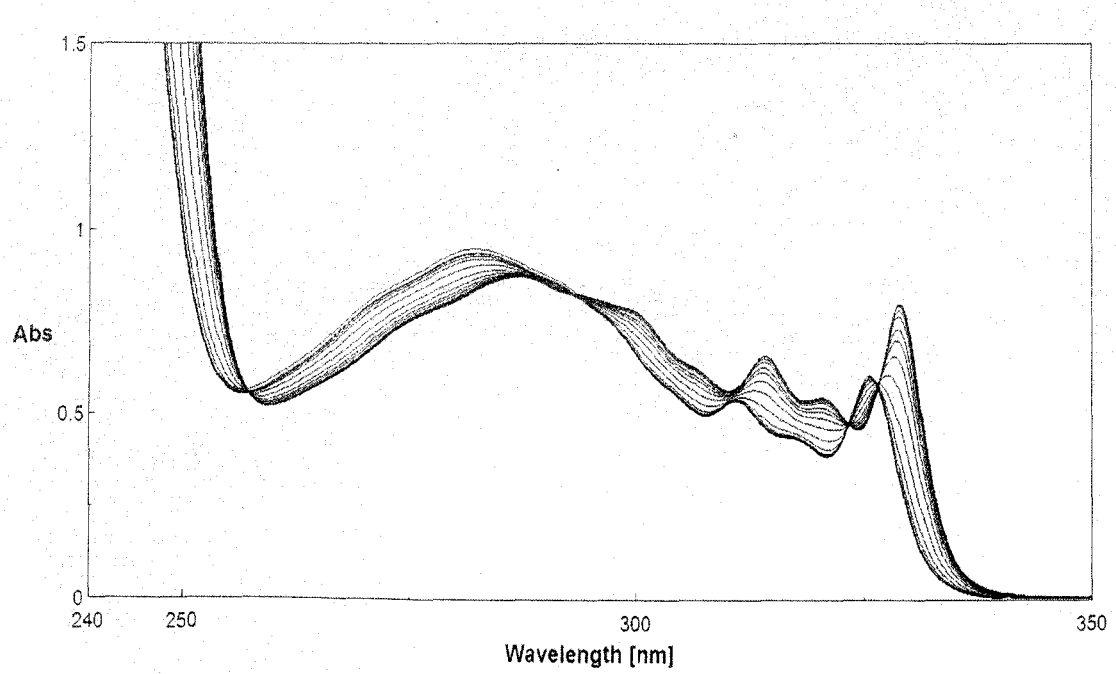

Figure 3.42: Absorption spectra of 2,7-dihydroxynaphthalene (0.25 mM) in water at varying concen-trations of DTAB at 25°C. [DTAB]: (1) 0.00 , (2) 6.23, (3) 8.31, (4) 9.97, (5) 11.96, (6) 13.05, (7) 14.24, (8) 15.53, (9) 16.95, (10) 18.49, (11) 20.17, (12) 24.20, (13) 29.04, (14) 34.85, (15) 41.82, (16) 50.19, (17) 60.23 mM

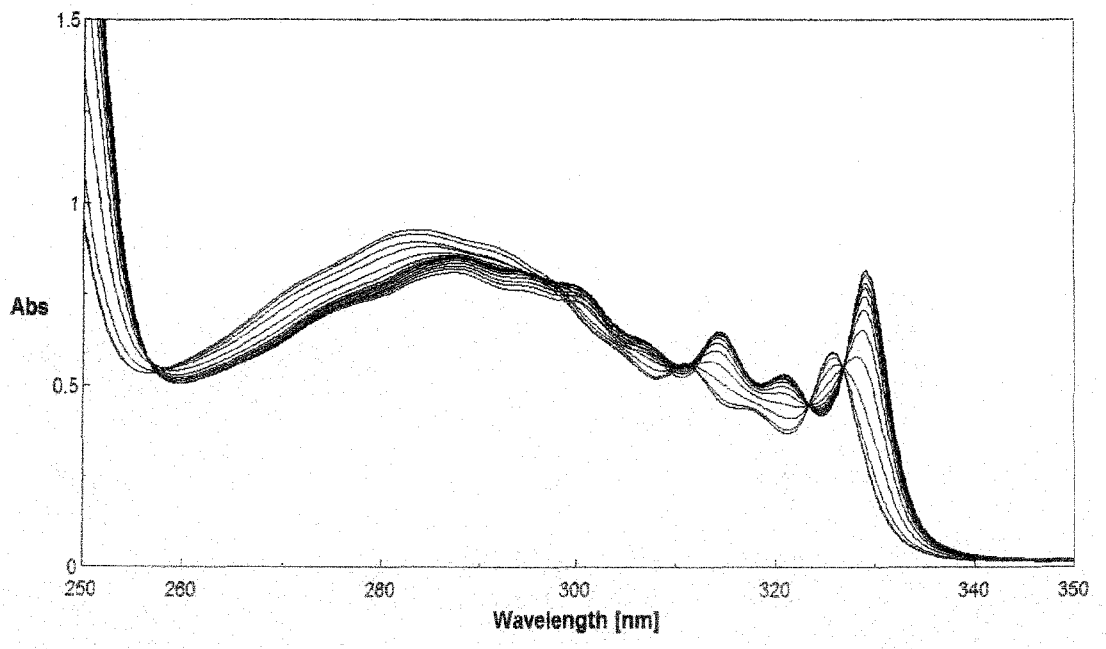

Figure 3.43: Absorption spectra of 2,7-dihydroxynaphthalene (0.25 mM) in water at varying concen-trations of TTAB at 25°C. [TTAB]: (1) 0.00 , (2) 1.56, (3) 2.09, (4) 2.79, (5) 3.35, (6) 4.02, (7) 4.82, (8) 5.78, (9) 6.94, (10) 8.33, (11) 10.00, (12) 15.00, (13) 21.38, (14) 25.66, (15) 30.80 mM

the result strongly indicates the presence of hydrogen bonding (as discussed for the naphthol/CTAB), between the micelle bound dopants and the surrounding interfacial water molecules.

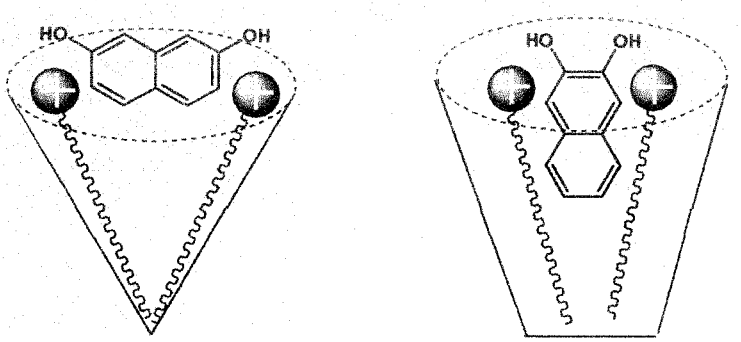

Figure 3.44: Schematic representation of the location and position of 2,3-DHN and 2,7-DHN in CTAB micelles.

From the above discussions, and the results obtained from ^{1}H NMR studies, the location and position of both the dihydroxynaphthalenes in micelles of CTAB can be understood. The schematic representation of the probable microstructure of the micelle in presence of the dopants is shown in figure 3.44. Because the polar hydroxyl groups must keep a certain contact with water, the positions of the hydroxyl groups in the naphthalene ring of 2,7-DHN prevents the ring from penetrating deeper into the micellar core. However, for 2,3-DHN the positions of the OH groups favour the entry of the hydrophobic aromatic part deep inside the micelle due to hydrophobic interactions. Thus, the packing of the 2,7-DHN /CTAB system should be less tight than for the 2,3-DHN/CTAB. The critical packing parameter of the 2,3-DHN/CTAB system most probably exceeds 1/3 and microstructural transition from micelles to worm like micelles take place in presence of strong cation- π interaction. On the other hand, such a possibility is remote in 2,7-DHN/CTAB system and the packing parameter value does not exceed 1/3. This corroborates the strong influence of the hydroxyl group, which apparently changes the orientation of the naphthalene ring at the micellar surface. Thus, unlike the hydroxynaphthalenes, the position of OH groups in dihydroxy-naphthalenes seems to be a decisive factor in the microstructural transiton of the micelles.

3.3.5 Surfactant Probe Binding Equilibrium

The enhancement of absorbance of the probe molecules in micellar solutions of alkyltrimethylammonium bromides can be rationalised in terms of binding of the probe with the micelle. As has already been mentioned, the most significant property of an organised assembly in spectroscopy is its ability to stabilise and bind solute molecules that are typically insoluble or sparingly soluble in bulk neat solvent [56]. However, the strength of binding can be identified through the determination of binding constant derived from the equilibrium between the probes and the micelle. Plots of absorbance at the longest wavelength band of all the dopants, against the concentrations of the surfactants, show discontinuity

at two critical points, one at the cmc and the other at the concentration beyond which no change in the position of the longest λ_{max} is observed. However, at concentrations between the two critical points, the curves are linear. For DTAB, linear plots are obtained between 14.6 to 20.0 mM and for TTAB and CTAB the linear portions are between 3.3 to 6.3 mM and 0.95 to 3.1 mm respectively. Hence, only the linear portions of the curve have been utilized to determine the binding constant in the present investigation. For the monohydroxy naphthalenes (1 and 2-naphthols) the values of the absorbance remains almost steady upon initial addition of surfactant, below the cmc, and then increases sharply and finally levels off to a plateau. The values of the absorbance of the probes in water and in presence of various concentrations of surfactants are utilized to obtain the strength of the binding between the two. The variation of absorbance of the monohydroxynaphthalenes (1- and 2-naphthols) and dihydroxynaphthalenes (2,3 and 2,7 –dihydroxynaphthalenes) against the concentration of the surfactants, viz; DTAB, TTAB and CTAB are shown in figure 3.45 to figure 3.56. It is interesting to note that the concentration from which a sharp rise in absorbance is observed, corresponds to the cmc of the individual surfactants. Therefore, the hydroxyaromatic compounds of the present investigation can serve to be potential probes for the determination of the critical micellisation concentrations as well. The values of cmc thus obtained are presented in table 3.1. As can be seen from figures 3.51 to 3.56, the dihydroxy naphthalenes (2,3-DHN and 2,7-DHN) too show break in the absorbance versus concentration plots. The values first decrease to a minimum and then increases. The minimum value is taken as the cmc of the surfactant. The values of cmc reported here are in good agreement with those reported in the literature [75, 76].

The binding constant K_s's (and surfactant c.m.c.'s) of the individual probe molecules, namely 1-naphthol, 2-naphthol, 2,3-dihydroxy-naphthalene and 2,7-dihydroxy-naphthalene along with the methoxynaphthalenes with alkyltrimethylammonium bromide micelles are determined from the study of the effect of added surfactant on the absorption spectra of the dopants using the following relationships:

$$f / (1- f) = K_s \{ [D] - [S]_t f \} - K_s \text{ cmc.}$$

Where, $f = [S_m] / [S_t]$ and $D_m = [D_t] - \text{cmc}$ (suffix t refers to total). Above equation is drawn assuming following equilibrium to hold between aqueous solubilisate (S_w) and the surfactant (D_m) to form the micelle embedded substrate (S_m),

$$S_w + D_m = S_m$$

Experimentally, f is calculated by, $f = (A - A_w) / (A_m - A_w)$, where A, A_w, and A_m are absorption intensities in surfactant, in water and at complete micellization of substrate, respectively. A plot of f/(1- f) against ([D] – $[S]_t$ f) shows discontinuity at two critical points (as mentioned above). The plot of f/(1- f) against ([D] – $[S]_t$ f) for the probe molecules in DTAB, TTAB, and CTAB gives good straight lines, from the slope of which the binding constant K_s is obtained. The plots utilized to obtain the binding constant values are shown in the inset of figures 3.45 to 3.56. The values of the binding constants with micelles of DTAB, TTAB and CTAB and the dopants are listed in table 3.1. The binding constants of the probe molecules with the surfactants increase with the increase in the chain length of the micelle and follow the order CTAB > TTAB > DTAB. Increase in the hydrocarbon chain length of surfactant increases the compactness of the micelle which in turn favours stronger binding with the additive molecules. The lesser hydration of CTAB micelles as compared to those of DTAB and TTAB may also be the reason for the stronger binding of probes with CTAB micelles.

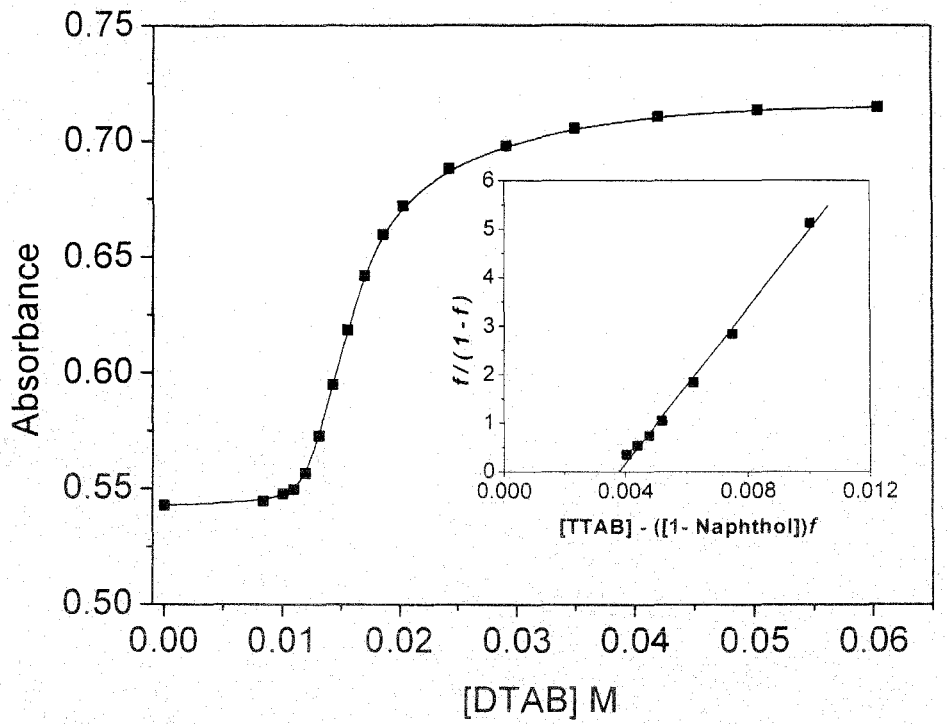

Figure 3.45: Plot of absorbance of 1-naphthol (0.25 mM) against the concentration of aqueous DTAB. The value of K_s (binding constant) were determined from the slope of the plot in the inset.

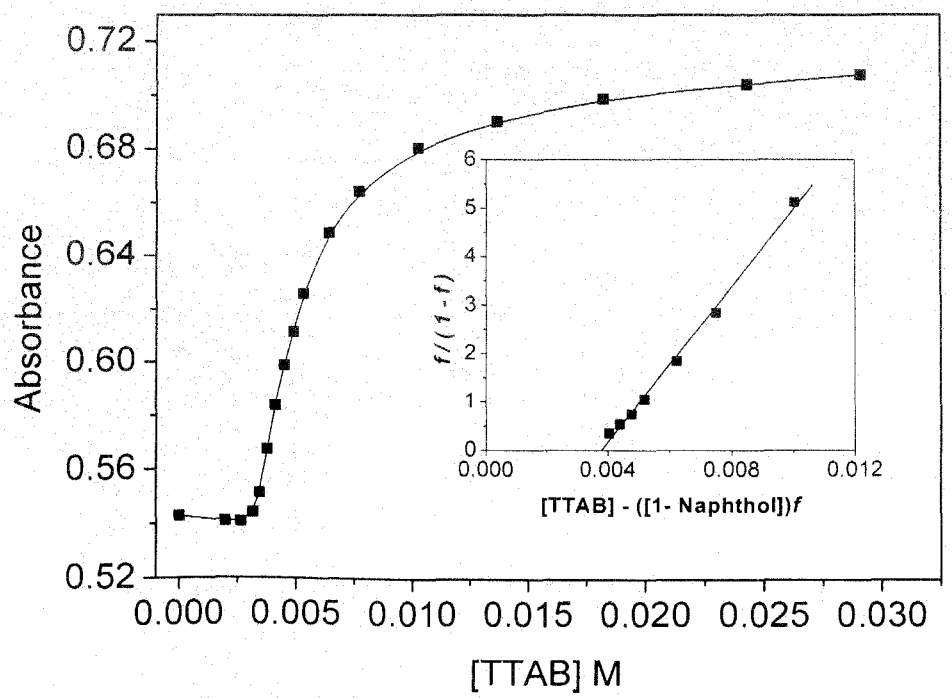

Figure 3.46: Plot of absorbance of 1-naphthol (0.25 mM) against the concentration of aqueous TTAB. The value of K_s (binding constant) were determined from the slope of the plot in the inset.

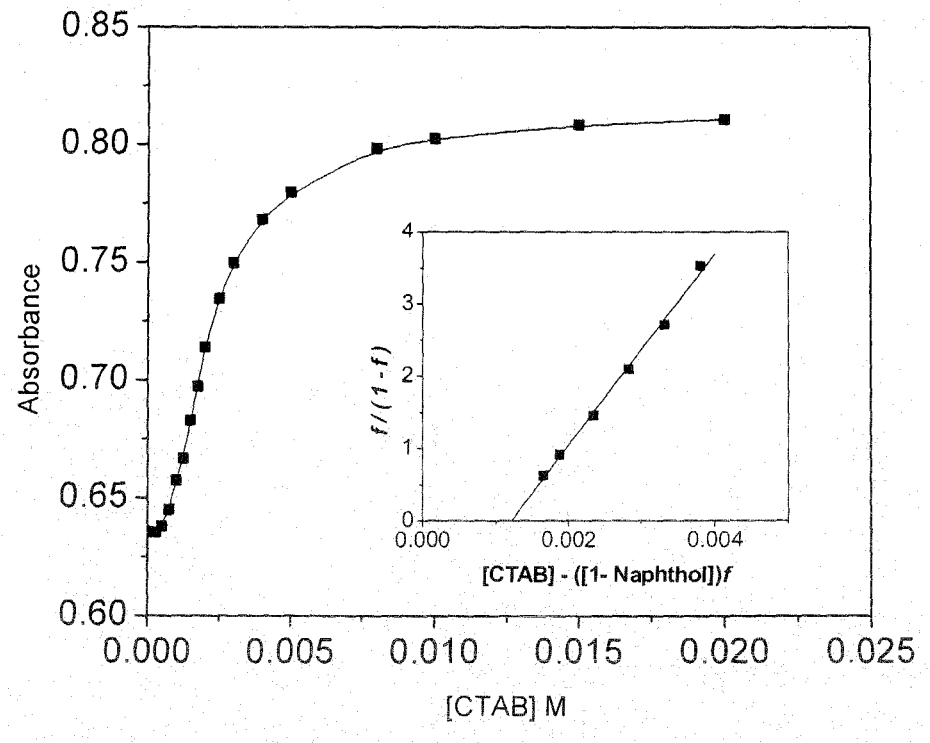

Figure 3.47: Plot of absorbance of 1-naphthol (0.25 mM) against the concentration of aqueous CTAB. The value of K_s (binding constant) were determined from the slope of the plot in the inset.

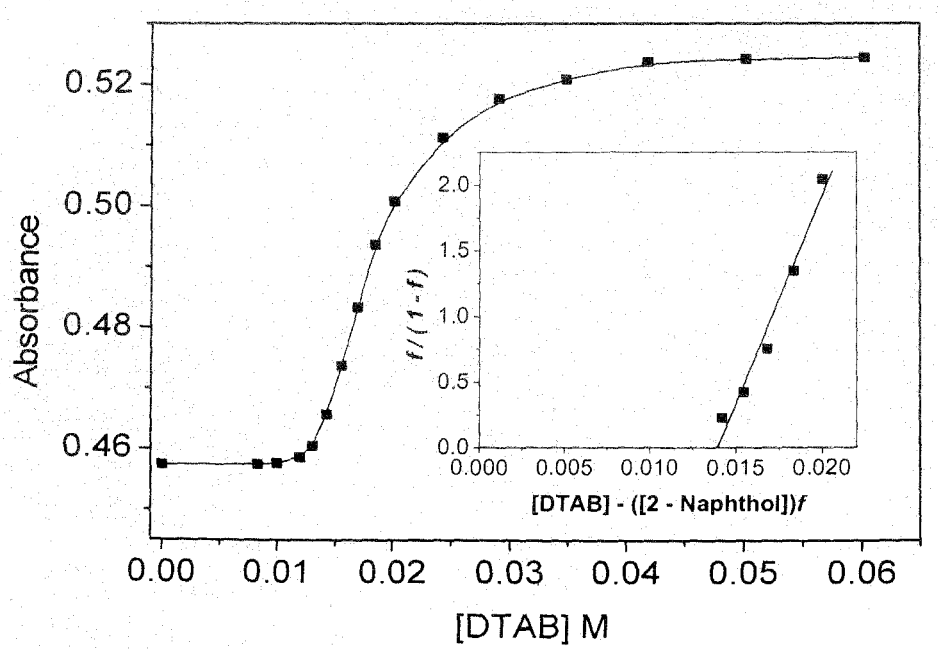

Figure 3.48: Plot of absorbance of 2-naphthol (0.25 mM) against the concentration of aqueous DTAB. The value of K_s (binding constant) were determined from the slope of the plot in the inset.

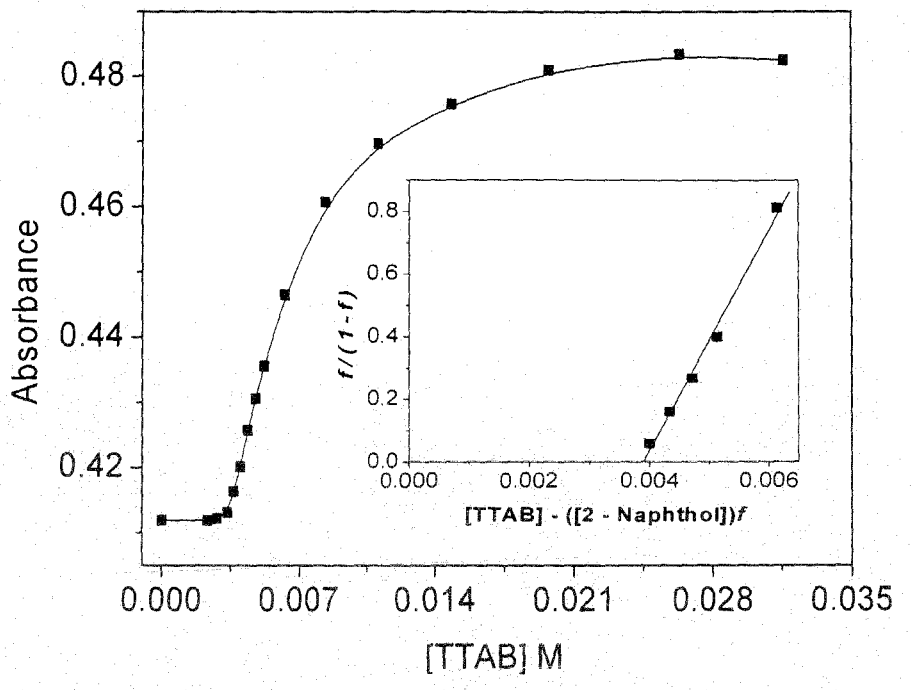

Figure 3.49: Plot of absorbance of 2-naphthol (0.25 mM) against the concentration of aqueous TTAB. The value of K_s (binding constant) were determined from the slope of the plot in the inset.

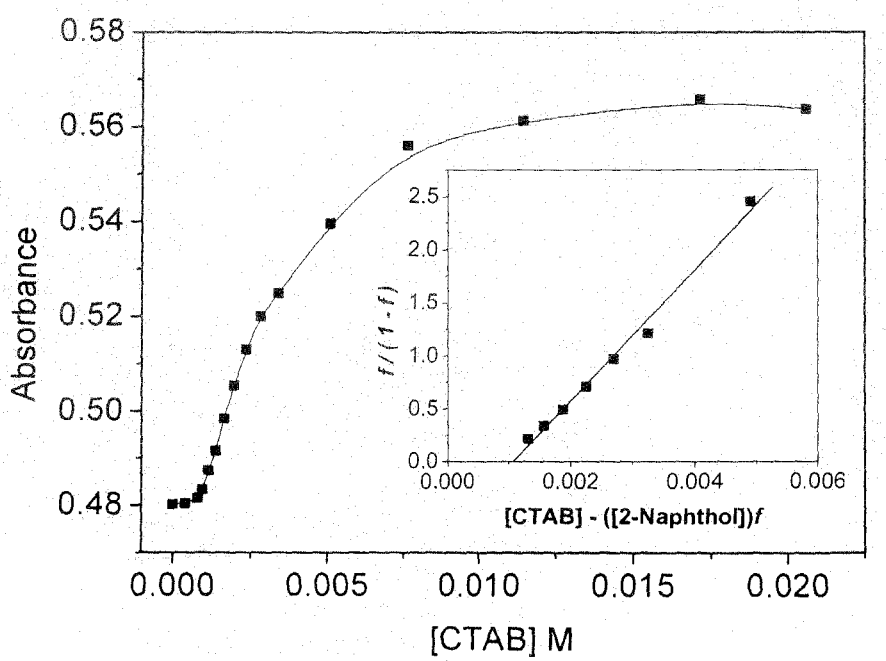

Figure 3.50: Plot of absorbance of 2-naphthol (0.25 mM) against the concentration of aqueous CTAB. The value of K_s (binding constant) were determined from the slope of the plot in the inset.

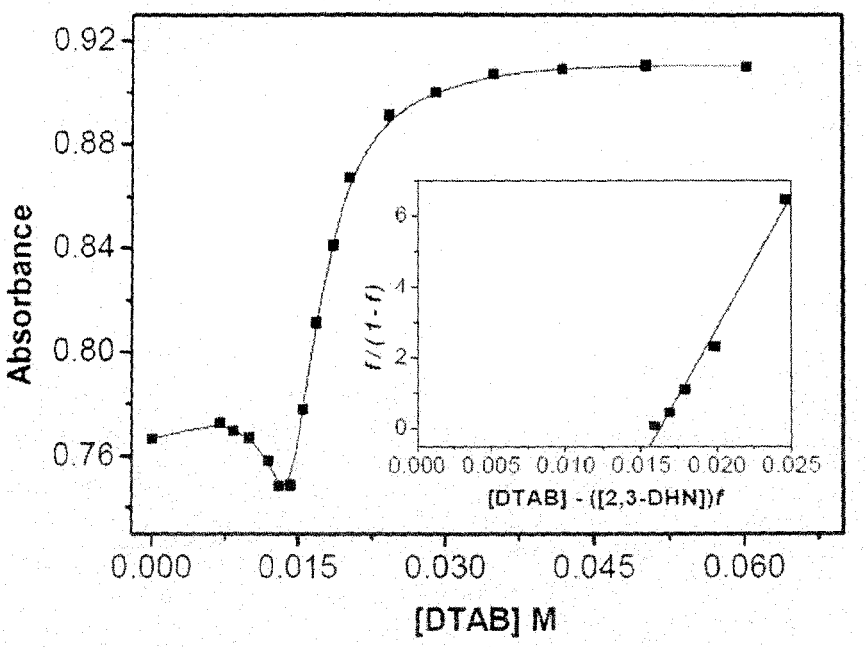

Figure 3.51: Plot of absorbance of 2,3-dihydroxynaphthalene (0.25 mM) against the concentration of aqueous DTAB. The value of K_s (binding constant) were determined from the slope of the plot in the inset.

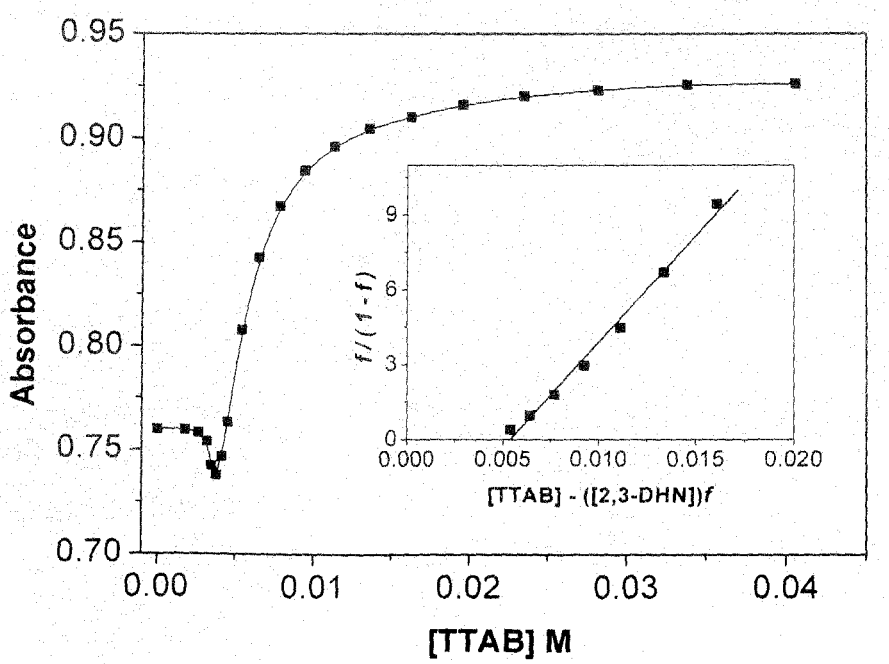

Figure 3.52: Plot of absorbance of 2,3-dihydroxynaphthalene (0.25 mM) against the concen-tration of aqueous TTAB. The value of K_s (binding constant) were determined from the slope of the plot in the inset.

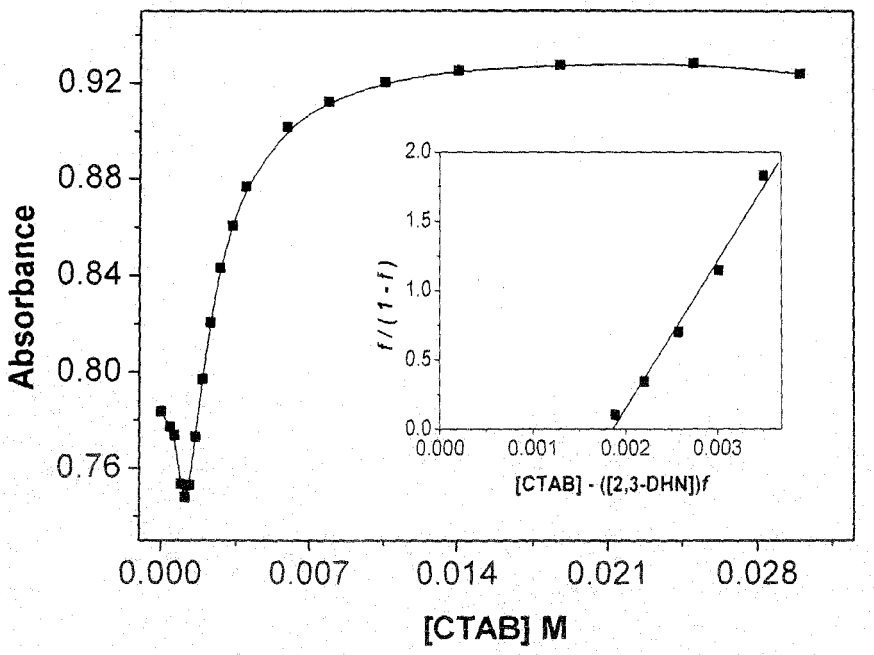

Figure 3.53: Plot of absorbance of 2,3-dihydroxynaphthalene (0.25 mM) against the concen-tration of aqueous CTAB. The value of K_s (binding constant) were determined from the slope of the plot in the inset.

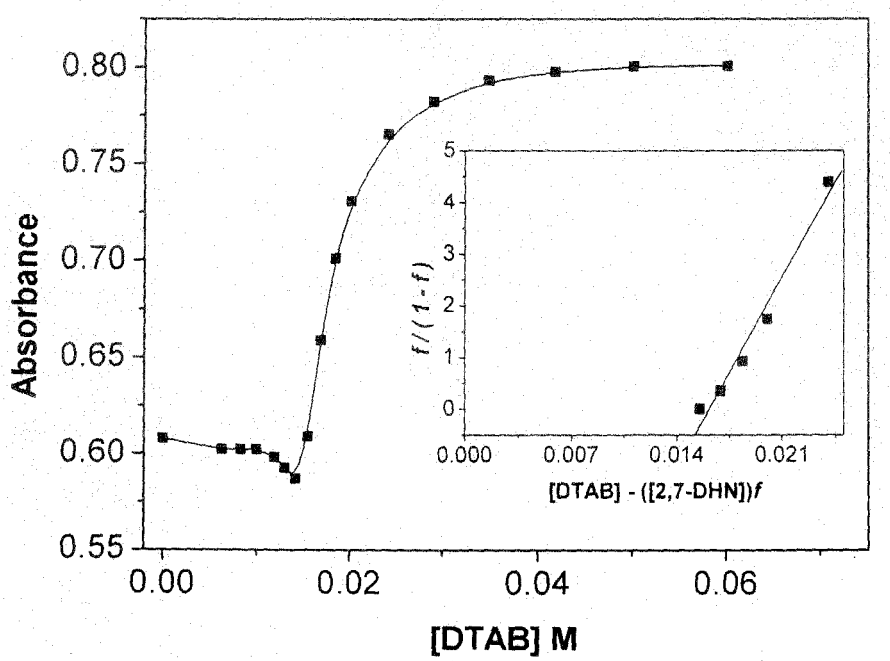

Figure 3.54: Plot of absorbance of 2,7-dihydroxynaphthalene (0.25 mM) against the concentration of aqueous DTAB. The value of K_s (binding constant) were determined from the slope of the plot in the inset.

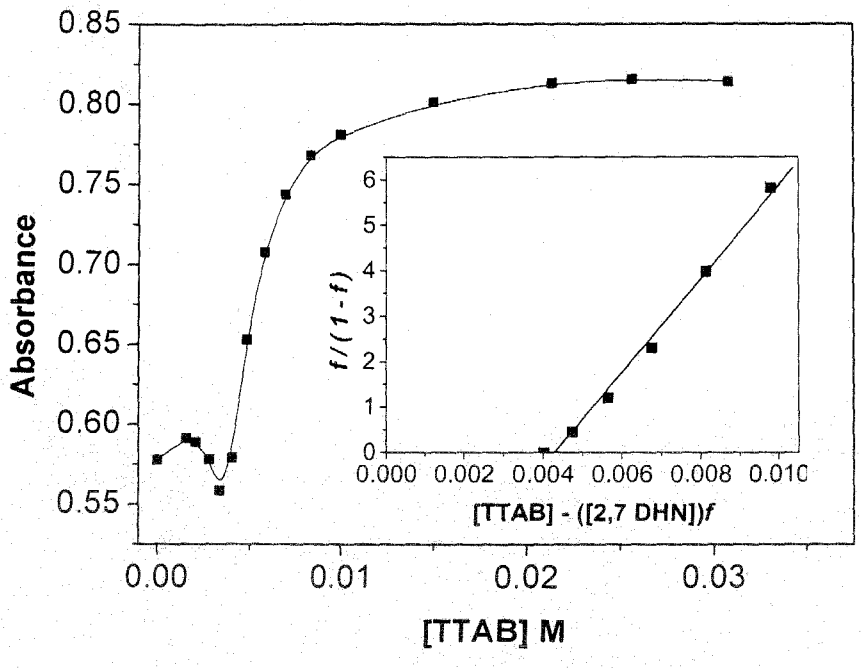

Figure 3.55: Plot of absorbance of 2,7-dihydroxynaphthalene (0.25 mM) against the concen-tration of aqueous TTAB. The value of K_s (binding constant) were determined from the slope of the plot in the inset.

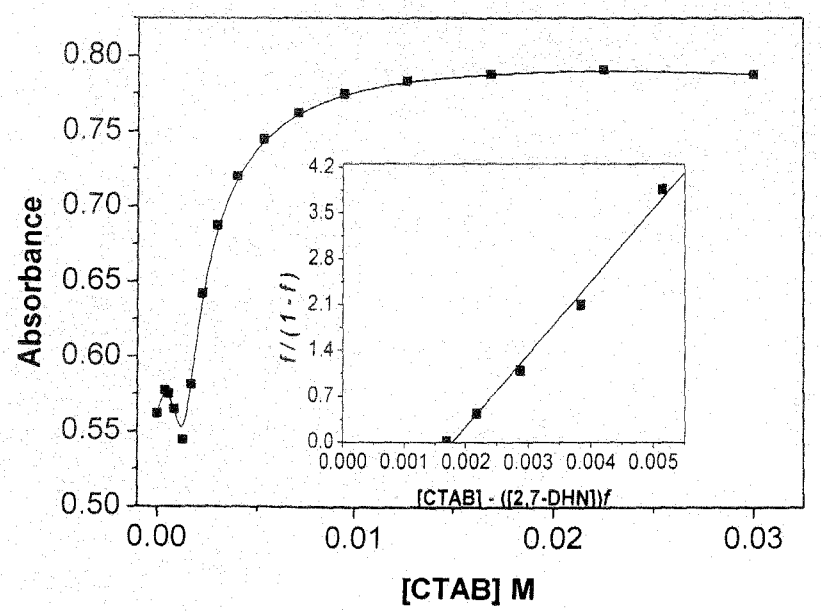

Figure 3.56: Plot of absorbance of 2,7-dihydroxynaphthalene (0.25 mM) againstthe concen-tration of aqueous CTAB. The value of K_s (bindingconstant)determined from the slope of the plot in the inset.

Table 3.1. Values of the binding constants and the cmc determined from the UV absorption studies.

Dopant	Surfactant	K_s	r	cmc x10^3 mM
	DTAB	514	0.9942	14.7
1-Naphthol	TTAB	801	0.9989	3.3
	CTAB	1325	0.9981	1.0
	DTAB	505	0.9840	14.5
2-Naphthol	TTAB	638	0.9918	3.2
	CTAB	723	0.9953	1.1
	DTAB	745	0.9925	14.7
2,3-DHN	TTAB	768	0.9974	3.4
	CTAB	1061	0.9845	1.1
	DTAB	529	0.9916	14.8
2,7-DHN	TTAB	1029	0.9964	3.4
	CTAB	1110	0.9896	1.1
1-MN	CTAB	448	0.9918	-
2-MN	CTAB	326	0.9848	-

Therefore, greater the compactness of the microstructure stronger is the binding between the probe and the micelle and vice-versa. Though the binding constant values of the surfactants follow the above order, no systematic trend was observed for the different probes in micellar media.

3.3.6 Cryogenic Transmission Electron Microscopy (cryo-TEM) Study

Cryo-TEM images of the CTAB-2-naphthol system at low and high pH's are shown in Figures 3.57 to 3.59. At low pH (pH ~5.5), the micrograph looks like a condense, isotropic, and continuous network (Figure 3.57) of worm ike micelles along with monodisperesed vesicles of very short diameters.

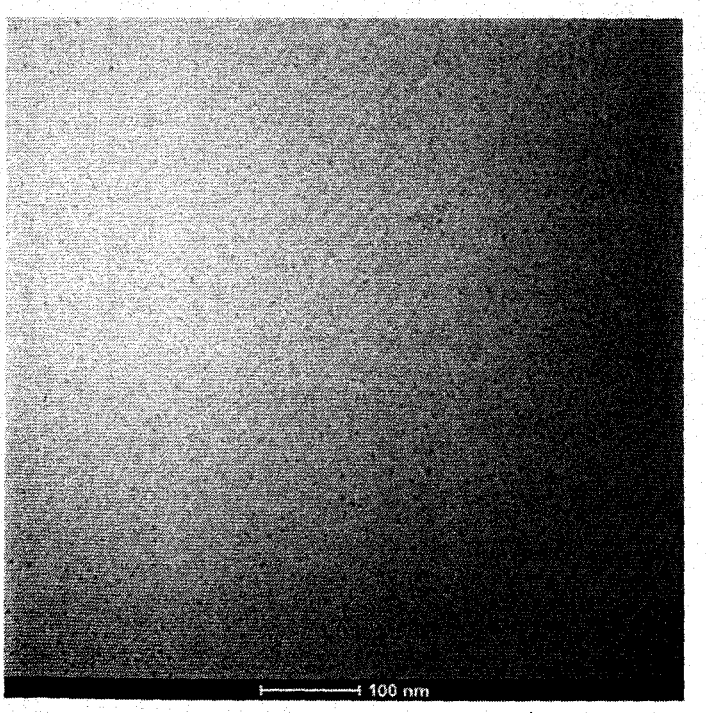

Figure 3.57: cryo-TEM micrographs of the CTAB-2-naphthol system (10 mM, 1:1) at pH ~5.5.

The micelles are slightly entangled and are shown in figure 3.58. At high pH (pH~9.4), the system contains very long (endless in micrograph) wormlike micelles, which coexist with large unilamellar vesicles. This is undoubtedly due to

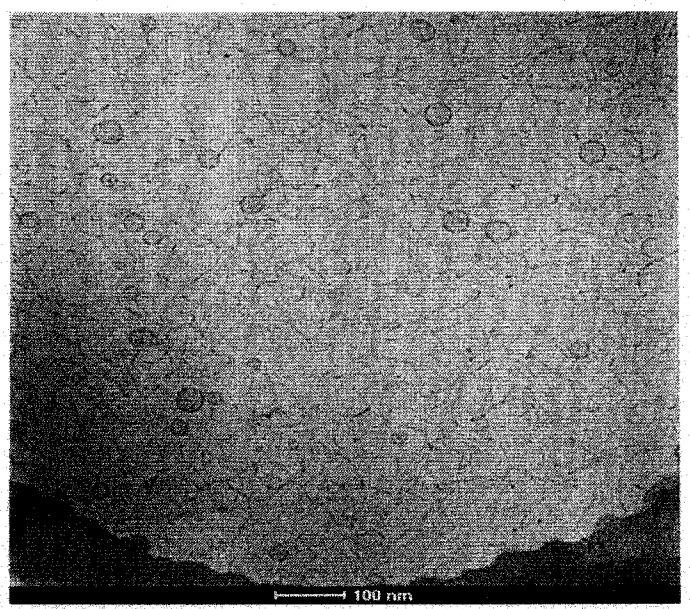

Figure 3.58: cryo-TEM micrographs of the CTAB-2-naphthol system (10 mM, 1:1) at pH of ~9.4)

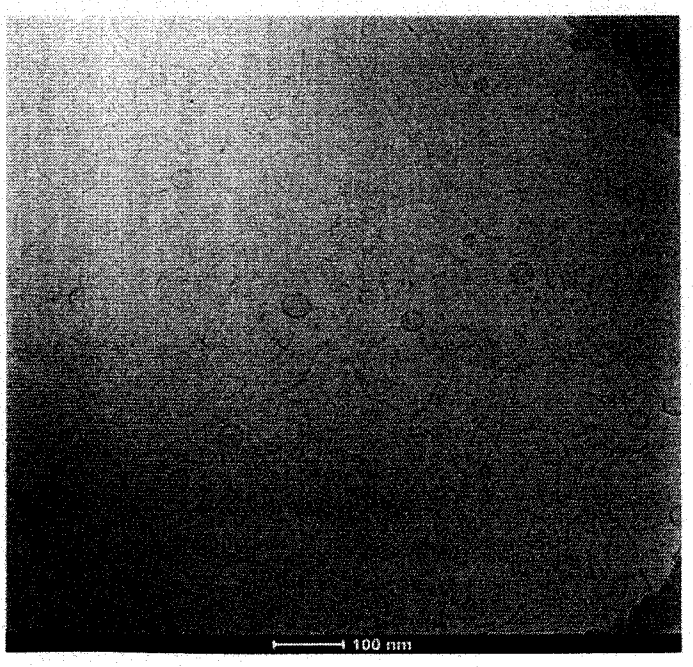

Figure 3.59: cryo-TEM micrographs showing linearly elongated worm-like micelles of the CTAB-2-naphthol system (10 mM, 1:1) at high pH (~9.4) under shear flow.

enhanced charge screening of micelles by naphtholate anions (discussed in section 3.3.3). The field is seen to populate mainly by large vesicles of diameter ~30 nm along with thinly populated smaller vesicles. It is also seen that the long worm-like micelles are highly entangled. Sometimes they are found to elongate linearly under shear flow (Figure 3.59). The solutions are completely transparent. The direct imaging by cryo-TEM supports the rheological observation as a function of pH. At low pH, the worm-like micelles are formed via headgroup charge shielding by aromatic π electrons, whereas, at high pH, ionization of OH groups takes place and the packing parameter exceeds the critical value of 1/2 via enhanced charge screening by naphtholate ions. This leads to unilamellar vesicle formation along with long worm-like micelles.

3.3.7 Orientation of water molecules at the micelle-water interface

Phospholipid bilayers, the main constituent of cell membranes, are important structural components in biological systems. The membrane/water interface provides a unique environment for many biochemical reactions, and the associated interfacial water is an integral part of such reactions. Water in this restrictive environment behaves differently, which affects many biochemical reactions. Therefore, a molecular level elucidation of the structure and orientation of water and lipid/water interfaces is essentially important to understand the adsorption and desorption of various biomolecules, ions and drugs at the biological interfaces [77-80]. In spite of its importance, we are yet to have a unanimous understanding of the water structure even for very simple lipid/water interfaces.

Recently vibrational sum frequency generation (VSFG) study, which is an interface specific spectroscopy, on charged lipid/water interfaces, confirms that the orientation of interfacial water is governed by the net charge on the lipid head group [78-80]. At an anionic lipid/water interface, water is in the hydrogen up

orientation, and at the cationic lipid/water interface, water is in the hydrogen down orientation. At the cationic and anionic lipid/water interface, interfacial water has comparable hydrogen bond strength, and it was analogous to the bulk water. In this section of the thesis spectroscopic results are revisited to confirm the orientation and restructuring of water molecules at the cationic micelle-water interface and demonstrated that H bonding and cationic- π interactions are involved in the formation of viscoelastic gels.

Micelles of different cationic surfactants viz., CTAB, OTAB, CPB, CPC etc., behave similarly in the presence of π-conjugated molecules with hydrogen bonding functionality like 1-naphthol, 2-naphthol, dihydroxynaphthalenes and alkyl substituted phenols [57, 81-84]. These systems form stimuli responsive viscoelastic gels at low surfactant concentrations. Role of aromatic π-electron systems in screening the charge of cationic head groups in spherical micelles is obvious. Interestingly, another aromatic π-electron system viz., methoxynaphthalenes failed to tune viscoelastic gelation in the above cationic surfactant system. In section 3.2.2 of the thesis it has been shown that the UV absorption spectra of micelle embedded naphthols provides some interesting results. The spectroscopic data strongly indicates the formation of unusual H-bond at the micellar interface by the dopant molecules with interfacial water. It has been argued that the OH groups of naphthols can act as both a proton donar as well as proton acceptor in forming intermolecular H bonds. H-bond in which the hydroxyl groups of naphthols is proton donor releases electron density from the O-H bond towards the oxygen and hence, by an inductive effect, toward the aromatic ring. This causes red shift of the π- π^* transition. Conversely, if the H-bond is formed in which the hydroxyl oxygen is a proton acceptor, electrons are withdrawn from the naphthalene ring, and an opposite shift is anticipated. In the present case, a significant red shift starts to occur (6.4 nm at λ_{max} ~293 nm) in the presence of CTAB just above its cmc (0.96 mM) with an well defined isobestic point at 296 nm. Such shifting of the λ_{max} continue to occur until most of the naphthols are partitioned in CTAB micelles at high surfactant concentration. The results suggest that the protruded OH groups of micelle embedded naphthols

form naphthols acts as H-donar and dioxane as the acceptor (figure 3.26). Previously, it has been shown that in the ground state 1-naphthol interacts with bulk water via

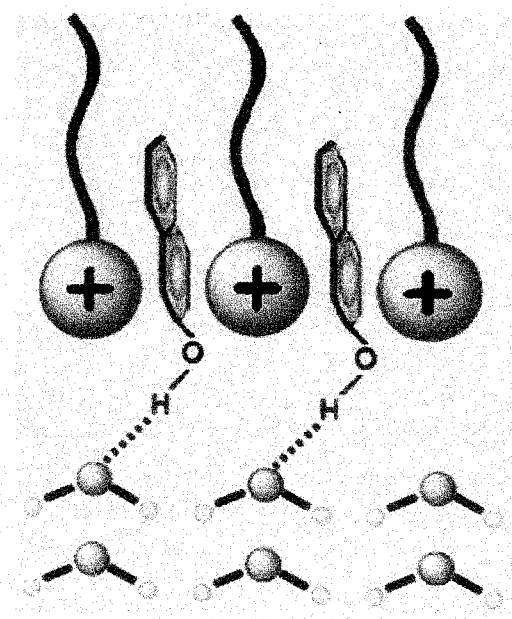

Figure 3.60: Schematic representation of the orientation of water molecules at the micelle water interface.

oxygen [66]. The nature of spectral modifications encountered by micelle free naphthol molecules in the presence of water is shown in figure 3.27. The figure shows that on every addition of water (upto 10 % v/v) substantial gain in intensity is displayed by 1-naphthol spectra with little change in wavelength. The result of the study confirms the orientation of water molecules at the micelle/water interface (figure 3.60) i.e., the electrostatic potential of the positive charges of surfactant head groups orient the water dipoles in hydrogen down direction such that the protruded OH groups can only form H-bonds with oxygen atoms of water as the acceptor site. In such a situation both the hydrogen atoms of water are directed away from the micellar head groups restricting the possibility of formation of H-bonds where water hydrogens might be donar. This result is in perfect agreement with the recent observation found via VSFG studies.

3.4 Refarence

1. J.H.Fuhrop, and J.Köning, *Membranes and Molecular Assemblies: the Synkietic Approach*, The Royal Society of Chemistry - Cambridge, (1994).
2. J. H. Clint, *Surfactant Aggregation*, Blackie - Glasgow/London, (1992).
3. M.J.Rosen, *Surfactants and Interfacial Phenomena*, Wiley-Interscience, New York, (2004).
4. F.Reiss-Husson and V. Luzzati, *J. Phys. Chem.*, **68**, 3504 (1964).
5. P. Ekwall, L. Mandell, and P. Solyom, *J. Colloid Interface Sci.* **35**, 519 (1971).
6. K .Fontell, A. Khan, B. Lindström, D. Maciejewska, and S. Puang-Ngern, *Colloid Polym. Sci.*, **269**, 727(1991).
7. G.Porte, Y. Poggi, J.Appell, and G. Maret, *J. Phys. Chem.* **88,** 5713 (1984).
8. P.Debye, and E.W. Anacker, *J. Phys. Chem.* **55**, 644(1950).
9. F.Quirion, and L. J. Magid, *J. Phys. Chem.* **90**, 5435 (1986)
10. S.J. Candau, E. Hirsch and R. Zana, *J. Colloid Interface Sci.* **105,** 521(1985).
11. P.J. Missel, N.A. Mazer, G.B. Benedeck and M.C. Carrey, *J. Phys. Chem.* **87**, 1264(1983)
12. L.J.Magid, Z. Li and P.D. Butler, *Langmuir.* **16**, 10028 (2000).
13. J. H. Mu, G. Z.Li, X. L. Jia, H. X.Wang, and G.Y. *J.* Zhang, *Phys. Chem. B.* **106**, 11685(2002).
14. J. H. Mu, G. Z.Li and H. X. Wang, *Rheol. Acta.*, **41**, 493(2002).
15. L.J.Yu, and A. Saupe, *Phys. Rev. Lett.* **45,** 1000(1980).
16. Y.Hendrikx, J. Charvolin, M. Rawiso, L.Liebert and M.C. Holmes, *J. Phys. Chem.* **87**, 3991(1983).
17. L.Q. Amaral and M.E.M. Helene, *J. Phys. Chem.* **92**, 6094(1988).
18. T. Thiele, J.F. Berret, S.Muller and C. Schmidt, *J. Rheol.* **45**, 29(2001).
19. G.Porte, R. Gomati, O.E. Haitamy, J. Appell, and J. Marignan, *J. Phys. Chem.* **90**, 5746(1986).
20. Y.A .Nastishin,. *Langmuir.* **11**, 5011(1996).
21. K.Bijma, and J.B.F.N. Engberts, *Langmuir* , **13**, 4843(1997).
22. K.Bijma, M.J. Bandamer and J.B.F.N. Engberts, *Langmuir.* **14**, 79(1998).

23. M.Bergström and J.S. Pedersen, *Langmuir.* **15**, 2250(1999).

24. H.Yin, M. Mao, J.Huang, and H. Fu, *Langmuir.* **18**, 9198(2002).

25. E.W. Kaler, K.L. Herrington, A.K. Murthy and J.A.N. Zasadzinski, *J. Phys. Chem.* **96**, 6698(1992).

26. R.D.Koehler, S.R.Raghavan, and E.W. Kaler, *J. Phys. Chem. B.* **104**, 11035(2000).

27. T. Nash, *J. Colloid Sci.* **13**, 134(1958).

28. J. Ulmius, H. Wennerström, L. B. Å. Johansson, G. Lindblom and S. Gravsholt, *J. Phys. Chem.* **83**, 2232(1979).

29. S. Gravsholt, *J. Colloid Interface Sci.* **57**, 575(1976).

30. M. Doi and S.F Edwards, *The Theory of Polymer Dynamics*, Oxford, Clarendon Press. (1986).

31. H.Rehage and H. Hoffmann, *Mol. Phys.* **74,** 933(1991).

32. H. Hoffmann, H. Löbl, H.Rehage and I.Wunderlich *Tenside Detergents.* **22**, 290(1985).

33. H. Rehage and H. Hoffmann *Phys. Chem.* **92**, 4712(1988).

34. T. Shikata, K. Hirata and T. Kotaka *Langmuir.* **3**, 1081(1987).

35. T. Shikata, K. Hirata and T. Kotaka *Langmuir.* **4**, 354(1988).

36. T. Shikata, K. Hirata and T. Kotaka *Langmuir.*, 5, 398(1989).

37. Shikata, T.; Hirata, K.; Kotaka, T. *J. Phys. Chem.* **94**, 3702(1990).

38. F.Kern, R.Zana and Candau, *Langmuir.* **7**, 1344(1991).

39. A.Khatory, F. Lequeux, F. Kern and S.J. Candau, *Langmuir.* **9,** 1456(1993).

40. J. Narayanan, E. Mende and C Monohar, *International Journal of Modern Physics B.* **16**, 375(2002).

41. E. Mendes, R.Oda, C.Monohar and J.Narayanan, *J. Phys. Chem. B* **71**, 338(1998).

42. S. Mishra, B. K. Mishra, S. D. Samant, J.Narayanan and C. Manohar, *Langmuir.* **9**, 2804(1993).

43. R. Oda ,J.Narayanan, P. A. Hassan, C. Manohar , R. A Salkar, F.Kern and S.J. Candau, *Langmuir* **14,** 4364(1998).

44. P. A. Hassan , S.J. Candau ,F.Kern Manohar, and C. Manohar, **14**, 6025(1998).

45. F. Lequeux, *Europhys. Lett.* **19**, 675(1992).

46. B. K. Mishra, S. D. Samant, P. Pradhan, B. Mishra and C. Manohar. *Langmuir* **9,** 894(1993).

47. P. A. Hassan, B. S. Valaulikar, C. Manohar, F. Kern, L. Bourdieu and S.J. Candau, *Langmuir* **12**, 4350(1996)

48. G. C. Kalur, B. D. Frounfelker, B. H. Cipriano, A. I. Norman, and S. R. Raghavan. *Langmuir* **21**, 10998(2005).

49. J. N. Israclachivli, D. J.Mitchell, and B. W. Ninham, *J. Chem. Soc.Faraday Trans.* **72,** 1525(1976).

50. U. R. K. Rao, C. Manohar, B. S. Valaulikar and R. M. Iyer, *J. Phys.Chem.* **91**, 3286(1987).

51. T. Takemura, K. Hara and H. Baba, *Bull. Chem. Soc. Jpn.* **44,** 977(1971).

52. K. Hara and H. Baba, *Mol. Phys.* **18**, 1100(1974).

53. N. Mataga and Y. Kaifu, J. *Chem. Phys.* **36**, 2804(1962).

54. H. Baba and S. Suzuki, *J. Chem. Phys.* **35**, 1118(1961).

55. A. Tramer, and M. Zaborowska, *Acta Phys. Pol.* **34**, 821(1968).

56. R.Karmakar and A. Samanta, *Chem. Phys. Lett.* **376**, 638(2003).

57. S.K. Saha, M. Jha, M. Ali, A. Chakraborty, G.Bit and S.K Das.. *J. Phys. Chem. B.* **112**, 4642(2008).

58. D. A. Dougherty, *Science* **271**, 163(1996).

59. I. Harwigsson and M. *J.* Hellsten *Am Oil Chem Soc* 73, 921(1996).

60. J. Myska and Z. Chara, *Exp Fluids* **30**, 229(2001).

61. Y. Lin, X. Han, J. Huang, H. Fu and C. Yu, *J. Colloid Interface Sci.* **330**, 449. (2009).

62. M. Tata, V. T.John, Y. Y. Waguespack and G. L McPherson,. *J. Phys. Chem.* **98,** 3809(1994).

63. F.Grieser and C. J. Drummond, *J. Phys. Chem.* **92**, 5580(1988).

64. S. K. Das, Ph.D. thesis, University of North Bengal, India,(2006).

65. G. Nemethy and A. Ray, *J. Phys. Chem.* **77**, 64(1973).

66. O. M. Zharkova, B. V.Korolev and Y. P. Morozova, *Russ. Phys. J.* **46,** 68(2003).

67. C.Ramachandran ,R. A. Pyter and P. Mukherjee, *J. Phys. Chem.* **86**, 3198(1982).

68. K. Bhattacharya, *J. Fluoresc.* **11**, 167(2001).

69. S.Balasubramanian, S. Pal and B. Bagchi, *Curr. Sci.* 82, 845(2002)

70. J. Gasjo, E. Anderson, J. Forsbeing, E. F. Aziz, B. Brena, C.Johansson, J. Nordgren, L.Duda, J. Adersson, F.Hennies, J. Rubensson and P. Hansson, *J. Phys. Chem. B 113*, 8201(2009).

71. A. Mallick. B. Haldar, S. Maiti and N.Chattopadhyay, *J. Colloid. Interface Sci.* 278, 215(2004).

72. S.Berr, R. R. M. Jones and J. S. Johnson, *J. Phys. Chem.* **96**, 5611(1992).

73. N. Muller In *Reaction Kinetics in Micelles*; Cordes, E. A., Ed.; Plenum Press: New York, (1973).

74. E.Bardez, E.Monnier and B. Valeur, *J. Colloid Interface Sci.* **112**, 200(1986).

75. H. Akbas and T. Taner, *Spectrochim. Acta A.* **73**, 150(2009).

76. K.Weidemaier, H.L. Tavernier and M.D. Fayer, *J. Phys. Chem. B.*, **101**, 9352(1997).

77. A.Yokota, K..Tsumoto, M.Shiroishi, H.Kondo, and I. Kumagai, *J. Biol. Chem.* **278**, 5410. (2003).

78. J.A. Mondal, , S. Nihonyanagi ,S. Yamaguchi and T. Tahara, *J. Am. Chem. Soc.* **132**, 10656(2010).

79. S. Nihonyanagi ,S. Yamaguchi and T. Tahara T. *J. Chem. Phys.* **130**, 204704(2009).

80. M.Savago, E. Vartianien, and H. Bonn, *J. Chem. Phys.* **131**, 161107(2009).

81. M. Ali, M. Jha, S. K. Das and S. K.; Saha, *J. Phys. Chem. B* **113,** 15563(2009).

82. M. Singh, C.Ford, V.Agarwal, G. Fritz, A. Bose, V. T. John and G. L. McPherson, *Langmuir* **20**, 9931(2004).

83. C.Ford, M. Singh ,L.Lawson, J.He, V.John, Y. K. Lu, and G. Papadopoulos, McPherson and Bose, *Colloids Surf.* **B. 39,** 143(2004).

84. V.;Agarwal, M. Singh.; G.; McPherson, V.;John and A. Bose, *Colloids Sur., A.* **281**, 246(2006).

Chapter 4

Interaction of cationic micelles with 1 and 2 naphthols: self fluorescence monitoring of stimuli-responsive viscoelasticity and location of surface activity

4.1 Introduction and Review of Previous Work

Stimuli-responsive properties of viscoelastic gels of long wormlike micelles are fascinating and have created a great deal of interest in recent years [1-4]. Most extensively studied system is the cetyltrimethylammonium bromide (CTAB) micelles in presence of a hydrotrope, sodium salicylate (SS). Unlike simple halides, salicylate promotes sphere to wormlike micellar transi-tion at very low concentrations, viz., near the normal critical micelle concentration (cmc, 1 mM) of CTAB. The flexible and elongated wormlike micelles under dilute conditions show complex and unusual rheological phenomena, which include strong viscoelasticity and shear-induced structure (SIS) formation[5-7]. It is particularly interesting that, while a wide variety of wormlike ionic micellar solutions display identical rheological responses, a common element in most of these systems is the presence of salt anions such as SS. Although a few examples are available in the literature where additives other than SS have been used, these molecules have never been considered as high up as the promoter like SS[8]. However, a number of studies on micellar shape transition in cationic, anionic, and catanionic surfactant systems induced by polar and nonpolar organic species under comparatively high concentration conditions have been reported in the literature [9-11]. While hydrophobic molecules with either aromatic ring or small polar group have shown better efficiency, no unusual rheological feature was apparent under this condition. The presence of an anionic charge on the promoter molecule has been considered pivotal in achieving low concentration shape transition of cationic micelles via charge screening because it decreases the average area per surfactant head group allowing the packing parameter to exceed the critical value of $^1/_3$[12]. However, other important factors including the role of OH group of the promoter molecule have not attracted much attention, and as such, the puzzling question as to why not only its presence but also its position in the aromatic ring of SS molecule is so vital remains broadly unanswered[13]. Therefore, to understand the role of the OH group precisely, it was tempting to check what would

happen if we use uncharged naphthols where the hydrophobic part is very strong and the anionic charge is absent. In this paper we have studied effect of neutral 1- and 2-naphthols on the shape transition of CTAB and CPB micelles and shown that inter-molecular H bonding between OH groups of micelle embedded naphthol molecules plays a key role in micellar shape transition in absence of any charge screening of head groups and imparts strong viscoelasticity to the dilute aqueous surfactant solution.

4.2 Experimental

1-Naphthol(puriss) and 2-naphthol(puriss)(Aldrich products) were purified further by vacuum sublimation followed by recrystallization from 1:1 aqueous methanol. CTAB (puriss, Aldrich) and CPB (Aldrich) were used as received. ^{1}H NMR and Fourier transform infrared (FTIR) were recorded on a Bruker (300 MHz) spectrometer and a Shimadzu (083000) spectrometer, respectively. Steady state fluorescence was measured on a Perkin-Elmer LS-55 luminescence spectrometer. UV absorption spectra were recorded on a Jasco (V-530) spectro-photometer. Shear-induced viscosity was measured on a rota-tional viscometer (Anton-Paar, DV-3P; accuracy (1% and repeatability (0.2%) equipped with temperature controller and with the facility of varying shear rates.

4.3 Results and Discussion

4.3.1 Microscopic polarity at the location of OH groups of embedded naphthols

It is believed that while the aromatic ring of naphthols are embedded in micelles the core of which having dielectric constant around 2-7 only, the OH groups are stood out toward water region. NMR study also confirms that the aromatic ring of the naphthol resides near the non-polar core in between tetraalkylammonium head

groups of the surfactants. Although almost all of the previous studies on the hydrotrope induced microstructural transitions of micelles argue that the OH groups are protruded out of the micellar surface and remains close to aqueous layer, no experimental verification has so far been reported. To understand the exact nature of the location of the OH group, the micropolarity of the residence sites is determined. Spectral characteristics, specially fluorescence spectra, are often very sensitive to the environments around the probe molecule. Because of this, fluorescence spectroscopy has become one of the important methods for the study of the structure and dynamics of the microheterogeneous systems. Unfortunately, the excited state proton transfer process (ESPT) of hydroxyaromatic compounds, viz., 1 and 2-naphthols complicates their spectral properties. The absorption spectra are also not sensitive to the environmental conditions in the present system. Moreover, information regarding the microenvironment of aromatic π-electron system which might have been obtained from the study of spectral characteristics , would not be helpful in determining the location of protruded OH groups of naphthol molecules. Therefore pK_a shift of the acid-base equilibrium of OH group of naphthols in microheterogeneous medium relative to aqueous solution would be the ideal route for getting such information precisely. This shift in pK_a in a cationic micelle like CTAB relative to aqueous solution may be due to the surface potential of the micelle and the polarity variation at the micellar interface from that of the bulk (in absence of any specific interaction). The theoretical background of the analysis of data pertaining to the interfacial acid-base equilibrium of naphthol molecules has been well documented for other similar probes[14, 15]. While determining pK_a values of the present system, let us assume that the acid-base equilibrium of the OH group of naphthols is described by

$$\Phi OH + H_2O \quad = \quad \Phi O^- \; + \; H_3O^+ \qquad (1)$$

Where ΦO^-, ΦOH and H_3O^+ are deprotonated and protonated (neutral) forms of the naphthols and the proton respectively. For the naphthol indicators in aqueous

micellar solution, the apparent pK_a values were obtained from the change in the ultraviolet absorption spectra as a

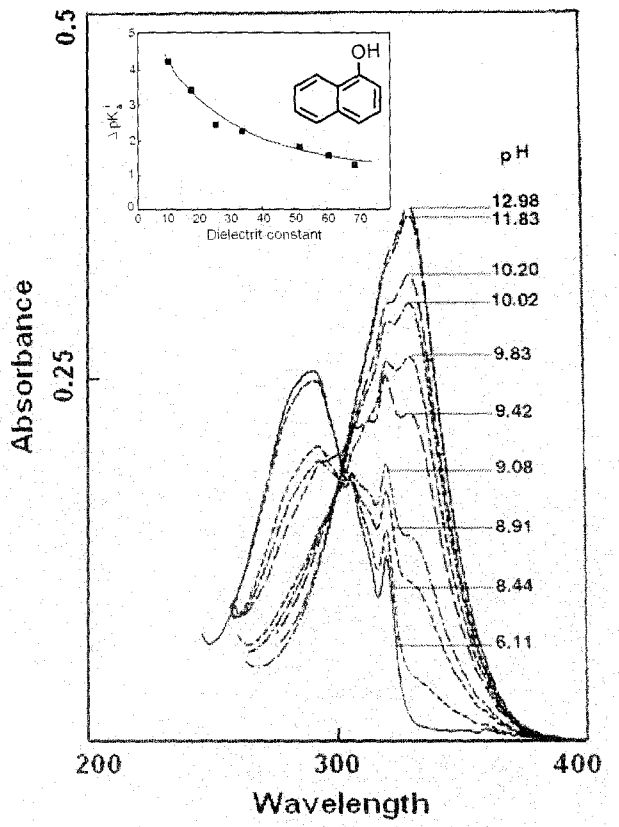

Figure 4.1: UV absorption spectra of 1-Naphthol (0.5 mM) in 5.0 mM CTAB at varying pH.

function of bulk aqueous pH by means of the following Handerson-Hasselbach equation (which considers only concentration terms at low concentration conditions) as follows (equation 2):

$$pK_a^{obs} = pH - \log [\Phi O^-] / [\Phi OH] \qquad (2)$$

provided that the quantity $[\Phi O^-] / [\Phi OH]$ is determined by $(A - A_{\Phi OH}) / (A_{\Phi O^-} - A)$ where A, $A_{\Phi OH}$ and $A_{\Phi O^-}$ are the absorbances of naphthols at experimental pH and low and high pH's respectively. The near uv spectra of 1-naphthol as a function of the bulk aqueous pH in CTAB micelle solution are shown in Figure 4.1 (unfortunately, the spectral profile of 2-naphthol is insensitive towards bulk aqueous pH and, therefore, can not be studied). For the acid-base equilibrium of the

interfacially located organic molecule, the pK_a^{obs} be now separated into two components viz., an electrostatic component and a non-electrostatic environmental component. This is formalised in relation 3,

$$pK_a^{obs} = pK_a^0 - e\,\Psi_0 / 2.303kT \qquad (3)$$

where, pK_a^0 is the apparent pK_a value if surface potential of the micelle, Ψ_0, is null. Information can be obtained about the acid-base equilibrium at the surfactant-water interfaces by comparing pK_a^0 values of naphthols in the aqueous micellar systems with the pK_a values for naphthols in the aqueous-organic mixtures, e.g., dioxane-water mixtures. The apparent pK_a in organic-aqueous mixture, pK_a^m , is defined in the following relation (equation 4).

$$pK_a^m = B + \log U_H^0 - \log [\Phi O^-] / [\Phi OH] - \log \gamma^m_{\Phi O^-} / \gamma^m_{\Phi OH} \qquad (4)$$

where, γ^m 's are activity coefficient terms in the medium, B is the pH meter reading and $\log U^0_H$ is the correction factor to be applied to pH meter reading to measure the actual hydrogen ion concentration in organic-aqueous mixtures. The pK_a^0 values relate to a system where the conjugate acid-base species reside in an interfacial microenvironment but the bulk aqueous solution pH is measured. Hence, the comparison between pK_a values in dioxane-water mixtures and pK_a^0 values in micelle systems should take into account the primary medium effect on the proton. In other words, pK_a^0 values need to compare to pK_a^i values rather than pK_a^m's where,

$$pK_a^i = pK_a^m + {}_m\gamma_H^+ \qquad (5)$$

and ${}_m\gamma_H^+$ denotes the primary medium effect on the proton. It is usual to assume that the mean primary medium effect on HCl, ${}_m\gamma_\pm$, approximates to ${}_m\gamma_H^+$. The $\log U_H^0$ and ${}_m\gamma_\pm$ values given in references 14, 15 were employed to derive pK_a^i values in dioxane-water mixtures. These pK_a^i ($\Delta pK^i_a = pK_a^i - pK_a^w$) values as a function of medium dielectric constant are shown in Figure 4 (inset). The pK_a^0 values of 1-naphthol in CTAB micelles are determined with the aid of eqn.3 and the known value of surface potential of CTAB micelles of +141 mV[14]. The effective dielectric constant (D_{eff}) values are obtained by comparing ΔpK^0_a's (Table 1) of 1-naphthol

in micellar surface with that of ΔpK^i_a values in 1,4-dioxane-water mixtures (Figure 4; inset). It may be noted that D_{eff} values are measured on the basis of several assumptions: (i) both the protonated and deprotonated forms of the naphthol indicator are quantitatively partitioned into the micellar phase at least at high surfactant: naphthol ratio (ii) the activity coefficient term ($\log \gamma^i_{\Phi O^-} / \gamma^i_{\Phi OH}$) is negligibly small so that ΔpK^0_a values are directly comparable with the ΔpK^i_a behaviour in different solvent dielectric constant bulk media (iii) although the OH groups of naphthol are protruded from the micellar surface, the acid-base equilibrium is still under the influence of micellar surface potential and (iv) it is evident that much like 1,4 dioxane-naphthol system, the interfacial water of CTAB micelles form H-bonds with micelle embedded naphthols (discussed later), which act as H-donor in both the above cases. No serious error in the evaluation of D_{eff} due to presence of this H-bond is thus anticipated because such effect, if any, would be compensated by the similar interaction present in the reference system (naphthols in dioxane-water)

Table 4.1. Results of pH titration of 1-naphthol in aqueous and aqueous CTAB micellar solution at 25°C.

Conc.of CTAB/mM (Conc. of 1-HN= 0.5mM)	pKa^w	pK_a^{obs}	ΔpK_a^{obs}	pK_a^0	ΔpK_a^0
20		8.623	0.765	11.007	1.619
50	9.388	8.679	0.709	11.063	1.675
100		8.914	0.474	11.298	1.910

Table 4.2 . D_{eff} values of OH group location of micellar interface

Conc. of CTAB/mM (Conc. of 1-HN = 0.5mM)	D_{eff}
20	51 ± 3
50	49 ± 3
100	45 ± 2

Table 4.2 shows that D_{eff} at the interface of CTAB micelles, as measured by the pK_a shift of interfacially located naphthols, vary from 51±3 to 45±2 as a function of CTAB concentration from 20mM to 100mM (concentration of naphthol being 0.5mM throughout). This result indicates that naphthols are increasingly partitioned in micelles as the CTAB concentration is increased. Utilising the solvatochromic visible absorption band maximum $E_T(30)$, D_{eff} estimates of 28-33 were obtained previously for CTAB micelles[16]. Therefore, in comparison to the previously determined micropolarity of CTAB micellar surface (D_{eff} ~ 30), the present value of 45 (under condition when most of the naphthol molecules are partitioned in micelles) is substantially high. This is an interesting observation. This clearly indicates that the OH groups are directed away from the surface of the micelles and are located around more polar region. Assuming a polarity gradient to exist with the distance from the micellar surface, one can have a rough idea of the location of the OH groups in the Stern layer. A recent application of numerical Poisson-Boltzman methods to the determination of the electrostatic potential and counter ion distribution around polyelectrolyte such as DNA may be relevant in this respect [17]. In this case the situation had prompted to choose a dielectric constant "field" , where low dielectric values exist near 30 at the polyelectrolyte surface and increasing away to the values near 78.5 in bulk water. A rough estimation following the above work, which takes on a cylindrical polyelectrolyte (e.g.,DNA) surface of radius 10A as the

low dielectric region, shows that the present D_{eff} value of 45 (compared to ~30 at the micellar surface) could be rationalised assuming OH group of naphthol to be protruded away from the CTAB micellar surface through nearly 1A distance toward the Stern layer[17].

4.3.2 Shear-Induced Viscosity and Fluorescence Intensity

Aqueous CTAB, CPB or OTAB (2-10 mM) and 1- or 2-naphthol (2-10 mM in 2-5% methanol, naphthols being sparingly soluble in water) solutions show viscosities similar to those of water. But as soon as these solutions are mixed together at room temper-ature, a thick gel-type fluid with high viscoelasticity is developed. Since viscoelasticity tends to disappear in high methanol concentrations, experimental solutions are prepared routinely by transferring the required amount of naphthol solutions (in pure methanol) in the experiment vial first, and then the alcohol was evaporated off completely before the addition of aqueous surfactant solution. Much like the CTAB-SS system, CTAB-naphthols, OTAB-naphthols and CPB-naphthols also display maximum viscoelasticity at a 1:1 molar ratio of surfactant and the promoter. The argument that an excess or deficiency of charge on the micelles due to adsorption of hydrotrope anions (e.g., SS) would shorten the micellar life time and size is not apparently true for the present system because under the present experimental condition of solution pH (6.5), the naphthols are mostly protonated, i.e., uncharged (pK_a's > 9.0). Therefore, it seems apparent that the symmetrical distribution of surfactant and the promoter molecules leading to highly compact spherical micelles facilitates an optimum surface curvature to attain in presence of H bonding (discussed later), and this results in the sphere to rod transition easily. For further experiments, naphthol to surfactant ratio was chosen to produce strongest viscoelasticity, i.e., 1:1 mole ratio. At low concentrations (<2 mM), CTAB, OTAB or CPB-naphthol solutions show shear thinning properties, typically observed in the case of a non-Newtonian fluid. But at higher concentrations (>2 mM; 25°C), present

experimental systems display interesting rheological phenomenon. Up to the applied shear rate of 52 s^{-1} (which is concentration dependent) for the CPB-2-naphthol system, solutions shear thin (Figure 4.3). An onset of viscosity rise is observed thereafter as a function of applied shear, and the viscosity share rate profile passes through a maximum, e.g., at 102 s^{-1} for the above system (Figure 4.3).

This behavior is consistent with building up of long wormlike micellar bundles[7]. The system recoils after the applied shear is withdrawn and takes a very long time (e.g., half-life period of viscosity decay of a CTAB-1-naphthol (7.0 mM) system equals 56 min; samples were sheared in a rotational viscometer at $100s^{-1}$ for ≥5 min to ensure that the high viscosity regime was reached) to recoil completely and to return to an equilibrium unsheared state. Shear rates at which viscosity transition takes place and the shear rates at which maximum viscosity is displayed by various systems vary to some extent from system to system (Figure 4.2 -4.7). Systems which display shear induced nonlinear rheological changes (such as the present systems) bring about formidable problem in measuring unperturbed solution viscosity because the measuring techniques (e.g., torsional shear rheometry) often apply considerable stress on the system during measurement, and thus the zero-shear viscosity becomes obscure. Both the naphthols are well-known fluophores, and significantly, the quantum yield of emission of the naphthols is found to be very sensitive to thesolution viscosity of the present systems.

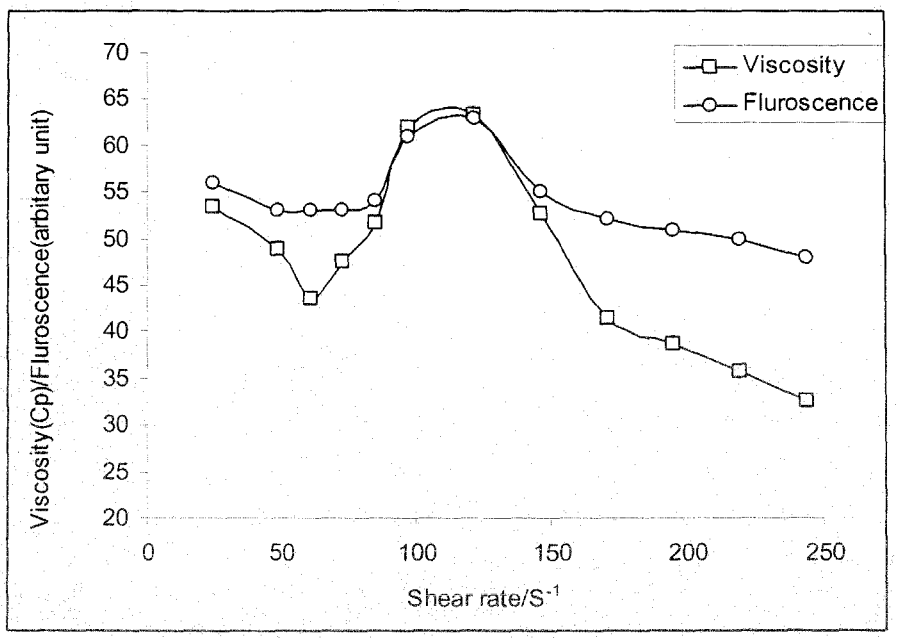

Figure 4.2: Variation of viscoelasticity and Fluorescence intensity of CPB-1-naphthol (10 mM) system with applied shear rate.

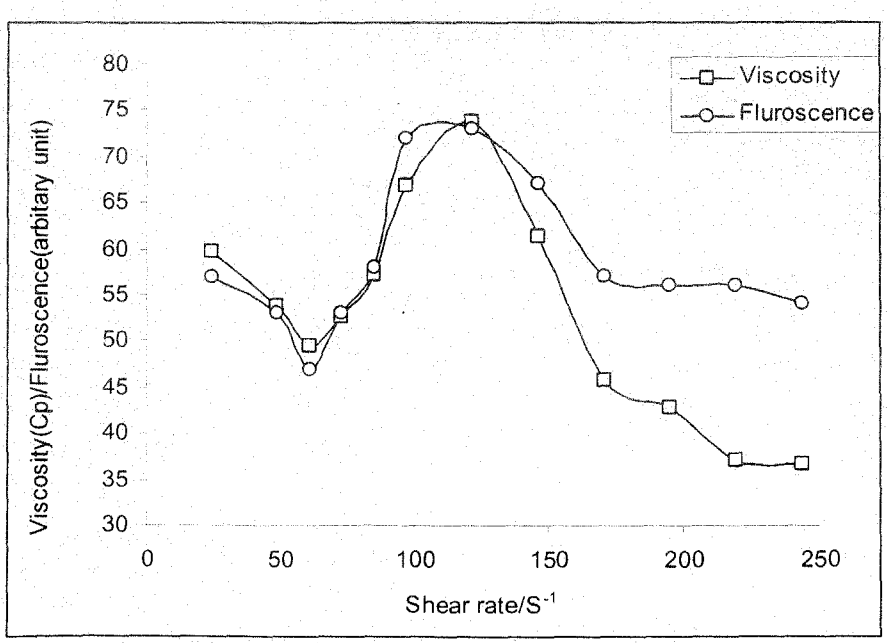

Figure 4.3: Variation of viscoelasticity and Fluorescence intensity of CPB-2-naphthol (10 mM) system with applied shear rate.

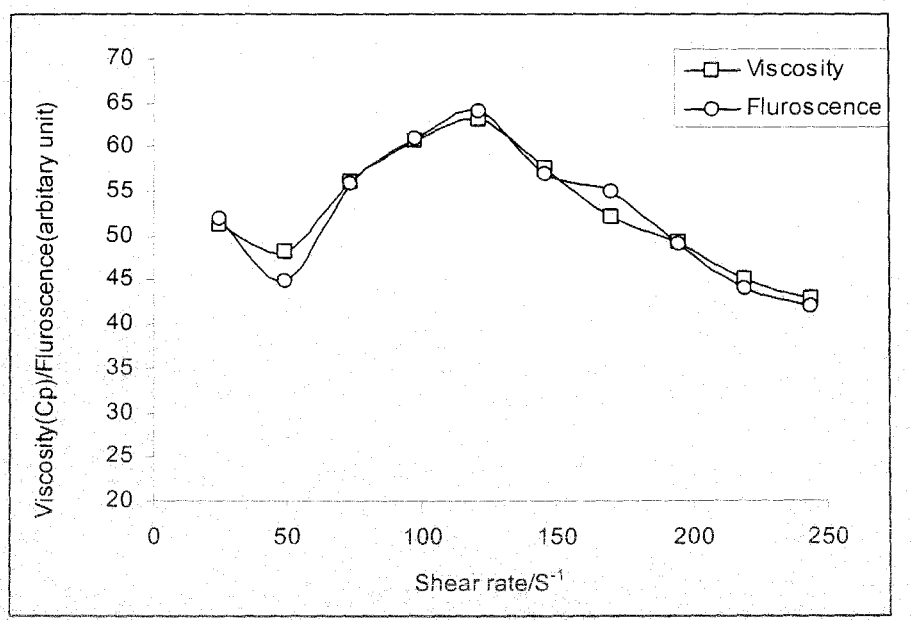

Figure 4.4: Variation of viscoelasticity of CTAB-1-naphthol (10 mM) system with applied shear rate.

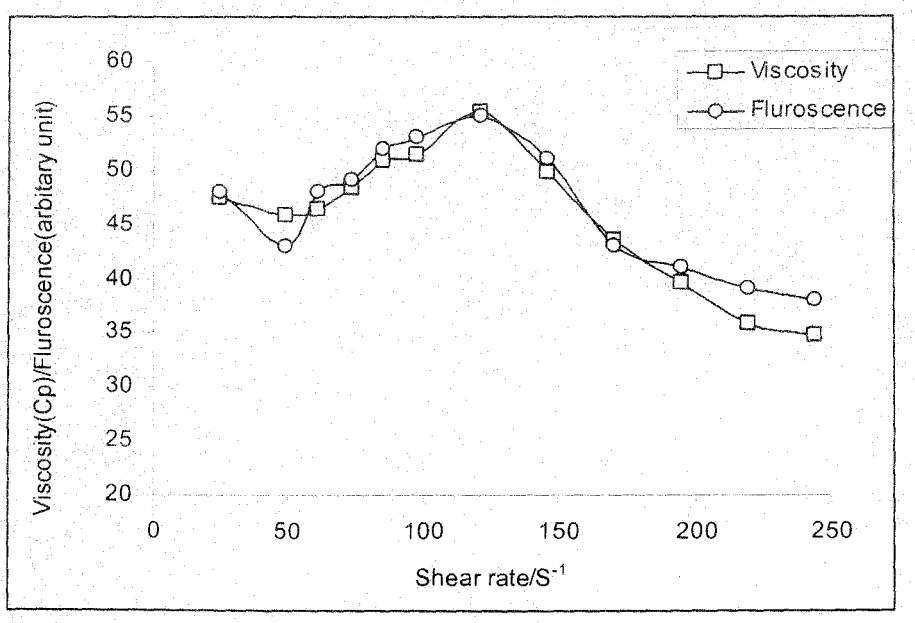

Figure 4.5: Variation of viscoelasticity of CTAB-2-naphthol (10 mM) system with applied shear rate.

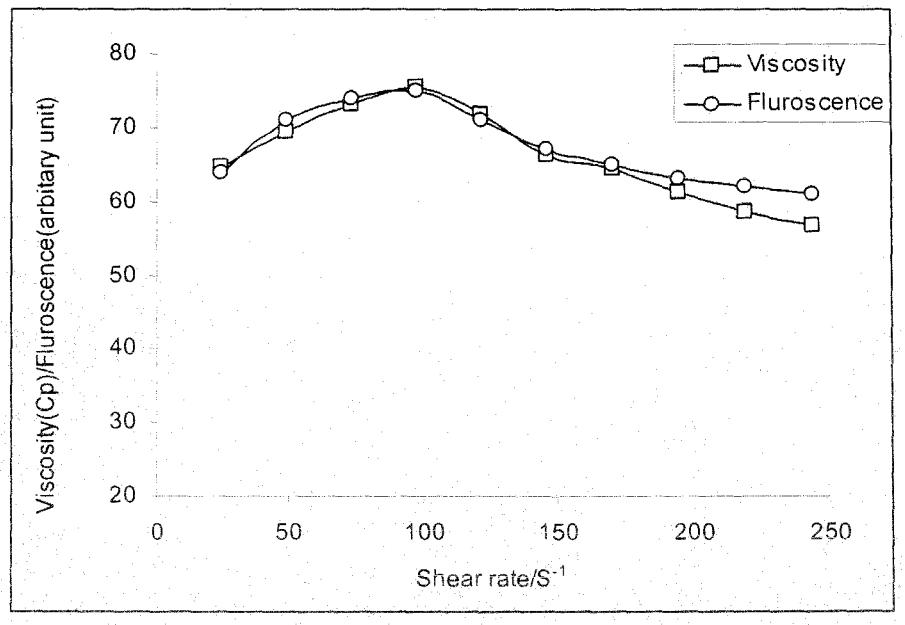

Figure 4.6: Variation of viscoelasticity of OTAB-1-naphthol (10 mM) system with applied shear rate.

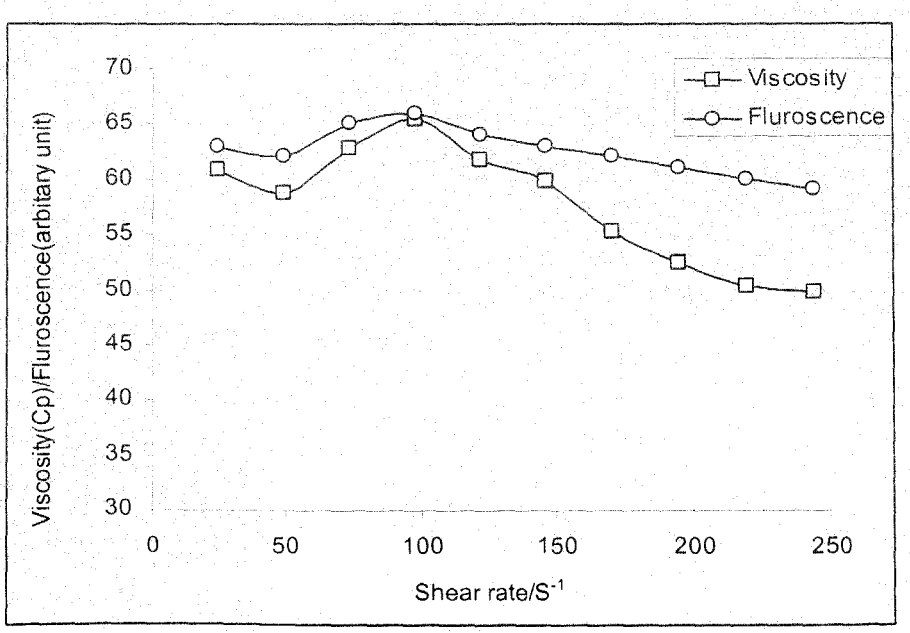

Figure 4.7: Variation of viscoelasticity of OTAB-2-naphthol (10 mM) system with applied shear rate.

This offers an interesting route for fluorescence monitoring of unperturbed viscosity as a function of applied shear (Figure 4.2-4.7). In a viscous medium, a fluophore cannot transfer energy efficiently via nonradiative means because of delayed collisions with the surrounding molecules resulting in the increased emission quantum yield. Moreover, the dipole moment of the probe in the excited state is greater than that in ground state, and hence interaction of the excited probe molecule with its surrounding molecules is different from that before absorption. Reorientation and translation of nearest-neighbor molecules allow the probe molecule to relax gradually to its equilibrium excited singlet state (S_1). In solutions of low viscoelasticity where these relaxations are very fast, fluorescence practically takes place from this equilibrium excited state S_1. In highly viscoelastic solutions, the relaxation of molecules surrounding the probe may be slow, and the probe molecules may emit before reaching their equilibrium excited state S_1, and a blue shift of the fluorescence spectrum may also be observed accompanying by an intensity enhancement. Similar situation is also encountered in a twisted intermolecular charge transfer state (TICT) formation where in a less viscous environment the probe molecules also display internal rotation and charge transfer, which results in the less emission quantum yield than that in a high viscous environment[18,19]. Furthermore, naphthols are weak acids in the ground state. In aqueous solution (pH 6.0-7.0), they exist almost completely in the acid forms. On excitation into the lowest singlet excited state, the pK_a values drop by several units (2-naphthol: pK_a* 2.78; 1-naphthol: pK_a* 0.40),[20-22] i.e., they undergo deprotonation in the excited state (DES)[23,24] As a result, the emission from the neutral forms of 1- and 2-naphthols at 360 and 357 nm, respectively, exhibits very low intensity than those of the anion forms near 450 or 420 nm, respectively. However, on binding to micelles, the DES process is restricted significantly causing a 20-90-fold increase in the intensity and life time of the neutral emission as well as in the rise time of the anion emission[25]. This is probably because of unavailability

of an adequate number of water molecules in the vicinity of the naphthol molecules embedded inside the micelle to hydrate the proton released during photolytic deprotonation[25]. Therefore, at low surfactant concentrations (<2 mM; DES is significant), emissions from the deprotonated anion forms of the napthols were monitored at higher wavelengths, whereas in the presence of high concentrations of surfactant, emission from neutral form of 2-naphthol were monitored at lower wavelengths (where DES is insignificant) in the present experiments (1-naphthol shows very low quantum yield for neutral emission). Figure 4.2-4.3 also compares the shear induced viscosity data with that of fluorescence intensity of the present CPB-2-naphthol system. While the overall feature of the shear-induced viscosity profile is identical with that of the emission, they are not exactly superimposed on one another possibly because of the perturbation imposed on the system during viscosity measurement. However, we failed to observe any direct effect of applied shear on the DES process. This is apparent from the nonvariant ratio of emission intensities of protonated to deprotonated naphthols as a function of applied shear. This also indicates that the shear does not influence the availability of water molecules to hydrate the liberated protons, i.e., the microstructure around the naphthol molecules in the wormlike micelles remains unchanged in SIS. However, as shown in Figure 4.2, it seems like that in the high applied shear rate (>180 s^{-1}) the viscosity and fluorescence have opposite variation with the applied shear rate. Partial modification/disruption of wormlike micelles under high shear may change the compactness causing redistribution of naphthols in the micellar gel expelling some of the inner site naphthols to the outer site (better accessible to water molecules), resulting in the slight increase in the fluorescence intensity due to modified DES process[26]. In an experiment where hydrotropic promoter for micellar shape transition is not a fluophore, a probe must be added from the outside for the above measurement. This, in turn, may alter the hydrophobic trait of the system and affect the rheology. Therefore, one should be careful in using external fluorescence probes for monitoring viscosity.

4.3.3 Fluorescence Spectroscopy

It has been reported that fluorescence quenching can be induced by the hydrogen-bonding interactions for fluophores in the hydrogen-bonding surroundings and is explained by the hydrogen bonding dynamics in the fluorescence state [27-32]. Therefore, it may be presumed that intermolecular H bonding in micelle-embedded naphthols can be studied effectively by observing fluorescence quenching (static and dynamic).

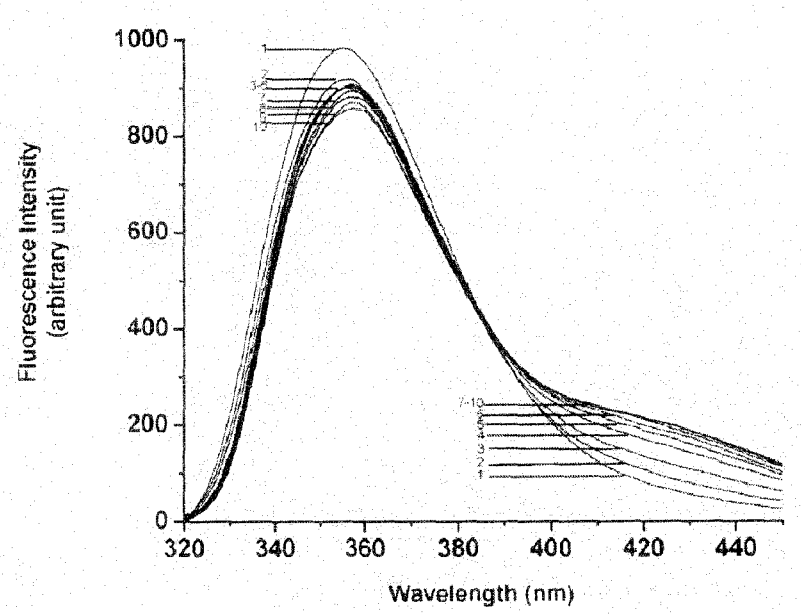

Figure 4.8: Fluorescence spectra of 2-naphthol ($0.25\ 10^{-5}$ mol/L) in aqueous CTAB solutions in presence of 0.1 M HCl. [CTAB]: (1) 0.0 mM, (2) 3 mM, (3) 2.5 mM, (4) 2 mM, (5) 1.5 mM, (6) 1 mM, (7) 0.75 mM, (8) 0.5 mM, (9) 0.25 mM, and (10) 0.12 mM

However, excited-state proton transfer (ESPT) or DES process of hydroxy aromatic compounds such as naphthols seems to make the situation somewhat difficult. The ESPT rates of these compounds in aqueous solutions are limited by the time water takes to wrap itself around the charge because a water cluster of 4 (1 molecules is the proton acceptor in each case[33]. The first two steps in the ESPT process are, therefore, (i) the H-bonded complex formation of electronically excited state of naphthols with water molecules and (ii) hydrogen-bonded complex formation with

water clusters required for protolytic dissociation[23]. ESPT process of 1- and 2-naphthols in organized media including different micelles have been investigated in considerable detail, but the results are not always unambigu-ous[23,24,34,35]. It has been shown that the ultrafast proton-transfer processes in ESPT became significantly retarded for 1-naphthol in micelles due to lack of water availability (as has already been mentioned), and the decay of the emissions are often multiex-ponential due to different solubilization sites in anionic and nonionic micelles, although a monoexponential decay process has also been observed for similar systems[34,35]. On the other hand, for CTAB micelles, the retardation effect is somewhat compensated by the catalytic effect of the micellar potential[35]. Although a previous study did not find convincing evidence that all of the naphthols in micelle are definitely in the form of H-bonded complex with several water molecules, which is required for photodissociation, possible existence of intermo-lecular H bond in electronically excited states of naphthols under identical condition of wormlike micelle formation have been re-examined in the present study[23]. Figures 4.8 and 4.9 show the emission spectra of 2- and 1-naphthols, respectively, in 0.1 M HCl in presence of CTAB. Addition of high excess of hydroxonium ion is to shift the acid-base equilibrium toward neutral naphthol (protonated) to facilitate intermolecular H-bond

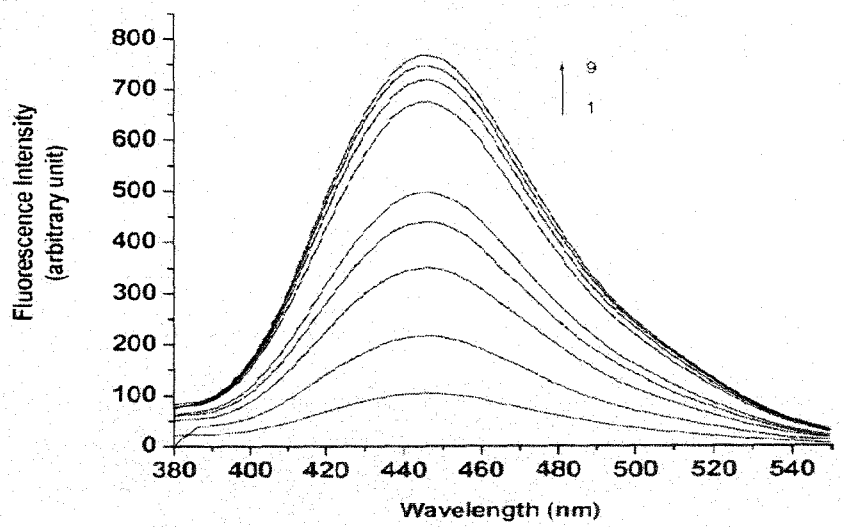

Figure 4.9. Fluorescence spectra of 1-naphthol (0.25 10^{-5} mol/L) in aqueous CTAB solutions in presence of 0.1 M HCl. [CTAB]: (1) 0.0 mM, (2) 0.25 mM, (3) 0.5 mM, (4) 0.75 mM, (5) 1.0 mM, (6) 1.5 mM, (7) 2.0 mM, (8), 2.5 mM, and (9) 3.0 mM.

formation. While 1-naphthol exhibits only anion emission (pK_a^* 0.40), which is enhanced substantially in presence of CTAB, emission from 2-naphthol in water was essentially from the neutral naphthol molecules under the above condition (pK_a^* 2.78). The effect of CTAB concentration on neutral as well as the anion emission of 2-naphthol is interesting (Figure 4.8). While addition of CTAB in the submicellar concentration range increases the intensity at 420 nm region depicting catalytic effect of CTAB charge on the excited-state deproto-nation, further addition of CTAB above the cmc (>1 mM) decreases the emission intensity indicating a retardation of the deprotonation rate for the lack of water availability in the micelles. Intensity of neutral emission, however, is increased slightly on the addition of CTAB in the submicellar concentration range, while in the post micellar concentration range no appreciable change of emission intensity is observed. Moreover, no detectable shift of neutral emission wavelength or the fluorescence quenching on CTAB addition is observed. Therefore, neither any extensive disruption of H bonds that might exist between the electronically excited state of naphthols and the water clusters nor the formation of new intermolecular H bond among the embedded naphthols in the photoexcited state is obvious from the above result.

4.3.4 FTIR Spectra:

The FTIR spectra of 2-naphthol in the presence and absence of CTAB micelles are shown in Figure 4.10 (A and B). The spectra of vacuum dried samples (25 ^{0}C) provided interesting results (in KBr pellets). (Studying the spectral feature of OH group of naphthols in aqueous solution was not possible (in CaF_2 cell) due to overlapping of IR peaks with that of water.) The broad band around 3354 cm^{-1}, which is assigned to the OH stretching of 2-naphthol (typically observed in phenols) is shifted to 3163 cm^{-1} due to partitioning in the micelles.

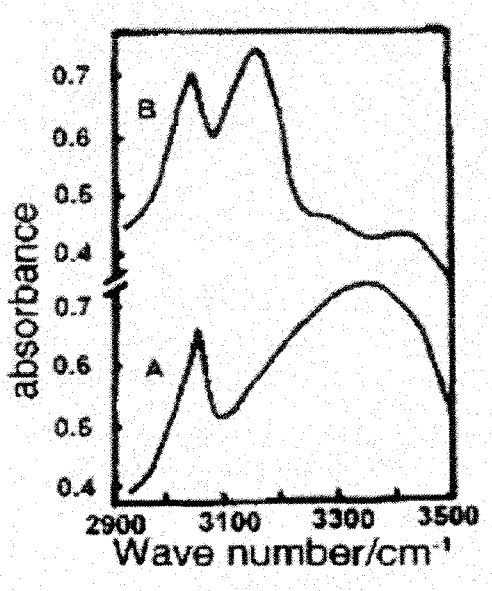

Figure 4.10. FTIR spectra of 2-naphthol (A) in the absence of CTAB and (B) in the presence of CTAB.

Comparatively sharper peak at higher wavelength confirms the presence of well-defined and stronger H bond in naphthols, which are embedded inside CTAB micelles. The peak at 3050 cm^{-1}, which remains almost unchanged upon gelation, may be assigned to aromatic CH stretch. Above shifting of OH stretching frequency is very much reproducible and consistently displayed by a wide variety of wormlike micellar systems promoted by naphthols. It seems apparent that H bonding plays an

important role in micellar shape transition[36]. The result also shows that vacuum drying at room temperature did not destroy the microstructure completely although may have modified it to some extent.

4.4 Reference

1. H. Rehage and H.Hoffmann, *J. Phys. Chem.*, **92,** 4712 (1988) .
2. H. Rehage and H. Hoffmann, *Mol. Phys.* **74,** 933 (1991) .
3. M. Cates and S. J. Candau, *J. Phys.: Condens. Matter* **2,** 6869 (1990).
4. Y. Hu, C. V.Rajaram, S. Q. Wang and A. M. Jamieson, *Langmuir* **10,** 80 (1994)
5. S. L. Keller, P. Boltenhagen,; D. J. Pine and J. A. Zasadzinski, *Phys. ReV. Lett.*, **80,** 2725 (1998)
6. B. Boltenhagen, Y.Hu, E. F.Matthys and D. J. Pine, *Phys. ReV. Lett.*, **79,** 2359 (1997)
7. C. Liu and D. J. Pine, *Phys. ReV. Lett.* **77,** 2121 (1996)
8. C. Manohar, In *Micelles, Microemulsions, and Monolayers*; *Science and Technology*; D. O. Shah, Ed.; Marcel Dekker, Inc.: New York, 145(1998)
9. P. M. Lindemuth and G. L. Bertrand, *J. Phys. Chem.*, **97**, 7769 (1993)
10. N. Hedin, R.Sitnikov, I.Furo, U.Henriksson and O. Regev, *J. Phys. Chem. B*, **103**, 9631 (1999
11. H. Yin, S. Lei, S.Zhu, J.Huang and J.Ye, *Chem.-Eur. J.*, **12,** 2825 (2006)
12. . N. Israclachivli, D. J. Mitchell and B. W. Ninham, *J. Chem. Soc., Faraday Trans.*, **72,** 1525(1976)
13. .R. K Rao, C.Manohar, B. S.Valaulikar and R. M. Iyer, *J. Phys. Chem.* **91**, 3286 (1987)
14. J. Drummond, F. Grieser and T.W. Healy,. *J. Chem. Soc. Faraday Trans. I*, **85,** 521 (1989)
15. C.J. Drummond, F. Grieser and T.W. Healy,*J. Chem. Soc. Faraday Trans. I*, **85,** 537 (1989)
16. C.J. Drummond, F. Grieser and T.W. Healy, *Faraday Discuss. Chem. Soc.*, **81**, 95 (1986)

17. G. Lamm and G.R. Pack, *J. Phys.Chem. B.*, **101**, 959 (1997).

18. C. E. Kung and J. K. Reed, *Biochemistry* **25,** 6114 (1986).

19. W. Retting and R. Lapouyade, In *Topics in Fluorescence Spectroscopy*; J. R. Lakowicz, Eds.; Plenum Press: New York, **4** 109(1994).

20. S. P. Webb, S. W.Yeh, L. A. Philips, M. A. Tolbert and J. H. Clark, *J.Am. Chem. Soc.*, **106,** 7286 (1984).

21. C. M. Harris and B. K. Selinger, *J. Phys. Chem.* **84** 1366 (1980).

22. C. M. Harris and B. K. Selinger, *J. Phys. Chem.* **84**, 891(1980).

23. K. M. Solntsev, Y. V. Ilichev, A. B. Demyashkevich and M. G. Kuzmin, *J. Photochem. Photobiol. A* **78,** 39 (1994).

24. Y. V. Ilichev, A. B. Demyashkevich and M. G. Kuzmin, *J. Phys. Chem.*, **95**, 3438 (1991).

25. D. Sukul, S. K. Pal, D. Mandal, S. Sen and K. Bhattacharya, *J. Phys. Chem. B*, **104,** 6128 (2000).

26. N. Pappayee and A. K. Mishra, *Photochem. Photobiol.*, **73**, 573 (2001).

27. S. Das, K. George Thomas, R. Ramanathan and M. V. George, *J. Phys. Chem.* **97,** 13625 (1993).

28. G. Zhao and K. Han, *J. Phys. Chem. A*, **111**, 2469 (2007).

29. G. Zhao and K. Han, *J. Phys. Chem. A*, **111**, 9218 (2007).

30. G. Zhao, J. Liu, L. Zhao and K. Han, *J. Phys. Chem. B*, **111**, 8940 (2007).

31. V. Samant, A. K. Singh, G. Ramakrishna, H. N. Ghosh, T. K. Ghanty and D. K. Palit, *J. Phys. Chem. A* **109**, 8693 (2005).

32. G. Zhao, *J. Chem. Phys.*, **127**, 024306 (2007).

33. .J Lee, G. W. Robinson, S. P. Webb, L. A. Philips and J. H. Clark, *J. Am. Chem. Soc.* **108,** 6538 (1986).

34. D.Mandal, S. K. Pal and K.Bhattacharyya, *J. Phys. Chem. A*, **102,** 9710 (1998).

35. S. Abou-al Einin, A. K. Zaitsev, N. K. Zaitsev and M. G. Kuzmin, *J. Photochem. Photobiol. A* **41,** 365 (1988) .

36. Y. Y.Waguespack, S.Banerjee, P. Ramannair, G. C. Irvin, V. T. John and G. L. McPherson, *Langmuir* **16,** 3036 (2000).

Section-B

In the treatment of the properties of very dilute polymer solutions it is convenient to represent the molecule as a statistical distribution of chain elements, or segments, about the centre of gravity. The average distribution of segments for a chain polymer molecule is approximately Gaussian [1] , its breadth depends on the molecular chain length and on the thermodynamic interaction between polymer segments and solvent. According to hydrodynamics, the specific viscosity of a Newtonian liquid containing a small amount of dissolved material should depend in first approximation only upon the volume concentration and the shapes of the suspended particles. By suitable application of such hydrodynamical considerations to solutions of long chain molecules, it is possible in a rough fashion to derive the Staudinger-Kraemer equation, denoting proportionality between specific or intrinsic viscosity and molecular weight[2]. It is an experimental fact, however, that the proportionality constant, K_m is dependent not only upon the type of polymer concerned, but also upon the temperature and the nature of the solvent. A relationship between intermolecular and intramolecular agglomeration tendency is established. Solutions of polystyrene, rubber and cellulose acetate in the solvent-non solvent systems were investigated by Alfrey and co-workers[2]. They observed that the specific viscosity of a dilute solution of polystyrene or rubber is strongly dependent upon the nature of solvent , the specific viscosity is high in a good solvent and low in a poor solvent or a solvent-non solvent mixture. This has been interpreted as being due to changes in mean molecular shape. The specific viscosities of cellulose acetate solutions are not so sensitive to the nature of solvent. Besides this, the extrapolated specific viscosity at the limit of solubility is in the same range for several different solvent-non solvent systems. The effect of temperature upon intrinsic viscosity should depend strongly upon the nature of solvent. Alfrey and co-workers also noted that the effect of a temperature increase is to lower the specific viscosity of rubber or polystyrene solutions in a good solvent, but to increase the specific viscosity in a mixture of solvent and non-solvent. Unperturbed dimensions of flexible linear macromolecules can be obtained from

intrinsic viscosity-molecular weight data in any solvent , good or poor, if (as is almost always true) the hydrodynamic draining effect is negligible and if an estimate can be made of the viscosity expansion factor α_n defined by[3]

$$[\eta] = K_\theta M^{1/2} \alpha_n^{\ 3} \qquad (1)$$

In principle this can be done graphically from the relation alone if a reliable expression is available for the dependence of α_n on M. In particular, it has been shown from theoretical considerations that the intrinsic viscosity should depend on the molecular weight M, temperature T and solvent type in accordance with the relationships,[4-6]

$$\alpha^5 - \alpha^5 = 2\psi C_M (1 - \theta/T) M^{1/2} \qquad (2)$$

where $K_\theta = k_1 T/\psi_1$

$$K_\theta = \phi_o (r^2_o/M)^{3/2} \qquad (3)$$

$$C_M = 27(d^{5/2}/\pi^{3/2} N) (\upsilon^{-2}/v_1) (M/r^2_o)^{3/2}$$

$$= 1.4238 \times 10^{-24} (v^2/v_1) (\theta_o/K_\theta) \qquad (4)$$

Where ψ_1 is entropy parameter, k_1 is the enthalpy parameter, θ is the temperature and K_θ is the unperturbed dimension of the polymer, ϕ_o is the Flory's universal constant. Here, υ is the partial specific volume of the polymer and v_1 is the molar volume of the solvent.

Intrinsic viscosities of polyisobutylene fractions ($M = 1.8 \times 10^5$ to 1.88×10^6) and polystyrene fractions ($M = 70 \times 10^4$ to 1.27×10^7) have been determined in various pure solvents and in several solvent mixtures at several temperatures by Fox and Flory[7-8]. They observed that the parameter K_θ in the equation (54) , is same in different solvents but decreases somewhat with temperature (1.08×10^{-3} at 24° to 0.91×10^{-3} at 105^0 for polyisobutylene and 8.0×10^{-4} at 34^0 to 7.3×10^{-4} at 70^0 for polystyrene). The root-mean square end-to-end $(r_o^2)^{1/2}$, unperturbed by

intramolecular interactions (other than hindrance to free rotation) for a polyisobutylene molecule and polystyrene molecule with $M=10^6$ has been calculated to be 795A□ and 730A□ at 25^0C respectively. The solution properties of poly (methyl acrylate) in various solvents by light scattering , osmometry, and viscosity techniques have been investigated by many co workers[9-21]. Many empirical and semi empirical methods for the estimation of K_θ from viscometric measurements in good solvents have recently been proposed[22-35].

The viscosity behaviour of poly (methyl methacrylate) in four solvents was studied within the temperature range of 25^0 to 60^0C and the thermodynamic parameters were evaluated and discussed using Fox-Flory[6], Burchard Stockmayer-Fixman[36,37], Kurata-Stockmayer[38,39] and Berry[40] equations by Lenka and Co-workers[41]. On the other hand, for evaluation of K_θ from $[\eta]$ at $T > \theta$ (in good solvent), a number of equations relating $[\eta]$ and M through K_θ (after eliminating linear expansion factor (α), hydrodynamic expansion factor (α_η), lattice co-ordination number (z) etc.) have been suggested. These equations are shown below (where symbols have their usual meanings). Fox and Flory equation[6]

$$[\eta]^{2/3}/M^{1/3} = K_\theta^{2/3} + K_\theta^{5/3} C_T (M/[\eta]) \quad (5)$$

Kurata-Stockmayer (K-S) equation[38,39]

$$[\eta]^{2/3}/M^{1/3} = K_\theta^{2/3} + 0.363\,\phi\, B[g(a_\eta)M^{2/3} / [\eta]^{1/3}] \quad (6)$$

Burchard-Stockmayer and Fixman (B.S.F) equation[36,39]

$$[\eta] / M^{1/2} = K_\theta + 0.51\phi\, BM^{1/2} \quad (7)$$

Berry equation[40]

$$([\eta] / M^{1/2})^{1/2} = K_\theta^{1/2} + 0.42\, K_\theta^{3/2}\, B(r_0^2/M)^{3/2}\, (M/[\eta]) \quad (8)$$

According to these equations, the value of K_θ may be obtained from the intercepts on the ordinates of the lots of the quantity on the left hand side versus a

function of M and [η] on the right hand side . The unperturbed dimensions for polymethylacrylate, polyethylacrylate, polybutylacrylate, polyacrylonitrile, and polyvinyl pyrrolidine have been calculated by Lenka and co-workers[42] using an expression relating to the cross- over point concentration, C_x, of the polymer in a number of solvents with the unperturbed dimension of polymer molecule ($r_o^{1/2}$).

$$([\eta] /M^{1/2})^{5/3} = K_\theta^{5/3} + 0.627\ \phi_o^{5/3} (<R^2> /M)\ BM^{1/2} \qquad (9)$$

And Bohdanecky derived the following equation[51]

$$[\eta] /M^{1/2} = 0.80\ K_\theta + 0.65\ K_\theta\ K^{0.7} M^{0.35} \qquad (10)$$

The unperturbed dimensions of polystyrene and poly (2-vinylpyridine) have been measured in solvent-precipitant mixtures of various compositions using the Stockmayer-Fixman representation by Dondos and Benoit[44]. They obtained a linear relationship between K_θ and ΔG^E (the excess free enthalpy of mixing of the solvents) if, instead of using the bulk composition of the mixture one introduces its 'local' composition. This composition is calculated from the values of the preferential adsorption coefficient measured by light scattering.

In a resin-solvent system, the change in temperature initiates conformational transition in polymer chains[3] and the process of aggregation on precipitation is caused ;by such transitions[45] Raju and Yaseen reported that the continuous decrease in limiting viscosity number of Nylon-6 in m-cresol at temperatures ranging from 20° to 75°C was due to the contraction of the dimensions of the polymer coil[46]. Quoting the view of other workers they explained that a partial helix-coil type polymer chain transition occurs in polyamide-6 in solution and results in higher value of limiting viscosity number of nylon-6 in m-cresol at lower temperatures which in turn favours the dissolution [47]. They also observed that limiting viscosity number of Nylon-6 in phenol increase with temperature and the system attained a state of optimum dissolution at 55°C and further increase in temperature and had adverse effect. Chatfield reports that solvent power of an alcohol-ether mixture for

nitrocellulose increases with lowering of temperature and at -50°C, methyl alcohol alone becomes a solvent for cellulose ethers[48]. Recently, Savas and Zuhal have determined the unperturbed dimensions of anionically polymerized poly (p-ter-butyl-styrene) at various temperatures and found the θ –temperature of the polymer of the order of 31°C and 32.7°C in 1-nitropropane and 2-octanol respectively[49]. Several other workers reported the conformational transition of polymers in solution with change in temperature.[31,50]. Coil dimensions of poly (methylacrylate) in the cosolvent medium of CCl_4 and MeOH have been investigated by Maitra and Nandi[52]. They observed that the intrinsic viscosity exhibited a maximum for all fractions of polymer at a composition, ϕ_{CH3OH} (volume fraction of methanol) = 0.33 and also Huggins constant showed a minimum at the same composition. The unperturbed dimension (K_θ) exhibited a maximum and molecular extension parameter α_n, showed a minimum at ϕ_{CH3OH} =0.33.The experimental data for the solution properties of poly (N,N- dimethylacrylamide) and poly (N-isopropylacrylamide) show that the hydrodynamic and configurational characteristics of these two N-substituted polyacrylamide, in methanol and water are different, showing a peculiar behaviour in water, which cannot be easily interpreted in terms of random coil molecules[53,54]. Also, the unperturbed dimensions dimensions estimated from data ion good solvents are found to depend more on the lateral substituent structure than on its dimensions. Chintore and co-workers found that behaviour of poly (N-methylacrylamide) molecules in aqueous solution was quite abnormal, as indicated by the values of the second virial coefficients, lower than those measured in methanol[53,54]. Therefore, the hypothesis was made that the solvation of N-substituted poly acrylamides by water would occur with large dipole interaction and/or hydrogen bonding with the structural units of the polymers in such a way as to give a large chain expansion with low chain flexibility, so that the polymer molecules could no more be treated as random coils in aqueous solutions. It has been pointed out that polyacrylamide, in which the lack of N-substituents increases the chances of intramolecular interactions, has the highest unperturbed

dimensions[55]. The aqueous solutions of polyacrylamides are suspected to contain fibrous aggregates of very high molecular weight. These aggregates were observed by electronic microscopy[56] and the disaggregation kinetics studied by viscometry[57,58]. This phenomenon is generally attributed to intermolecular hydrogen bonds and is evidenced by an important decrease of viscosity with time. Boyadijian and co-workers have noticed differences of measured molecular weight by light scattering, according to the nature of solvent and have concluded the presence of aggregates broken up by the effect of salts in pure water but not in formamide[59] However, even for non-hydrolysed polyacrylamide, there is a lack of reliable data in the literature concerning the chain conformation in salt water solutions and its relation to intrinsic viscosity, particularly in the range of molecular weights of interest[60,61]. However, Francois and Sarazin and co-workers were successful in studying molecular weight dependence of radius of gyration, viscosity sedimentation and diffusion on a set of fractions in the same range of molecular weight[35]. It has been shown recently that, the unperturbed dimensions of polyacrylamide could be determined by light scattering measurements in methanol-water system[61]. These authors concluded that the high value of the exponent (0.64) of the molecular weight dependence of the radius of gyration was not related to a great expansion of the macro molecular coil, and the determination of the unperturbed dimensions by extrapolation of viscosity measurements in good solvents at $M \rightarrow O$ should be possible and works of Okada and Yamaguchi provide such determinations[62,63]. Fundamental parameters of poly (2-acrylamido-2-methyl propane sulphonamide) which is soluble in water and formamide are obtained by light scattering, and viscometry in these good solvents by Gooda and Huglin[64] and has been analysed by extrapolation procedures to yield the unperturbed dimensions $(r^2_o /M_w)^{1/2}$, steric factor (σ) and characteristic ratio (C_∞). There was a good accord between the values of $(\langle r^2\rangle_o /M_w)^{1/2}$, σ and C_∞ thereby obtained directly and those derived indirectly, the mean values being 8.73×10^{-9} $cmg^{1/2}$ $mol^{1/2}$, , 4.07 and 32 respectively. Bohdanecky and Petrus and co-workers investigated the solution of 9

polyacrylamide fractions (molecular weight 3300-800,000) in water at 25°C and in a mixed θ solvent (3.2 volume, H_2O-MeOH) at 20°C by light scattering, sedimentation and viscometry[65]. Measurements in water gave the configuration character ratio $C_\infty = 8.5$

The fundamental parameters of the polyacrylamide obtained previously by viscometry in good solvent i.e. water and in a θ solvents have been analysed by viscosity molecular weight relationship procedures suggested by several workers (Scholtan[60], Newman[66] and Misra[67]). High value of excluded volume exponent, as was observed in some cases, once thought to be the result of great expansion of polyacrylamide in aqueous solution as mentioned above[35,61]. This arose doubts on the applicability of the method of extrapolation of the viscosity data in determining unperturbed dimension of the polymer in water. Further study, however, confirmed that the high value of the exponent of molecular weight dependence of the radius of gyration was not due to a great expansion of the macromolecular coil in water and it is now believed that determination of the unperturbed dimension by extrapolating viscosity data in good solvents is possible[61]. Although some studies on the solution viscosity properties of acrylamide in water are available in the literature, similar studies in other solvents or cosolvent systems are surprisingly little[61-65] in a binary liquid mixture. It is the interaction between the liquids that governs the solubility of a polymer in the mixture. Expansion of coil are also occurred due to two main reasons (i) variation of molecular extension factor (α_n) and (ii) change of the unperturbed dimension of the polymer due to interactions of two component liquids[68,69]. In the present chapter , the results of our investigation on unperturbed dimension, interaction parameter and related aspects of unhydrolized polyacrylamide in water –DMSO mixtures have been described. The intrinsic viscosities [η] of the polymer have been measured for different molecular weight fractions of the polymer and also in different compositions (water/DMSO) of the cosolvent mixture . From the[η] – M relation, the unperturbed dimension (K_θ) and molecular extension factor (α_n) have been measured. The

Huggins constant value in each case was also determined in order to study the influence of cosolvent system on the aggregation of polymer[52]. While DMSO is a poor solvent for PAM, water-DMSO mixture acts as a cosolvent in all proportions. In the previous chapters, we have reported the technique by which the molecular weight of the polyacrylamide in aqueous solution may be controlled by trapping the initiator component in the interlayer space of montmorillonite. This method has been adopted selectively to prepare polymers of varying molecular weights for the solution property studies as presented in this chapter.

Reference

1. P. Devye and I. M. Krieger (unpublished) have shown that the average distribution of each segment about the centre of gravity is exactly Gaussian for random chain unperturbed by intramolecular interactions
2. T. Lafrey, A Bartovics and H. Mark, *J. Am. Chem. Soc.*, **64,** 1557 (1942)
3. P.J.Flory, Principles of Polymer Chemistry, Cornell University Press, Ithaca, N.Y. , Chap. XIV, (1953).
4. P.J. Flory, *J.Chem.Phys.*, **17**303 (1949).
5. T.G.Fox, Jr., and P.J.Flory, *J. Phys. Colloid Chem* **53** 197 (1947).
6. P.J.Flory and T.G.Fox, *Jr., J. Am. Chem. Soc***73** , 1904 (951)
7. T.G.Fox, Jr.[2] and *P.J.Flory, J.Am.Chem.Soc.*, **73,** 1909 (1951)
8. P.J.Flory, Jr[2], and *P.J.Flory, J.Am.Chem.Soc.*, **73, 1915 (**1951**)**
9. J.M.G. Cowie, *Polymer,* **7**, 487 (1966)
10. T. Brandrup and E.H.Immergut (eds), Polymer Handbook, Wiley interscience, New York, p. 47 (1966).
11. G.V. Schulz and R.Kriste, *Z.Phys, Chem*(F. furt), **30,** 171 (161)
12. S.N.Chinal and C.W.Bondurant, *Jr. J.Polymer. Sci.,* **22**, 555 (1956)
13. H. Lutje and G. Meyerhoff, , *Markromol. Chem.,* **68**, 180 (1963)
14. T.G.Fox, *Polymer,* **3**, 111 (1962).
15. M. Bohdanecky, *Collect. Czech. Chem. Commun.,* **30,** 1576 (1965)
16. H. Inagaki and S. Kawai, *Makromol. Chem.,* **79**, 42 (1964)
17. M. Bohdanecky, *Collec. Czech. Chem. Commun.,* **34**, 407(1969)
18. V.V.Varadaiah and V.S.R. Rao, *J. Sci, Ind. Res.*, **20B**, 280 (1961)
19. S.N.Chinal, J.D.Matlack, A.L. Resnick, and R.S.Samuels, *J. Polym.; Sci.,***17,** 391 (1955).
20. W.R.Moore and R.J.Fort., *J. Polym.; Sci.,***A1**, 929 (1963)..
21. S. Gundiah, R.B.Mohite and S.L.Kapur, *Makromol. Chem.,* **123**, 151(1969)
22. S.Arichi, *Bull. Chem. Soc. Jpn.*, **39**, 439 (1966).
23. U.Bianchi and A.Peterlin, *J.Polym.Sci., A-2,* **6**, 1759 (1968)
24. D.W.Van Krevelen and P.J.Hoftyzer, *J. Appl. Polym. Sci.,* **11**, 1409 (1967).

25. D.W.Van Krevelen and P.J.Hoftyzer, *J. Appl. Polym. Sci.*, 10, 1331 (1968).
26. K.Kanide, Kobunshi Kagaku, 25, 781 (1968); *Chem. Abst.*, **70**, 88348Y (1969).
27. V. S. R., Rao, *J.Polym.Sci.*, **62**, S157 (1962).
28. H.L.Bhatnagar, A.B. Biswas and M.K.Gharpurey, *J. Chem. Phys.*, **23**, 88 (1958)
29. H. Yamakawa, *J.Chem. Phys.*, **34**, 1360 (1961).
30. T. Sakai., *J.Polym.Sci.*, A-2, **6**, 1535 (1968)
31. P.Vasudevan and Santappa, *Makromol. Chem.*, **137**, 261 (1970)
32. S.Gundiah, R.B.Mohite, and S.L.Kapur, *Markromol. Chem.*, **123**, 151 (1969)
33. P. Vasudevan and M. Sentappa, Unpublished Result.
34. P.C.Deb and S.R.Chatterjee, *Makromol. Chem.*, **120**, 49(1968).
35. P.C.Deb and S.R.Chatterjee, *J. Indian Chem. Soc.*, **46**, 468 (1969)
36. W.Burchard, *Makromol Chem.*, **50**, 20 (1960)
37. W. H. Stockmayer and M. Fixman, *J.Polym. Sci.*, **C1**, 137 (1963)
38. M.Kurata, W.H.Stockmayer , *Fortschr, Hochpolym. Forsch*, **3**, 196(1963).
39. H. Kurata, W.H.Stockmayer, and A. Roig, *J. Chem. Phys.*, **33**, 151 (1960)
40. G.C.Berry, *J.Chem. Phys.* **46**, 1338 (1967)
41. S.Lenka, P.Nayak and M.Dash, *J. Macromol. Sci. Chem.*, **A 20 (4)** 467 (1983)
42. S.Lenka, P.Nayak and M.Dash, *J. Macromol. Sci. Chem.*, **A 19 (3)** 321 (1983)
43. G. Tanaka, *Macromolecules,* **15,** 1028 (1982)
44. A. Dondas and H. Benoit, *Macromolecules,* **6 (2)**, 242 (1973)
45. I.W. Vanden Berg, G. Vande Ridder, and C.A. Smoldevs, *Eur, Poly. J.*, **17**, 935 (1981)
46. G. Tanaka, K.V.S.N. Raju and M. Yaseen, *J. Appl. Polym. Sci.*, **43**,1533 (1991)
47. H. Haneczek, E. Turska, *Polymer*, **24**, 1590 (1983)

48. H.W. Chatfield, "Varnish Constituents", Leonard Hill Ltd., London, 412, 419 (1953)
49. K.Savas and K. Zuhal, *Polymer Communications*, **31 (1)**, 35 (1990)
50. I. Nishio, S.T. Sun, G. Swislow and T. Tanaka, *Nature*, **281**, 208 (1979)
51. M. Bohdanecky, *J. Polym. Sci. (B)*, **3**, 201 (1965)
52. B. Maitra and A.K. Nandi, *Polymer*, **34 (6)**, 1260, 1993
53. O. Chintore, M. Guaita and L. Trossarelli, *Makromol. Chem.*, **180**, 2019 (1979)
54. O. Chintore, M. Guaita and L. Trossarelli, *Makromol. Chem.*, **180**, 969 (1979)
55. M. Kurata, Y. Tsunashima, M. Iwama and K. Kamada, in : "Polymer Handbook", edited by J. Brandrup and E. H. Immergut, 2nd edition, Wiley-Interscience, NewYork, IV- 36, (1975)
56. J. W. Herr and W. G. Routson, paper number SPE 5098, 49th Ann. Fall. Meeting (1974)
57. W.P. Shyluk and F.S. Stow, Jr, *J. Appl. Polym. Sci.*, **13**, 1023 (1969)
58. N. Narkis and M. Rebhun, *Polymer*, **6**, 507 (1966)
59. R. Boyadjian, G. Seytre, P. Berticat and G. Vallet, *Eur. Polym. J.*, **12**, 401 (1975)
60. W. Scholtan, *Makromol. Chem.*, **14**, 169(1954)
61. T. Schwartz, J. Sabbadin and J. Francois, *Polymer*, **22**, 609 (1954)
62. C. Okada, K. Kamada, T. Yoshihara, J. Hasoda and A. Fumuro, 'Reports on Progress on Polymer Phymer Physics in Japan', XX5, (1977)
63. N. Yamaguchi, N. Onda and Y. Hirai, 'Reports on Progress on Polymer Phymer Physics in Japan', XX1, 63 (1978)
64. S. R. Gooda and M. B. Huglin, *Polymer*, **34 (9)**, 1913 (1993)
65. M. Bohdanecky, V. Petrus and B. Sadlacek, *Makromol. Chem.*, **184 (10)**, 2061 (1983)
66. S. Newman, W. R. Krigbaum, C. Laugier and P.J. Flory, *J.Polym. Sci.*, **14**, 451 (1954)
67. G. S. Misra and S. H. Bhattacharya, *Eur. Polym. J.*, **15**, 125 (1979)

Chapter 5

Determination of unperturbed dimension and interaction parameters of sodium alginate in binary solvent mixtures by viscosity measurements

5.1 Introduction

Alginate is a water-soluble linear polysaccharide and is the only polysaccharide which naturally contains carboxyl groups in each constituent residue, and possesses various abilities for functional materials [1,2]. Due to the presence of the carboxylic acid groups in the saccharides residue, alginic acid has an anionic nature, forming alginate salts with cationic metals, such as Ca^{2+} and Na^{+}. Calcium alginate is insoluble and appears a swelling behaviour in water, whereas sodium alginate is soluble in water [3].

Furthermore, sodium alginate is a biodegradable polymer [4]. In the treatment of the properties of very dilute polymer solutions it is convenient to represent the molecule as a statistical distribution of chain elements, or segments, about the centre of gravity. The average distribution of segments for a polymer molecule is approximately gaussian; its breadth depends on the molecular chain length and thermodynamic interaction between polymer segments and solvent. According to hydrodynamics, the specific viscosity of a Newtonian liquid containing a small amount of dissolved material should depend in the first approximation only upon the volume concentration and the shapes of the suspended particles. Alginates are insoluble in water-miscible solvents such as alcohols and ketones. Aqueous solutions (1%) of most alginates would tolerate the addition of 10-20% of these solvents; propylene glycol alginate tolerates 20-40% while up to 65% ethanol can be added to triethanolamine alginate without causing precipitation. The presence of such solvents in water, before dissolving the alginate, will hinder hydration. An even more efficient method of diluting the alginate particles is to use liquid-mixture dispersion in which they are wetted with a non-solvent. This can be either a water-miscible non- aqueous liquid (such as ethanol or glycerol) or a water-immiscible liquid (such as a vegetable oil). The particles are dispersed and the rate of hydration, and solution, would depend on the time taken for the non-solvent liquid to diffuse from the surface of the particles. The behavior of dilute polymer solutions, expressed

by different parameters, the second virial coefficient, the mean dimensions, the intrinsic viscosity (η) and influenced by temperature, solvent quality, molecular weight domain, can be discussed through different excluded volume theories [5]. The theoretical approaches mutually differ in the mathematical methods approximations used, but all of them relate the excluded volume effects to measurable quantities, by considering different possible interactions. The unperturbed dimension (UD) of a given polymer in a solvent does not depend on the nature of the solvent, as long as the solvent has no influence on the rotation of the chain segments [6,7]. This is true in many cases, especially for nonpolar polymer-solvent pairs, but in the cases of polar polymer - polar solvents systems, the unperturbed dimension vary considerably with the nature of the solvent. Most of the polymeric materials are soluble only in a limited number of primary solvents, but they could be made soluble in all proportions in mixtures consisting of two or more solvents, which may be individually poor solvent for the polymers [8]. Several mixtures of nonsolvent are also known which produce good solvent systems or at least increase the solvency power of primary solvents [9-16]. The intrinsic viscosity [η] is related to unperturbed dimension K_θ, molecular weight M, and the hydrodynamic expansion factor α_η by the relation [17,18]

$$[\eta]=\Phi(r_o^2/M)^{3/2}M^{1/2}\alpha_\eta^3=K_\theta M^{1/2}\alpha_\eta^3 \qquad (1)$$

where Φ is universal parameter ($\Phi = 2.5\times10^{23}$ mol^{-1}) and r_o^2 is the unperturbed mean square end- to end distance. At theta temperature $\alpha=\alpha_\eta=1$ and hence evaluation of K_θ is possible using this equation. On the other hand, for evaluation of K_θ from intrinsic viscosity at temperature other than theta temperature, a number of equations have been proposed [19-21].

The unperturbed dimension of polystyrene and poly (2- vinylpyridine) has been measured in solvent-precipitant mixtures of various compositions using the Stockmayer-Fixman representation by Dondos and Benoit [22]. Recently Savas and Zuhal have determined the unperturbed dimensions of anionically polymerized poly

(p-tert-butyl-styrene) at various temperatures and found the theta temperature of the polymer of the order of 31^0 and 32.7^0C in nitropropane and 2-octanol respectively [23]. Several other workers reported the conformational transition of polymers in solution with change of temperature [24,25]. Coil dimension of poly(methyl methacrylate) in the cosolvent medium of carbontetrachloride CCl_4 and methanol have been investigated by Maitra and Nandi [26]. They observed that the intrinsic viscosity exhibited a maximum for all fractions of polymers at a composition, $\Phi_{methanol}$=0.33 and also Huggins constant showed a minimum at the same composition. The experimental data for the solution properties of poly(N,N-dimethyl acrylamide) and poly (n-isopropylacrylamide) show that the hydrodynamic and configurational characteristics of these two polymers in methanol and water are different, showing a peculiar behavior in water, which cannot be easily interpreted in terms of random coil molecules. Chintore and co-workers found that the behavior of poly(N-methylacrylamide) molecule in aqueous solution was quite abnormal, as indicated by the values of second virial coefficients, lowered than those measured in methanol solutions by the large difference of estimated unperturbed dimensions [27,28]. Therefore, the hypothesis was made that the solvation of N-substituted polyacrylamide by water would occur with large dipole interaction and/or hydrogen bonding with the structural units of the polymers in such a way as to give a large chain expansion with low chain flexibility, so that the polymer molecules could no more be treated as random coil in aqueous solutions. It has been pointed out that polyacrylamide, in which lack in N-substations increases the chances of intramolecular interactions, has the highest unperturbed dimensions [29]. It has been shown that, the unperturbed dimension of polyacrylamide could be determined by light scattering measurement in methanol-water system [30]. These authors concluded that the high value of the exponent (0.64) of the molecular weight dependence of radius of gyration was not related to a great expansion of macromolecular coil, and the determination of unperturbed dimension by extrapolaton of viscosity measurements in good solvent at $M \rightarrow 0$ should be possible

and the work of Okada and Yamaguchi provides such determinations [31, 32]. The fundamental parameters of polyacrylamide obtained previously by viscometry in good solvent and in θ solvents have been analyzed by viscosity -molecular weight relationship procedures as suggested by several workers [15, 33]. High value of excluded volume exponent, as was observed in some cases, once thought to be the result of great expansion of polyacrylamide in aqeous solution as mentioned earlier. This arose doubts on the applicability of the method of extrapolation of the viscosity data in determining unperturbed dimension of the polymer in water. Further study, however, confirmed that high value of exponent of molecular weight dependence of the radius of gyration was not due to great expansion of the macromolecular coil in water and it is now believed that determination of unperturbed dimension by extrapolating viscosity data in good solvents is possible [30]. Saha and coworkers [34] have determined the unperturbed dimension of polyacrylamide (synthesized by them using a novel method to increase the chain length) in water-dimethylsulphoxide, water-1,4 dioxan, water-dimethyl formamide mixtures at 30-50^{0}C by different methods of extrapolation and found minimum value of unperturbed dimension at different fractions of nonsolvent depending on the nature of the polymer and nonsolvent, and obviously the temperature.

From the above literature it appears that in some cases the estimated unperturbed dimensions of chains may depend on the method of measurement in some cases and in other instances these are consistent. The extrapolation procedures often yield much higher values for unperturbed dimensions as compared to the real one, due to the curvatures appearing in the linear dependences given by the experimental data for high values of the excluded volume [35-37].

An alginate molecule can be regarded as a block copolymer containing M, G, and MG blocks, the proportion of these blocks varying with the seaweed source. Viscosity measurements performed by Celine Sartori [38] on high-G and medium-G sodium alginate solutions gave values of 13,400 and 3,800 mPa.s respectively. This was indicative of a higher inflexibility of the G sequences in solution. The

observed low value of in dynamic viscosity and average molecular weight of alginate from Laminaria digitata during alkaline extraction [39] may be due to treatment of alkali because a significant decrease in alginate dynamic viscosity was observed after 2 h of alkaline treatment in a control experiment. Further, the intrinsic viscosity and average molecular weight of alginates from alkaline extractions (1–4 h) were determined, indicating depolymerization of alginates, average molecular weight decreased significantly during the extraction, falling by a factor of 5 between 1 and 4 h of extraction. These results suggest that reduction of extraction time could enable preserving the rheological properties of the extracted alginates.

In the present section, the results of our investigation on unperturbed dimension, interaction parameter of sodium alginate in water-acetone and water-ethoxy ethanol have been described. The intrinsic viscosities of the polymer have been measured in different compositions (water-acetone and water-ethoxy ethanol) of the cosolvent mixture at different temperatures. From the relation between [η] and M, the unperturbed dimension and molecular expansion factor have been measured. The Huggins constant value in each case was also determined in order to study the influence of co-solvent system [34, 40].

5.2 Experimental

In the present study, an Ubbelohde viscometer was used to measure the relative viscosities of polymer solutions. The related definitions are as follow:

Specific viscosity, $\eta_{sp} = (t - t_o)/t_o$ (2)

Reduced viscosity, $\eta_{red} = \eta_{sp}/C$ (3)

Intrinsic viscosity, $[\eta] = (\eta_{sp}/C)_{C \to o}$ (4)

and the Huggins equation is

$$\eta_{sp}/C = [\eta] + K_H [\eta]^2 C, \quad (5)$$

where K_H is the Huggins constant. In the above relations, the symbol η refers to the viscosity of solution, t is the efflux time of the solution, t_o is the efflux time of solvent and C is the polymer concentration. .

The viscosity average molecular weights of the sodium alginate (S.D Fine chemical India (High molecular weight), Loba, India (Medium molecular weight) and Fluka, Switzerland (Low molecular weight)) were determined using a suspended level Ubbelohde Viscometer placed in thermostated water bath at appropriate temperature (accuracy, ±0.1°C). A digital stopwatch with accuracy ±0.1 sec was used for measuring the flow time. Double distilled water was used throughout the experiment. Acetone (E Mark) and ethoxy ethanol (E Mark) were purified before used by fractional distillation following the usual procedure before use. A series of sodium alginate solutions of different concentrations in aqueous 0.1 M NaCl were prepared and the times of flow of the solutions were measured. Specific viscosity

$$[\eta] = \eta_{sp}/C, \text{ Lim } _{C \rightarrow O} \quad (6)$$

Where C stands for concentration of polymer solution. The molecular weight of the Sodium Alginate was finally calculated by using the model proposed by Mancini et al. [41].

$$[\eta] = 1.228 \times 10^{-4} M^{0.963} \text{ cm}^3/\text{g}. \quad (7)$$

The high, medium and low molecular weights of sodium alginates used in the study are listed in Table 1.

Table 1. Molecular weights of Sodium alginates

Sodium alginates types	$M_v \times 10^{-5}$
High Molecular weight (Type-A)	3.80
Medium Molecular weight (Type-B)	2.20
Low molecular weight (Type-C)	1.40

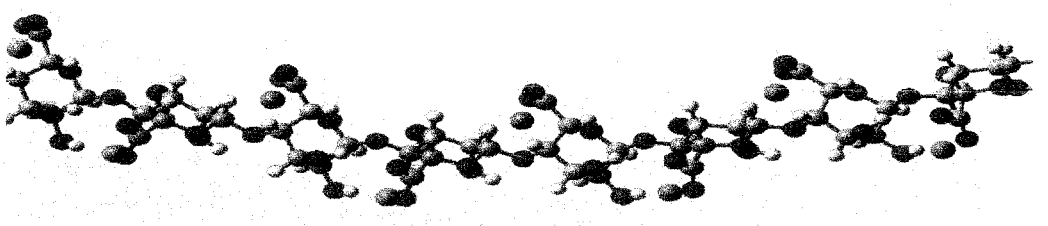

Scheme I: Molecular structure of sodium alginate (Grey; Carbon, Red: Oxygen;White: Hydrogen; Violate: Sodium)

5.2.1 Result and discussion

5.2.2 Intrinsic viscosity

Nature of the interaction between the liquids governs the solubility of a polymer in a binary liquid mixture. The changes in the molecular dimensions of the polymer in the varied molecular extension parameter (α_η) and the unperturbed dimensions due to the interaction with two component liquid have been studied [42]. In general for a flexible polymer in poor solvent, the intrinsic viscosity [η] increases with rise in temperature, whereas in good solvent it decreases with temperature. In athermal solvent, however, it is independent of temperature [43]. The polymer chains are expanded most at the temperature at which [η] is maximum. The variation of [η] in the acetone of all three types of sodium alginates (Type-A, B and C) at different temperatures and solution compositions are shown in Figure 5.1-5.3. The result shows that with increasing the amount of non-solvent (acetone) up to certain limit, intrinsic viscosity also increases for the all types of sodium alginate (Type-A, B and C). This variation is, however, distinguishable from the variation observed in case of a pure solvent system [5]. Intrinsic viscosity reaches its maximum value near

Φ_{ACE} =0.2 (Φ being the relative volume composition in the mixture) for the all three types of sodium alginates (Figure 5.1-5.3). This indicates that energetically the most favorable solvent composition is same for all three types of different sodium alginates (Type-A, B and C). The decreases in [η] after the maximum are explained by the decrease in unperturbed mean square end-to-end distance [5]. At a higher co-solvency condition, the energetic weighting factor favors the extended configuration of the sodium alginates molecules. For the sodium alginate of high molecular weight (Type-A), however, there is no such definite maxima in the plot of [η] vs. Φ_{ACE} has been observed (Figure 5.1). The higher the molecular weight of the polymer, lower concentration of acetone is required for showing the co-solvency effect. The extended long chains are surrounded by the solvated hull and longer the chain lesser is the amount of acetone required for attaining the co-solvency condition. An increase in the temperature of a polymer solution generates two antagonistic effects [44,45]. This is apparent in case of higher molecular weight sodium alginate at higher concentration of acetone. Firstly, an increase in temperature generally leads to an increase in the solubility. This results in uncoiling of the polymer chain leading to an increase in intrinsic viscosity with temperature at 25^0C Further increase in temperature may lower the rotational barrier, thereby enhancing the degree of rotation about a skeletal bond, forcing the molecular chains to assume more compact coiled configuration. This leads to decrease in intrinsic viscosity with the increase in temperature at 30^0C. On the other hand, in water-ethoxy ethanol mixture the variation of [η] of all three types sodium alginates at different temperatures and solution compositions are shown in Figure 5.4-5.6. The result shows that with increasing the amount of non-solvent (ethoxy ethanol) up to a certain limit ($\Phi_{E.E.} \leq 0.2$), intrinsic viscosity decreases for all types of sodium alginates. With increasing ethoxy ethanol (poor solvent) concentration, the intrinsic viscosity decreases due to contraction of the dimensions of polymer coil as well as the degree of intermolecular agglomeration. This variation is, however, distinguishable from the variation observed in case of a pure solvent system.

Intrinsic viscosity reaches its maximum value near $\Phi_{E.E.}$ =0.3 for all type of sodium alginates. This indicates that energetically the most favorable solvent composition is same for all the types of sodium alginates. The decrease in [η] after the maximum is explained by the decrease in unperturbed mean square end-to-end distance [5]. At a higher co-solvency condition, the energetic weighting factor favors the extended configuration of the sodium alginates molecules.

The co-solvency and the intermolecular interaction of polymers are also manifested in the Huggins constant values when the composition of the solvent is varied (equation-5). K_H values are used to predict the degree of interaction between polymer and the solvent. The sign of K_H is also often taken as a measure of the type of interaction in the polymer chain. The general positive nature of the K_H values and their increment indicate enhanced inter unit attractive interactions. Values of Huggins constant are presented in Table 5.1 and 5.2 for water-acetone and water-ethoxy ethanol mixture respectively. The K_H values are calculated from the least square slopes of equation 5. It is observed that K_H values are maximum at the solvent composition, Φ_{ACE} = 0.3 for water-acetone mixture and $\Phi_{E.E.}$ =0.1 for water-etoxy ethanol mixture respectively in all of the types of the polymers (Type-A, B and C) and the value decreases with deceasing molecular weight of the polymer, indicating lowering of the tendency of intermolecular aggregation with lower molecular weight fractions of the polymers (Type-A→Type-C). K_H has the smallest value at Φ_{ACE} =0.4 for water-acetone mixture and $\Phi_{E.E.}$= 0.4 for water-etoxy ethanol mixture respectively. Under this condition, both type of solvent pulls the distance between polymer molecules closer to make polymer side chains twisted around each other. This action makes polymer main chain wind around polymer side chain and agglomerates.

5.2.3 Unperturbed dimension (UD)

The UD of a polymer chain is the dimension where volume exclusion due to long range segmental interaction is nullified by its interaction with a definite solvent

(theta solvent) [46]. UD is the end-to-end distance of the polymer chain under theta condition and can be determined from intrinsic viscosity measurement at this condition using the following equation 47,48).

$$[\eta]_\theta = \Phi_o(r_o^2/M)^{3/2}M^{1/2}\alpha_n^3 = K_\theta M^{1/2}\alpha_n^3 \quad (8)$$

But, under non-theta conditions various equations are employed to derive K_θ of sodium alginates in different water-acetone and water-ethoxy ethanol mixtures. The required equations for the evaluation of K_θ are as followes [19-21, 49]

$$([\eta]/M)^{1/2}=K_\theta+0.51\Phi BM^{1/2}\text{[Burchard-Stockmayer and Fixman(BSF)]} \quad (9)$$

$$\{(\eta/M)^{1/2}\}^{1/2}=K_\theta^{1/2}+0.42K_\theta^{3/2}B(r_o^2{}_{/M})^{3/2}(M/[\eta])\text{-} \quad \text{[(Berry] (10)}$$

$$[\eta]^{4/5}/M^{2/5}=0.786K_\theta^{4/5}+0.454\,K_\theta^{2/5}B^{2/3}\Phi^{2/3}M^{1/3}\text{ [Inagaki-Suzuki-Kurat (ISK)] (11)}$$

The value of K_θ obtained from three different methods of measurements viz., BSF, Berry ISK and agree well with each other except in a few compositions of the solvents. The results are summarized in Table 5.3 and 5.4 for water-acetone and water-ethoxy ethanol mixture respectively. The representative BSF plots for sodium alginate fractions for various cosolvent compositions at 20^0C, 25^0C and 30^0C temperature are shown in Figures 5.7 and 5.9 for water-acetone and in Figures 5.10-5.12 for water-ethoxy ethanol mixture respectively. In the case of water-acetone mixture it is apparent that at Φ_{ACE}=0.4, the sodium alginate has the lowest unperturbed dimension and this result is in general true for all the adopted methods for K_θ calculation (BSF, Berry and ISK). Above the Φ_{ACE}=value of 0.4 the co-solvency of the system is lost and the sodium alginate is precipitated out from the solution. The effect of temperature is interesting for BSF Plot of sodium alginate in both the acetone and ethoxy ethanol fraction at various co-solvent compositions (Figure 5.7-5.11). At Φ_{ACE} =0.1 the sodium alginate shows highest K_θ value for all the methods which are used (.BSF, Berry and ISK). With an increase in temperature K_θ decreases due to greater freedom of rotation around the skeletal

bonds [85]. However, such a temperature dependence of K_θ can be attributed not only to the change in flexibility of macromolecular chain but also to the specific polymer solvent interaction [86]. The effect may also be correlated to the cohesive energy density of the polymer and the solvent. In case of ethoxy ethanol, the sodium alginate has the lowest unperturbed dimension value at $\Phi_{E.E.}$ =0.2 (true for all the methods for K_θ calculation). Strong attraction of two solvents (water and ethoxy ethanol), causes the sodium alginate to have the lowest value of unperturbed chain at above relative volume composition in the mixture where as at $\Phi_{E.E.}$ =0.4 the sodium alginate has the highest unperturbed dimension and this result is in general true for all the methods which are adopted for K_θ measurement. Above $\Phi_{E.E.}$ =0.4, the co-solvency effect is the same as that found at the Φ_{ACE} =0.1 in the water-acetone mixture.

5.2.4 Molecular extension factor (α_n)

The molecular expansion factor (α_n), which represents the effect of long-range interaction, can be described as an osmotic swelling of the chain by the solvent-polymer interaction. It has been calculated from the relation [26],

$$\alpha_n^3=[\eta]/K_\theta M_v^{1/2} \qquad (12)$$

Where K_θ has been taken from the BSF plot. The actual end-to-end distance, $\alpha_n K_\theta$, of the polymer molecule is also computed, which is shown in Table 5.5 for water-acetone and Table 5.6 for water-ethoxy ethanol mixtures respectively .It is observed that $\alpha_n K_\theta$ attains its highest value at Φ_{ACE} =0.1 for all the fractions of the sodium alginate in water-acetone mixture and at $\Phi_{E.E.}$=0.4 for all the fractions in water-ethoxy ethanol mixture respectively. As the number of segmental interaction of the polymer molecules increases with molecular weight, the value of α_n also increases. This trend is observed at all the temperatures under the study.

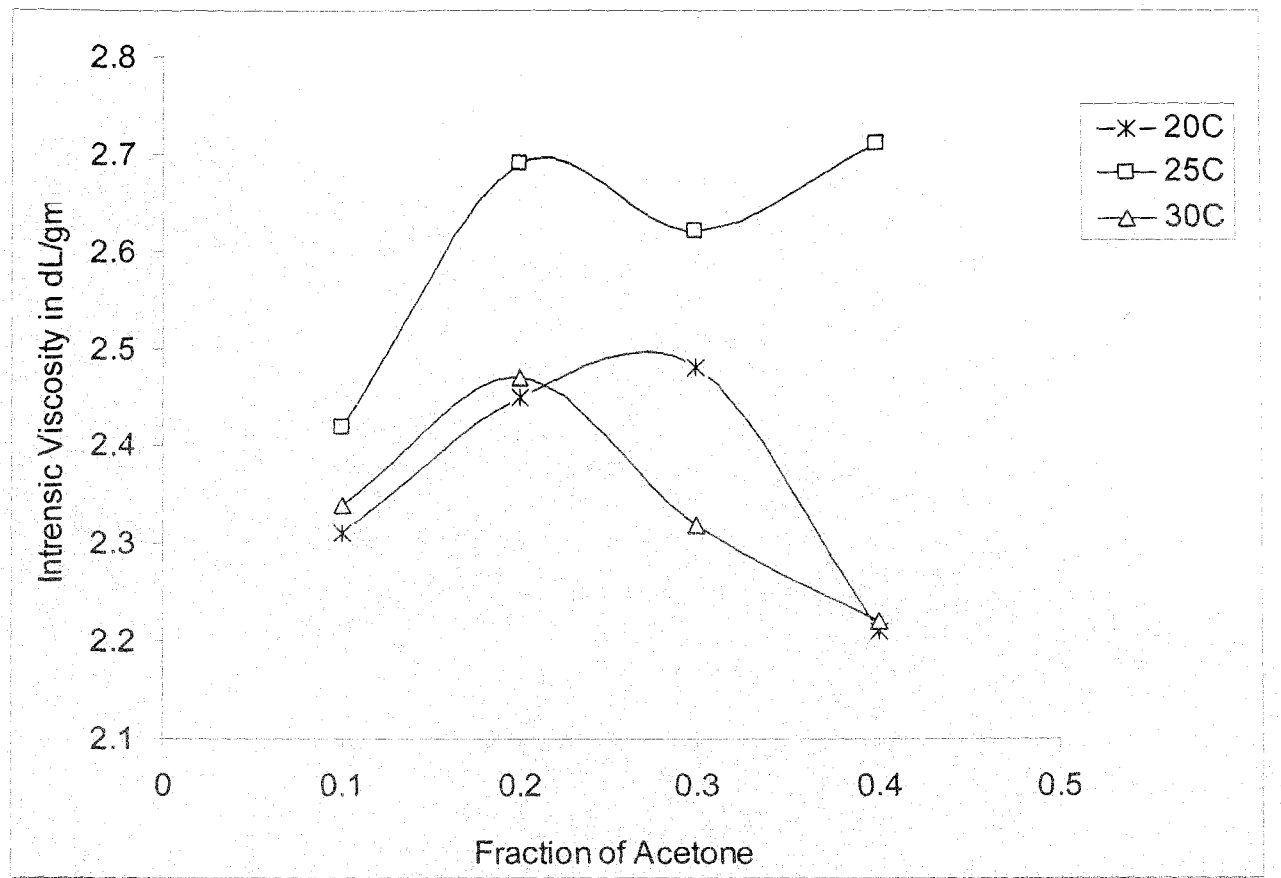

Figure 5.1: Change in intrinsic viscosity with fraction of acetone for sodium alginate of (type-A)

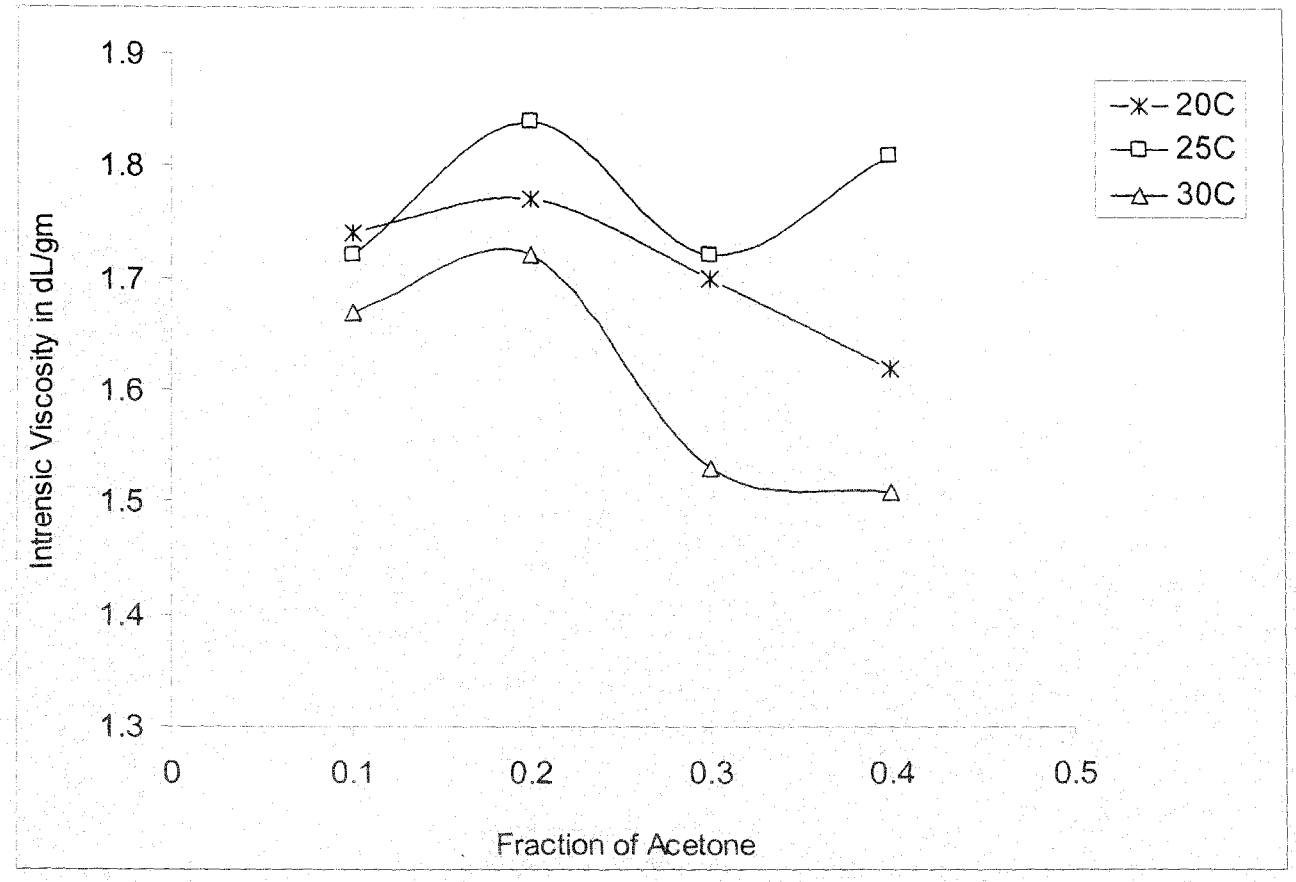

Figure 5.2: Change in intrinsic viscosity with fraction of acetone for sodium alginate of (Type-B)

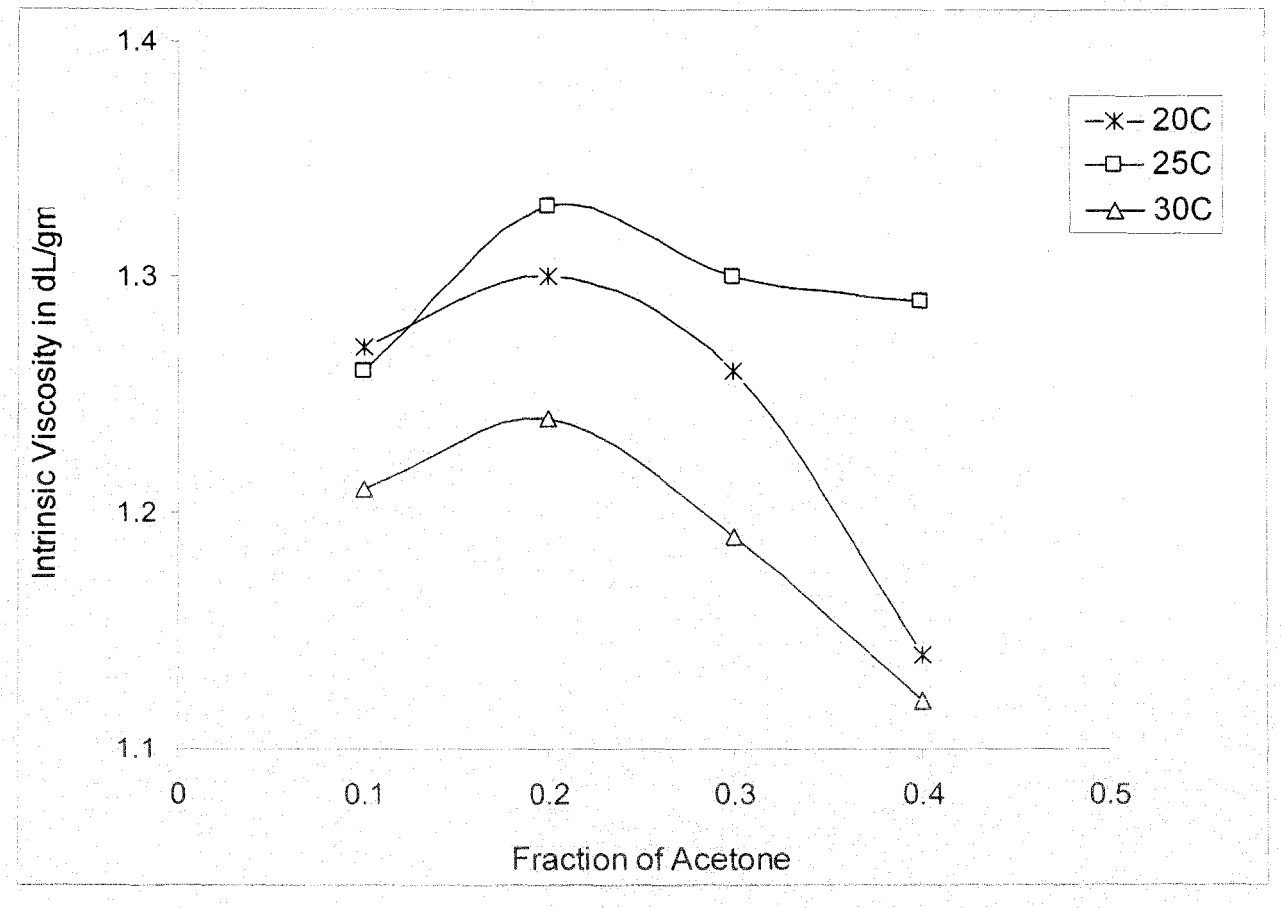

Figure 5.3: Change in intrinsic viscosity with fraction of acetone for sodium alginate of (Type-C)

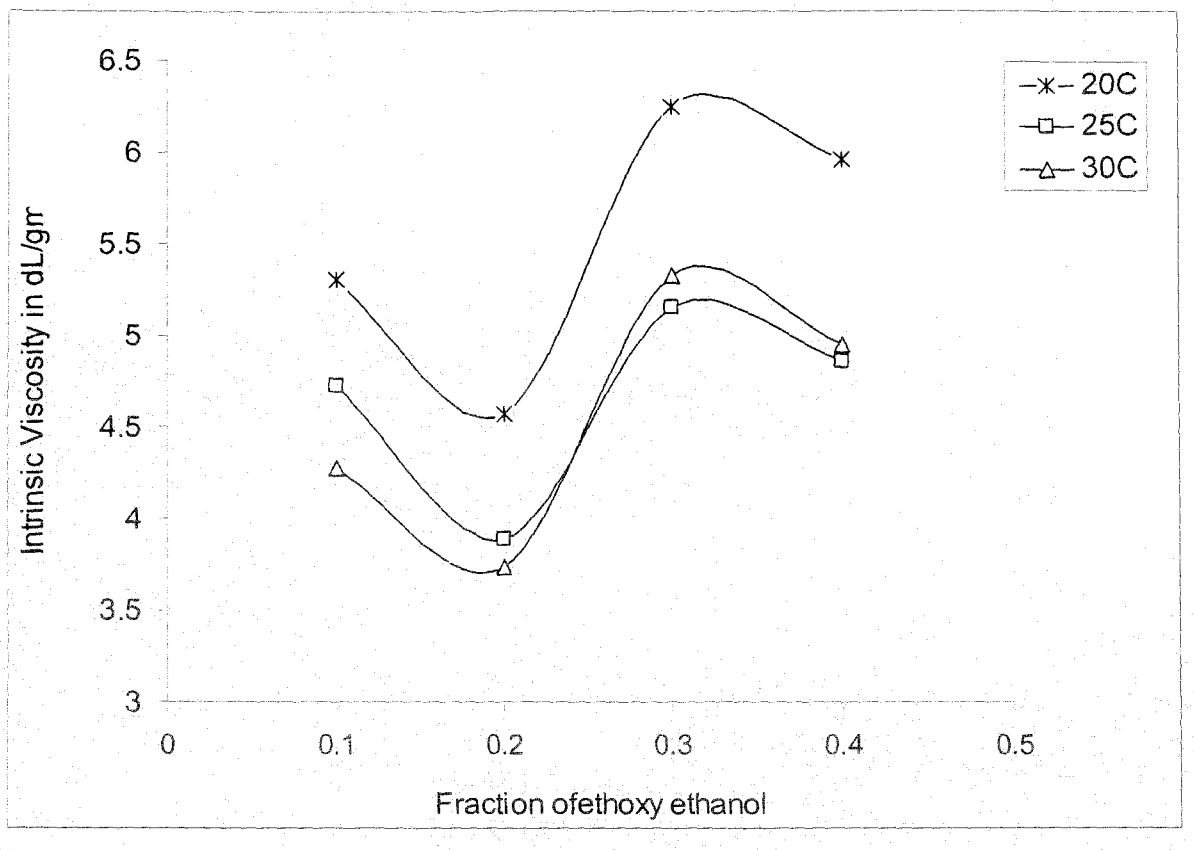

Figure 5.4: Change in intrinsic viscosity with fraction of ethoxy ethanol for sodium alginate of (type-A)

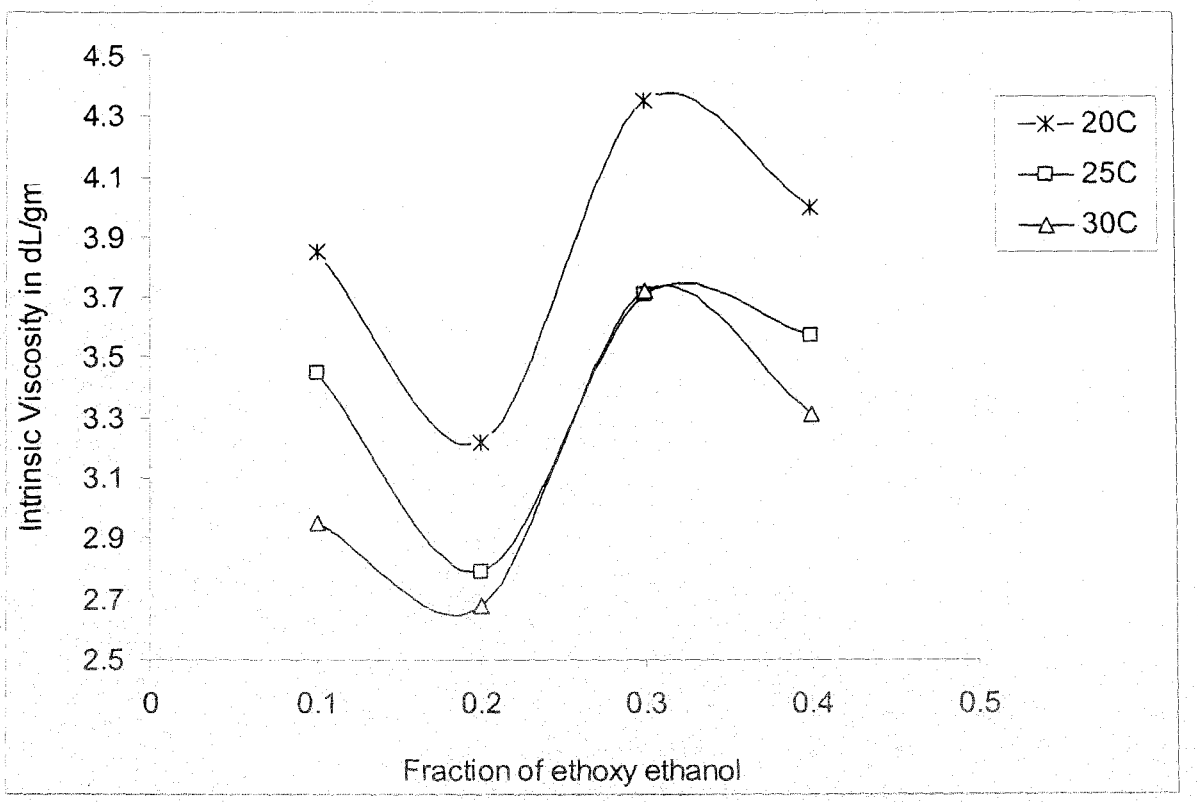

Figure 5.5: Change in intrinsic viscosity with fraction of ethoxy ethanol for sodium alginate of (type-B)

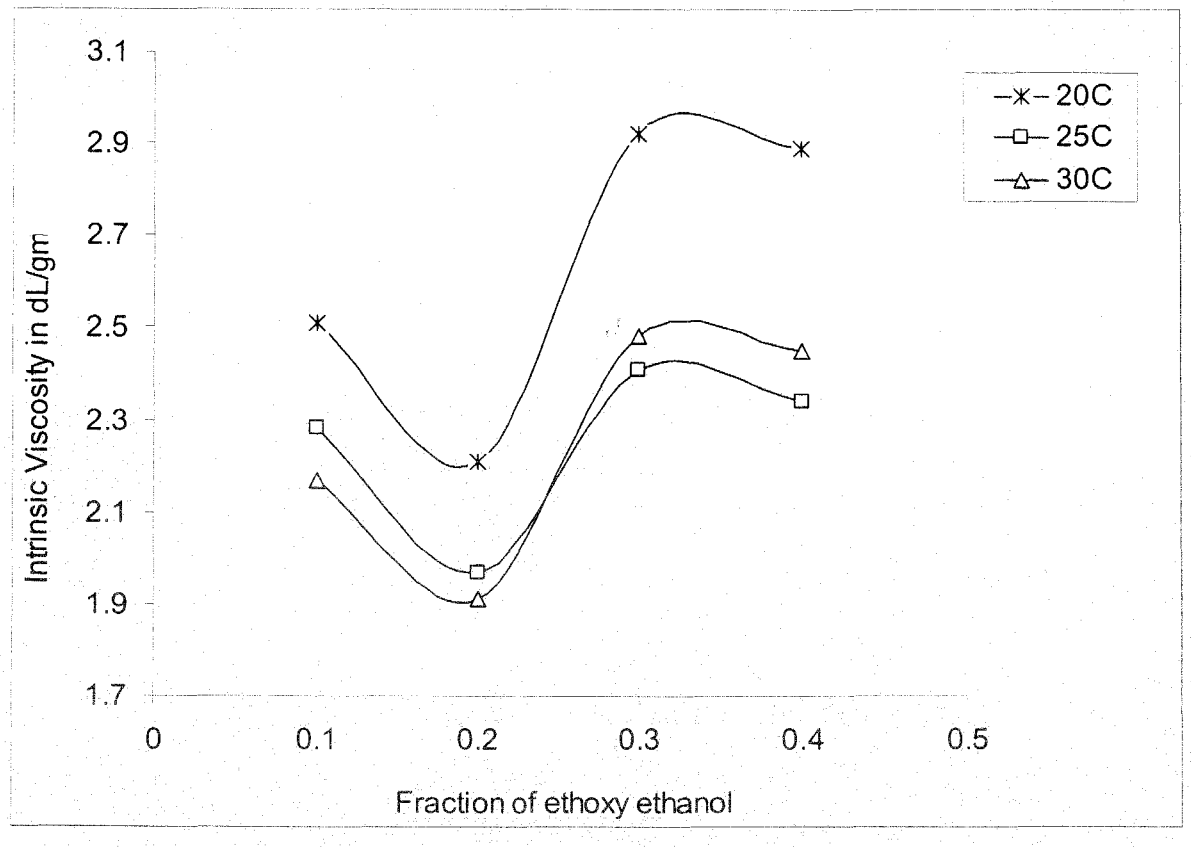

Figure 5.6: Change in intrinsic viscosity with fraction of ethoxy ethanol for `sodium alginate of (type-C)

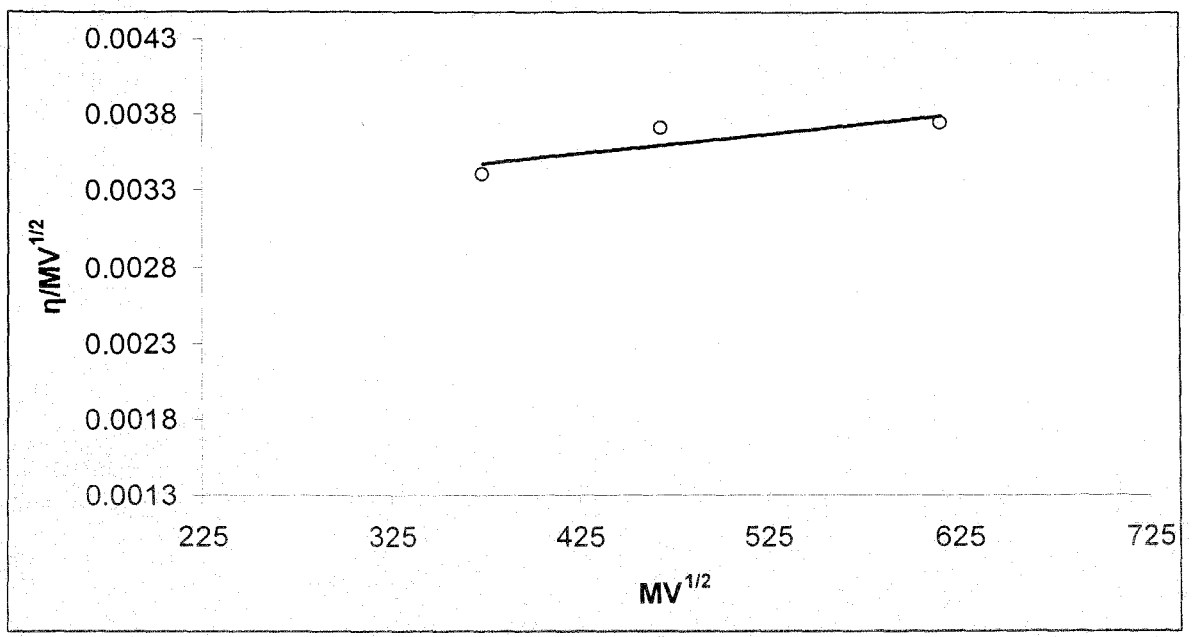

Figure 5.7: BSF plot at 20^{0}C: Φ_{ACE}=0.1 for sodium alginate.

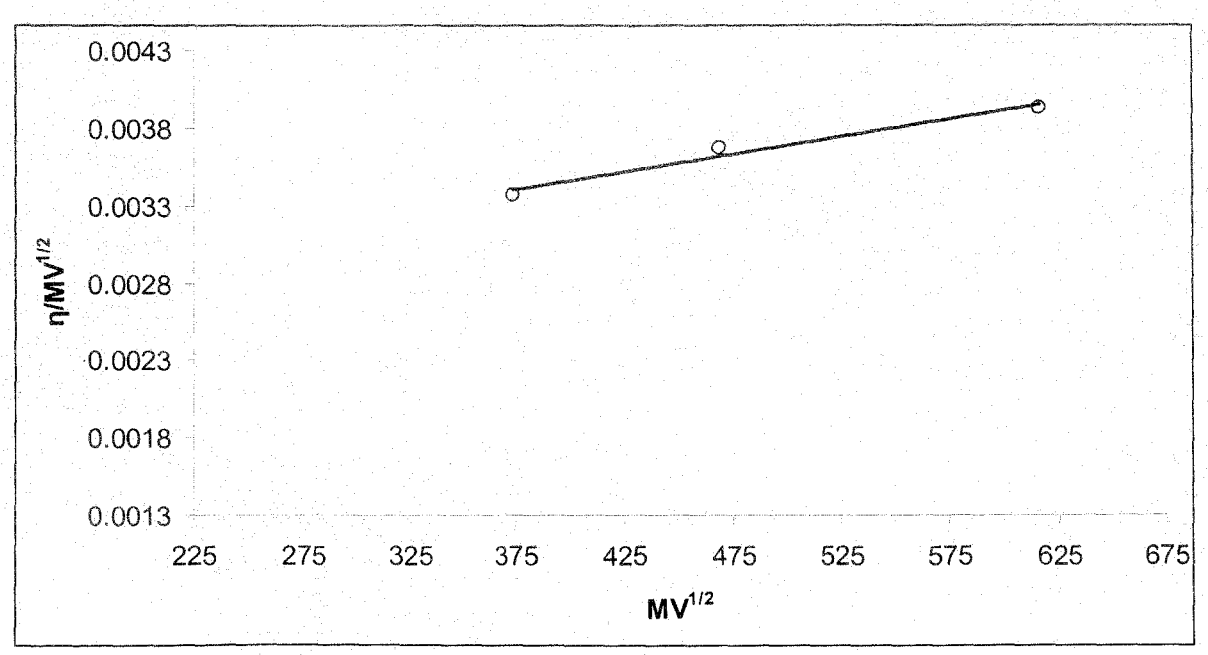

Figure 5.8: BSF plot at 25^{0}C: Φ_{ACE}=0.1for Sodium Alginate

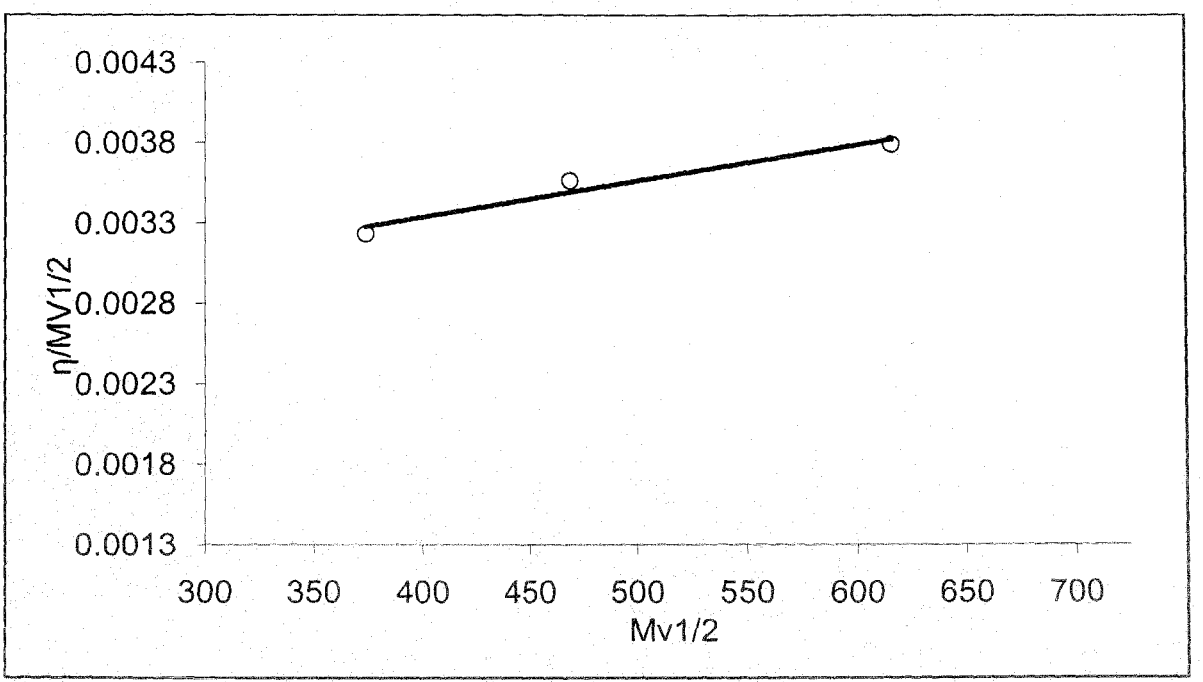

Figure 5.9: BSF plot at 30°C: Φ_{ACE}=0.1for Sodium Alginate

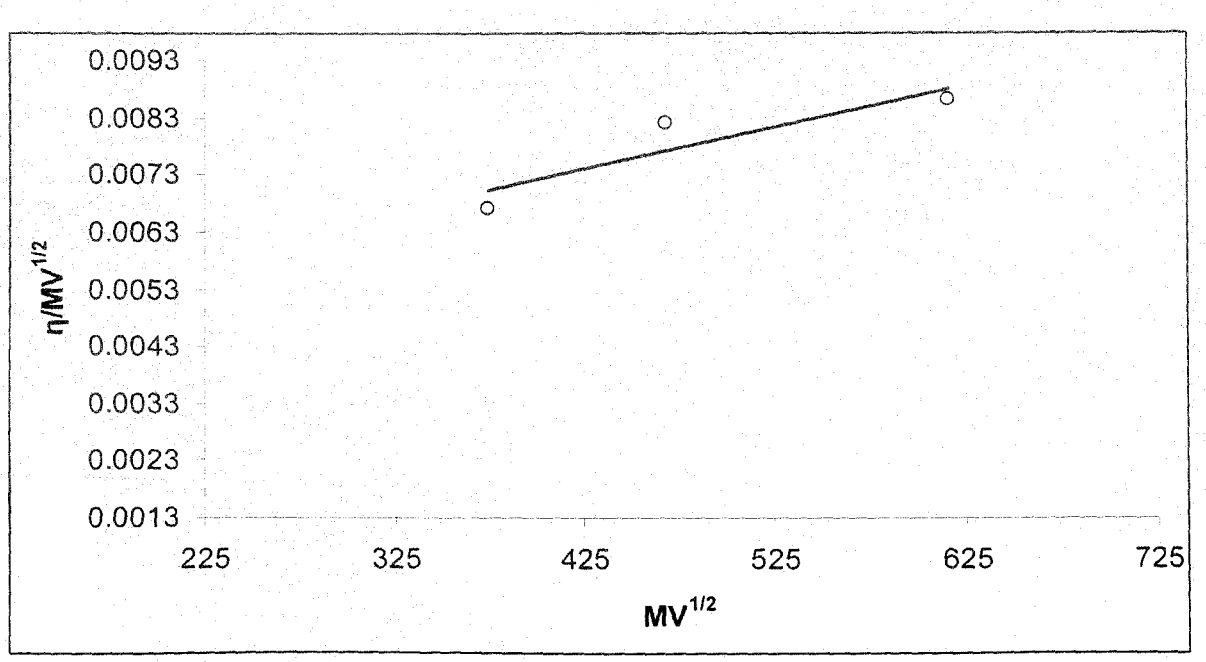

Figure 5.10: BSF plot at 20°C: $\Phi_{E.E.}$=0.1 for sodium alginate

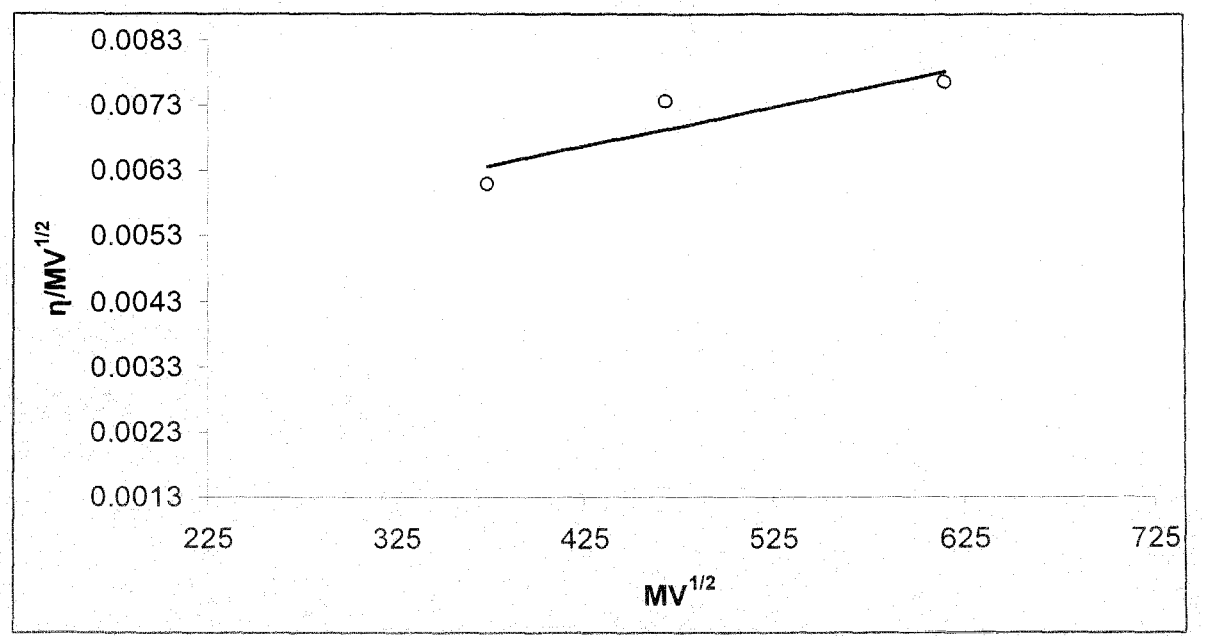

Figure 5.11: BSF plot at 25^{0}C: $\Phi_{E.E.}$=0.1 for sodium alginate

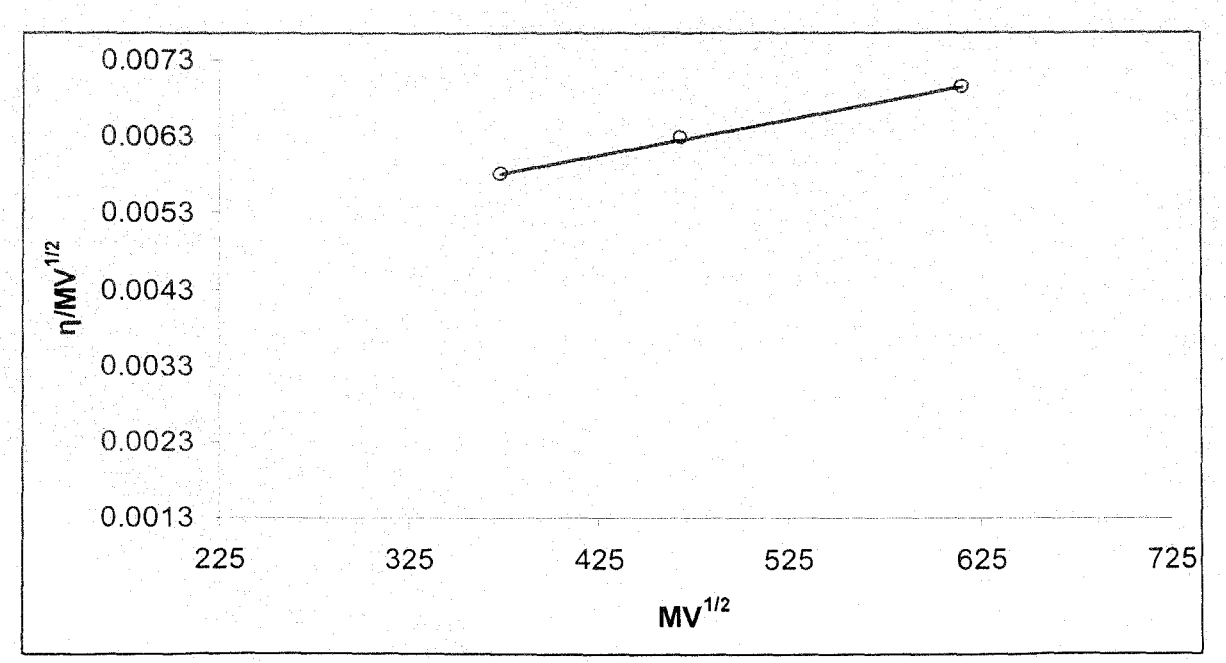

Figure 5.12: BSF plot at 30^{0}C: $\Phi_{E.E.}$=0.1for sodium alginate

Table 5.1

Huggins constant of different fractions of sodium alginate at different temperature and various solvent compositions (water-acetone).

Temp. in °C	Φ_{ACE}	Sodium alginate		
		Type-A . K_H	Type-B K_H	Type-C. K_H
20	0.1	1.242	1.131	0.968
	0.2	1.513	1.317	1.072
	0.3	1.628	1.431	1.163
	0.4	0.752	0.533	0.279
25	0.1	0.973	0.857	0.629
	0.2	1.171	0.972	0.752
	0.3	1.214	1.102	0.925
	0.4	0.472	0.386	0.296
30	0.1	1.163	1.118	0.861
	0.2	1.214	1.127	1.154
	0.3	1.246	1.238	1.179
	0.4	0.641	0.527	0.438

Table 5.2

Huggins constant of different fractions of Sodium alginate at different temperature and various solvent compositions (water-etoxy ethanol)

Temp. in °C	$\Phi_{E,E}$	Sodium alginate		
		Type-A . K_H	Type-B . K_H	Type-C. K_H
20	0.1	2.107	1.628	1.197
	0.2	1.734	1.218	1.041
	0.3	1.518	1.108	0.975
	0.4	1.445	0.873	0.448
25	0.1	1.749	1.292	1.021
	0.2	1.441	1.172	0.964
	0.3	1.138	1.008	0.825
	0.4	0.942	0.852	0.727
30	0.1	1.772	1.318	1.263
	0.2	1.460	1.284	1.154
	0.3	1.397	1.225	1.109
	0.4	1.274	0.937	0.878

Table 5.3

Unperturbed Dimension of Sodium alginate in water- acetone mixtures at different temperatures determined by different methods.

Temp. in °C	Φ_{ACE}	$K_\theta x10^4 (mol^{1/2}g^{-3/2}.dL)$		
		BSF	BERRY	ISK
20	0.1	29.60	29.11	35.69
	0.2	27.70	25.54	31.52
	0.3	23.60	19.08	24.60
	0.4	23.40	21.42	25.46
25	0.1	25.60	22.59	28.14
	0.2	23.40	16.93	22.98
	0.3	22.10	16.53	21.62
	0.4	20.10	10.86	17.69
30	0.1	24.30	21.35	26.48
	0.2	22.90	18.11	23.46
	0.3	21.90	19.04	23.08
	0.4	20.50	16.14	21.02

Table 5.4

Unperturbed Dimension of Sodium alginate in water- ethoxy ethanol mixtures at different temperatures determined by different methods.

Temp. in °C	$\Phi_{E.E.}$	$K_\theta x10^4 (mol^{1/2}g^{-3/2}.dL)$		
		BSF	BERRY	ISK
20	0.1	42.30	35.41	37.76
	0.2	38.10	27.64	35.79
	0.3	45.70	27.76	38.91
	0.4	47.50	30.09	44.17
25	0.1	40.80	35.74	38.76
	0.2	38.20	32.63	40.02
	0.3	39.30	16.53	34.00
	0.4	41.80	37.66	39.44
30	0.1	40.60	21.35	42.24
	0.2	37.90	33.09	40.60
	0.3	38.30	19.04	31.97
	0.4	42.10	30.41	41.29

Table 5.5

Molecular extension factor and coil dimensions of sodium alginate at different temperature in various solvent composition (water-acetone).

Temp. in°C	Φ_{ACE}	Sodium alginate					
		Type-A		Type-B		Type-C	
		α_n	$\alpha_n x K_\theta x 10^4$	α_n	$\alpha_n x K_\theta x 10^4$	α_n	$\alpha_n x K_\theta x 10^4$
20	0.1	1.082	32.021	1.078	31.913	1.047	30.982
	0.2	1.128	31.242	1.109	30.707	1.078	29.873
	0.3	1.195	28.192	1.154	27.228	1.126	26.569
	0.4	1.153	26.976	1.139	26.643	1.092	25.252
25	0.1	1.153	29.521	1.127	28.858	1.096	28.050
	0.2	1.231	28.803	1.188	27.798	1.150	26.899
	0.3	1.244	27.483	1.184	26.164	1.163	25.697
	0.4	1.298	26.091	1.243	24.982	1.197	24.001
30	0.1	1.160	28.195	1.136	27.600	1.100	26.729
	0.2	1.205	27.595	1.170	26.791	1.131	25.903
	0.3	1.198	26.232	1.142	25.011	1.132	24.800
	0.4	1.207	24.736	1.162	23.828	1.134	23.257

Table 5.6

Molecular extension factor and coil dimensions of sodium alginate at different temperature in various solvent composition (water-ethoxy ethanol).

Temp. in°C	$\Phi_{E.E.}$	Sodium alginate					
		Type-A		Type-B		Type-C	
		α_n	$\alpha_n x K_\theta x 10^4$	α_n	$\alpha_n x K_\theta x 10^4$	α_n	$\alpha_n x K_\theta x 10^4$
20	0.1	1.267	53.594	1.247	52.761	1.166	49.328
	0.2	1.248	47.549	1.217	46.362	1.157	44.095
	0.3	1.303	59.547	1.266	57.859	1.195	54.624
	0.4	1.267	60.183	1.215	57.731	1.175	55.856
25	0.1	1.233	50.326	1.217	49.656	1.143	46.637
	0.2	1.182	45.157	1.159	44.276	1.113	42.512
	0.3	1.285	50.532	1.263	49.619	1.179	46.335
	0.4	1.236	51.645	1.221	51.043	1.144	47.808
30	0.1	1.196	48.551	1.157	46.977	1.126	45.725
	0.2	1.169	44.296	1.147	43.458	1.104	41.855
	0.3	1.312	50.243	1.275	48.818	1.201	45.983
	0.4	1.240	52.211	1.188	50.010	1.159	48.778

5.3 Reference:

1. G.Meera and T. E. Abraham, "Polyionic hydrocolloids for the intestinal delivery of protein drugs: Alginate and chitosan-a review",*Journal of Controlled Release,* **114** ,1,(2006)
2. A. Ikeda, A. Takemura and H. Ono. *Carbohydr .Polym.*, **42** ,421 (2000)
3. K .Jun-ichi ,S.Shingo, S.Shin-ichiro, "Preparation of alginate- polymethacrylate hybridmaterial by radical polymerization of cationic methacrylate monomer in the presence of sodium alginate"_*Carbohydrate polymers,* **60,** 253 (2005)
4. McNeely WH and Pettitt DJH. 1973. Algin. In: Polysaccharides and Their Derivatives. 2nd ed.Whistler RL and BeMiller JN, eds. Academic Press, New York, US, pp. 49-81
5. P.J Flory, Principles of polymer, Ithaca:Cornell university Press; 1953
6. A. Dondos and H. Benoit, *Macromolecules,* **4**(3), 279 (1971).
7. R. Tajero, C. Gomez, B. Celda, R. Gavara, and A. Campos, *Makromol. Chem*, **189** (7), 1643 (1988).
8. I.A. Katime and J.R. Quintana,. *J. Macromol. Chem.*, **189**(6), 1373 (1988).
9. L. Katime and J.R. Schio, *Eur. Polym. J.*, **20**(1), 99 (1984).
10. T. Scwartz, J. Sabbadin, and J. Francois, *J. Polymer*, **22,** 609 (1979).
11. J. Francois,.D. Sarazin, T.S chwartz and G. Weill , *Polymer*, **20**, 969(1979).
12. T. Scwartz,. J. Francois, and G. Weill. *Polymer*, **21**, 247 (1980).

13. W. Scholtan, *Macromol Chem*, **14**(1), 169, (1954)

14. S. Newman, S. Krigbaum, W.R. Laugier, and P.J. Flory, *J. Polym Sci*, **14**, 451 (1954).

15. G.S. Misra and S.H. Bhattacharya, *Eur Polym J.*, **15**, 125(1979).

16. M. Bohdonecky, V. Petrus and B. Sedlacek, *Makromol Chem,* **184**, 2061 (1983).

17. P.J. Flory and T.G. Fox, *J Am Chem Soc*, **73**:1904 and 1915. (1951).

18. H. Kurata, W.H. Stockmayer and A. Roig, *J Chem Phys*, **33**(1), 151 (1960).

19. W.H. Stockmayer and M. Fixman, *J. Polym. Sci.*, **C 1**,137 (1963).

20. G.C. Berry and E.F. Casassa, *J Polym Sci-Macromolecular reviews*, **4 (1),** 1-66. (1970)

21. W. Buchard, *Makromol. Chem.* **50,** 20(1960).

22. A. Dondos and H. Benoit, *Macromolecules.* **6(2)**, 242(1973).

23. K. Savas and K. Zuhal, *Polymer Communications*, **31(1)**, 35(1990).

24. P. Vasudevan and M. Santappa, *Makromol. Chem.*, **137,**261(1970).

25. I. Nishio, S. T. Sun, G. Swislow and T.Tanaka,*Nature*,**281**,208(1979).

26. B. Maitra and A.K. Nandi, *Polymer*, **34(6)**,1261(1993).

27. O.Chintore, M.Guaita and L.Trossarelli, *Makromol.Chem.* **180,** 2019(1979).

28. O.Chintore, M.Guaita and L.Trossarelli, *Makromol.Chem.* **180,**969(1979).

29. M. Kurata, Y. Tsunashima, M. Iwama and K. Kamada, in: "Polymer Handbook", edited by J. Brandrup and E.H. Immergut, 2nd edition, Wiley-Interscience, New york,IV-36,(1975).

30. T. Schwartz, J. Sabbadin and J. Francois, *Polymer*. **22,**609 (1981).

31. C. Okada, K. kamada, T. Yoshihara, J. Hosoda and A. Fumuro, 'Reports on Progress in Polymer Physics in Japan' XX5, (1977).

32. N. Yamaguchi, N. Onda and Y. Hirai, 'Reports on progress in Polymer physics in Japan' XXI, 63 (1978).

33. S. Newman, W.R. Krigbaum, C. Laugier and P.J. Flory, *J. Polym. Sci.*, **14**, 451 (1954)

34. P. Bera and S.K. Saha, *Eur. Polym. J*, **37**, 2327 (2001)

35. C.I. Simionescu, S. Ioan, and B.C. Simionescu, *Rev Roum Chim.*, **31**, 995 (1986).

36. M. Bercea , S. Morariu ,S. Ioan and B.C. Simionescu , *Synth Polym J.*, **1**, 81 (1994)

37. M. Bercea, C. Ioan, S. Morariu, S. Ioan, and B.C. Simionescu, *Polym Plast. Technol. Eng.*, **37,** 295,(1998).

38. Celine Sartori , Ph.D thesis, Department of Materials Engineering, Brunel University May 1997

39. V.Peggy, A.Abdellah L.Jack, K.Raymond and B.Régis *Journal of Phycology*, **44(2)** 515 (2008)

40. G. Bit, B. Debnath, S. K. Saha, *Eur. Polym. J*, 42 (2006) 544

41. M.Mancini,M.Moresi and F.Sappino, Rheological behavior of aqueous dispersions of algal sodium alginates, *J. Food Eng.* ,**28**,283 (1996).

42. A.Dondos,P.Rempp and H.Benoit,*J.Polym.Sci,***C30**,9 (1970).

43. A.Dondos and H.Benoit ,*Macromolecules,***4,** 279 (1971).

44. T. Alfrey, A. Bartovics and H. Mark *J Am Chem Soc*, **64**, 1557(1942).

45. I.Noda, T.T. Suge, M. Nagasawa, *J Phys Chem*, **74**(Feb.19): 710 (1970).

46. V. Vangani and A. K. Rakshit, *J Appl Polym Sc*, **60**(**7**), 1005(1996).

47. P.J. Flory and T.G.Fox, J Am Chem Soc,73,1904 and 1915 (1951)

48. H.Kurata W.H. Stockmayer and A. Roig, J Chem Phys, 33(1),151 (1960)

49. H. Inagaki, H Suzuki, M. Kurata. J Polym Sci, C15,409(1966)

50. S. Ioan, M. Bercea, C.I. Simionescu and B.C. Simionescu. In: Salamon JC, editor. The polymeric encyclopaedia: synthesis, properties and applications, 11. Boca Raton FL:CRC Press, 8417 (1996).

CHAPTER 6

Studies on solution properties of Poly (Vinyl Alcohol) in water-acetone and water-tetra hydro furan mixtures

6.1. Introduction and review of the previous work

Poly(vinyl alcohol) (PVA) has attracted much attention due to its excellent flexibility, transparency, toughness, and relatively low cost, especially in the era of high price petroleum. PVA has been widely used in different fields including textile sizing and is utilized as a finishing agent, an emulsifier, a photosensitive coating, and as an adhesive for paper, wood, textiles, and leather [1,2] In addition, it is a biologically friendly polymer because of its biodegradability and biocompatibility [3] The unperturbed dimention (K_θ) of a polymer sample may be used to assess the viscosity expansion (α_η) of a flexible polymer chain [4,5].This important parameter K_θ, is conventionally determined by the solution-viscosity method at theta condition.

One of the most important methods utilizes Mark- Hownik-Sakurda (MHS) eqution at theta condition (Equation 1)

$$[\eta]_\theta = K_\theta M^{1/2} \qquad (1)$$

Where K_θ is the unperturbed dimension of the polymer which can be calculated from a number of graphical procedures based on the various theories of dilute polymer solution in non theta solvents.(as shown in Chapter 5)

Poly (vinyl alcohol) is an industrially important polymer, and this is shown by the fact that its production increases every year [6-10]. It exhibits a high degree of compatibility with inorganic salts [11], natural and synthetic resins, and other chemicals [12,13]. Small amount of PVA effectively stabilize emulsions [14], dispersions, and suspensions [15]. It also forms chemical complexes of practical importance [16]. The intrinsic viscosity [η], which is a measure of the hydrodynamic size of the isolated molecules, and Huggin's constant K_H [17] which is a measure of their interactions with solvent, are both influenced by changes of solvent power[18] and temperature[19]. Besides theoretical interest, such measurements are also important for technical reasons such as the technique of polymer addition in motor oil recovery. Advances in the preparation of stereoregular polymers have stimulated the need to characterize their microtacticity and fine structure [20]. A

number of studies and experimental techniques were used to characterize the nature of polymers in different solvents, but there seems to be few systematic studies of the dilute solution properties in different solvents, and these are restricted to one or two temperatures.[21,22] As far as the polymers are concerned, the viscosity method can be successfully employed for the determination of the nature of the compound and their behavior in different solvents.

6.2 Exeperimental

High molecular weight Poly vinyl alcohol(Type-A) (average molecular weight $1.24x10^5$), medium molecular weight Poly vinyl alcohol(Type-B) (average molecular weight $0.95x10^5$) and low molecular weight Poly vinyl alcohol(Type-C) (average molecular weight $0.72x10^5$) were purchased from Aldrich, Belgium, Across organics,USA and Fluka,Switzerland respectively. An Ubbelohde viscometer was used to mesure the relative viscosities of polymer solutions. The Viscometer was placed in thermostated water bath at appropriate temperature, controlled within the range of $\pm 0.1^{\circ}C$ and a digital stopwatch with accuracy ± 0.1 sec was used to measure flow time. The definitions of the important quantities and parameters are as follow:

Specific viscosity, $\eta_{sp} = (t - t_o)/t_o$ (2)

Reduced viscosity, $\eta_{red} = \eta_{sp}/C$ (3)

Intrinsic viscosity, $[\eta] = (\eta_{sp}/C)_{C \to o}$ (4)

and the Huggins equation is

$\eta_{sp}/C = [\eta] + K_H [\eta]^2 C,$ (5)

where K_H is the Huggins constant. In the above relations, the symbol [η] refers to as the viscosity of solution, t is the efflux time of the solution, t_o is the efflux time of solvent and C is the polymer concentration.

6.2.1 Result and Discussion

6.2.2 Intrinsic viscosity

The nature of interaction between liquids governs the solubility of a polymer in binary liquid mixtures. The changes in molecular dimension of the polymer in these systems are manifested in the varied molecular extension parameters and the unperturbed dimension due to the interaction with two component liquid mixtures. In general, for a flexible polymer in poor solvent, the intrinsic viscosity increases with temperature, whereas in good solvent it decreases with temperature. In athermal solvent, however, viscosity is independent of temperature (As has been already mentioned in Chapter 5) [23]. The polymer chains are expanded most at the temperature at which intrinsic viscosity ([η]) is the maximum. The variation of [η] in the water-acetone mixture of all three types of PVA at different temperatures and solution compositions are shown in Figure 6.1-6.3. The result shows with the increase in the amount of nonsolvent (acetone) up to a certain limit, intrinsic viscosity also increases for all types of Poly (vinyl alcohol). Intrinsic viscosity reaches its maximum value near Φ_{ACE} = 0.4 (Φ being the relative volume composition in the mixture) for all types of Poly (vinyl alcohol). This indicates that energetically the most favorable solvent composition is same all types of PVA. It is found that for all the molecular weight fractions, the intrinsic viscosity attains the minimum near Φ_{ACE}= 0.3, indicating energetically the most unfavorable solvent composition for the polymer. The lowest value of [η] at Φ_{ACE}= 0.3 indicates the maximum degree of intermolecular aggregation of the polymer at this solvent composition. The decrease in [η] after a certain limit is explained by the decrease in unperturbed mean square end-to-end distance. Instead of giving a minimum with the variation of solution composition, the [η] reaches a maximum for all the polymer fractions at Φ_{ACE} = 0.4 due to most powerful co-solvent effect. On the

other hand, the variation of [η] in the water-tetrahydrofuran (THF) mixture of all three types of Poly vinyl alcohol at different temperatures and solution compositions are shown in Figure 6.4-6.6. The result shows that with the increase in the THF (poor solvent) concentration, the intrinsic viscosity decreases due to the contraction of the dimensions of polymer coil as well as for the higher degree of intermolecular agglomeration. However, at high value of Φ_{THF} the [η] value tends to increase again for preferential solvation of the polymer due to high co-solvent effect. It is found that for all the molecular weight fractions, the intrinsic viscosity attains the minimum near Φ_{THF}= 0.2 indicating energetically most unfavorable solvent composition for the polymer. The [η] reaches a maximum for all the polymer fractions at Φ_{ACE} = 0.3 due to most powerful co-solvent effect. The decrease in [η] after the maximum is explained by the decrease in unperturbed mean square end-to-end distance. Moreover the effect of temperature on [η] is also important. In case of both the binary solvent mixtures (i.e. water-acetone mixture and water- THF mixture) with increasing temperature the value of [η] decreases due to lowering of the rotational barrier of the polymer. This enhance the degree of rotation about a skeletal bond, forcing the molecular chains to be more compact.

The co-solvency and the intermolecular interaction of polymers are also manifested in the Huggins constant (K_H) values when the composition of the solvent is varied. K_H values are used to predict the degree of interaction between polymer and the solvent. The sign of K_H is also often taken as a measure of the type of interaction in the polymer chain. The general, positive value of the K_H values and their increment with the medium composition indicate enhanced interunit attractive interactions. Values of Huggins constant are presented in Table 6.1and 6.2 for water- acetone mixture and for water-THF mixture respectively. The K_H values are calculated from the least square slopes of equation (5). It is observed that K_H values are maximum at the Φ_{ACE} = 0.1 for water- acetone mixture and also at the Φ_{THF} = 0.1 for the water- THF mixture respectively for all the types of polymers, indicating higher tendency of intermolecular aggregation at this composition of the solvent. K_H is the smallest for Φ_{ACE} = 0.4 and for Φ_{THF}=0.3

under this condition, the nonsolvents pull the distance between polymer molecules closer to make polymer side chains twisted around each other. This action makes polymer main chain winds around polymer side chain and agglomerates.

6.2.3 Unperturbed dimension (UD)

The unperturbed dimension of a polymer chain is important in understanding the physical properties of the polymer both in solution as well as in the solid state. It is the dimension of the polymer chain where volume exclusion due to long range segmental interaction is nullified by its interaction with a definite solvent (θ) [24, 25]. UD is the end-to-end distance of the polymer chain under theta condition and can be determined from intrinsic viscosity measurement at this condition. In the present study, BSF equation under non-theta condition [26] has been used to derive K_θ (UD) of PVA in different water- acetone mixtures and water- THF mixtures respectively. The results are summarized in Table 6.3 for water- acetone mixtures and in Table 6.4 for water- THF mixtures respectively. Some of the BSF plots are shown (Chapter 5) in figures 6.7- 6.9 for water-acetone mixtures and in figures 6.10-6.12 for water- THF mixtures respectively. Plots are essentially linear. The value of K_θ obtained from various methods of measurements viz. BSF, ISK and Berry agree well with each other except for a few composition conditions of the solvents. It is apparent that at Φ_{ACE} =0.4 and Φ_{THF}=0.1 polymer have the lowest unperturbed dimension (this result is in general true for all the adopted methods for K_θ calculation). Strong attraction of two solvents (water- acetone mixtures at Φ_{ACE} =0.4), causes the Poly (vinyl alcohol)s to have the lowest value of unperturbed chain .On the other hand, . It is observed that at Φ_{ACE} =0.2 and Φ_{THF}=0.4, the polymer have the highest unperturbed dimension (this result is in general true for all for all the methods which are mentioned for K_θ calculation) which indicates that above Φ_{ACE}=0.2 water - acetone mixtures have the same co-solvency effect as was found at the Φ_{THF}=0.4 in the water - THF mixtures. The effect of temperature is interesting. With an increase in temperature, r_0^2 and hence K_θ, increase due to greater bindness of rotation around the skeletal bonds. However, such a

temperature dependence of K_θ can be attributed not only to the change in flexibility of macromolecular chain but also to the specific polymer solvent interaction [27]. The effect may also be correlated to the cohesive energy density of the polymer and the solvent.

6.2.4 Molecular extension factor (α_n)

The molecular extension factor (α_n), which represents the effect of long-range interaction, can be described as an osmotic swelling of the chain by the solvent-polymer interaction.

α_n has been calculated from the relation given below

$$\alpha_n^3 = [\eta]/K_\theta M_v^{1/2} \qquad (6)$$

where K_θ has been taken from the BSF plot.

The actual end-to-end distance, $\alpha_n K_\theta$, of the polymer molecule is also computed, which is shown in Table 6.5 for water - acetone mixtures and in Table 6.6 for water - THF mixtures .It is observed that $\alpha_n K_\theta$ do not attains a definite lowest value at any fraction for water -acetone mixture but at Φ_{THF} =0.1 (water - THF mixtures) it is minimum. However, α_n value is the highest at the above composition .The intermolecular interaction is probably responsible for the high value of α_n at that (Φ_{THF} =0.1) composition for the solvent mixtures (water - THF mixtures). The molecular weight dependency of α_n is probably clear from the Table 6.5 and 6.6. α_n generally increases with increase in molecular weight of the polymer. As the molecular weight of the polymer increases, the number of segmental interaction of the polymer molecules with the solvent molecule increases, resulting in a large value of α_n.

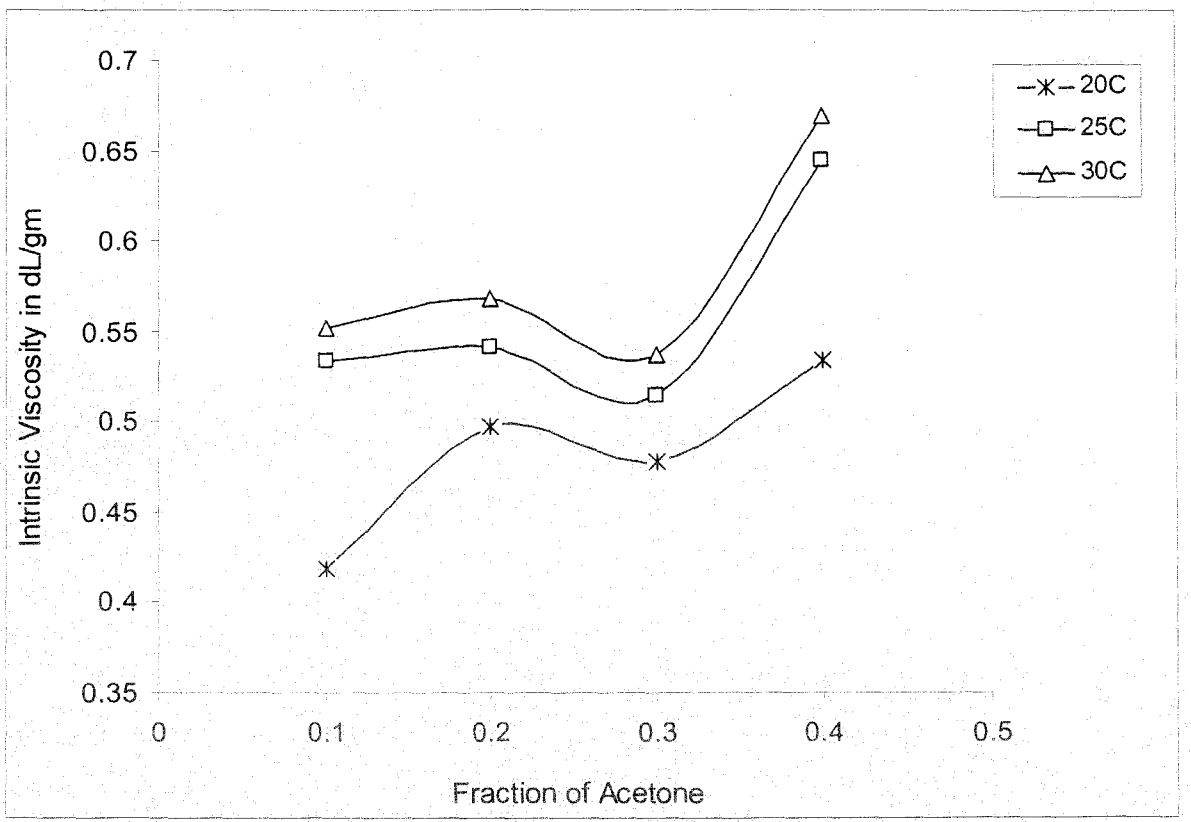

Figure 6.1: Change in intrinsic viscosity with fraction of acetone for PVA of (Type-A.)

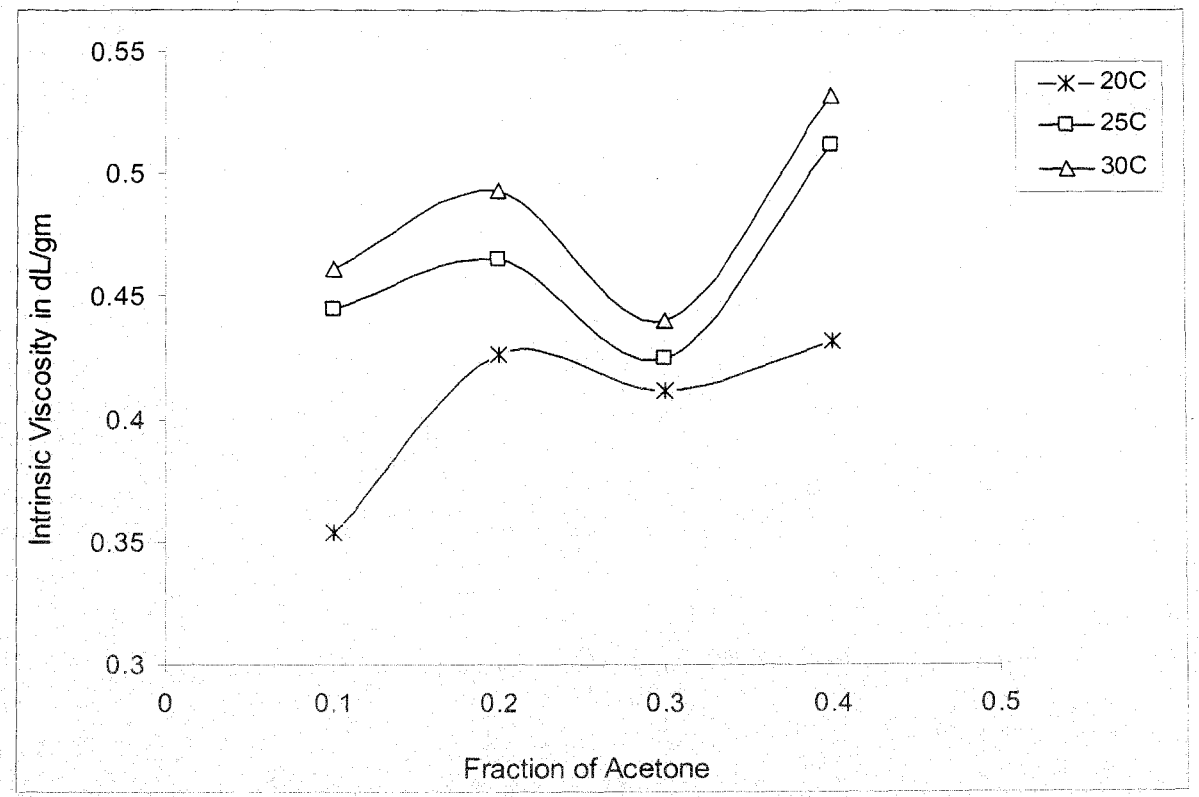

Figure 6.2: Change in intrinsic viscosity with fraction of acetone for PVA of (Type-B)

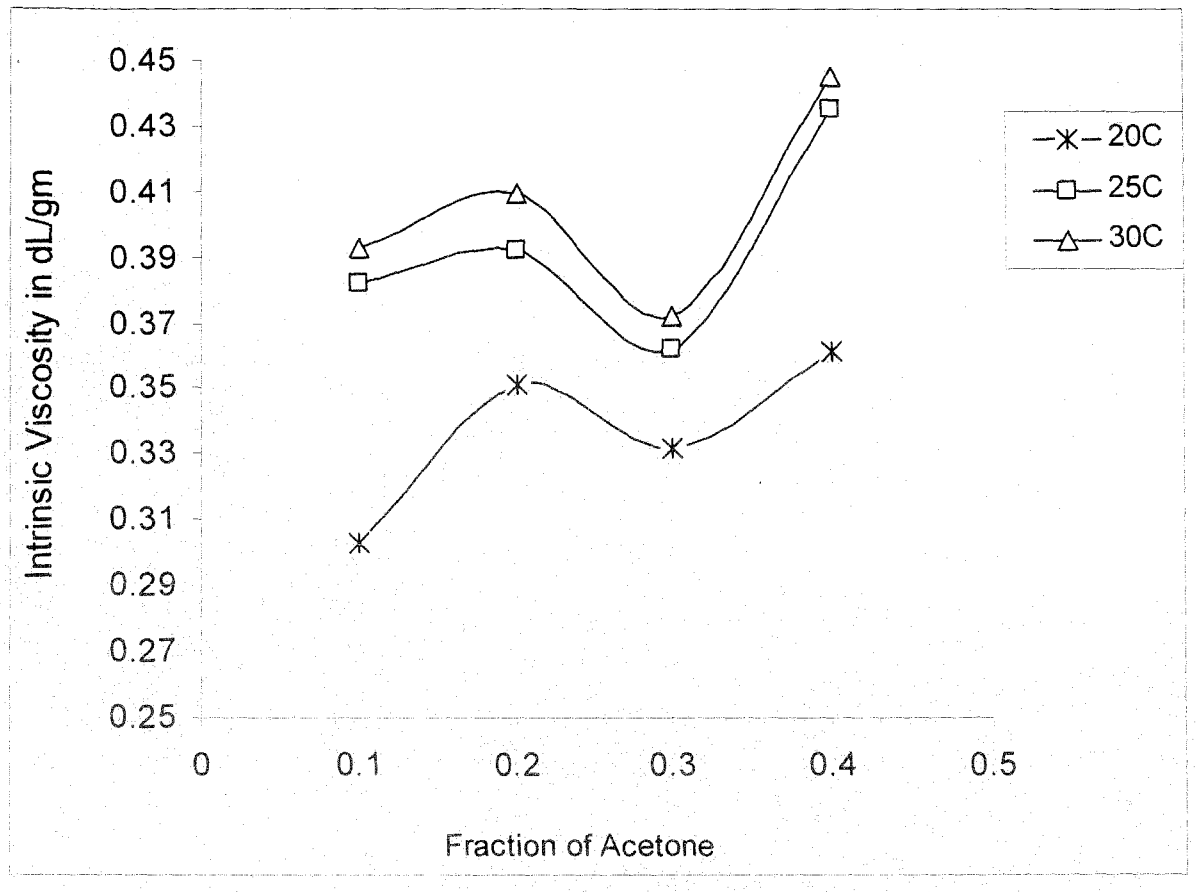

Figure 6.3: Change in intrinsic viscosity with fraction of acetone for PVA of (Type-C)

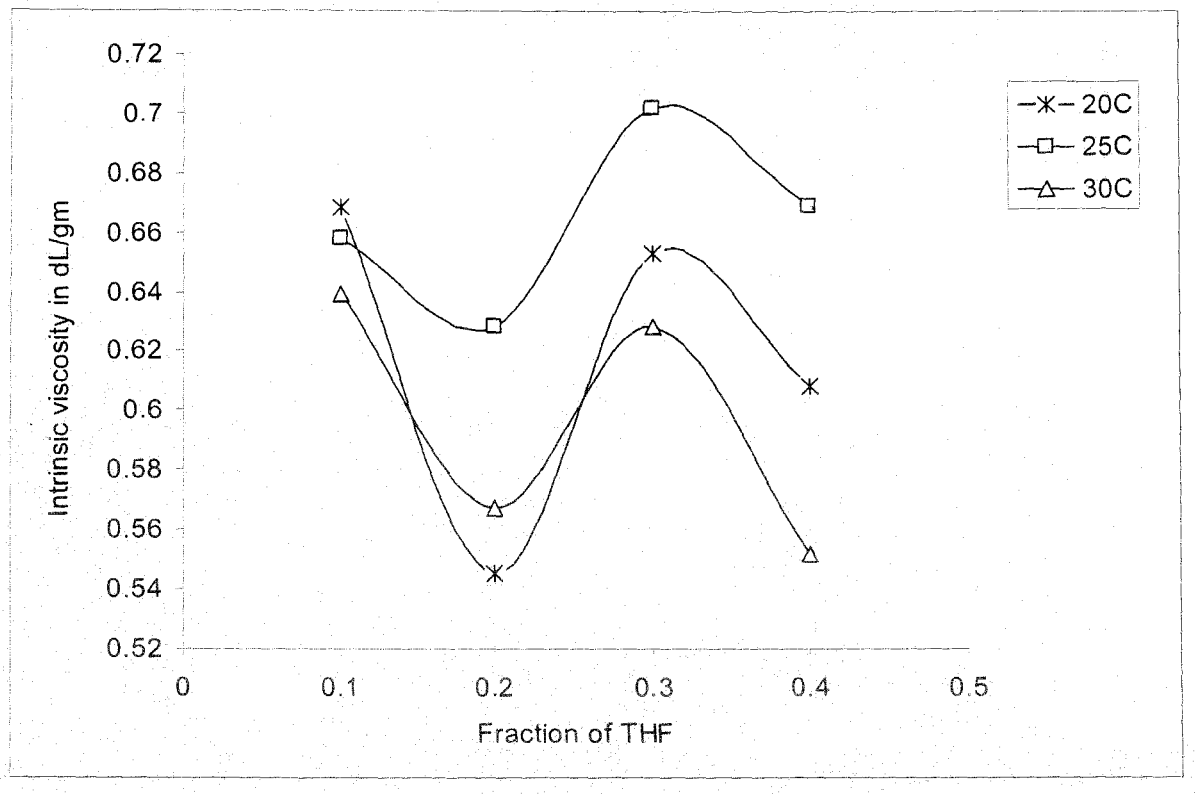

Figure 6.4: Change in intrinsic viscosity with fraction of THF for PVA of (Type-A)

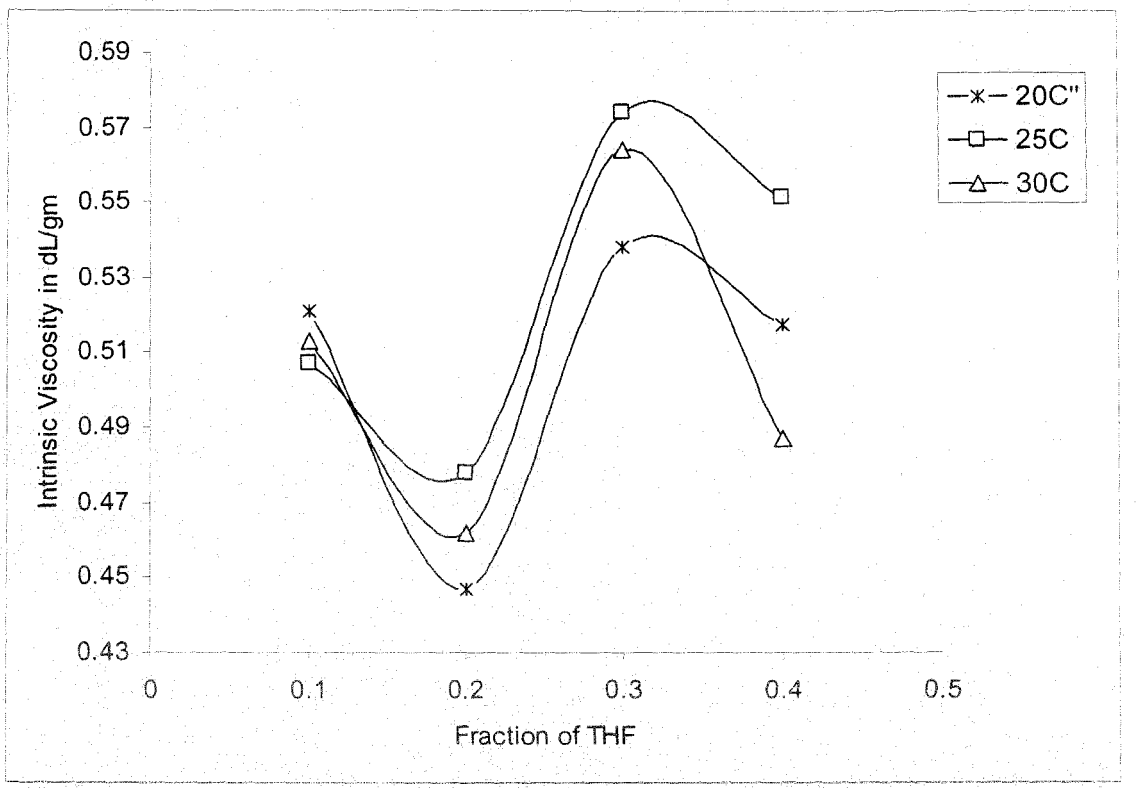

Figure 6.5: Change in intrinsic viscosity with fraction of THF for PVA of (Type-B)

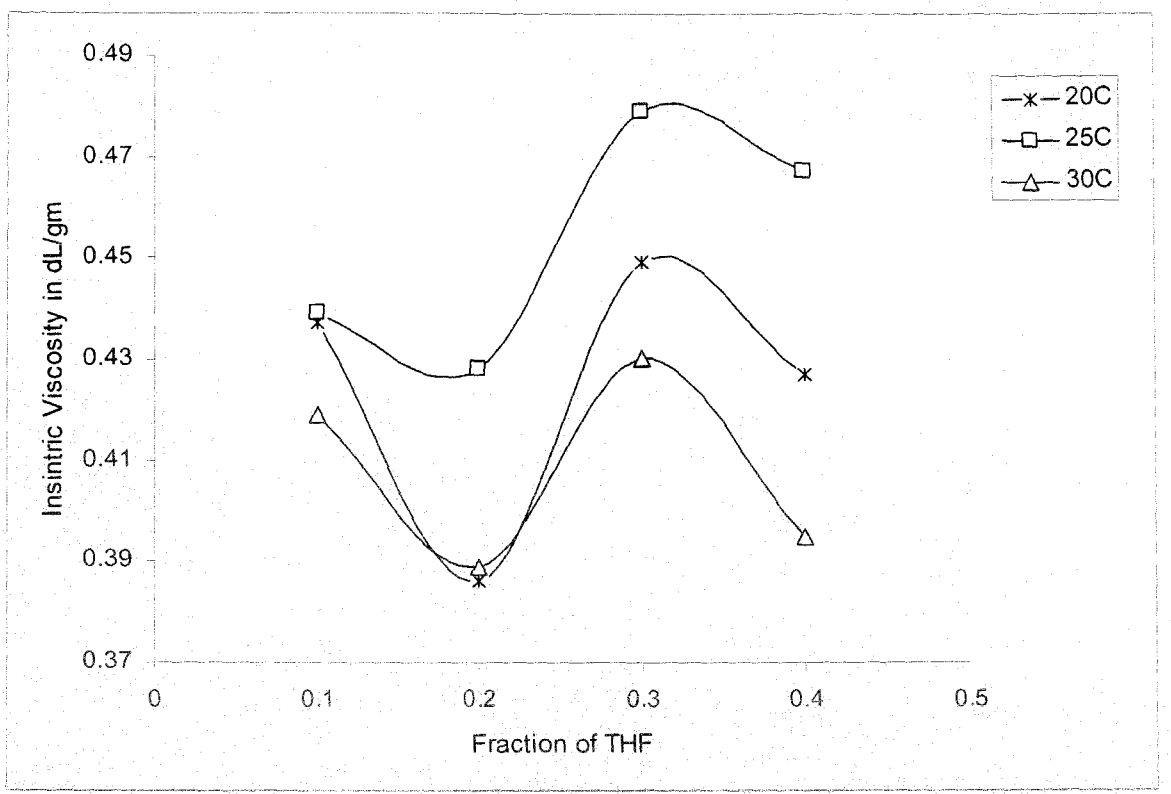

Figure 6.6: Change in intrinsic viscosity with fraction of THF for PVA of (Type-C)

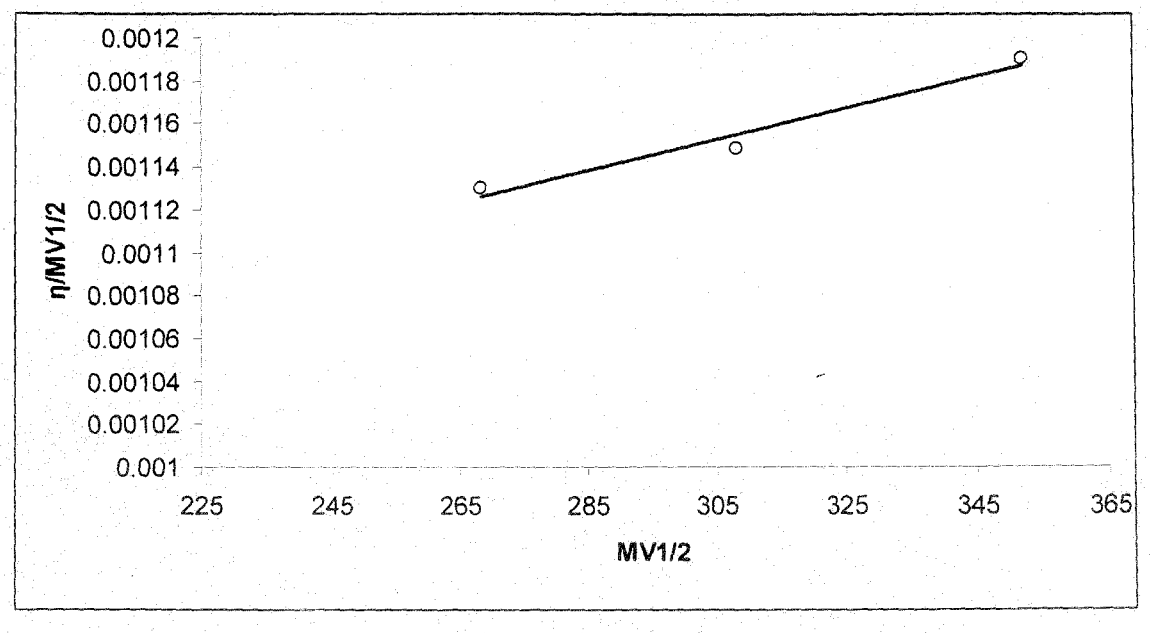

Figure 6.7: BSF plot at 20°C : Φ_{ACE} =0.1 for PVA

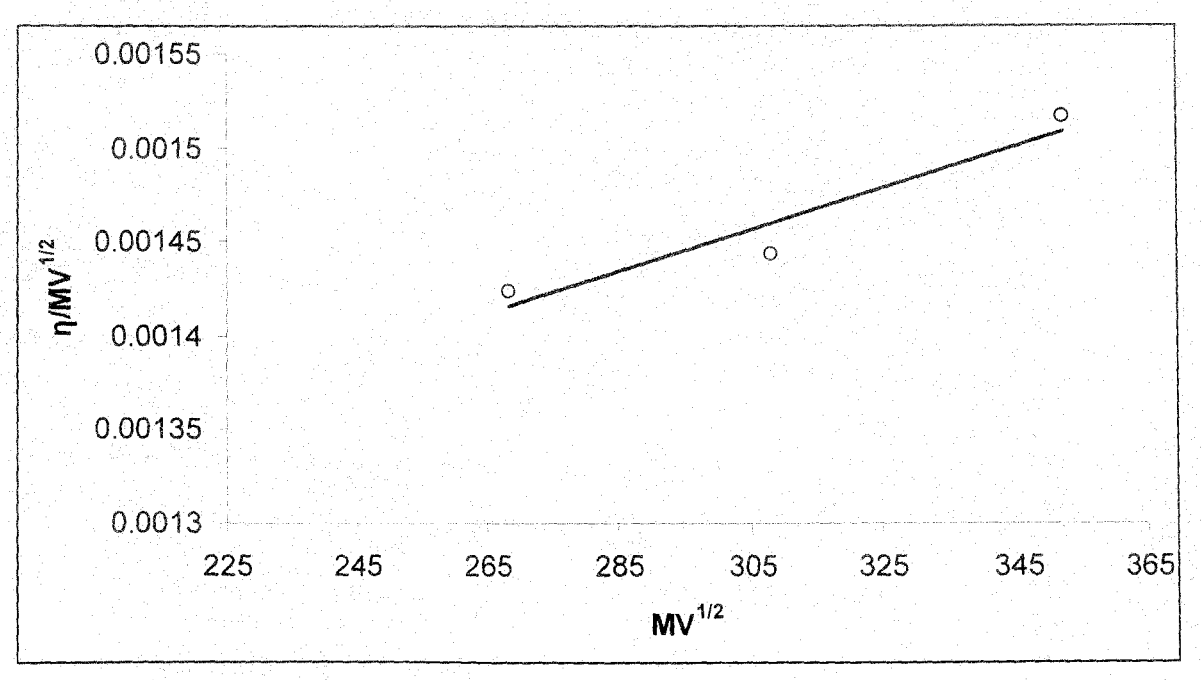

Figure 6.8:BSF plot at 25°C : Φ_{ACE} =0.1 for PVA

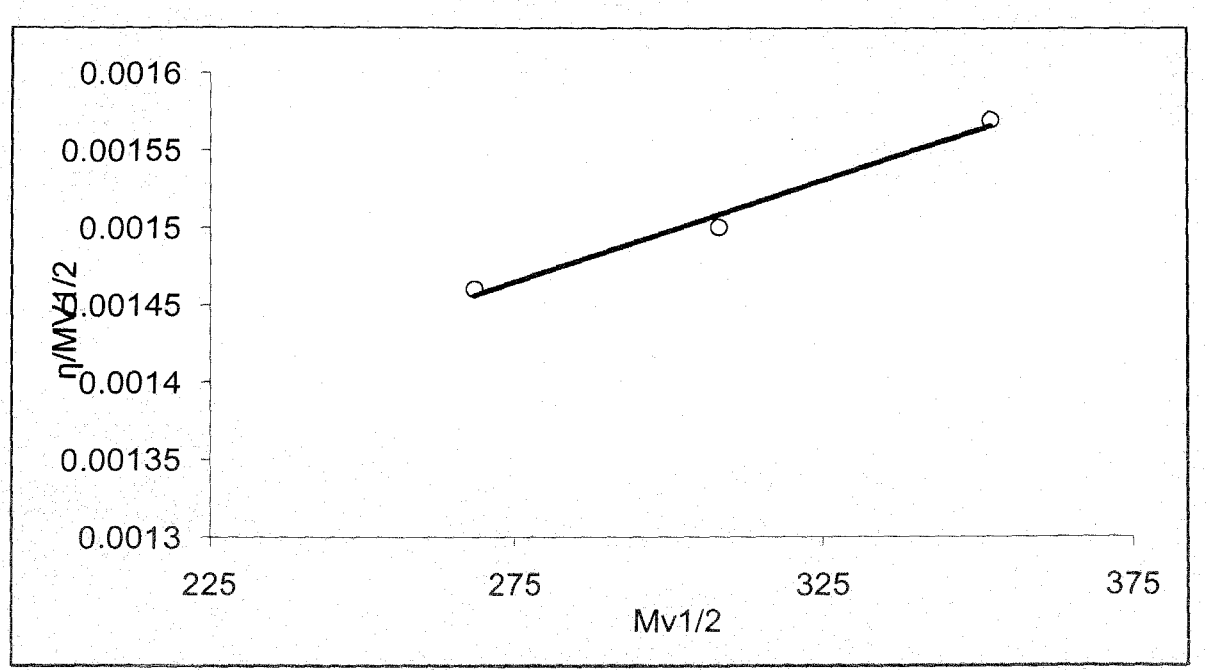

Figure 6.9: BSF plot at 30^{0}C : Φ_{ACE} =0.1 for PVA

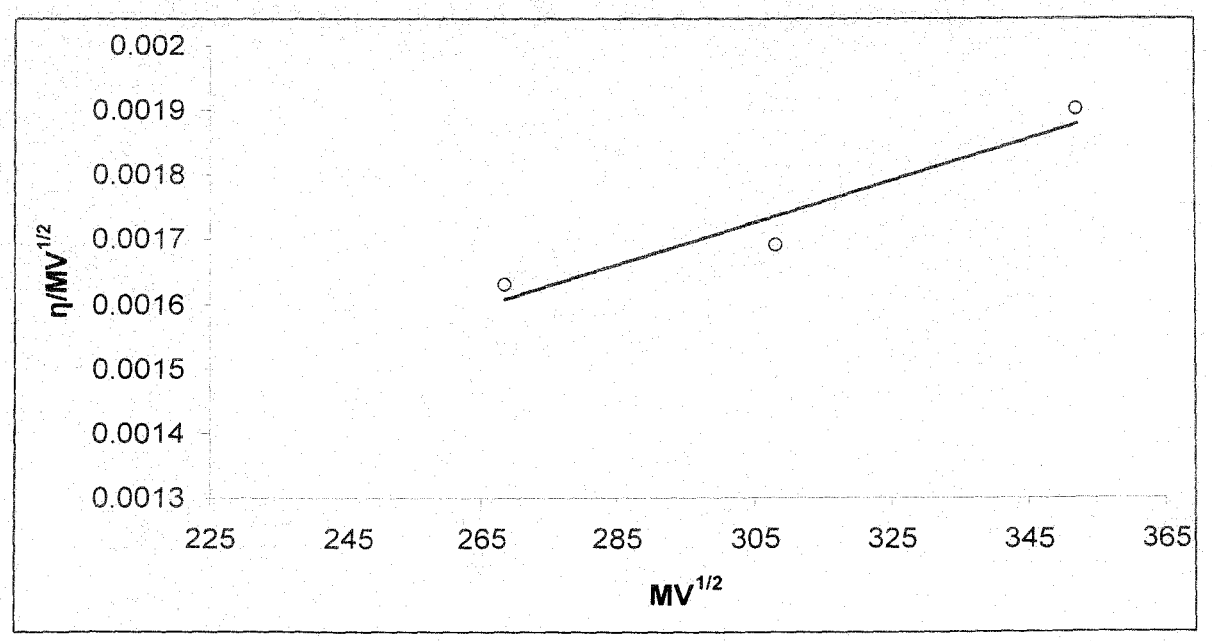

Figure 6.10:BSF plot at 20^{0}C : Φ_{THF} =0.1for PVA

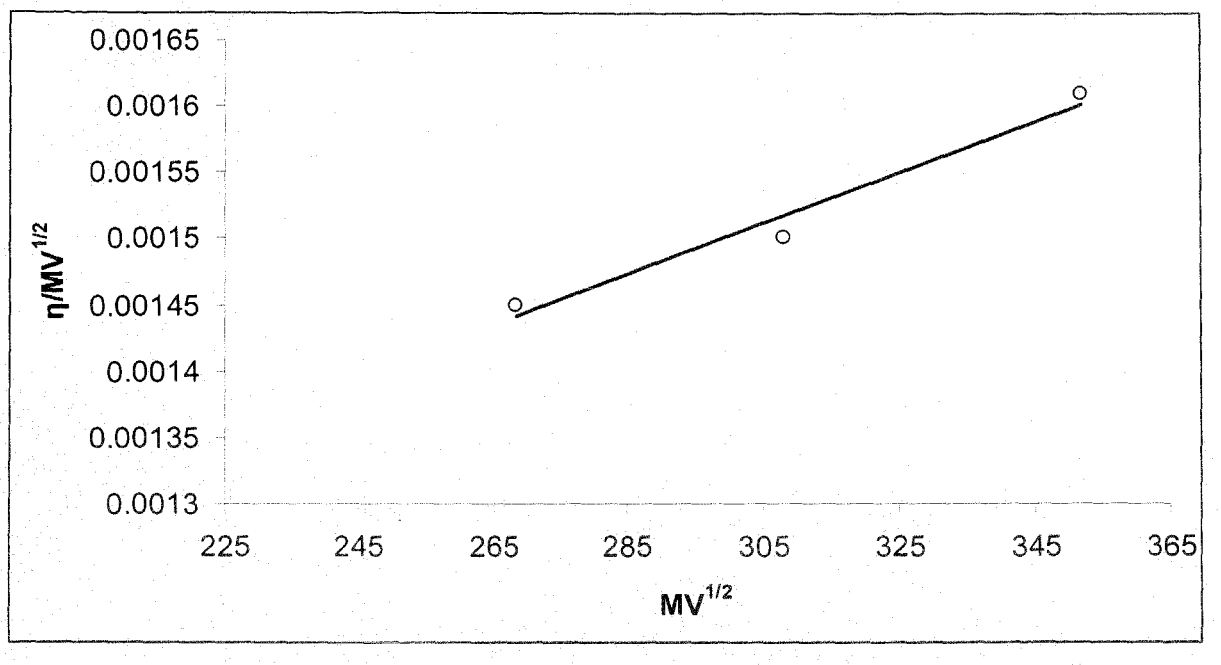

Figure 6.11:BSF plot at 25^{0}C : Φ_{THF} =0.1for PVA

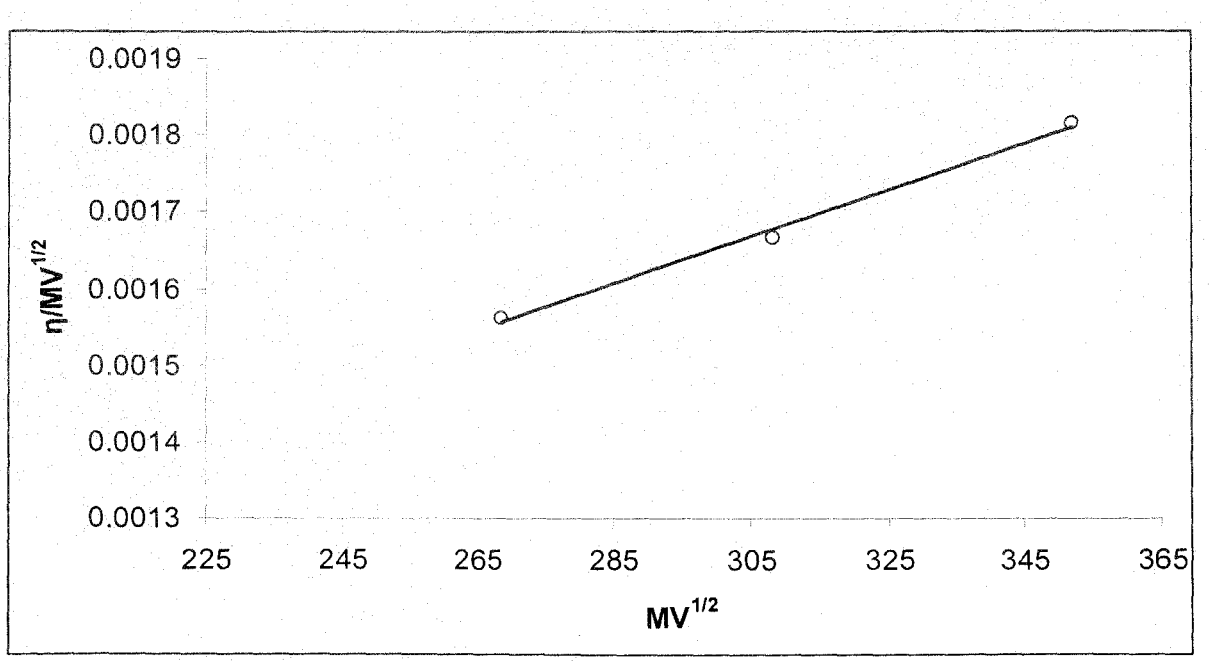

Figure 6.12 :BSF plot at 30^{0}C: Φ_{THF} =0.1 for PVA

Table 6.1

Huggins constant of different fractions of Poly Vinyl Alcohol at different temperature and various solvent compositions(water-acetone)..				
Temp. in °C	$\Phi_{E.E}$	Poly Vinyl Alcohol		
		Type-A . K_H	Type-B . K_H	Type-C. K_H
20	0.1	0.594	0.638	0.645
	0.2	0.518	0.537	0.583
	0.3	0.453	0.478	0.514
	0.4	0.373	0.392	0.416
25	0.1	0.626	0.697	0.736
	0.2	0.598	0.562	0.674
	0.3	0.498	0.534	0.578
	0.4	0.422	0.475	0.517
30	0.1	0.783	0.734	0.796
	0.2	0.629	0.684	0.737
	0.3	0.573	0.622	0.684
	0.4	0.482	0.542	0.438

Table 6.2

Huggins constant of different fractions of Poly Vinyl Alcohol at different temperature and various solvent Compositions(water-THF).				
Temp. in °C	Φ_{THF}	Poly Vinyl Alcohol		
		Type-A . K_H	Type-B . K_H	Type-C. K_H
20	0.1	0.414	0..398	0.341
	0.2	0.374	0.352	0.297
	0.3	o.239	0.193	0.174
	0.4	0.297	0.287	0.256
25	0.1	0.578	0.483	0.437
	0.2	0.426	0.386	0..227
	0.3	0.278	0.232	0.437
	0.4	0.284	0.252	0.238
30	0.1	0..473	0.422	0.419
	0.2	0.369	0.338	0.317
	0.3	0.234	0.221	0.216
	0.4	0.254	0.236	0.214

Table 6.3

Unperturbed Dimension of Poly vinyl Alcohol in water -acetone mixtures at different temperatures determined by different methods.

Temp. in °C	Φ_{ACE}	$K_\theta x10^4 (mol^{1/2}g^{-3/2}.dL)$		
		BSF	BERRY	ISK
20	0.1	9.306	7.800	9.963
	0.2	9.886	9.078	11.134
	0.3	8.702	7.775	9.250
	0.4	7.862	5.470	7.400
25	0.1	11.200	10.608	13.042
	0.2	12.200	11.833	14.835
	0.3	9.847	8.946	10.971
	0.4	9.296	7.403	8.703
30	0.1	11.300	10.517	13.000
	0.2	12.500	12.159	14.964
	0.3	9.313	10.654	9.804
	0.4	8.641	5.317	7.402

Table 6.4

Unperturbed Dimension of Poly Vinyl Alcohol in water -tetra hydro furan mixtures at different temperatures determined by different methods.

Temp. in °C	Φ_{THF}	$K_\theta x10^4 (mol^{1/2}g^{-3/2}.dL)$		
		BSF	BERRY	ISK
20	0.1	7.395	4.397	10.890
	0.2	10.700	10.182	12.164
	0.3	10.900	8.538	11.093
	0.4	11.700	10.407	12.916
25	0.1	8.456	8.928	7.327
	0.2	9.316	12.702	9.093
	0.3	11.100	8.237	10.930
	0.4	12.200	10.641	13.169
30	0.1	7.432	2.595	5.750
	0.2	9.237	7.349	9.330
	0.3	10.900	13.169	10.930
	0.4	11.900	11.999	13.975

Table 6.5

Molecular extension factor and coil dimensions of Poly Vinyl Alcohol at different temperature in various solvent composition (water- acetone).

Temp. in°C	Φ_{ACE}	Poly Vinyl Alcohol					
		Type-A		Type-B		Type-C	
		α_n	$\alpha_n x K_\theta x 10^4$	α_n	$\alpha_n x K_\theta x 10^4$	α_n	$\alpha_n x K_\theta x 10^4$
20	0.1	1.085	10.101	1.073	9.982	1.067	9.925
	0.2	1.126	11.132	1.118	11.054	1.098	10.853
	0.3	1.160	10.092	1.153	10.033	1.124	9.785
	0.4	1.245	9.787	1.213	9.532	1.196	9.404
25	0.1	1.106	12.390	1.088	12.189	1.082	12.132
	0.2	1.079	13.175	1.073	13.095	1.061	12.955
	0.3	1.140	11.228	1.119	11.017	1.110	10.936
	0.4	1.253	11.648	1.213	11.281	1.203	11.189
30	0.1	1.115	12.603	1.041	11.764	1.090	12.320
	0.2	1.089	13.609	1.020	12.751	1.068	13.354
	0.3	1.179	10.973	1.090	10.253	1.141	10.636
	0.4	1.300	11.236	1.186	10.155	1.242	10.738

Table 6.6

Molecular extension factor and coil dimensions of Poly Vinyl Alcohol at different temperature in various solvent composition (water- tetra hydro furan).

Temp. in°C	Φ_{THF}	Poly Vinyl Alcohol					
		Type-A		Type-B.		Type-C	
		α_n	$\alpha_n x K_\theta x 10^4$	α_n	$\alpha_n x K_\theta x 10^4$	α_n	$\alpha_n x K_\theta x 10^4$
20	0.1	1.369	10.123	1.317	9.741	1.301	9.621
	0.2	1.098	12.844	1.107	11.841	1.104	11.809
	0.3	1.194	13.012	1.17	12.752	1.154	12.574
	0.4	1.139	13.321	1.128	13.193	1.108	12.963
25	0.1	1.303	11.014	1.248	10.556	1.246	10.537
	0.2	1.242	11.567	1.185	11.041	1.196	11.145
	0.3	1.216	13.492	1.188	13.190	1.172	13.005
	0.4	1.159	14.141	1.136	13.857	1.126	13.734
30	0.1	1.347	10.008	1.308	9.723	1.281	9.518
	0.2	1.198	11.223	1.170	10.959	1.157	10.837
	0.3	1.178	12.844	1.188	12.955	1.137	12.394
	0.4	1.096	13.045	1.099	13.079	1.073	12.774

6.3 Reference

1 C. A Finch,. PolyVinyl Alcohol; Wiley: New York, pp 1-3 and12-18(1992).

2 N.Nakano, S.Yamane, K. Toyosima, PoVal(polyVinyl-alcohol); Japan Polymer Society: Kyoto,p 3 (1989)

3 E.Chiellini, A. Corti, , S. D. Antone and R Solaro, Biodegradation of poly (vinyl alcohol) based materials. *Prog. Polym. Sci.* **28,** 963(2003).

4 P. J.Flory and F. S. Leutner, 1. Polym. Sci. **3**, 880 (1948); **5**, 267 (1950).

5 H. yamakwa modern theory of polymer solutions.New York ,Harper and `Row,(1971)

6 N. Gungor and S. Dilmac, The effects of some salts and $(NaPO_3)n$ polymer on viscosity `of Na-Montmoillanite slurry. *J. Chem. Soc.* Pak. ,**19**, 14 (1997).

7 F.Uddin, R.Saeed and R. Talib, Temperature Dependence of the Intermolecular Activation Energy for Flow in Strontium Nitrate And Barium Nitrate Solution in Aqueous 2- Propanol Mixtures. *J. Saudi Chem. Soc.* 2, 101(1998).

8 R. H. Stokes and R. Mills, Viscosity Electrolyte and Related Properties; Pergamon Press: New York, (1965).

9 N. Ahmed, S.Akber, I. Khan and A. Saeed, Viscosity Parameters and Energy of Activation ` of Dilute Aqueous Polyvinyl Alcohol (PVOH) Solutions. *J. Chem. Soc.* Pak. ,10, 43 (1998).

10 M. S. Khan, and F.anwal, Degradation of PVC in Air. *J. Chem. Soc.* Pak. 19, 8 (111997).

11 H. Yang, P.Zhu, C. Png, S. Ma, Q.Zhu and C. Fan, Viscometric Study of Polyvinyl Alcohol in NaCl/Water Solutions ranged from Dilute to Extremely Dilute`Concentration *Eur. Polym. J.*, **9**, 1939 (2001)..

12 N. M. Claramma and N. M. Mathew, Rheological Behavior of Prevuleanized Natural Rubber Latex; Huething Gm B H: Heidelberg,Germany, (1998.)

13 T.Okaya, H. Kohna, K. Terada, T. Sato, H. Maruyams and J. Yamauchi, Specific Interaction of Starch and Polyvinyl Alcohols having Long Alkyl Groups. J. *Appl. Polym. Sci.*, **45**, 1127(1992).

14 M.Nakamae, K.Yuki, T.Sato and H. Maruyama, Colloids and Surfaces, A: Physicochemical and Engineering Aspects; Elsevier Science Publishers B. V: Amsterdam, The Netherlands, (1997).

15 W. S. Lyoo, S. M. Lee, K.Koo, J. S. Lee, H. D..Ghim, J. Kim and P. J. Lee, Effect `of Emulsion Polymerization Conditions of Vinyl Acetate on the Viscosity Fluctuation and Gelatinous Behavior of Aqueous Poly (Vinyl Alcohol) Solution. *J.`Appl. Polym. Sci.* **82,** 1897(.2001).

16 M. Shibayama, F. Ikkai, R. Moriwaki and S. Nomura, Complexation of Poly (Vinyl Alcohol) Congo Red Aqueous Solutions. 1.Viscosity Behav. Gelatin Mech.*Macromol.* **27**,1738(1994)

17 K.Lewandowska, D. U.Staszewska, and M. Bohdanecky, Huggins Viscosity Coefficient of Aqueous Solutions of Poly (Vinyl Alcohol), *Eur. Polym. J.* **37**,25(2001)

18 G. O Yahya, A. Ali, M. Al-Naafa and A. E. Z. Hammad, *J. Appl. Polym. Sci.* **57**,343(1995).

19 K.Koga, A.Takada and N. Nemoto, Dynamic Light Scattering and Dynamic Viscoelasticity of Poly(VinylAlcohol) in Aqueous Bora Solutions5.Temperatures Effects. *Macromolecules*, ***32***, 8872(1999).

20 N.Ahmed,.and B. Ahmed, Intrinsic Viscosity, Huggins Constant and Unperturbed Chain Dimension of Poly Vinyl Pyrolidone. *J. Chem. Soc. Pak.*, **12**, 246(1990)

21 M. Liu, R.Cheng, C. Wu and R. Qian, Viscometric Investigation of Intramolecular Hydrogen Bonding Cohesional Entanglement in Extremely Dilute Aqueous Solutions of Polly Vinyl Alcohol. *J. Polym. Sci., Part B: Polym. Phys.*, ***35***, 2421(1997).

22 G.Jones, and M. Dole, The Viscosity of Aqueous Solutions of Strong Electrolytes with Special Reference of Barium Chloride. *J. Am. Chem. Soc.(*1929).

23 T. Alfrey, A. Bartovics and H. Mark *J Am Chem Soc.*, **64**, 1557 (1942).

24. P.L. Nayak and M.Santappa *Ind.J appl. Chem*,**35**,662 (1976)

25. J.M.G. Cowie, *Polymer;* **7(10),** 487(1966).

26. A. Dondos and H. Benoit, *Macromolecules*, **4(3)**, 279 (1971).

27. A. Dondos and H. Benoit, *Macromolecules,* **6(2)**, 242(1973

CHAPTER 7

Summary and conclusion

7. Summary and Conclusion

Many everyday materials – food, medicines, cleaning agents, paints, plastics – are highly complex at the microscopic levels and consist of several kinds of molecules or tiny particles, which are held together by weak electrostatic forces in a highly organized way. At room temperature, these forces are usually not strong enough to prevent the materials from deforming under stress – which is why they are 'soft'. Generally the materials which consist of very large molecules and easily deformable are usually referred to as "soft matter". The concept of "soft matter" covers a large class of molecular materials, including e.g. polymers, thermotropic liquid crystals, micellar solutions, microemulsions and colloidal suspensions, and also includes biological materials, e.g. membranes and vesicles. Two major focuses of the present study have been fixed. In Section A of the thesis, a detail study has been undertaken on the surfactant aggregation in aqueous solutions in presence of additives. Special emphasis has been given to the spherical to rod/worm like micelle transition at low surfactant concentrations, particularly in presence of neutral additives. Rheological and spectroscopic behaviour of the systems are also examined. The section B of the thesis constitutes studies on the physicochemical characteristic of some biopolymer viz, Sodium alginate and Poly (vinyl alcohol) in solution phase.

A chapter wise summary of the study and the conclusions drawn from the experimental work is summarized below. The references have been cited at the end of each chapter.

The First Chapter [**Chapter-1: General Introduction**] describe the general introduction to the various basic concepts and parameters dealt in the present work.

The second Chapter [**Chapter-2:Scope and object**] of the thesis describes the scope and object of the present study.

Chapter Three [**Chapter-3: Studies on Microstructural Transition of Micellar Aggregates in Presence of hydroxyaromatic compounds: Rheology and Spectroscopy**] of the thesis describes the effect of neutral hydroxyaromatic

dopants on the microstructural transition of CTAB micelles, from spherical to wormlike micelles and vesicles. Micellar aggregates that can grow anisotropically under appropriate conditions, changing their shapes from spheres to rods or highly flexible wormlike aggregates, provide some analogies between giant flexible cylindrical micelles and conventional polymeric solutions. The polymerlike micelles (wormlike micelles) which are formed by certain ionic surfactants in solution exhibit very interesting rheological properties. At high concentrations, these solutions show typical viscoelastic behaviour while at very low concentrations more complex and unusual rheological phenomena is observed. Stimuli-responsive properties of viscoelastic gels of long wormlike micelles are fascinating and have created a great deal of interest in recent years.

The most extensively studied system is the cetyltrimethylammonium bromide (CTAB) micelles in presence of a hydrotrope, sodium salicylate. The presence of an anionic charge on the promoter molecule has been considered pivotal in achieving low concentration shape transition of cationic micelles via charge screening because it decreases the average area per surfactant head group allowing the packing parameter to exceed the critical value of ⅓. However, other important factors including the role of OH group of the promoter molecule have not attracted much attention, and as such, the puzzling question as to why not only its presence but also its position in the aromatic ring of NaSal molecule is so vital remains broadly unanswered. Therefore, to understand the role of the OH group precisely, it was tempting to check what would happen if we use uncharged naphthols where the hydrophobic part is very strong and the anionic charge is absent. In this chapter we have studied effect of neutral 1- and 2-naphthols and also the dihydroxy derivatives, 2,3- dihydroxynaphthalene (2,3-DHN) and 2,7-dihydroxynaphthalene (2,7-DHN), on the shape transition of CTAB micelles and shown that intermolecular H bonding between OH groups of micelle embedded naphthol molecules plays a key role in micellar shape transition in absence of any charge screening of head groups and imparts strong viscoelasticity to the dilute aqueous surfactant solution. The viscosity of the systems comprising of CTAB and the hydroxyaromatic dopants are maximum at the surfactant to dopant mole ratio

of 1:1. Therefore, the shear induced rheological studies were carried out at a mole ratio of 1:1.

To understand the exact role of hydrogen bonding in the above mentioned shape transition, studies with methoxynaphthalenes were also carried out at similar conditions. The methoxynaphthalene-CTAB systems (1-methoxynaphthalene/CTAB and 2-methoxynaphthalene/CTAB), on the other hand, neither display the ability to develop viscoelasticity in the system nor exhibit any viscosity modification with applied shear, and behave completely like a Newtonian liquid. This result is quite surprising in view of the fact that much like 1- and 2-naphthols, both 1- and 2-methoxynaphthalenes are expected to embed into the micelles of CTAB. Though methoxynaphthalenes (MN) possess a similar structure and hydrophobicity to that of the hydroxyl naphthalene (HN) molecules but because the methoxynaphthalenes cannot act as hydrogen bond donors, they fail to assist the micellar shape transition and impart viscoelasticity to the CTAB solution.

The effect of temperature and pH on the shear induced viscoelasticity of the systems showed interesting results. With increasing temperature the viscosity of the system increased upto a critical temperature of ~26°C and then decreased. As the temperature was increased, naphthol molecules (uncharged) becomes more soluble and gets partitioned more strongly in the micellar phase. This favors the formation of longer wormlike micelles up to the critical temperature, above this temperature the increased kinetic energy allows the surfactant unimers to hop more frequently between the body and the end cap resulting in the breaking up of the wormlike micelles, thus decreasing the effective viscosity. The motivation behind carrying out the study at different pH stems from the fact that the hydroxyaromatic dopants which, under neutral conditions activate the formation of worm-like micelles at pH ~5.0 may on partial ionization of the OH group increase the packing parameter further via charge screening. This in turn could stimulate in designing a route for pH-responsive vesicle formation. As expected the systems showed a transition of morphology from highly viscous wormlike micelles to less viscous globular vesicles. The results were further confirmed by cryo-TEM images.

To understand the kind of interactions which are operative in the micelle-dopant systems, spectroscopic studies were also carried out. The spectral characteristics of naphthols (which contain OH) were compared with those of methoxy naphthalenes (which do not contain OH) under various conditions in order to visualize a consistent molecular picture. The location and orientation of the additive molecules in the micelles were ascertained by ^1H NMR studies. The signals from the aromatic ring protons of the naphthol molecules were shifted upfield when D_2O solutions of CTAB and naphthols were mixed in 1:1 mole ratio. The CH_3 protons of CTAB head group and the adjacent CH_2 protons, which resonate at 3.132 and 3.289, respectively, in D_2O, were shifted upfield and were found to resonate at 2.746 and 2.397, respectively, in the presence of naphthol. However, CH_2 protons adjacent to CTAB head group, were affected the most in presence of naphthols, and unlike pure CTAB, the signal from CH_2 protons emerged on the other side of CH_3 protons of CTAB head groups. From the above observation it was concluded that the solubilized naphthol molecules were penetrated not deep inside the micellar core but were present near the surface probably with a well-defined orientation in which the OH groups are protruded from the micellar surface toward the polar aqueous phase. The degree of upfield shift of the signals from methoxynaphthalenes (in CTAB micelles) were less than those of the naphthols, indicating a stronger partitioning of the naphthols in the micelles.

The possibility of hydrogen bonding and π-π interaction in naphthols were been checked by observing the effect of CTAB micelles on the absorption spectrum of the hydroxyaromatic compounds. UV absorption spectra of the dopants were modified in their ground electronic state showing significant red-shifting and presence of isobestic points. The modifications are explained in terms of the formation of hydrogen bonding network between the micelle embedded naphthol molecules and the interfacial water molecules. The relatively less polar and less mobile water molecules compared to bulk water forms strong H-bond with the OH group of embedded naphthols, which act as H-donors and results in an optimum orientation of aromatic π-electron systems in the micelles to shield the surfactant headgroup charges efficiently; maybe via cation-π interaction; i.e., the cation

charge of surfactant head groups interacts with the quadrupole moment of the aromatic π-system of naphthols. The methoxynaphthalenes on the other hand showed very little shift. Moreover, no isobestic point could be observed. In methoxynaphthalenes the ability of intermolecular H-bond formation disappears and therefore, the small red-shift, with the absence of any isobestic point(s), compared to that in naphthols indicates that a weaker noncovalent interaction takes place. The chapter concludes with the cryo-TEM investigations, which strongly proves the existence of wormlike micelles at ordinary pH and vesicles at high pH value

Chapter Four [**Chapter-4: Interaction of Cationic Micelles with 1 and 2 Naphthols: Self Fluorescence Monitoring of Stimuli-Responsive Viscoelasticity and Location of Surface Activity**] describes a novel technique of fluorescence monitoring of viscoelasticity of the system and the location of the OH groups of micelle-embedded napthol molecules via measuring the micropolarity of the sites. It is believed that while the aromatic ring of naphthols are embedded in micelles the core of which having dielectric constant around 2-7 only, the OH groups are stood out toward water region. Nmr study also confirms that the aromatic ring of the naphthol resides near the non-polar core in between tetraalkylammonium head groups of the surfactants. Although almost all of the previous studies on the hydrotrope-induced microstructural transitions of micelles argue that the OH groups are protruded out of the micellar surface and remains close to aqueous layer, no experimental verification has so far been reported. To understand the exact nature of the location of the OH group, the micropolarity of the residence sites are determined. Moreover, information regarding the microenvironment of aromatic π-electron system which might have been obtained from the study of spectral characteristics , would not be helpful in determining the location of protruded OH groups of naphthol molecules. Therefore, pK_a shift of the acid-base equilibrium of OH group of naphthols in microheterogeneous medium relative to aqueous solution is considered as the ideal route for getting such information precisely. This shift in pK_a in a cationic micelle like CTAB relative to aqueous solution may be due to the surface potential of the micelle and the polarity variation

at the micellar interface from that of the bulk (in absence of any specific interaction). 1 and 2 naphthols with aromatic π-system in their structures, are fairly surface active and embedded in aqueous CTAB micelles strongly. The success of naphthols in effecting microstructural transition of micelles lies in their unique ability to form H-bonding with interfacial water molecules, which have shown unusual H-bond donating property compared to bulk water. The OH groups of micelle-embedded naphthols are protruded toward the Stern layer through ~1 A and the dielectric constant of OH sites has been measured as 45±2 by observing pK_a-shift of acid-base equilibrium of naphthols at the interface relative to that in bulk water. Stimuli-responsive viscoelastic gels of long wormlike CTAB and CPB micelles are formed at low surfactant concentrations in presence of 1- and 2-naphthols. Systems which display shear induced nonlinear rheological changes (such as the present systems) bring about formidable problem in measuring unperturbed solution viscosity because the measuring techniques (e.g., torsional shear rheometry) often apply considerable stress on the system during measurement, and thus the zero-shear viscosity becomes obscure. Both the naphthols are well-known fluophores, and significantly, the quantum yield of emission of the naphthols is found to be very sensitive to the solution viscosity of the present systems. This offers an interesting route for fluorescence monitoring of unperturbed viscosity as a function of applied shear. In a viscous medium, a fluophore cannot transfer energy efficiently via nonradiative means because of delayed collisions with the surrounding molecules resulting in the increased emission quantum yield.

In the Chapter Five [**Chapter-5: Determination of unperturbed dimension and interaction parameters of sodium alginate in binary solvent mixtures by viscosity measurements**] the results of the investigation on unperturbed dimension, interaction parameter and related aspects of sodium alginate in water-acetone and water-ethoxy ethanol mixtures have been described. The intrinsic viscosities [η] of three different samples of the polymer having different molecular weights were measured in various fractions of solvent composition. Acetone and ethoxy ethanol is a poor solvent for PVA but water-acetone and water- ethoxy

ethanol mixtures act as a cosolvent in certain proportions. From the relation between [η] and M, the unperturbed dimension and molecular expansion factor have been measured. The Huggins constant value in each case was also determined in order to have ideas on the influence of cosolvent system on the aggregation of the polymer. It is observed that there are a maximum in [η] vs. Φ_{ACE} and [η] vs. $\Phi_{E.E.}$ plots at the solvent composition Φ_{ACE} = 0.2 and $\Phi_{E.E.}$ =0.3 respectively for Sodium alginate. It is observed that K_H values are maximum at the solvent composition Φ_{ACE} =0.3 and $\Phi_{E.E.}$ =0.2 for all types of aliginate polymers respectively indicatinting that all types of polymers have higher tendency of intermolecular aggregation at this fraction of the solvent. K_H is smallest Φ =0.4 for both the solvent mixture (Acetone and ethoxy ethanol) under this condition polymer molecules are held closer and make side chains twisted around each other. Unperturbed dimensions under non-theta condition were calculated using various equations in different water-acetone and water- ethoxy ethanol mixtures. The value of K_θ obtained from three different methods of measurements viz., BSF, I-S-K and Berry agree well with each other except in a few compositions of solvents. It is apparent that at Φ_{ACE} =0.4 and $\Phi_{E.E.}$ =0.2 the polymer has the lowest unperturbed dimensions and at Φ_{ACE} =0.1 and at $\Phi_{E.E.}$ =0.4 the polymer has the highest unperturbed dimensions. Volume related parameter ($\alpha_{n.}$) are also computed in this chapter.

In the Chapter Six [**Chapter-6: Studies on solution properties of poly (vinyl alcohol) in water-acetone and water-tetrahydro furan**] unperturbed dimension, Huggins constant (K_H) and volume related parameter (α_n), are determined via the measurement of intrinsic viscosity [η] of PVA with two different types of binary solvent mixtures (water- acetone and water- tetrahydrofuran) in the similar way as has been done in the previous chapter for sodium aliginate in water-acetone and water- ethoxyethanol mixtures.

The last chapter of the thesis [**Chapter-7: Summary and conclusion**] summaries the overall work presented in the thesis and describes the conclusions drawn from the experimental section.

List of Publications:

1. Micellar Shape Transition under Dilute Salt-Free Conditions: Promotion and Self-Fluorescence Monitoring of Stimuli-Responsive Viscoelasticity by 1- and 2-Naphthols, Swapan K. Saha, Mrinmoy Jha, Moazzam Ali, Amitabha Chakraborty, Goutam Bit, and Susanta K. Das, ***J. Phys. Chem. B***, 2008,112,4642-4647.

2. Hydrogen-Bond-Induced Microstructural Transition of Ionic Micelles in the Presence of Neutral Naphthols: pH Dependent Morphology and Location of Surface Activity, Moazzam Ali, Mrinmoy Jha, Susanta K. Das, and Swapan K. Saha, ***J. Phys. Chem. B***, 2009,113,15563–15571.

3. Determination of unperturbed dimension and interaction parameters of sodium alginate in binary solvent mixtures by viscosity measurements, Mrinmoy Jha, Soumik Bardhan, Gulmi Chakraborty, Bidyut Debnath, Swapan K. Saha, ***J. Colloid Polymer Sc.,*** 2015 (Submitted)

4. Studies on Solution Properties of Poly (Vinyl Alcohol) in Water-Acetone and Water-Tetra Hydro Furan Mixtures, Mrinmoy Jha, Soumik Bardhan, Gulmi Chakraborty, Swapan K. Saha, ***J. Chem. Eng. Data,*** 2015 (Submitted)

Micellar Shape Transition under Dilute Salt-Free Conditions: Promotion and Self-Fluorescence Monitoring of Stimuli-Responsive Viscoelasticity by 1- and 2-Naphthols

Swapan K. Saha,* Mrinmoy Jha, Moazzam Ali, Amitabha Chakraborty, Goutam Bit, and Susanta K. Das

Department of Chemistry, University of North Bengal, Darjeeling 734 013, India

Received: October 9, 2007; In Final Form: February 2, 2008

Effect of 1 and 2-naphthols on the shape transition of cetyl trimethylammonium bromide (CTAB) and cetylpyridinium bromide (CPB) micelles are studied. Stimuli-responsive viscoelastic gels of long wormlike micelles are formed at low surfactant concentrations in the presence of neutral naphthols, where H-bonding plays a key role in micellar shape transition in the absence of any charge screening. Micelle-embedded naphthols also act as novel self-fluorescence probes for monitoring viscoelasticity of the system as a function of applied shear. ^{1}H NMR study shows that the solubilization sites of naphthols in the micelle are located near the surface. While UV absorption and Fourier transform infrared studies confirm the presence of intermolecular H-bonds in micelle embedded naphthols, transmission electron micrographs of vacuum-dried samples at room temperature demonstrate the transition in shape from sphere to rodlike micelles.

Introduction

Stimuli-responsive properties of viscoelastic gels of long wormlike micelles are fascinating and have created a great deal of interest in recent years.[1−4] Most extensively studied system is the cetyltrimethylammonium bromide (CTAB) micelles in presence of a hydrotrope, sodium salicylate (SS). Unlike simple halides, salicylate promotes sphere to wormlike micellar transition at very low concentrations, viz., near the normal critical micelle concentration (cmc, ~1 mM) of CTAB. The flexible and elongated wormlike micelles under dilute conditions show complex and unusual rheological phenomena, which include strong viscoelasticity and shear-induced structure (SIS) formation.[5−7] It is particularly interesting that, while a wide variety of wormlike ionic micellar solutions display identical rheological responses, a common element in most of these systems is the presence of salt anions such as SS. Although a few examples are available in the literature where additives other than SS have been used, these molecules have never been considered as high up as the promoter like SS.[8] However, a number of studies on micellar shape transition in cationic, anionic, and catanionic surfactant systems induced by polar and nonpolar organic species under comparatively high concentration conditions have been reported in the literature.[9−11] While hydrophobic molecules with either aromatic ring or small polar group have shown better efficiency, no unusual rheological feature was apparent under this condition. The presence of an anionic charge on the promoter molecule has been considered pivotal in achieving low concentration shape transition of cationic micelles via charge screening because it decreases the average area per surfactant head group allowing the packing parameter to exceed the critical value of $^1/_3$.[12] However, other important factors including the role of OH group of the promoter molecule have not attracted much attention, and as such, the puzzling question as to why not only its presence but also its position in the aromatic ring of SS molecule is so vital remains broadly unanswered.[13] Therefore, to understand the role of the OH group precisely, it was tempting to check what would happen if we use uncharged naphthols where the hydrophobic part is very strong and the anionic charge is absent. In this paper we have studied effect of neutral 1- and 2-naphthols on the shape transition of CTAB and CPB micelles and shown that intermolecular H bonding between OH groups of micelle embedded naphthol molecules plays a key role in micellar shape transition in absence of any charge screening of head groups and imparts strong viscoelasticity to the dilute aqueous surfactant solution.

* To whom correspondence should be addressed. E-mail: ssahanbu@hotmail.com.

Experimental

1-Naphthol(puriss) and 2-naphthol(puriss) (Aldrich products) were purified further by vacuum sublimation followed by recrystallization from 1:1 aqueous methanol. CTAB (puriss, Aldrich) and CPB (Aldrich) were used as received. ^{1}H NMR and Fourier transform infrared (FTIR) were recorded on a Bruker (300 MHz) spectrometer and a Shimadzu (083000) spectrometer, respectively. Steady-state fluorescence was measured on a Perkin-Elmer LS-55 luminescence spectrometer. UV absorption spectra were recorded on a Jasco (V-530) spectrophotometer. Shear-induced viscosity was measured on a rotational viscometer (Anton-Paar, DV-3P; accuracy ±1% and repeatability ±0.2%) equipped with temperature controller and with the facility of varying shear rates.

Results and Discussion

Shear-Induced Viscosity and Fluorescence Intensity. Aqueous CTAB or CPB (2−10 mM) and 1- or 2-naphthol (2−10 mM in 2−5% methanol, naphthols being sparingly soluble in water) solutions show viscosities similar to those of water. But as soon as these solutions are mixed together at room temperature, a thick gel-type fluid with high viscoelasticity is developed. Since viscoelasticity tends to disappear in high methanol concentrations, experimental solutions are prepared routinely by transferring the required amount of naphthol solutions (in pure methanol) in the experiment vial first, and

10.1021/jp709850u CCC: $40.75
Published on Web 03/22/2008

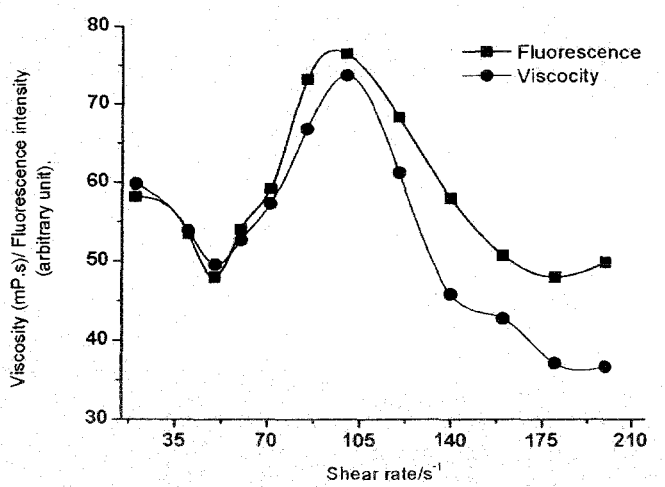

Figure 1. Variation of viscoelasticity of CPB−2-naphthol (10 mM) system with applied shear rate.

then the alcohol was evaporated off completely before the addition of aqueous surfactant solution. Much like the CTAB−SS system, CTAB−naphthols and CPB−naphthols also display maximum viscoelasticity at a 1:1 molar ratio of surfactant and the promoter. The argument that an excess or deficiency of charge on the micelles due to adsorption of hydrotrope anions (e.g., SS) would shorten the micellar life time and size is not apparently true for the present system because under the present experimental condition of solution pH (~6.5), the naphthols are mostly protonated, i.e., uncharged (pK_a's > 9.0). Therefore, it seems apparent that the symmetrical distribution of surfactant and the promoter molecules leading to highly compact spherical micelles facilitates an optimum surface curvature to attain in presence of H bonding (discussed later), and this results in the sphere to rod transition easily. For further experiments, naphthol to surfactant ratio was chosen to produce strongest viscoelasticity, i.e., 1:1 mole ratio. At low concentrations (<2 mM), CTAB or CPB−naphthol solutions show shear thinning properties, typically observed in the case of a non-Newtonian fluid. But at higher concentrations (>2 mM; 25 °C), present experimental systems display interesting rheological phenomenon. Up to the applied shear rate of ~52 s^{-1} (which is concentration dependent) for the CPB−2-naphthol system, solutions shear thin (Figure 1). An onset of viscosity rise is observed thereafter as a function of applied shear, and the viscosity share rate profile passes through a maximum, e.g., at 102 s^{-1} for the above system (Figure 1).

This behavior is consistent with building up of long wormlike micellar bundles.[7] The system recoils after the applied shear is withdrawn and takes a very long time (e.g., half-life period of viscosity decay of a CTAB−1-naphthol (7.0 mM) system equals ~56 min; samples were sheared in a rotational viscometer at 100s^{-1} for ≥5 min to ensure that the high viscosity regime was reached) to recoil completely and to return to an equilibrium unsheared state. Shear rates at which viscosity transition takes place and the shear rates at which maximum viscosity is displayed by various systems are shown in Table 1.

Systems which display shear induced nonlinear rheological changes (such as the present systems) bring about formidable problem in measuring unperturbed solution viscosity because the measuring techniques (e.g., torsional shear rheometry) often apply considerable stress on the system during measurement, and thus the zero-shear viscosity becomes obscure. Both the naphthols are well-known fluophores, and significantly, the quantum yield of emission of the naphthols is found to be very sensitive to the solution viscosity of the present systems. This

TABLE 1: Shear-Induced Viscoelastic Characteristics of CTAB and CPB Micelles in Presence of 1- and 2-Naphthols

viscoelastic system (10 mM, 1:1)	transition shear rate/s^{-1}	shear rate at maximum viscosity/s^{-1}
1-naphthol−CTAB	60	115
2-naphthol−CTAB	42	100
1-naphthol−CPB	63	106
2-naphthol−CPB	52	102

offers an interesting route for fluorescence monitoring of unperturbed viscosity as a function of applied shear. In a viscous medium, a fluophore cannot transfer energy efficiently via nonradiative means because of delayed collisions with the surrounding molecules resulting in the increased emission quantum yield. Moreover, the dipole moment of the probe in the excited state is greater than that in ground state, and hence interaction of the excited probe molecule with its surrounding molecules is different from that before absorption. Reorientation and translation of nearest-neighbor molecules allow the probe molecule to relax gradually to its equilibrium excited singlet state (S_1). In solutions of low viscoelasticity where these relaxations are very fast, fluorescence practically takes place from this equilibrium excited state S_1. In highly viscoelastic solutions, the relaxation of molecules surrounding the probe may be slow, and the probe molecules may emit before reaching their equilibrium excited state S_1, and a blue shift of the fluorescence spectrum may also be observed accompanying by an intensity enhancement. Similar situation is also encountered in a twisted intermolecular charge transfer state (TICT) formation where in a less viscous environment the probe molecules also display internal rotation and charge transfer, which results in the less emission quantum yield than that in a high viscous environment.[14,15] Furthermore, naphthols are weak acids in the ground state. In aqueous solution (pH ≈ 6.0−7.0), they exist almost completely in the acid forms. On excitation into the lowest singlet excited state, the pK_a values drop by several units (2-naphthol: $pK_a^* \approx 2.78$; 1-naphthol: $pK_a^* \approx 0.40$),[16−18] i.e., they undergo deprotonation in the excited state (DES).[19,20] As a result, the emission from the neutral forms of 1- and 2-naphthols at 360 and 357 nm, respectively, exhibits very low intensity than those of the anion forms near 450 or 420 nm, respectively. However, on binding to micelles, the DES process is restricted significantly causing a 20−90-fold increase in the intensity and life time of the neutral emission as well as in the rise time of the anion emission.[21] This is probably because of unavailability of an adequate number of water molecules in the vicinity of the naphthol molecules embedded inside the micelle to hydrate the proton released during photolytic deprotonation.[21] Therefore, at low surfactant concentrations (<2 mM; DES is significant), emissions from the deprotonated anion forms of the napthols were monitored at higher wavelengths, whereas in the presence of high concentrations of surfactant, emission from neutral form of 2-naphthol were monitored at lower wavelengths (where DES is insignificant) in the present experiments (1-naphthol shows very low quantum yield for neutral emission). Figure 1 also compares the shear induced viscosity data with that of fluorescence intensity of the present CPB−2-naphthol system. While the overall feature of the shear-induced viscosity profile is identical with that of the emission, they are not exactly superimposed on one another possibly because of the perturbation imposed on the system during viscosity measurement. However, we failed to observe any direct effect of applied shear on the DES process. This is apparent from the nonvariant ratio of emission intensities of protonated to deprotonated naphthols as a function of applied shear. This also indicates that the shear does not influence the availability of water molecules to hydrate

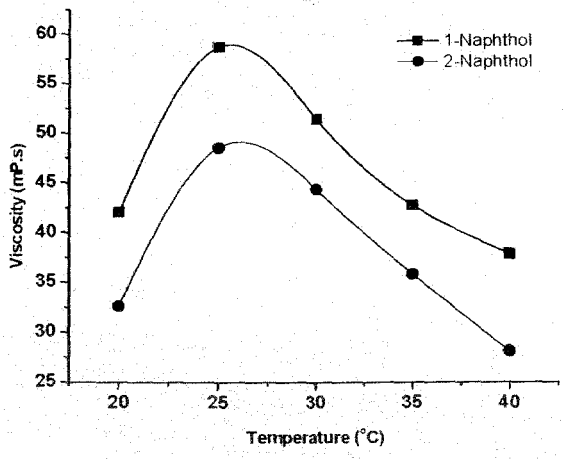

Figure 2. Variation of viscosity of CTAB−naphthol systems (10 mM; shear rate 30 s^{-1}) with temperature.

the liberated protons, i.e., the microstructure around the naphthol molecules in the wormlike micelles remains unchanged in SIS. However, as shown in Figure 1, it seems like that in the high applied shear rate (> 180 s^{-1}) the viscosity and fluorescence have opposite variation with the applied shear rate. Partial modification/disruption of wormlike micelles under high shear may change the compactness causing redistribution of naphthols in the micellar gel expelling some of the inner site naphthols to the outer site (better accessible to water molecules), resulting in the slight increase in the fluorescence intensity due to modified DES process.[22] In an experiment where hydrotropic promoter for micellar shape transition is not a fluophore, a probe must be added from the outside for the above measurement. This, in turn, may alter the hydrophobic trait of the system and affect the rheology. Therefore, one should be careful in using external fluorescence probes for monitoring viscosity.

Effect of Temperature. Typically, when a wormlike micellar solution is heated, the micellar contour length decays exponentially with temperature. At higher temperatures, surfactant unimers can move more rapidly between the cylindrical body and hemispherical end cap of the worm (the end cap is energetically unfavorable over the body by a factor equal to the end-cap energy). Thus, because end-cap constraint is less severe at higher temperatures, the worms grow to a lesser extent. However, an opposite trend in the rheological behavior is observed in CTAB/CPB−naphthol systems. Instead of a decrease in viscosity, it is increased with temperature steadily up to a critical temperature value (26 °C for CTAB−naphthols) and then decreases (Figure 2).

This transition as a function of temperature is reversible, i.e., if the temperature is lowered down from a high value, viscosity of the system follows the same viscosity−temperature profile. This observation is unusual, and the only example of this kind is found in a recent reference where wormlike micelle formation was promoted by sodium salt of hydroxy naphthalene carboxylate (SHNC).[23] However, any explanation emphasizing charge screening of surfactant head groups by the added salt anions as has been put forward in above experiments is not applicable. On the other hand, hydrophobic interaction between micellar core and the aromatic ring of the naphthol molecules seems to be an important factor, which imparts the thermoreversible viscoelastic property to the present system. As the temperature is increased, naphthol molecules (uncharged) are more soluble and perhaps are partitioned more strongly in the micellar phase. This favors the formation of longer wormlike micelles up to the critical temperature, above which the increased kinetic energy allowing surfactant unimers to hop more frequently

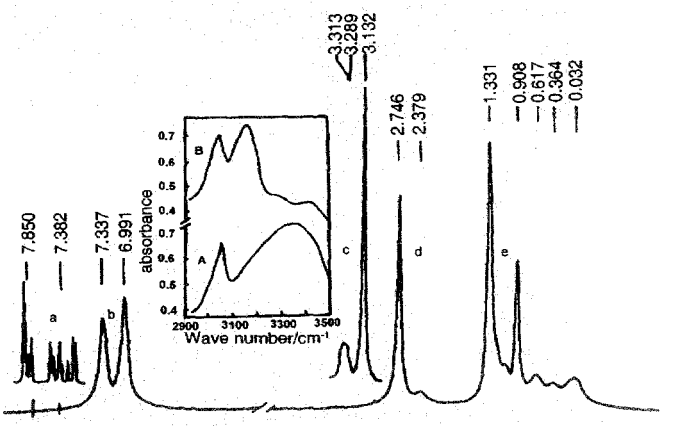

Figure 3. ^{1}H NMR and FTIR spectra of CTAB−2-naphthol system. (a) ^{1}H signal from 2-naphthol, (c) ^{1}H signal from CTAB, (b, d, e) NMR spectrum of CTAB−2-naphthol (1 mM, 1:1). Insets: FTIR spectra of 2-naphthol (A) in the absence of CTAB and (B) in the presence of CTAB.

between the body and the end cap results in the breaking up of the wormlike micelles.[23]

^{1}H NMR Study. To ascertain the location and orientation of the additive naphthol molecules in the micelles and to understand the nature of interaction in micellar shape transitions, ^{1}H NMR experiments were performed along with the absorption and emission spectroscopies. NMR spectrum of 2-naphthol in D_2O (in absence of CTAB) shows clusters of signals centered at δ values of 7.850 and 7.382, respectively, due to the resonance of the aromatic ring protons (Figure 3a). These two sets of signals are shifted upfield, broadened, and merged to give two broad signals at δ values of 7.337 and 6.991, respectively, when D_2O solution of CTAB and naphthols are mixed in 1:1 molar ratio (1.0 mM; Figure 3b). This large shift of aromatic proton resonance to low δ values clearly indicates the location of naphthol rings in the less polar environment than that of water. Previous studies with CTAB−SS system also showed similar upfield shift of proton resonance of the aromatic moiety of SS molecule, and it was argued that this was due to insertion of SS molecules into the micelles.[13] On the other hand, CH_3 protons of CTAB head group and the adjacent CH_2 protons, which resonate at 3.132 and 3.289, respectively, in D_2O (Figure 3c), are shifted upfield and resonate at 2.746 and 2.397, respectively, in the presence of 2-naphthol (Figure 3d). However, CH_2 protons adjacent to CTAB head group, are affected most in the presence of naphthols, and unlike pure CTAB, the signal from CH_2 protons emerges on the other side of CH_3 protons of CTAB head groups in the presence of naphthols. This identification is important because it indicates the presence of aromatic ring of naphthol near the surfactant head groups and close to adjacent CH_2 group. Signals from protons of other parts of hydrocarbon chain, however, remain unaffected in presence of naphthols (Figure 3e). The NMR spectra of 10 mM CTAB−2-naphthol (1:1) have further subtle features (Figure 4). While the signals from water protons remain well resolved (not shown), the signals from the aromatic protons of the naphthol molecules are broadened dramatically (Figure 4a). This means that on the NMR time scale, the motion of the naphthol molecules is highly restricted in viscoelastic phase, but water molecules rotate freely.[24] The signals from CTAB protons are, however, broadened to a lesser extent but appear structureless preventing further analysis (parts b and c of Figure 4). It seems that the naphthol molecules are held tightly in the micelles by means of strong hydrophobic interaction and H bonding. Above observation conclusively proves that the solubilized naphthol molecules are

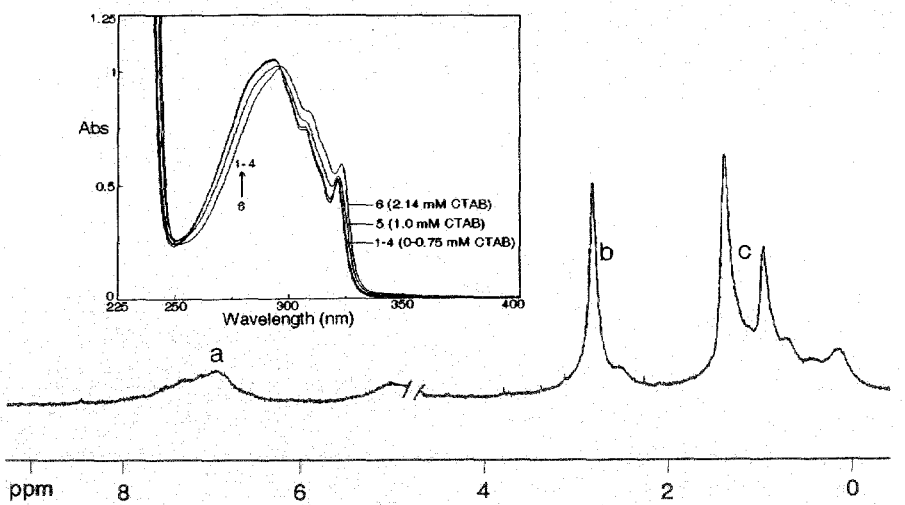

Figure 4. ^{1}H NMR and UV absorption spectra of CTAB−naphthol system: (a, b, c) NMR spectrum of CTAB−2-naphthol (10.0 mM, 1:1). Inset: UV absorption spectra of aqueous 1-naphthol (0.25 mM) solution at various CTAB concentrations.

penetrated not deep inside the micellar core but present near the surface probably with a well-defined orientation in which the OH groups are protruded from the micellar surface toward the polar aqueous phase. A previous study on the measurement of "apparent" shift of pK_a of 1-naphthol at the micellar surface of CTAB yielded an effective dielectric constant value of ~45, indicating that the location of OH groups of naphthol at the micellar surface is fairly polar in nature.[25,26]

UV Absorption and Emission Studies. Possibilities of the H bonding and $\pi-\pi$ interaction in naphthols have been checked by observing the effect of CTAB micelles on the absorption spectrum. The near-UV absorption of 1-naphthol (250−335 nm), which arises from two strongly overlapping $\pi-\pi^*$ transition, viz., $^1L_a \leftarrow {}^1A_1$ and $^1L_b \leftarrow {}^1A_1$, however, remains unaffected in presence of submicellar aqueous CTAB solution (Figure 4, inset) indicating absence of any appreciable interactions. But interestingly, a significant red-shift is observed in the spectrum at 293, 307, and 321 nm in presence of CTAB just above its cmc (1.0 mM) with a well-defined isobestic point at 296 nm. Previously, a similar red-shift of absorption spectrum of 2-naphthol in AOT reverse micelle relative to the spectrum of free naphthol was observed when this molecule acts as hydrogen-bond donor because of the perturbation by the negative charge carried on oxygen atom of the partner molecule.[27] The same reasoning applies to the present case also and the nature of spectral change indicates in favor of H bonding between naphthol molecules (red-shift is observed in 2-naphthol−CTAB system also), which are embedded increasingly in the micelle as the CTAB concentration (> 1.0 mM) is increased (Figure 4, inset).

It has been reported that fluorescence quenching can be induced by the hydrogen-bonding interactions for fluophores in the hydrogen-bonding surroundings and is explained by the hydrogen-bonding dynamics in the fluorescence state.[28−33] Therefore, it may be presumed that intermolecular H bonding in micelle-embedded naphthols can be studied effectively by observing fluorescence quenching (static and dynamic). However, excited-state proton transfer (ESPT) or DES process of hydroxy aromatic compounds such as naphthols seems to make the situation somewhat difficult. The ESPT rates of these compounds in aqueous solutions are limited by the time water takes to wrap itself around the charge because a water cluster of 4 ± 1 molecules is the proton acceptor in each case.[34] The first two steps in the ESPT process are, therefore, (i) the H-bonded complex formation of electronically excited state of naphthols with water molecules and (ii) hydrogen-bonded

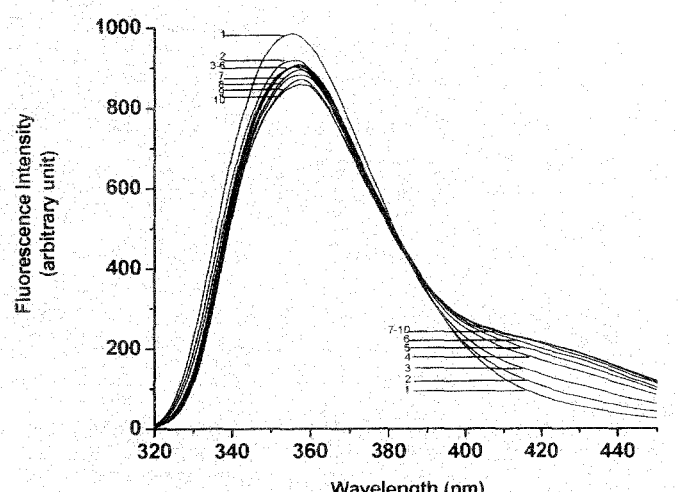

Figure 5. Fluorescence spectra of 2-naphthol (0.25×10^{-5} mol/L) in aqueous CTAB solutions in presence of 0.1 M HCl. [CTAB]: (1) 0.0 mM, (2) 3 mM, (3) 2.5 mM, (4) 2 mM, (5) 1.5 mM, (6) 1 mM, (7) 0.75 mM, (8) 0.5 mM, (9) 0.25 mM, and (10) 0.12 mM.

complex formation with water clusters required for protolytic dissociation.[19] ESPT process of 1- and 2-naphthols in organized media including different micelles have been investigated in considerable detail, but the results are not always unambiguous.[19,20,35,36] It has been shown that the ultrafast proton-transfer processes in ESPT became significantly retarded for 1-naphthol in micelles due to lack of water availability (as has already been mentioned), and the decay of the emissions are often multiexponential due to different solubilization sites in anionic and nonionic micelles, although a monoexponential decay process has also been observed for similar systems.[35,36] On the other hand, for CTAB micelles, the retardation effect is somewhat compensated by the catalytic effect of the micellar potential.[36] Although a previous study did not find convincing evidence that all of the naphthols in micelle are definitely in the form of H-bonded complex with several water molecules, which is required for photodissociation, possible existence of intermolecular H bond in electronically excited states of naphthols under identical condition of wormlike micelle formation have been re-examined in the present study.[19] Figures 5 and 6 show the emission spectra of 2- and 1-naphthols, respectively, in 0.1 M HCl in presence of CTAB. Addition of high excess of hydroxonium ion is to shift the acid−base equilibrium toward neutral naphthol (protonated) to facilitate intermolecular H-bond

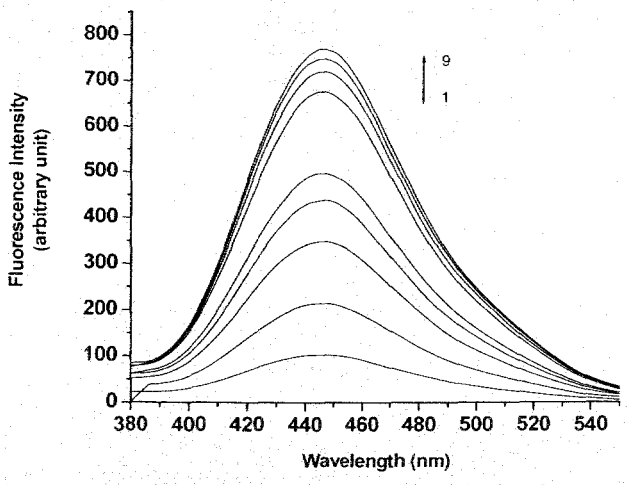

Figure 6. Fluorescence spectra of 1-naphthol (0.25×10^{-5} mol/L) in aqueous CTAB solutions in presence of 0.1 M HCl. [CTAB]: (1) 0.0 mM, (2) 0.25 mM, (3) 0.5 mM, (4) 0.75 mM, (5) 1.0 mM, (6) 1.5 mM, (7) 2.0 mM, (8), 2.5 mM, and (9) 3.0 mM.

formation. While 1-naphthol exhibits only anion emission ($pK_a^* \approx 0.40$), which is enhanced substantially in presence of CTAB, emission from 2-naphthol in water was essentially from the neutral naphthol molecules under the above condition ($pK_a^* \sim 2.78$). The effect of CTAB concentration on neutral as well as the anion emission of 2-naphthol is interesting (Figure 5). While addition of CTAB in the submicellar concentration range increases the intensity at ~420 nm region depicting catalytic effect of CTAB charge on the excited-state deprotonation, further addition of CTAB above the cmc (>1 mM) decreases the emission intensity indicating a retardation of the deprotonation rate for the lack of water availability in the micelles. Intensity of neutral emission, however, is increased slightly on the addition of CTAB in the submicellar concentration range, while in the post-micellar concentration range no appreciable change of emission intensity is observed. Moreover, no detectable shift of neutral emission wavelength or the fluorescence quenching on CTAB addition is observed. Therefore, neither any extensive disruption of H bonds that might exist between the electronically excited state of naphthols and the water clusters nor the formation of new intermolecular H bond among the embedded naphthols in the photoexcited state is obvious from the above result.

FTIR and Transmitting Electron Microscopic (TEM) Studies. The FTIR spectra of 2-naphthol in the presence and absence of CTAB micelles are shown in Figure 3 (insets A and B). The spectra of vacuum-dried samples (25 °C) provided interesting results (in KBr pellets). (Studying the spectral feature of OH group of naphthols in aqueous solution was not possible (in CaF_2 cell) due to overlapping of IR peaks with that of water.) The broad band around 3354 cm^{-1}, which is assigned to the OH stretching of 2-naphthol (typically observed in phenols) is shifted to 3163 cm^{-1} due to partitioning in the micelles. Comparatively sharper peak at higher wavelength confirms the presence of well-defined and stronger H bond in naphthols, which are embedded inside CTAB micelles. The peak at 3050 cm^{-1}, which remains almost unchanged upon gelation, may be assigned to aromatic CH stretch. Above shifting of OH stretching frequency is very much reproducible and consistently displayed by a wide variety of wormlike micellar systems promoted by naphthols. It seems apparent that H bonding plays an important role in micellar shape transition.[37] The result also shows that vacuum drying at room temperature did not destroy the microstructure completely although may have modified it

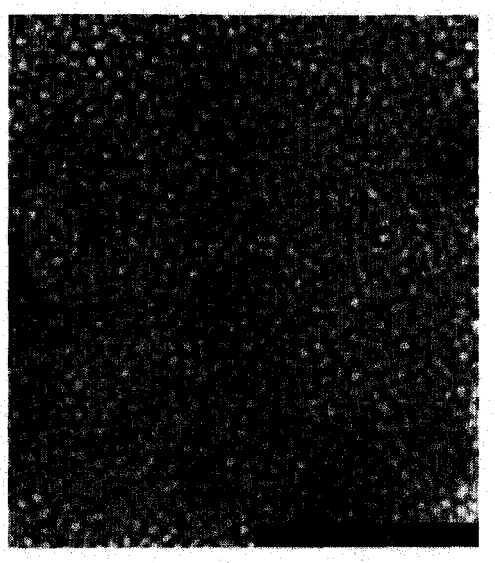

Figure 7. TEM micrographs of CTAB−2-naphthol system (10 mM, 1:1).

to some extent. This observation is also supported by TEM experiments done under identical conditions. The sample preparation on TEM grid was done according to the method described elsewhere followed by vacuum drying at room temperature as above.[38] The TEM micrograph looks like a condense, isotropic, and continuous network (Figure 7). The structure represents the transition in shape from spherical to rodlike micelles. Interestingly, this TEM picture is almost identical with that of the microstructure observed under cryoTEM for cetyltrimethylammonium hydroxide (100 mM) in presence of 2-hydroxy 1-naphthoic acid (55 mM) by a previous worker.[39] Freeze-fracture electron microscopy done with CTAB-SS system also indicated the formation of isotropic wormlike micelles similar to one shown in Figure 7,[5] along with other morphologies. This result clearly suggests that specific and stronger H bonds are formed between naphthol molecules, which are embedded in micelles because of their close proximity. In absence of charge screening, these H bonds force to decrease the surface area per surfactant head group causing micellar shape transition to occur. In the presence of hydrotropes like SS, however, both the phenomena, viz., charge screening as well as H bonding may be operative simultaneously.

Conclusion

Stimuli-responsive viscoelastic gels of long wormlike CTAB and CPB micelles are formed at low surfactant concentrations in presence of 1- and 2-naphthols. In the absence of charge screening of surfactant head groups, H bonding among micelle-embedded naphthol molecules probably plays the key role in micellar shape transition. Micelle-embedded naphthols act as novel self-fluorescence probes for monitoring viscoelasticity as a function of applied shear. The viscoelastic gels formed in presence of naphthols are thermoreversible in nature, and the viscosity−temperature profile of each system passes through a maximum. ^1H NMR confirms that solubilization sites of naphthols in the micelle are located near the surface. The above study also shows that, on the NMR time scale, the motion of the naphthol molecules is highly restricted in viscoelastic phase, but water molecules rotate freely. While fluorescence quenching via H-bond strengthening is not observed in the micellar phase, UV absorption spectra demonstrate the presence of inter-

molecular H bond in micelle-embedded naphthols in their ground electronic states, which was confirmed by FTIR. The ESPT of 2-naphthol is facilitated in presence of CTAB in the submicellar concentration range due to the catalytic effect of surfactant charge where as, ESPT is hindered in postmicellar concentrations due to lack of water accessibility. TEM micrographs of vacuum-dried samples demonstrate spherical to rodlike micellar transition of CTAB and CPB in presence of naphthols, as seen in Figure 7.

Acknowledgment. This work was funded by the Council of Scientific and Industrial Research, New Delhi.

References and Notes

(1) Rehage, H.; Hoffmann, H. *J. Phys. Chem.* **1988**, *92*, 4712−4719.
(2) Rehage, H.; Hoffmann, H. *Mol. Phys.* **1991**, *74*, 933−943.
(3) Cates, M.; Candau, S. J. *J. Phys.: Condens. Matter* **1990**, *2*, 6869−6877.
(4) Hu, Y.; Rajaram, C. V.; Wang, S. Q.; Jamieson, A. M. *Langmuir* **1994**, *10*, 80−85.
(5) Keller, S. L.; Boltenhagen, P.; Pine, D. J.; Zasadzinski, J. A. *Phys. Rev. Lett.* **1998**, *80*, 2725−2728.
(6) Boltenhagen, B.; Hu, Y.; Matthys, E. F.; Pine, D. J. *Phys. Rev. Lett.* **1997**, *79*, 2359−2362.
(7) Liu, C.; Pine, D. J. *Phys. Rev. Lett.* **1996**, *77*, 2121−2124.
(8) Manohar, C. In *Micelles, Microemulsions, and Monolayers; Science and Technology*; Shah, D. O., Ed.; Marcel Dekker, Inc.: New York, 1998; p 145.
(9) Lindemuth, P. M.; Bertrand, G. L. *J. Phys. Chem.* **1993**, *97*, 7769−7773.
(10) Hedin, N.; Sitnikov, R.; Furo, I.; Henriksson, U.; Regev, O. *J. Phys. Chem. B* **1999**, *103*, 9631−9639.
(11) Yin, H.; Lei, S.; Zhu, S.; Huang, J.; Ye, J. *Chem.−Eur. J.* **2006**, *12*, 2825−2835.
(12) Israelachivli, J. N.; Mitchell D. J.; Ninham, B. W. *J. Chem. Soc., Faraday Trans.* **1976**, *72*, 1525−1568.
(13) Rao, U. R. K.; Manohar, C.; Valaulikar, B. S.; Iyer, R. M. *J. Phys. Chem.* **1987**, *91*, 3286−3291.
(14) Kung, C. E.; Reed, J. K. *Biochemistry* **1986**, *25*, 6114−6121.
(15) Retting, W.; Lapouyade, R. In *Topics in Fluorescence Spectroscopy*; Lakowicz, J. R., Eds.; Plenum Press: New York, 1994; Vol. 4, p 109.
(16) Webb, S. P.; Yeh, S. W.; Philips, L. A.; Tolbert, M. A.; Clark, J. H. *J. Am. Chem. Soc.* **1984**, *106*, 7286−7288.
(17) Harris, C. M.; Selinger, B. K. *J. Phys. Chem.* **1980**, *84*, 1366−1371.
(18) Harris, C. M.; Selinger, B. K. *J. Phys. Chem.* **1980**, *84*, 891−898.
(19) Solntsev, K. M.; Ilichev, Y. V.; Demyashkevich, A. B.; Kuzmin, M. G. *J. Photochem. Photobiol. A* **1994**, *78*, 39−48.
(20) Ilichev, Y. V.; Demyashkevich, A. B.; Kuzmin, M. G. *J. Phys. Chem.* **1991**, *95*, 3438−3444.
(21) Sukul, D.; Pal, S. K.; Mandal, D.; Sen, S.; Bhattacharya, K. *J. Phys. Chem. B* **2000**, *104*, 6128−6132.
(22) Pappayee, N.; Mishra, A. K. *Photochem. Photobiol.* **2001**, *73*, 573−578.
(23) Kalur, G. C.; Frounfelker, B. D.; Cipriano, B. H.; Norman, A. I.; Raghvan, S. R. *Langmuir* **2005**, *21*, 10998−11004.
(24) Tata, M.; John, V. T.; Waguespack, Y. Y.; McPherson, G. L. *J. Phys. Chem.* **1994**, *98*, 3809−3817.
(25) Grieser, F.; Drummond, C. J. *J. Phys. Chem.* **1988**, *92*, 5580−5593.
(26) Das, S. K. Ph.D. thesis, University of North Bengal, India, 2006.
(27) Bardez, E.; Monnnier, E.; Valeur, B. *J. Colloid Interface Sci.* **1986**, *112*, 200−207.
(28) Das, S.; George Thomas, K.; Ramanathan, R.; George, M. V. *J. Phys. Chem.* **1993**, *97*, 13625−13628.
(29) Zhao, G.; Han, K. *J. Phys. Chem. A* **2007**, *111*, 2469−2474.
(30) Zhao, G.; Han, K. *J. Phys. Chem. A* **2007**, *111*, 9218−9223.
(31) Zhao, G.; Liu, J.; Zhao, L.; Han, K. *J. Phys. Chem. B* **2007**, *111*, 8940−8945.
(32) Samant, V.; Singh, A. K.; Ramakrishna, G.; Ghosh, H. N.; Ghanty, T. K.; Palit, D. K. *J. Phys. Chem. A* **2005**, *109*, 8693−8704.
(33) Zhao, G. *J. Chem. Phys.* **2007**, *127*, 024306−024306.
(34) Lee, J; Robinson, G. W.; Webb, S. P.; Philips, L. A.; Clark, J. H. *J. Am. Chem. Soc.* **1986**, *108*, 6538−6542.
(35) Mandal, D.; Pal, S. K.; Bhattacharyya, K. *J. Phys. Chem. A* **1998**, *102*, 9710−9714.
(36) Abou-al Einin, S.; Zaitsev, A. K.; Zaitsev, N. K.; Kuzmin, M. G. *J. Photochem. Photobiol. A* **1988**, *41*, 365−373.
(37) Waguespack, Y. Y.; Banerjee, S.; Ramannair, P.; Irvin, G. C.; John, V. T.; McPherson, G. L. *Langmuir* **2000**, *16*, 3036−3041.
(38) Liu, Z.; Cai, J. J.; Scriven, L. E.; Davis, H. T. *J. Phys. Chem.* **1994**, *98*, 5984−5993.
(39) Abdel-Rahem, R. Ph.D. thesis, University of Bayreuth, Germany, 2003.

Hydrogen-Bond-Induced Microstructural Transition of Ionic Micelles in the Presence of Neutral Naphthols: pH Dependent Morphology and Location of Surface Activity

Moazzam Ali, Mrinmoy Jha, Susanta K. Das, and Swapan K. Saha*

Department of Chemistry, University of North Bengal, Darjeeling 734 013, India

Received: August 9, 2009

The effect of naphthols and methoxynaphthalenes on the microstructure transition of cetyltrimethylammonium bromide (CTAB) micelles is studied. Although the surface activities of these two types of organic dopants are strong, methoxynaphthalenes failed to promote spherical to worm-like micellar transition and to impart viscoelasticity to the aqueous CTAB solution, presumably due to their inability to form unique H-bonds with interfacial water. The micropolarity of OH sites of micelle-embedded naphthols is measured by observing the pK_a shift at the micellar surface relative to bulk water. On the basis of spectroscopic and other data, the microstructures formed by both classes of dopants at the micellar surface are predicted. On the basis of hydroxyaromatic dopants, a simple and effective route to design pH-responsive viscoelastic worm-like micelles and the vesicles of single tail cationic surfactant (CTAB) is reported. Results are confirmed by observing cryogenic transmission electron microscopy (cryo-TEM) images.

Introduction

Organic π-conjugated molecules are effective tuners in the formation of various nanostructured materials, and the entailed route is potentially facile and efficient for the development of functional materials of technological and biological importance.[1−4] Microstructural transitions of micellar aggregates, especially the nature of transition from ordinary micelles to long worm-like giant micelles and the vesicles, mediated by organic π-electron systems are of fundamental scientific interest and have been reported in several papers recently.[5−8] Moreover, synthetic vesicular systems are interesting from a number of standpoints, not the least being their structural similarity with the constituent of the biomembrane, viz., phospholipid. They offer a convenient way to probe interactions involving membrane systems. Vesicle aggregation or adhesion is the primary step for the fusion of the vesicles in membrane. Therefore, the elucidation of the molecular mechanism of vesicular aggregation would greatly contribute to a better understanding of these biological phenomena. Single chain ionic surfactants, e.g., cetyltrimethylammonium bromide (CTAB), favor convex-up surface geometry of the micelles due to strong headgroup repulsion and form spherical or near spherical micelles at the critical micelle concentration (cmc), while either at much higher surfactant concentrations (~1.0 M) or in the presence of high inorganic salt concentrations (>0.1 M), morphological changes occur to rod-like micelles and vesicles.[9−12] Hydrotropic salts like sodium salicylate (SS) also promote sphere to worm-like micellar transition at considerably lower concentration (e.g., ~1.0 mM in CTAB) by increasing the packing parameter above the critical value of 1/3 via efficient charge screening of the surfactant head groups.[13] These worm-like micellar solutions at low concentrations show complex and unusual rheological phenomena. They exhibit some fascinating shear dependent properties and have been the subject of much discussion for a long time.[14−18] For example, when sheared below a critical shear rate which depends on temperature, surfactant, and salt concentrations, dilute worm-like micellar solutions shear thin. On the contrary, above a critical shear rate, micellar solutions show time dependent behavior. Initially, the solutions shear thin, and after an induction period, the solutions exhibit a shear thickening property. It has been suggested that shear thickening occurs because free worm-like micelles join a transient network under shear; the microstructures have been broadly named shear-induced structure or phase (SIS or SIP, respectively).[19−21] However, in certain systems, e.g., cetyltrimethylammonium chloride/sodium 3-methyl salicylate dispersion, vesicle to worm-like micellar transition and vice versa have been claimed to occur under shear, leading to rheological modification of the system.[22] A recent discovery of the flow-induced structure transition between vesicle and micelle is also interesting. The structural transition induced by flow in the cetyltrimethylammonium 3-hydroxy naphthalene 2-carboxylate micelles and the mixture of hexadecylpydinium chloride and sodium chlorate caused initial confusion because there has been apparently no reason for how the structural transition takes place.[22,23] As has already been pointed out, a facile and interesting route of lowering the surface curvature of micelles of single chain cationic surfactants is to increase the effective cross-sectional area of the hydrocarbon tail and to shield the headgroup charges by embedding neutral aromatic compounds with hydrogen bonding functionalities (e.g., 1- and 2-naphthols).[5] These dopants upon embedding in the micelle hinder any curvilinear displacement of head groups to take place via a comparatively rigid network of hydrogen bonding at the micelle surface and at the same time decrease the area of the surfactant head groups efficiently. The efficiency of hydroxy aromatic compounds in micellar shape transition is very high, and an aqueous mixture of CTAB and 2,3-dihydroxy naphthalene which gives highly viscous rod-like nanoaggregates has been used as a template for the sol−gel synthesis, providing an aqueous route for tube silicate preparation.[7] Altering the structure of the micellar system by phenolic dopant is an easy way to tailor the structure and properties of mesoporous materials which are synthesized on the micellar templates.[24] UV absorption spectra are modified due to the presence of an intermolecular H-bond in micelle-embedded naphthols in their ground elec-

* To whom correspondence should be addressed. E-mail: ssahanbu@hotmail.com.

10.1021/jp907677x CCC: $40.75
Published on Web 10/28/2009

tronic states, and this was confirmed by FTIR. The excited state proton transfer (ESPT) of 2-naphthol is facilitated in the presence of CTAB in the submicellar concentration range due to the catalytic effect of surfactant charge, whereas ESPT is hindered in post-micellar concentrations due to lack of water accessibility. However, the exact nature of H-bonding in the micellar phase is not understood completely. Moreover, together with hydrogen bonding, the $\pi-\pi$ and cation$-\pi$ interactions between favorably arranged micelle-embedded naphthol molecules may also be involved in modifying the absorption spectra.[25] Therefore, in order to further examine the exact nature of the noncovalent interaction that is involved in the above modification of the spectra, it is tempting to check what would happen if we replace the hydroxyl group of the promoter naphthol molecules by methoxy groups. Methoxy naphthalenes (MN) possess a similar structure and hydrophobicity to that of the naphthol (HN) molecules but cannot act as hydrogen bond donors. It would be interesting to compare the efficiency of methoxy naphthalenes with that of naphthols in effecting microstructural transitions of micelles and to discuss the result in the light spectroscopic observations. Further, it may be anticipated that a simple and effective route to design a pH-responsive microstructure could well be based on the neutral naphthol dopants, which form salts only at high pH ($pK_a > 9.2$). As a function of pH, ionization of the OH group of naphthol molecules may switch the onset of charge screening, paving the way to effect further morphological transitions (viz., vesicle formation). An objective of the present work is, therefore, to design a simple effective route of pH-responsive morphological transition for the aqueous molecular aggregates of single chain cationic surfactant, viz., CTAB from micelles to long worm-like micelle to unilamelar vesicles.

Finally, it is important to note that although the last two decades have witnessed a strong excitement among the researchers on the microstructural transitions of micelles at low concentrations, induced by hydrotropes like sodium salicylate and other similar dopants, leading to stimuli-responsive viscoelasticity, the exact role and the location of the protruded polar groups (e.g., OH groups) of the hydrotropes toward the Stern layer have not been firmly ascertained. This is particularly an interesting basic element to investigate for the present system where intermolecular H-bonding through OH groups of the micelle-embedded naphthols seems to play the pivotal role in the transition of the micellar morphology. In this work, therefore, micropolarity has been determined at the OH group sites by monitoring the pK_a shift at the micellar interface relative to bulk water in an attempt to determine the location of the protruded OH groups in the Stern layer.[26,27]

Experimental Section

1- and 2-Naphthols (puriss, Aldrich) were purified by vacuum sublimation followed by crystallization from 1:1 aqueous methanol. 1- and 2-Methoxynaphthalenes (Acros-Organics, Belgium) were recrystallized from 1:1 aqueous methanol before use. CTAB (puriss, Aldrich) was used as received. ^{1}H NMR and UV absorption spectra were recorded on a Bruker (300 MHz) spectrometer and a Jasco (v-530) spectrophotometer, respectively. Shear-induced viscosity was measured on a rotational viscometer (Anton-Paar, DV-3P; accuracy ±1% and repeatability ±0.2%) equipped with a temperature controller and with the facility of varying shear rates. A Kruss tensiometer (K 9) was used for surface tension measurements. Sample preparation on a TEM grid for cryo-TEM study was done following a similar method to that described in a previous paper.[5]

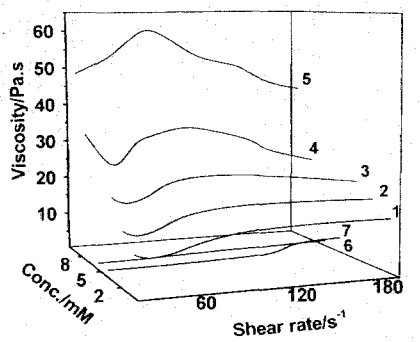

Figure 1. Steady shear viscosity as a function of the applied shear rate for dilute and concentrated solutions of 2-naphthol/CTAB at 25 °C. The molar concentration ratio, [2-naphthol]/[CTAB], was fixed at unity. (1) 1.0, (2) 1.5, (3) 2.0, (4) 5.0, (5) 8.5 mM. (6) and (7) are plots for 1- and 2-methoxynaphthalene−CTAB (5 mM, 1:1) systems, respectively.

Results and Discussion

Shear-Induced Viscoelasticity and Surface Activity: Role of the OH Group of the Dopant. Figure 1 shows the rheological responses for a representative viscoelastic system, viz., an aqueous CTAB−1-naphthol system as a function of concentration (1:1 mol ratio; this composition yields the strongest viscoelasticity) at 25 °C (pH ~5.0). At low concentrations (<2 mM), this system shows a shear thinning property up to a shear rate of 25 s^{-1} and then the shear thickening phenomenon starts to occur, but above a shear rate of 60 s^{-1}, the fluid shows a Newtonian type behavior (Figure 1(1,2)). However, an overall non-Newtonian nature is apparent as the concentration of the CTAB and naphthol (1:1) system is raised above 2.0 mM. At still higher concentrations (>5.0 mM), the nature of the rheological response changes dramatically and the system starts displaying an unusual rheology as a function of shear rate (Figure 1(4)). Up to a shear rate of 60 s^{-1}, the fluid shear thins. An onset of viscosity rise is observed at the shear rate of 60 s^{-1}, and the system again shear thins, passing through a maximum at 70 s^{-1}. At further higher concentrations (8.5 mM), the viscosity−shear rate profile again changes feature; the initial shear thinning characteristics disappear. The overall behavior is consistent with building up of long worm-like micellar bundles at relatively high concentrations. Therefore, it appears that the shear thinning viscosity in low shear rates is indicative of the flow-induced alignment toward the flow directions. Meanwhile, when the CTAB concentration is above 10.0 mM in the equimolar CTAB/naphthol solutions, the micelles are much longer and entangled with each other in the solution. In this case, the shear viscosity increases much higher and the micellar solution behaves like entangled polymer solutions exhibiting typical nonlinear viscoelastic behavior such as a stress plateau. The contour length of the worm-like micelles is highly dependent on the concentrations of the surfactant and the promoter.

The methoxynaphthalene−CTAB systems, on the other hand, neither display the ability to develop viscoelasticity (6,7 of Figure 1) in the system nor exhibit any viscosity modification with applied shear, and behave completely like a Newtonian liquid. This result is quite surprising in view of the fact that much like 1- and 2-naphthols, both 1- and 2-methoxynaphthalene are expected to embed into the micelles of CTAB. Therefore, to ascertain the location and orientation of the additive methoxy naphthalene molecules in the micelles and to understand the nature of the interaction with micelles, ^{1}H NMR experiments were performed (Figure 2).

The NMR spectrum of 1-MN in D_2O (in the absence of CTAB) shows four sets of signals, centered at δ values of 8.151,

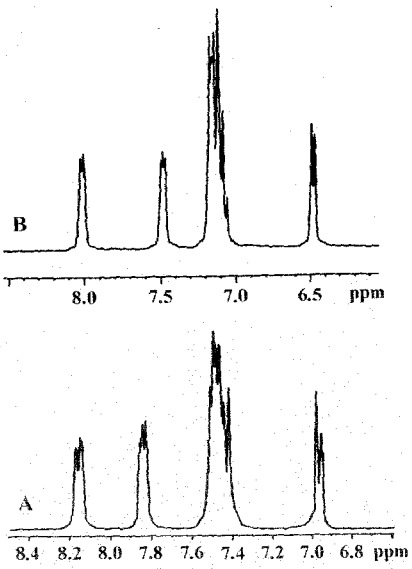

Figure 2. ^{1}H NMR spectra of 1-methoxynaphthalene in the absence (A) and presence (B) of CTAB (7.5 mM, 1:1).

7.853, 7.482, and 6.947, respectively, due to the resonance of the aromatic ring protons (Figure 2A). All four sets of signals are shifted upfield, remain well resolved, and appear at δ values of 8.013, 7.492, 7.147, and 6.487, respectively, when D_2O solutions of CTAB and 1-MN are mixed in 1:1 molar ratio (7.5 mM; Figure 2B). The methoxy protons which resonate at a δ value of 3.953 in water (not shown) are also shifted upfield and resonate at a δ value of 3.561 in CTAB. A similar upfield shift of aromatic and methoxy proton signals is observed in the CTAB−2-MN system as well. This large shift of either aromatic proton resonance or methoxy proton resonance to low δ values clearly indicates the location of naphthalene rings as well as the methoxy group of methoxy naphthalene molecules in the less polar environment than that of water. A previous study with the CTAB−naphthol system also showed a similar upfield shift of proton resonance of the aromatic moiety of the naphthol molecule, and it was argued that this was due to insertion of naphthol molecules into the micelle.[5] Unlike naphthol−CTAB systems, absence of line broadening and the well resolved structures of the NMR signals clearly indicates fast rotation of naphthalene rings in the CTAB−MN systems (on the NMR time scale). However, the degree of upfeild shift of the signals is less in 1-MN than that in naphthols; this indicates a stronger partitioning of naphthol molecules in the micelles. In this context, comparison of surface activities of methoxynaphthalenes and naphthols may also be interesting.

Figure 3 clearly shows that both 1- and 2-naphthols reduce the surface tension (ST) of water to a considerable extent, indicating that naphthols are surface active. Previously, it has been shown that 3-hydroxynaphthalene 2-carboxylate (SHNC) also reduces the surface tension in a similar manner and it also effectively promotes micellar shape transition.[28] Interestingly, while SHNC decreased the surface tension of water from a value of 75 to 60 N/m in the presence of 60 mM concentration of SHNC, an identical decrease in surface tension has been brought about by naphthols in the presence of only 0.4 and 0.5 mM concentrations. On the other hand, the surface tension of water is decreased to a similar extent by an even lesser amount of 1- and 2-MN's. While 1-MN decreases the ST of water up to the extent of 58 mN in the presence of 0.31 mM concentration, 2-MN did the identical ST lowering in the presence of only 0.16 mM concentration. While the extents of surface activity displayed by both naphthols are very close to each other, for 1- and 2-MN molecules, it differs quite significantly (Figure 3). The result indicates that 1- and 2-methoxy naphthalenes are stronger surface active agents than 1- and 2-naphthols, and accordingly, these molecules are expected to be embedded into the micelle strongly. Therefore, the findings of the NMR experiment are further strengthened by this fresh evidence of surface activities exhibited by methoxy naphthalene molecules. However, in spite of the strong surface activity shown by 1- and 2-MN, they fail to induce a microstructural transition in CTAB micelles. It seems apparent that OH groups in naphthol molecules play an important role in this respect. The results show that the naphthols are involved in a stronger and different kind of interaction with CTAB micelles as compared to methoxy naphthalenes. The surfactant, viz., CTAB, forms spherical micelles in the presence of methoxynaphthalene (2−10 mM; 1:1), whereas in the presence of naphthols CTAB forms long worm-like micelles and even vesicles (discussed in a later part).

Microscopic Polarity at the Location of OH Groups of Embedded Naphthols. It is believed that while the aromatic rings of naphthols are embedded in micelles, the core of which having a dielectric constant around 2−7 only, the OH groups stand out toward the water region. NMR study also confirms that the aromatic ring of the naphthol resides near the nonpolar core in between tetraalkylammonium head groups of the surfactants. Although almost all of the previous studies on the

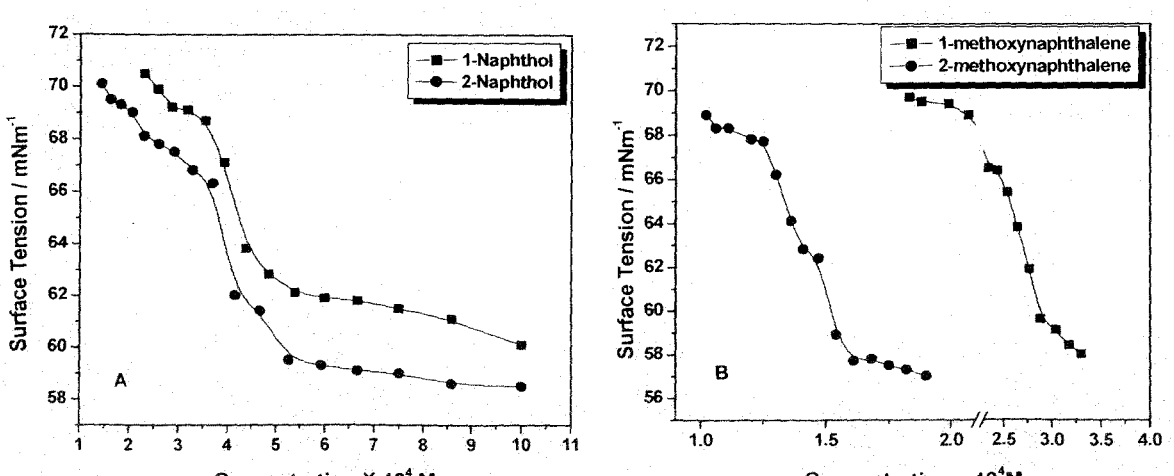

Figure 3. Surface tension of naphthols (A) and methoxynaphthalenes (B) as a function of concentration in water at 25 °C.

hydrotrope-induced microstructural transitions of micelles argue that the OH groups protrude out of the micellar surface and remain close to the aqueous layer, no experimental verification has so far been reported. To understand the exact nature of the location of the OH group, the micropolarity of the residence sites is determined. Spectral characteristics, especially fluorescence spectra, are often very sensitive to the environments around the probe molecule. Because of this, fluorescence spectroscopy has become one of the important methods for the study of the structure and dynamics of the microheterogeneous systems. Unfortunately, the excited state proton transfer process (ESPT) of hydroxyaromatic compounds, viz., 1- and 2-naphthols, complicates their spectral properties. The absorption spectra are also not sensitive to the environmental conditions in the present system. Moreover, information regarding the microenvironment of the aromatic π-electron system, which might have been obtained from the study of spectral characteristics, would not be helpful in determining the location of protruded OH groups of naphthol molecules. Therefore, pK_a shift of the acid–base equilibrium of the OH group of naphthols in a microheterogeneous medium relative to aqueous solution would be the ideal route for getting such information precisely. This shift in pK_a in a cationic micelle like CTAB relative to aqueous solution may be due to the surface potential of the micelle and the polarity variation at the micellar interface from that of the bulk (in the absence of any specific interaction). The theoretical background of the analysis of data pertaining to the interfacial acid–base equilibrium of naphthol molecules has been well documented for other similar probes.[26,27] While determining pK_a values of the present system, let us assume that the acid–base equilibrium of the OH group of naphthols is described by

$$\Phi OH + H_2O = \Phi O^- + H_3O^+ \qquad (1)$$

where ΦO^-, ΦOH, and H_3O^+ are deprotonated and protonated (neutral) forms of the naphthols and the proton, respectively. For the naphthol indicators in aqueous micellar solution, the apparent pK_a values were obtained from the change in the ultraviolet absorption spectra as a function of bulk aqueous pH by means of the following Henderson–Hasselbach equation (which considers only concentration terms at low concentration conditions) as follows (eq 1):

$$pK_a^{obs} = pH - \log[\Phi O^-]/[\Phi OH] \qquad (1a)$$

provided that the quantity $[\Phi O^-]/[\Phi OH]$ is determined by $(A - A_{\Phi OH})/(A_{\Phi O^-} - A)$, where A, $A_{\Phi OH}$, and $A_{\Phi O^-}$ are the absorbances of naphthols at experimental pH and low and high pH's, respectively. The near UV spectra of 1-naphthol as a function of the bulk aqueous pH in CTAB micelle solution are shown in Figure 4 (unfortunately, the spectral profile of 2-naphthol is insensitive toward bulk aqueous pH and, therefore, cannot be studied). For the acid–base equilibrium of the interfacially located organic molecule, the pK_a^{obs} is now separated into two components, viz., an electrostatic component and a nonelectrostatic environmental component. This is formalized in relation 2

$$pK_a^{obs} = pK_a^0 - e\Psi_0/2.303kT \qquad (2)$$

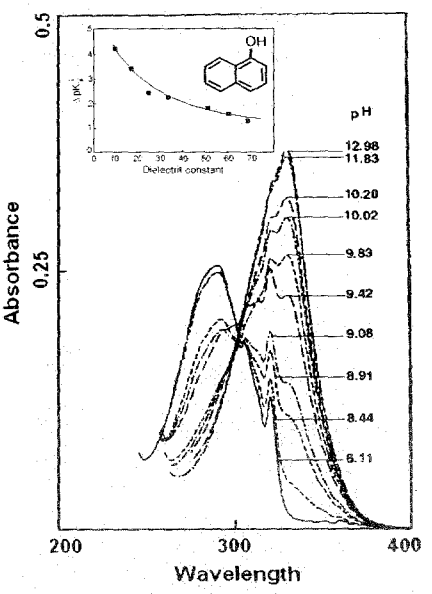

Figure 4. UV absorption spectra of 1-naphthol (0.5 mM) in 5.0 mM CTAB at varying pH.

where pK_a^0 is the apparent pK_a value if the surface potential of the micelle, Ψ_0, is null. Information can be obtained about the acid–base equilibrium at the surfactant–water interfaces by comparing pK_a^0 values of naphthols in the aqueous micellar systems with the pK_a values for naphthols in the aqueous–organic mixtures, e.g., dioxane–water mixtures. The apparent pK_a in organic–aqueous mixture, pK_a^m, is defined in the following relation (eq 3).

$$pK_a^m = B + \log U_H^0 - \log[\Phi O^-]/[\Phi OH] - \log \gamma^m_{\Phi O^-}/\gamma^m_{\Phi OH} \qquad (3)$$

where γ^m's are activity coefficient terms in the medium, B is the pH meter reading, and $\log U_H^0$ is the correction factor to be applied to pH meter reading to measure the actual hydrogen ion concentration in organic–aqueous mixtures. The pK_a^0 values relate to a system where the conjugate acid–base species reside in an interfacial microenvironment but the bulk aqueous solution pH is measured. Hence, the comparison between pK_a values in dioxane–water mixtures and pK_a^0 values in micelle systems should take into account the primary medium effect on the proton. In other words, pK_a^0 values need to compare to pK_a^i values rather than pK_a^m's where

$$pK_a^i = pK_a^m + {}_m\gamma_H^+ \qquad (4)$$

and ${}_m\gamma_H^+$ denotes the primary medium effect on the proton. It is usual to assume that the mean primary medium effect on HCl, ${}_m\gamma_\pm$, approximates to ${}_m\gamma_H^+$. The $\log U_H^0$ and ${}_m\gamma_\pm$ values given in refs 26 and 27 were employed to derive pK_a^i values in dioxane–water mixtures. These pK_a^i ($\Delta pK_a^i = pK_a^i - pK_a^w$) values as a function of medium dielectric constant are shown in Figure 4 (inset). The pK_a^0 values of 1-naphthol in CTAB micelles are determined with the aid of eq 2 and the known value of the surface potential of CTAB micelles of +141 mV.[26] The effective dielectric constant (D_{eff}) values are obtained by comparing ΔpK_a^0's (Table 1) of 1-naphthol on a micellar surface with ΔpK_a^i values in 1,4-dioxane–water mixtures (Figure 4; inset). It may be noted that D_{eff} values

TABLE 1: Results of pH Titration of 1-Naphthol in Aqueous and Aqueous CTAB Micellar Solution at 25°C

conc. of CTAB/mM (conc. of 1-HN = 0.5 mM)	pK_a^w	pK_a^{obs}	$-\Delta pK_a^{obs}$	pK_a^0	ΔpK_a^0
20		8.623	0.765	11.007	1.619
50	9.388	8.679	0.709	11.063	1.675
100		8.914	0.474	11.298	1.910

TABLE 2: D_{eff} Values of OH Group Location of Micellar Interface

conc. of CTAB/mM (conc. of 1-HN = 0.5 mM)	D_{eff}
20	51 ± 3
50	49 ± 3
100	45 ± 2

are measured on the basis of several assumptions: (i) both the protonated and deprotonated forms of the naphthol indicator are quantitatively partitioned into the micellar phase at least at high surfactant/naphthol ratio; (ii) the activity coefficient term ($\log \gamma^i_{\Phi O^-}/\gamma^i_{\Phi OH}$) is negligibly small so that ΔpK_a^0 values are directly comparable with the ΔpK_a^i behavior in different solvent dielectric constant bulk media; (iii) although the OH groups of naphthol protrude from the micellar surface, the acid−base equilibrium is still under the influence of micellar surface potential; (iv) it is evident that much like the 1,4-dioxane−naphthol system, the interfacial water of CTAB micelles forms H-bonds with micelle-embedded naphthols (discussed later), which act as a H-donor in both of the above cases. No serious error in the evaluation of D_{eff} due to the presence of this H-bond is thus anticipated because such an effect, if any, would be compensated by the similar interaction present in the reference system (naphthols in dioxane−water).

Table 2 shows that D_{eff} at the interface of CTAB micelles, as measured by the pK_a shift of interfacially located naphthols, varies from 51 ± 3 to 45 ± 2 as a function of CTAB concentration from 20 to 100 mM (concentration of naphthol being 0.5 mM throughout). This result indicates that naphthols are increasingly partitioned in micelles as the CTAB concentration is increased. Utilizing the solvatochromic visible absorption band maximum $E_T(30)$, D_{eff} estimates of 28−33 were obtained previously for CTAB micelles.[29] Therefore, in comparison to the previously determined micropolarity of the CTAB micellar surface (D_{eff} ~30), the present value of 45 (under conditions when most of the naphthol molecules are partitioned in micelles) is substantially high. This is an interesting observation. This clearly indicates that the OH groups are directed away from the surface of the micelles and are located around the more polar region. Assuming a polarity gradient to exist with the distance from the micellar surface, one can have a rough idea of the location of the OH groups in the Stern layer. A recent application of numerical Poisson−Boltzmann methods to the determination of the electrostatic potential and counterion distribution around polyelectrolyte such as DNA may be relevant in this respect.[30] In this case, the situation had prompted us to choose a dielectric constant "field", where low dielectric values exist near 30 at the polyelectrolyte surface and increase away to the values near 78.5 in bulk water. A rough estimation following the above work, which takes on a cylindrical polyelectrolyte (e.g., DNA) surface of radius 10 Å as the low dielectric region, shows that the present D_{eff} value of 45 (compared to ~30 at the micellar surface) could be rationalized assuming the OH group of naphthol to be protruded away from the CTAB micellar surface through a nearly 1 Å distance toward the Stern layer.[30]

Spectral Modification of Micelle-Embedded Dopants: Contribution of H-Bonding, $\pi-\pi$ or Cation$-\pi$ Interactions? In view of the differences in the viscoelastic responses and the morphological transitions of CTAB micelles (Figure 1) induced by neutral naphthols and the methoxy naphthalenes, UV absorption spectra of these dopants may be interesting to study in micellar media. To understand the kind of interactions which are operative in the micelle−dopant systems, the key element of the present study is to compare the spectral characteristics of naphthols (HNs which contain OH) with those of methoxy naphthalenes (MNs, which do not contain OH) under various conditions in order to visualize a consistent molecular picture eliminating the untenable suggestions. Aromatic compounds, e.g., naphthalene, in general, have two strongly overlapped bands in the near UV region, viz., the longitudinally polarized $^1L_a \leftarrow {}^1A$ band and the transversely polarized $^1L_b \leftarrow {}^1A$ band. While the vibrational structure of these bands appears differently in different substituted compounds, effects of extending conjugation in 1 and 2 positions by OH or CH_3O groups in naphthol and methoxynaphthalene molecules, respectively, are interesting. Both in 1-naphthol and 1-methoxy, naphthalene conjugation is extended in the transverse direction and, therefore, it affects the transverse polarized ^1L_a band. In 2-naphthol and 2-methoxy naphthalene, on the other hand, conjugation is primarily extended in the longitudinal direction, affecting both the intensity and the frequency of the longitudinally polarized ^1L_b band compared to the unsubstituted naphthalene.

It is well-known that the near UV spectra of aromatic compounds are affected by specific interactions like hydrogen bonding. Noncovalent interactions like $\pi-\pi$ and cation$-\pi$ also cause shifts in the electron distributions of the molecule. The OH group of naphthols can act as both a proton donor as well as a proton acceptor in forming intermolecular hydrogen bonding. A hydrogen bond in which the hydroxyl groups of naphthols is a proton donor releases electron density from the O−H bond toward the oxygen and hence, by an inductive effect, toward the aromatic ring. This causes a red-shift of the $\pi-\pi^*$ transition. Conversely, if a hydrogen bond is formed in which the hydroxyl oxygen is a proton acceptor, electrons are withdrawn from the naphthalene ring, and an opposite shift is anticipated. If both bonds could form at the same time and with equal ease, since their effects on the partial charges of the oxygen are opposite, the net change on the oxygen and hence on the aromatic ring may be small. Therefore, in such a situation, the spectral shift relative to the position of the band in a non-hydrogen-bonding situation ought to be small.[32] The near UV absorption of 1-naphthol which arises from two strongly overlapped $\pi-\pi^*$ transitions remains unaffected in the presence of submicellar aqueous CTAB solution, indicating the absence of any appreciable interaction (Figure 5) (the effect of CTAB micelles on the UV spectra of 2-naphthol is also similar). However, interestingly, significant red-shift starts to occur (6.4 nm at λ_{max} ~293 nm) in the presence of CTAB just above its cmc (0.96 mM) with a well-defined isobastic point at 296 nm. Such shifting of λ_{max} continues until most of the naphthol molecules are partitioned in the micellar phase at high surfactant/naphthol ratio (80:1; Figure 5A). The result suggests that the protruded OH groups of micelle-embedded naphthols form a H-bond with interfacially located (D_{eff} ~45) water molecules and act as a H-donor. It may also be argued that at a mole ratio of 1:1 of naphthol and the CTAB, at which maximum viscoelastic response is observed under shear due to the presence

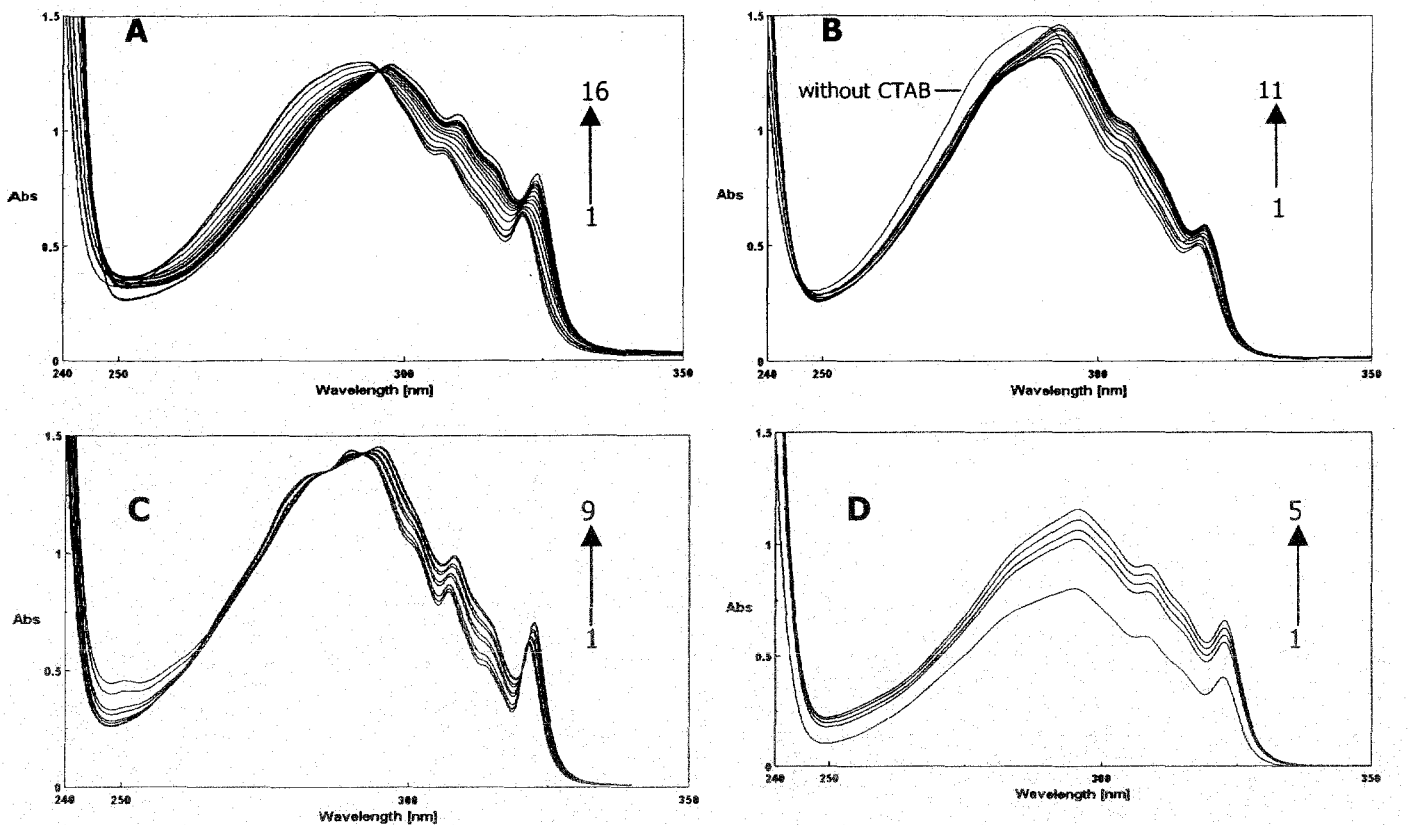

Figure 5. (A) Absorption spectra of 1-HN (0.25 mM) in water at varying concentrations of CTAB at 25 °C. [CTAB]: (1) 0.0, (2) 0.44, (3) 0.55, (4) 0.75, (5) 1.00, (6) 1.25, (7) 1.50, (8) 1.75, (9) 2.00, (10) 2.50, (11) 3.00, (12) 3.50, (13) 4.00, (14) 5.00, (15) 15.00, (16) 20.00 mM. (B) Absorption spectra of 1-MN (0.25 mM) in water at varying concentrations of CTAB at 25 °C. [CTAB]: (1) 0.33, (2) 0.50, (3) 0.75, (4) 1.00, (5) 1.50, (6) 2.00, (7) 2.50, (8) 3.00, (9) 3.50, (10) 4.00, (11) 5.00 mM. (C) Absorption spectra of 1-HN (0.25 mM) in isooctane at various concentrations of 1,4-dioxane at 25 °C. [Dioxane]: (1) 0.00, (2) 13, (3) 20, (4) 40, (5) 50, (6) 80, (7) 100, (8) 160, (9) 200 mM. (D) Absorption spectra of 1-HN (0.25 mM) in acetonitrile at different percentages of water at 25 °C. % of water: (1) 0.00%, (2) 4%, (3) 6%, (4) 8%, (5) 10%.

of entangled worm-like micelles, not all of the naphthol molecules are embedded in the micelles, but some are located in the palisade layer. These naphthols may, however, be involved in H-bond network formation with embedded molecules via interfacial water.

The spectral feature (Figure 5A) and the nature and degree of shift undoubtedly resemble the spectra of naphthol in isooctane at various dioxane concentrations (red-shift of 6.3 nm at λ_{max} ~293 nm, Figure 5C, as compared to a red-shift of 6.4 nm at λ_{max} ~293 nm, Figure 5A) where naphthol acts as the hydrogen bond donor and dioxane as the acceptor (Figure 5 C).[31]

Previously, it has been shown that, in the ground state, 1-naphthol interacts with water via oxygen, whereas with alcohols (ethanol and isopropanol) and acetonitrile it interacts via hydrogen from the hydroxyl group.[33] The nature of spectral modification encountered by micelle free naphthol molecules in the presence of water is shown in Figure 5D. This figure shows that on every addition of water (up to 10% v/v) substantial gain in intensity is displayed by 1-naphthol spectra (in acetonitrile) with little change of wavelength. The nature of spectral modification of 1-HN due to H-bond formation is quite different from that of micelle-embedded naphthol. It may be argued that, like alcohols and acetonitrile media, naphthols at the interface (D_{eff} ~45) act as H-donating agents and water as a H-acceptor at the oxygen atom. This is indeed interesting. The low D_{eff} value found for the interfacial microenvironment of CTAB micelles may be attributed to a low interfacial water activity. Nevertheless, it has also been argued that the low interfacial D_{eff} value may be a result of the H-bond donor properties of the water in the interfacial region being different from that of bulk water, and/or the presence of electrostatic image interactions caused by the proximity of the low dielectric hydrocarbon core. Present experiments indeed justify the former conjecture precisely.[34] It is known that the water molecules at the micellar interface have some strange properties.[35,36] The solvation dynamics are slowed down by several orders of magnitude relative to bulk water. The reorientational motion is also restricted. The dynamics of water molecules near an aqueous micellar interface has been a subject of intense current interest because such a system serves as a prototype of complex biological system. Furthermore, oxygen K absorption and emission spectra of water molecules in the micellar interface also show that the local electronic structure of water molecules is dramatically different from that of bulk water.[37] The relatively less polar and less mobile water molecules compared to bulk water form a strong H-bond with the OH group of embedded naphthols, which act as H-donors and result in an optimum orientation of aromatic π-electron systems in the micelles to shield the surfactant headgroup charges efficiently; maybe via cation$-\pi$ interaction; i.e., the cation charge of surfactant head groups interacts with the quadrupole moment of the aromatic π-system of naphthols. On the other hand, as the H atom of OH is replaced by a CH_3 group (viz., the methoxy naphthalene molecule), the ability of intermolecular H-bond formation disappears. Instead, the H-accepting tendency from a potential donor is enhanced. The nature of changes encountered in the UV spectra of methoxy naphthalenes on the addition of CTAB above its cmc indicates the permeation of the dopant molecules in the micelles (Figure 5B). The small red-shift compared to

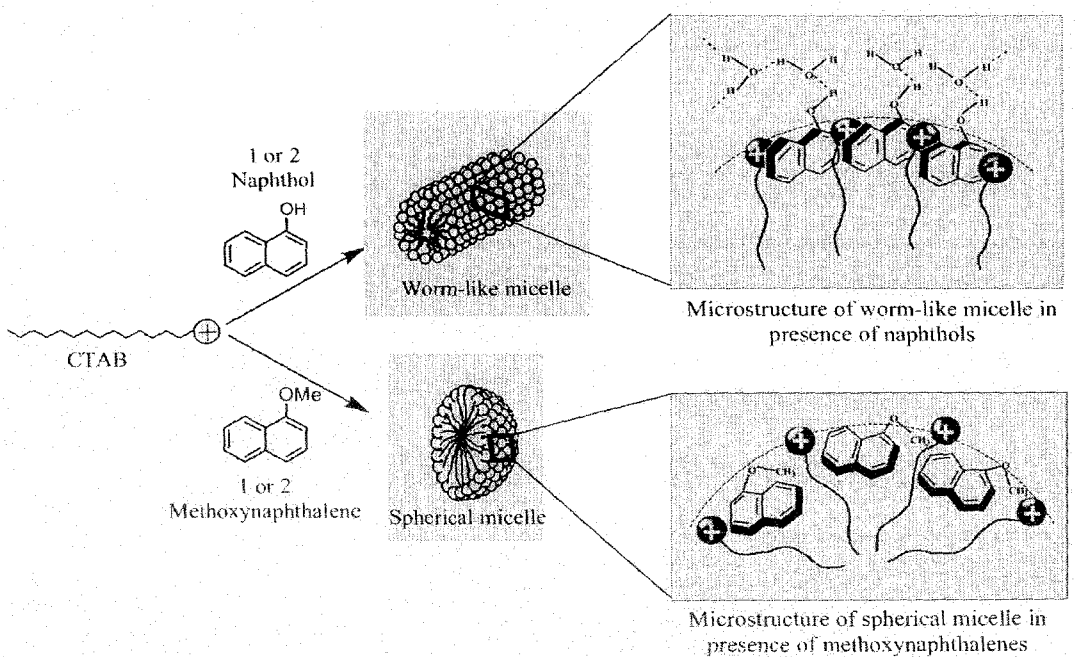

Figure 6. Schematic representation of the microstructures found in worm-like micelles formed by naphthols and spherical micelles formed by methoxynaphthalenes with CTAB.

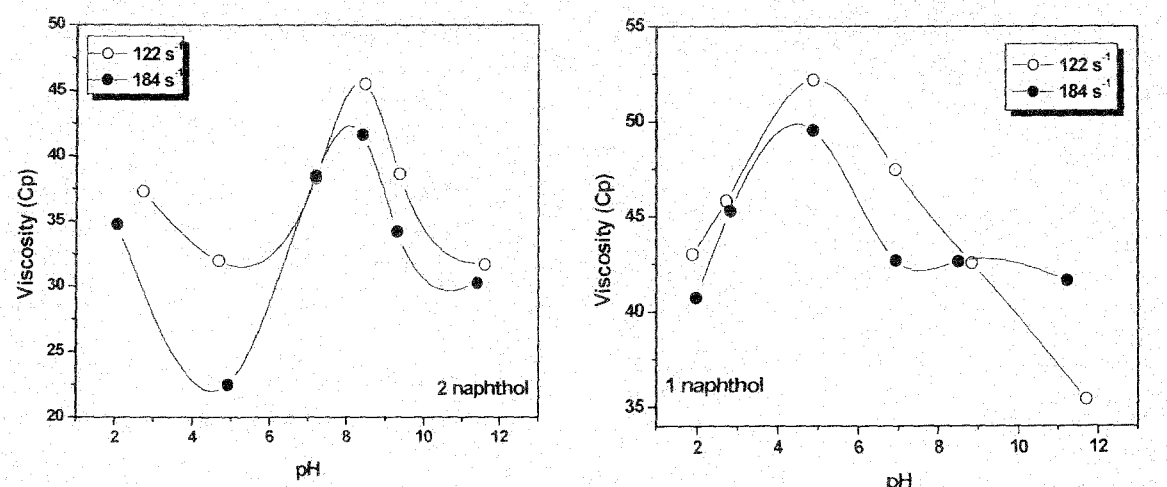

Figure 7. Viscosity vs pH profile for naphthol/CTAB systems at fixed shear rates of 122 and 184 s^{-1}.

that in naphthols indicates a weaker noncovalent interaction takes place. The large drop in intensity on first addition of 0.33 mM CTAB is the signature of breaking of a H-bond with bulk water molecules. Due to their directionality and spatial arrangement, complementary multiple H-bonding interactions at the micellar interface lead to engineering well-defined supramolecular structure via micellar headgroup charge shielding by π-electron systems of naphthols (Figure 6). This result of unusual H-bonding may be relevant, not only when considering the H-bonding of the interfacial water molecules in the specific micelle and dopant studied here but also for the H-bonding interaction of other micelle−dopant systems as well.

Shear-Induced Viscosity and pH. The role of neutral hydroxyaromatic dopants, viz., 1- and 2-HN, which are found to be efficient in bringing about microstructural transition in CTAB and CPB micelles, stimulates the idea of designing a route for pH-responsive vesicle formation.[5] This idea stems from the fact that the dopants, which under neutral conditions activate the formation of worm-like micelles at pH ~5.0, may on partial ionization of the OH group increase the packing parameter further via charge screening. This idea tempted us to study the pH dependent viscosity changes of the present viscoelastic gel system.[38] Figure 7 shows the viscosity−pH profiles of the 1-HN−CTAB and 2-HN−CTAB systems at constant shear of 122 and 184 s^{-1}, respectively. The general nature of the variation of viscosity as a function of pH for both 1- and 2-naphthol−CTAB systems is similar in high shear regime (viz., 122 and 184 s^{-1}, respectively). However, morphological responses are not identical for both of the systems. While the viscosity of both, 2- as well as 1-HN−CTAB systems, is quite high (35−45 Cp) due to formation of long worm-like micelles at low pH, the viscosity of the former system falls initially, indicating formation of shorter micelles with pH until pH ~5.0 is reached. On the other hand, for 1-HN−CTAB, the onset of viscosity rise as a function of pH is found to occur from very low pH (pH ~2.0). For 2-naphthol−CTAB, the onset of viscosity rise is observed at higher pH (>5.0) and the viscosity−pH profile passes through a maximum at pH ~8.5. The onset of viscosity rise is observed due to the partial titration of OH group, leading to charge screening of surfactant head groups by the naphtholate anion and at pH ~8.5 the worm-like micelles grow maximum. Further increase in pH results in the ionization of OH group further,

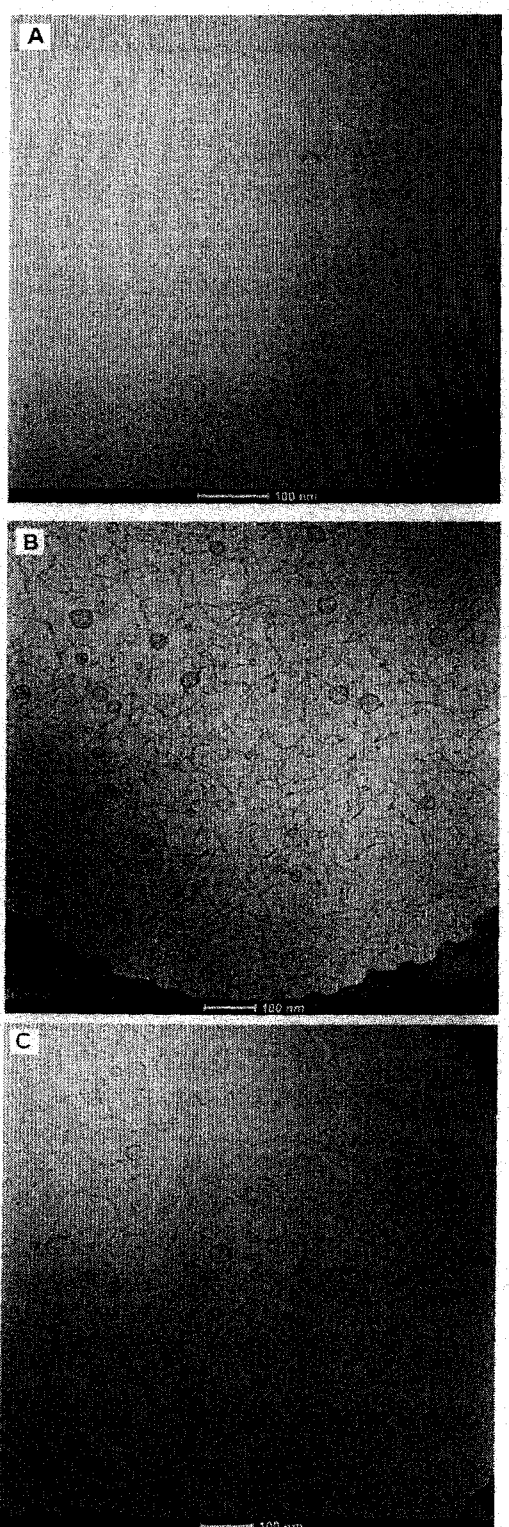

Figure 8. cryo-TEM micrographs of the CTAB−2-naphthol system (10 mM, 1:1) at normal pH (~5.5) (A) and at high pH (~9.4) (B). Part C shows linearly elongated worm-like micelles under shear flow.

and the packing parameter probably exceeds the critical value of 1/2 via enhanced charge screening, leading to vesicle formation (for naphthols, $pK_a > 9$, which means 50% ionization of the OH group at pH ~9.0). This results in the fall of viscosity of the system. Since 1-naphthol could modulate the micellar surface curvature more efficiently, a little dissociation of the OH group (at low pH range) leads to an appreciable decrease of surface curvature via charge screening and promotes long worm-like micelle formation. In fact, for the 1-HN−CTAB system, vesicles start to form even at slightly higher than pH ~5.0 (Figure 7). A simple and effective route to design pH-responsive viscoelastic worm-like micelles and less viscous globular vesicles based on naphthol dopants may be tuned by controlling the degree of charge screening of CTAB micelles via controlled ionization of naphtholic OH groups. The result of pH-responsive morphology modification is further investigated by means of cryo-TEM.

Cryogenic Transmission Electron Microscopic Study. Cryo-TEM images of the CTAB−2-naphthol system at low and high pH's are shown in Figure 8. At low pH (pH ~5.5), the micrograph looks like a condense, isotropic, and continuous network (Figure 8A) of worm-like micelles along with monodisperesed vesicles of very short diameters.

The micelles are slightly entangled. At high pH (pH~9.4), the system contains very long (endless in micrograph) worm-like micelles, which coexist with large unilamellar vesicles. This is undoubtedly due to enhanced charge screening of micelles by naphtholate anions. The field is seen to populate mainly by large vesicles of diameter ~30 nm along with thinly populated smaller vesicles. It is also seen that the long worm-like micelles are highly entangled. Sometimes they are found to elongate linearly under shear flow (Figure 8c). The solutions are completely transparent. The direct imaging by cryo-TEM supports the rheological observation as a function of pH (Figure 7). At low pH, the worm-like micelles are formed via headgroup charge shielding by aromatic π electrons, whereas, at high pH, ionization of OH groups takes place and the packing parameter exceeds the critical value of 1/2 via enhanced charge screening by naphtholate ion. This leads to unilamellar vesicle formation along with long worm-like micelles.

Conclusion

Neutral naphthols and methoxynaphthalenes, both with an aromatic π-system in their structures, are fairly surface active and embedded in aqueous CTAB micelles strongly. However, unlike methoxynaphthalenes, only naphthols can promote spherical to long worm-like micellar transition at room temperature and impart strong viscoelasticity and unusual rheology to the system. The success of naphthols in effecting microstructural transition of micelles lies in their unique ability to form H-bonds with interfacial water molecules, which have shown unusual H-bond donating properties compared to bulk water. The OH groups of micelle-embedded naphthols are protruded toward the Stern layer through ~1 Å and the dielectric constant of OH sites has been measured as 45 ± 2 by observing the pK_a shift of acid−base equilibrium of naphthols at the interface relative to that in bulk water. The result of unusual H-bonding may be relevant, not only when considering the H-bonding of the interfacial water molecules in the specific micelle and dopant studied here but also for the H-bonding interaction of other micelle−dopant systems as well. On the basis of hydroxyaromatic dopants like naphthols, a simple and effective route to design pH-responsive viscoelastic worm-like micelles and the vesicles of single tail cationic surfactant (CTAB) is reported. Results are confirmed by observing cryogenic transmission electron microscopy (cryo-TEM) images.

Acknowledgment. The authors are thankful to Council of Scientific and Industrial Research, New Delhi, for financial support. Dr. Wins Busing of FEI Company, The Netherlands, is gratefully acknowledged for help in acquiring the cryo-TEM data.

References and Notes

(1) Hoeben, F. J. N.; Jonkheijin, P.; Meijer, E. W.; Schenning, A. P. J. H. *Chem. Rev.* **2005**, *105*, 1491–1498.
(2) Guldi, D. M.; Zerbetto, F.; Georgakilas, V.; Prato, M. *Acc. Chem. Res.* **2005**, *38*, 38–42.
(3) Yoosaf, K.; Belbakra, A.; Nichola, A.; Llanes-Pallas, A. *Chem. Commun.* **2009**, 2830–2832.
(4) Cui, S.; Liu, H.; Gan, L.; Li, Y.; Zhu, D. *Adv. Mater.* **2008**, *20*, 2918–2923.
(5) Saha, S. K.; Jha, M.; Ali, M.; Chakraborty, A.; Bit, G.; Das, S. K. *J. Phys. Chem. B* **2008**, *112*, 4642–4647.
(6) Tan, G.; Ford, C.; John, V. T.; He, J.; McPherson, G. L.; Bose, A. *angmuir* **2008**, *24*, 1031–1036.
(7) Isayama, M.; Nomiyama, K.; Yamaguchi, T.; Kimizuka, N. *Chem. tt.* **2005**, *34*, 462–463.
(8) Singh, M.; Ford, C.; Agarwal, V.; Fritz, G.; Bose, A.; John, V. T.; Pherson, G. L. *Langmuir* **2004**, *20*, 9931–9937.
(9) Clint, J. H. *Surfactant Aggregation*; Blakie & Son Ltd.: London, 1992; p 147.
(10) Manohar, C. In *Micelles, Microemulsions and Monolayers, Science and Technology*; Shah, O. D., Ed.; Marcel Dekker, Inc.: New York, 1998; p 145.
(11) Davis, T. S.; Ketner, A. M.; Raghavan, S. R. *J. Am. Chem. Soc.* **2006**, *128*, 6669–6675.
(12) Tung, S.-H.; Lee, H.-Y.; Raghavan, S. R. *J. Am. Chem. Soc.* **2008**, *130*, 8813–8817.
(13) Israelachivili, J. N.; Mitchell, D. J.; Ninham, B. N. *J. Chem. Soc., Faraday Trans. 2* **1976**, *72*, 1525–1568.
(14) Rehage, H.; Hoffman, H. *J. Phys.Chem.* **1988**, *92*, 4712–4719.
(15) Rehage, H.; Hoffman, H. *Mol. Phys.* **1991**, *74*, 933–943.
(16) Cates, M.; Candau, S. J. *J. Phys.: Condens. Matter* **1990**, *2*, 6869–6877.
(17) Hu, Y.; Rajaram, C. V.; Wang, S. Q.; Jamieson, A. M. *Langmuir* **1994**, *10*, 80–85.
(18) Ketner, A. M.; Kumar, R.; Davies, T. S.; Elder, P. W.; Raghavan, S. R. *J. Am. Chem. Soc.* **2007**, *129*, 1553–1557.
(19) Keller, S. L.; Boltenhagen, P.; Pine, D. J.; Zasadzinski, J. A. *Phys. Rev. Lett.* **1998**, *80*, 2725–2728.
(20) Boltenhagen, B.; Hu, Y.; Matthys, E. F.; Pine, D. J. *Phys. Rev. Lett.* **1997**, *79*, 2359–2362.
(21) Liu, C.; Pine, D. J. *Phys. Rev. Lett.* **1996**, *77*, 2121–2124.
(22) Zheng, Y.; Lin, Z.; Zakin, J. L.; Talmon, Y.; Davis, H. T.; Scriven, L. E. *J. Phys. Chem. B* **2000**, *104*, 5263–5271.
(23) Mendes, E.; Narayanan, J.; Oda, R.; Kern, F.; Candau, S. J. *J. Phys. Chem. B* **1997**, *101*, 2256–2258.
(24) Agarwal, V.; Singh, M.; McPherson, G.; John, V.; Bose, A. *Colloids Surf., A* **2006**, *281*, 246–253.
(25) Dougherty, D. A. *Science* **1996**, *271*, 163–168.
(26) Drummond, C. J.; Grieser, F.; Healy, T. W. *J. Chem. Soc., Faraday Trans. 1* **1989**, *85*, 521–535.
(27) Drummond, C. J.; Grieser, F.; Healy, T. W. *J. Chem. Soc., Faraday Trans. 1* **1989**, *85*, 537–550.
(28) Mishra, B. K.; Samant, S. D.; Pradhan, P.; Mishra, S. B.; Manohar, C. *Langmuir* **1993**, *9*, 894–898.
(29) Drummond, C. J.; Grieser, F.; Healy, T. W. *Faraday Discuss. Chem. Soc.* **1986**, *81*, 95–102.
(30) Lamm, G.; Pack, G. R. *J. Phys. Chem. B* **1997**, *101*, 959–965.
(31) Baba, H.; Suzuki, S. *J. Chem. Phys.* **1961**, *35*, 1118–1127.
(32) Nemethy, G.; Ray, A. *J. Phys. Chem.* **1973**, *77*, 64–68.
(33) Zharkova, O. M.; Korolev, B. V.; Morozova, Y. P. *Russ. Phys. J.* **2003**, *46*, 68–74.
(34) Ramachandran, C.; Pyter, R. A.; Mukherjee, P. *J. Phys. Chem.* **1982**, *86*, 3198–3205.
(35) Bhattacharya, K. *J. Fluoresc.* **2001**, *11*, 167–179.
(36) Balasubramanian, S.; Pal, S.; Bagchi, B. *Curr. Sci.* **2002**, *82*, 845–848.
(37) Gasjo, J.; Anderson, E.; Forsbeing, J.; Aziz, E. F.; Brena, B.; Johansson, C.; Nordgren, J.; Duda, L.; Adersson, J.; Hennies, F.; Rubensson, J.; Hansson, P. *J. Phys. Chem. B* **2009**, *113*, 8201–8205.
(38) Lin, Y.; Han, X.; Huang, J.; Fu, H.; Yu, C. J. *Colloid Interface Sci.* **2009**, *330*, 449–455.

JP907677X